NSPORTATION

UNIVERSITY OF MINNESOTA

BOND BEHAVIOR OF UNCOATED AND EPOXY-COATED REINFORCEMENT IN CONCRETE

Catherine French,
Roberto Leon, and
Timothy Grundhoffer
Civil and Mineral Engineering

Sponsored by:
Center for Transportation Studies

Structural Engineering Report No. 92-04

Bond Behavior of Uncoated and Epoxy-Coated Reinforcement in Concrete

Prepared by

Timothy Matthew Grundhoffer
Catherine W. French
Roberto T. Leon

Final Report Prepared for

UNIVERSITY OF MINNESOTA
CENTER OF TRANSPORTATION STUDIES
and
NATIONAL SCIENCE FOUNDATION
Research Grant No. BCE-8451536

May 1992

ABSTRACT

This report summarizes an experimental program conducted to investigate the bond behavior of epoxy-coated and uncoated reinforcement in concrete. The objectives were to investigate the effect of bar surface (epoxy, uncoated), concrete strength (6, 10, 12, 14 ksi), addition of micro silica to concrete (6, 10, 12 and 14 ksi concrete with micro silica and 6 and 10 ksi concrete without micro silica), and bar size (No. 6, No. 8, No. 11). Undisturbed rebar strain distribution along the development length was determined for epoxy-coated and uncoated bars using strain gages embedded inside the rebar. This was the first time the strain distribution of epoxy-coated rebar had been measured.

Ninety-six inverted half-beam specimens were tested while monitoring load, initial cracking load, free-end slip, and loaded-end slip. Four of the 96 specimens (2 uncoated, 2 epoxy-coated) had test bars with internally embedded strain gages. All of the specimens were designed to fail in bond by splitting of the concrete. All of the bars were cast with at least 12 in. of concrete above the bar (bottom cast). The reinforcement of a particular size was from the same heat of steel with the N type deformation pattern.

A bond failure hypothesis for epoxy-coated bars is presented. The results were evaluated and compared to current design codes and previous research.

ACKNOWLEDGEMENTS

The University of Minnesota Center for Transportation Studies and the National Science Foundation Grant No. BCS-8451536 provided funding for the project. Generous material donations provided by North Star Steel, Simcote Inc., and Minnesota Rebar were greatly appreciated.

TABLE OF CONTENTS

TABLE OF CONTENTS
(continued)

TABLE OF CONTENTS
(continued)

LIST OF TABLES

LIST OF FIGURES

LIST OF FIGURES
(continued)

LIST OF FIGURES
(continued)

LIST OF FIGURES
(continued)

LIST OF FIGURES
(continued)

Chapter 1: Introduction

1.1 General

The use of epoxy-coated reinforcing steel and micro silica concrete has become common place in the design of reinforced concrete structures. Epoxy coating is used to protect the reinforcing steel from corrosive agents, thus prolonging the life of the structure. Micro silica is added to the concrete to increase its impermeability, stiffness, and strength. The increased impermeability is used to protect the rebar from the penetration of deicing salts. The increased stiffness aids in decreasing elastic shortening of columns and also decreasing deflection due to creep. The increased strength allows for smaller sections which provides the owner with more usable space. The combined increase in stiffness and strength associated with higher strength concrete is used in composite columns of tall buildings to resist lateral loads.

In general coated and uncoated bars are used with both normal concrete and micro silica concrete in a wide range of structures. Micro silica concrete is used with normal uncoated reinforcement in multi-story buildings where no corrosion resistance is necessary and concrete strengths are well above 10000 psi. Micro silica concrete combined with the use of epoxy-coated reinforcing steel has been widely

used in parking ramp structures as an "ultra" corrosion resistant system. The micro silica slows the flow of chloride ions to the reinforcing steel. Chloride ions which reach the level of reinforcement are then resisted by the epoxy coating. Currently in bridge decks, the State of Minnesota requires epoxy-coated reinforcement without micro silica concrete.

A disadvantage of epoxy-coated reinforcement is that longer lengths are required to fully develop the reinforcement. Current ACI and AASHTO codes [1,2] recognize the decreased ultimate bond strength of epoxy-coated reinforcement by requiring amplified development lengths for epoxy-coated reinforcement. The amplified development lengths are 20 to 50 percent greater than those of uncoated reinforcement.

The objective of this project was to investigate the bond and development of epoxy-coated and uncoated reinforcement in concrete with and without micro silica over a range of concrete strengths (6000-14000 psi). Prior to the start of this project no research had investigated the bond and development length of epoxy-coated reinforcement in micro silica concrete. Research conducted at University of California, Berkeley by Gjorv, Monteiro, and Mehta (1986) [3] had shown the addition of micro silica can improve the bond strength of uncoated reinforcement as compared to uncoated reinforcement embedded in normal concrete of the same

strength. It was of interest to investigate if micro silica could also improve the bond of epoxy-coated reinforcement. Relatively little research involving bond of reinforcement had been done with high strength concrete(above 10000 psi).

1.2 Background

Research began on the bond strength of steel reinforcement in concrete in the early 1900's and is still continuing. The use of epoxy coating was manifested by research starting in 1974 by Clifton et al. [4]. Thus epoxy-coated rebar is a relatively new construction material. Since 1974 the interest in research and use of epoxy-coated rebar has grown. The following two sections provide a basic background in understanding bond and highlight previous research on the bond strength of epoxy-coated rebar and/or micro silica concrete as related to this study.

1.2.1 Background on Bond of Deformed Reinforcement in Concrete

The definition of bond stress is taken from the ACI Committee 408, Report "Bond under Cyclic Loading", 1990 [5]. Bond stress is defined as the shear force per unit area of bar surface between two sections along a bar.

The equation for bond stress is given by:

$$\sigma_b = \frac{q}{\Sigma o} = \frac{\Delta F}{\Delta L \Sigma o} = \frac{\Delta f_s (\pi d_b^2/4)}{\Delta L (\pi d_b)} = \frac{d_b \Delta f_s}{4 \Delta L} \qquad (1\text{-}1)$$

where q = change of bar force per unit length of bar
Σo = nominal perimeter of the bar
d_b = nominal diameter of the bar
Δf_s = change of steel stress over length ΔL
ΔL = length of bar over which bond stress is computed
ΔF = change of force over length ΔL

The Δ's imply small increments of force and length. In this report the bond stress will be defined as the average bond stress over a development length which is considered large compared to ΔL above. The average bond stress can be defined by removing the Δ's from the above equation and thus representing the average bond stress over the entire development length.

Bond strength can be defined by different limits. The ultimate bond strength is defined as the maximum average bond stress developed. Another limit for bond strength may be identified at a stated amount of slip (displacement of the bar relative to the concrete).

The following subsections describe basic bond mechanisms, failure modes, slip, and bond specimens.

1.2.1.1 Bond Mechanisms

The bond of deformed reinforcement in concrete is a complicated mechanism which is mostly understood in a qualitative nature. It is essential that the bar force is transferred to the concrete to maintain structural integrity. The bar force is transferred to the concrete by adhesion, friction and mechanical bearing between the deformation and concrete. Figure 1.1 illustrates schematically the three mechanisms of bond. Upon initial loading the forces are transferred by adhesion created through chemical bonding between the steel and concrete. The adhesion is not a sustained resistance; at low bar stresses the adhesion is lost. After adhesion is lost the bar slips relative to the concrete which enables development of the friction and mechanical bearing mechanisms. Due to the rib face angle (Figure 1.1) the forces are transferred to the concrete by bearing perpendicular to the rib face and friction between the rib face and the adjacent concrete. The resultant force of the bearing and friction forces produces radial tension in the concrete surrounding the bar.

1.2.1.2 Bond Failure Modes

Two types of bond failures exist: pullout failure and splitting failure. If adequate confinement exists in the

form of transverse steel, large cover, or a combination thereof, a pullout failure occurs. A pullout failure is a direct shear failure of the concrete key at the level of the outer edge of the deformation (Figure 1.2). The confinement allows the tensile stresses in the concrete to be resisted. This allows the bearing pressures between the rib face and the concrete to increase with increasing bar load and the frictional component becomes less significant. The high bearing pressures result in failure of the concrete keys in shear.

If sufficient concrete cover and/or transverse confinement are not provided to resist the radial tension stress in the concrete, a splitting failure occurs (Figure 1.3). Once the concrete cracks, the deformations push the concrete away from the bar by wedge action. As the concrete starts to ride up the rib face the component of friction between the rib face and the concrete becomes more significant.

Because the ratio of typical development length to concrete cover is large, splitting bond failures are more likely to occur in slabs and other structural members without transverse reinforcement or large concrete cover. The study, conducted at the University of Minnesota, focussed on splitting bond failures.

1.2.1.3 Bar Slip

Slip is the movement of the bar relative to the concrete in the direction of the load. Slip occurs by crushing of the concrete in front of the deformation or by wedge action. Wedge action forces the concrete to move transversely away from the bar as the bar slips relative to the concrete in the direction of load.

As the bar is loaded, elongation occurs within the bonded region and is thus a component of slip. Depending on the type of specimen and instrumentation, separation of the elongation and slip is not always possible. However, a strict definition of slip does not include the elongation of the bar in the bonded region.

1.2.1.4 Related Rib Area

In Europe related rib area is used to gage the performance of deformed bar patterns. The related rib area, α_{sb} is a term that defines quantitatively the geometry of the deformation pattern. It is proportional to the ratio of rib height to rib spacing.

The related rib area is defined by the following equation:

$$\alpha_{sb}=\frac{kF_R\sin\beta}{\pi\phi c_s} \qquad (1\text{-}2)$$

where F_R = area of transverse rib above bar core
c_s = distance between transverse ribs
k = number of transverse ribs around the perimeter
β = angle between rib and longitudinal axis of the bar
ϕ = nominal bar diameter

It has been found that bars with different deformation patterns and the same related rib area have nearly the same bond behavior (Rehm, 1961 [19], Soretz and Hölzenbein, 1980 [20]). Soretz and Hölzenbein also found that with simultaneous reduction in rib height and rib spacing while keeping the related rib area constant produced similar slip behavior. Also, the smaller rib heights and rib distances reduce the splitting ability of the bar.

Martin and Noakowski (1981) [21] showed the bond strength and pure slip stiffness increased when the related rib area, α_{sb}, was increased. However as α_{sb} increases the bond failure became more brittle and it was suggested that the range for α_{sb} should be between 0.05 and 0.08.

The related rib area is a very informative parameter and should be discussed when studying deformed reinforcement in concrete.

1.2.1.5 Type of Bond Test Specimens

There are generally three types of bond specimens: pullout, inverted half-beam, and splice type specimens.

Pullout type specimens consist of a test bar cast uniaxially in a small block or cylinder of concrete. The test bar is usually loaded by reacting off the concrete surrounding the bar. When loaded in this manner, the stress in the concrete around the bar is therefore in compression (Figure 1.4). These specimens are considered unrealistic because the primary use of reinforcement is to carry tensile stress with the concrete around the bar in tension (flexural tension zone). However, the tests are very economical and allow preliminary relative comparisons.

Inverted half-beam specimens are used as a more realistic bond test. A typical specimen is shown in Figure 1.5. The specimen allows the test bar to be in an area of flexural tension under a moment gradient and constant shear.

The slip can be measured at the free end and the loaded end (Figure 1.5). The slip at the free end represents pure slip relative to the concrete and does not include elongation of the bar. The loaded-end slip includes the pure slip and elongation of the bonded bar. Loaded-end slip is measured by placing a displacement transducer on the external portion of the bar to monitor relative movement between a point on the bar and the concrete face. This loaded end displacement

measurement includes slip, elongation of the bar in the bonded region, and elongation of the bar outside the concrete. Loaded-end slip is defined as the loaded end displacement minus the elongation of the bar outside the bonded region. If the free-end slip is subtracted from the loaded-end slip the elongation of the bar within the bonded region is obtained. If flexural cracking has occurred within the bonded region, the elongation within the cracks is not detected by the instrumentation. The instrumentation cannot detect the elongation because the loaded end displacement is referenced off the concrete face.

As shown in Figure 1.5, a length of the bar is unbonded near the loaded end. This length is known as the lead length. Lead lengths used by past researchers were intended to prevent a conical pullout failure. Lead lengths in older specimens were as long as 10 inches. As more experience with these specimens was gained, it was realized when using longer bonded lengths a conical failure would not govern. Current lead lengths range from 0 to 3 inches. Section 2.3.1 in Chapter 2 explains the lead length selected for the current study with inverted half-beam specimens.

Splice type bond specimens are considered the most realistic and costly. They consist of full scale beams with two point loads (Figure 1.6). Two bars are spliced in an area of constant moment and zero shear. As the specimen is loaded the specimens fail in bond in the splice region. The

stress in the bar at failure can be determined by beam theory or by installing strain gages just outside of the splice region. Without the use of strain gages an uncertainty in the actual bar stress exists. Slip is not easily measured when using splice type specimens, and therefore it is not measured. The specimens also provide comparisons of deflection and overall structural performance.

1.2.2 Previous Research

1.2.2.1 Previous Research on Bond and Epoxy-Coated Bars

Clifton et al. [4] (February 1974) conducted a study that addressed the feasibility of using nonmetallic organic coatings for corrosion protection of reinforcement in concrete.

It was determined that fusion bonded epoxy coating performed the best against corrosion, abrasion, and impact. The effect of epoxy coating on bond strength was evaluated by testing 32 pullout type specimens. Twenty three specimens were fabricated with epoxy-coated No. 6 rebar, and 5 had uncoated rebar. Coating thicknesses varied from 1 to 11 mils with two rebar having coating thicknesses of 25 mils.

The test specimens consisted of the bar cast uniaxially in a 10 X 10 12 in. prism with a 2 in. diameter wire cage for confinement. As the bar was loaded, the concrete surrounding the rebar was put into compression (Figure 1.4). In reality,

the concrete around the bar should be in tension when the rebar is in tension.

The bond performance of the epoxy-coated rebar was compared to the uncoated rebar using a slip criteria. The critical bond stress was determined using the lesser of the steel stresses occurring at a free-end slip of 0.002 in. or a loaded-end slip of 0.01 in. The test results showed the epoxy-coated rebar with coating thicknesses between 1 to 11 mils had a critical bond stress 6 percent lower than the uncoated rebar specimens. The two bars having a coating thickness of 25 mils failed by pullout while all other bars yielded. It was recommended that the coating thickness should not exceed 10 mils.

Johnston and Zia [7] (August 1982) conducted a study to compare the bond characteristics of epoxy-coated rebar specimens to uncoated rebar specimens under static and fatigue loadings.

Slab specimens with uncoated or coated reinforcement were tested to compare cracking, deflection, and flexural strength among specimens. Inverted half-beam specimens (Figure 1.5) were tested under static and fatigue loadings to investigate the ultimate bond strength and rebar slip relative to the concrete.

A total of 6 slabs were tested, 3 with epoxy-coated rebar and 3 with uncoated rebar. The ultimate deflection of

the epoxy-coated rebar slabs was on the order of 20 percent greater than that of the uncoated rebar slabs. A 4 percent reduction in ultimate strength was exhibited by the epoxy-coated rebar slab specimens as compared to the uncoated rebar slab specimens.

There were 26 inverted half-beam specimens for the static tests and 14 inverted half-beam specimens for the fatigue tests. The test variables in the inverted half-beam tests included the rebar surface condition, bar size, and development length. The rebar surface conditions were normal black, epoxy-coated and blast clean. The specimens included No. 6 rebar with 8, 13, and 18 inch development lengths and No. 11 rebar with 16, 24, and 30 inch development lengths. All uncoated rebar specimens had identical epoxy-coated companion specimens. Additionally, four specimens with a blast clean surface condition were cast. Two blast clean No. 6 rebar specimens with a 13 inch development length and two blast clean No. 11 rebar specimens with a 24 inch development length were tested.

The performance of the epoxy-coated rebar was compared to that of the uncoated rebar using a slip criteria and ultimate bond strengths. The slip criteria comparisons were based on the lesser bar stress that occurred at a free-end slip of 0.002 inch or a loaded-end slip of 0.01 inch. From this bar stress an average bond stress was obtained. The ultimate strength comparisons could only be done on specimens

that experienced bond failure. In this study only the No. 6 rebar with 8 inch development length and the No. 11 rebar with 16 inch development length failed in bond. The other specimens were loaded to 1.25 times their nominal yield stress without a bond failure.

In both comparisons the average bond stress of the coated rebar was divided by the average bond stress of the uncoated rebar to obtain a performance ratio. The slip criteria ratios for all but the No. 6 rebar with 8 in. development length varied from 1.06 to 1.29 with an overall average ratio of 1.15. The No. 6 bars with 8 in. development length had a ratio of 2.16. The ultimate strength ratios were 1.17 for both the No. 6 and No. 11 rebar. However, as stated in the previous paragraph, the ultimate strength data is limited because only a few bars failed in bond. The ultimate bond strengths from the fatigue tests were similar to the results from the static tests. Using a weighted average of the slip and bond strength comparison, a ratio of 1.15 was obtained. It was recommended for design that the basic development lengths for epoxy-coated rebar be multiplied by 1.15.

Treece and Jirsa (January 1987) [8] tested 21 splice-type beam specimens (Figure 1.6) to compare the ultimate bond strength of epoxy-coated rebar with that of uncoated rebar. The test variables included bar size, coating thickness,

concrete strength, and casting position. The specimens included No. 6 or No. 11 spliced rebar with coating thicknesses varying from 5 to 12 mils. The concrete strengths were 4, 8, and 12 ksi. Seventeen specimens were cast with the spliced bars in the top position. The remainder of the specimens were cast with the spliced bars in the bottom position. The concrete cover was 2 in. for the No. 11 rebar and varied from 5/8 to 2 in. for the No. 6 rebar. The specimens were designed to fail in bond before yielding the rebar.

The bond strength was determined by averaging the stress developed in the rebar over the splice length at failure, thus giving an ultimate bond strength comparison. All of the specimens exhibited a splitting failure.

The performance of the epoxy-coated rebar specimens was compared to that of the uncoated rebar specimens using a bond efficiency ratio. The efficiency ratio was defined as the measured bond strength divided by the theoretical bond strength.

The theoretical bond strength was determined using the following equation developed by Orangun, Jirsa, and Breen (1975) [9].

The equation was a result of studying the test data from previous research with splice type bond specimens.

$$U_{OJB}=\sqrt{f'c}\left[1.2+3\left(\frac{c}{d_b}\right)+50\left(\frac{d_b}{l_s}\right)\right] \qquad (1\text{-}3)$$

where
U_{OJB} = ultimate bond stress, psi
$f'c$ = concrete compressive strength, psi
c = lesser of the side cover and bottom cover, in.
d_b = nominal rebar diameter, in.
l_s = splice or development length, in.

The above equation will be referred to as the OJB equation for the remainder of this paper. The final comparison between the epoxy-coated rebar specimens and the uncoated rebar specimens was obtained by dividing the bond efficiency ratio for the epoxy-coated rebar by the bond efficiency ratio of the uncoated rebar. It was shown that the bond strength of the epoxy-coated rebar was 67 percent of the uncoated rebar bond strength. The report stated the reduction was independent of the bar size, coating thickness (5 to 12 mils), and concrete strength. It was recommended that epoxy-coated rebar with a cover less than 3db or a clear spacing less than 6db have its required basic development length multiplied by a factor of 1.5. The development length for all other epoxy-coated rebar should be multiplied by 1.15 as found by Johnston and Zia.

Choi et al. [10] (July 1990) conducted a study at the University of Kansas Center for Research. The study considered the effects of bar size, coating thickness, deformation pattern, concrete cover, and casting position. Inverted half-beam specimens and splice type specimens were used.

Bar sizes of No. 5, No. 6, No. 8, and No. 11 were used with coating thicknesses varying from 3 to 17 mils. Three deformation patterns were used and designated by the S, C, and N shapes. None of these deformation patterns were the same as the diamond shape deformation patterns used by Johnston et al. and Treece et al., two of the studies described above. Clifton et al. (1974) also used a barrel shape similar but not identical to the S shape. Top and bottom casting positions along with bar covers of 1, 2 and 3 bar diameters were also studied.

A total of 394 inverted half-beam tests and 4 splice type tests were conducted. In an effort to reduce variability, adjustments were made to the bond strengths to account for the actual concrete cover. The results of the No. 5 epoxy-coated rebar were adjusted to account for the different coating thicknesses. The correction for cover and coating thickness was based on parallel best fit lines obtained using regression and the method of "Dummy Variables". The bond strengths for No. 6 and larger bars were found to be independent of the coating thickness and

were not corrected. All of the bond strength results were normalized to a concrete strength of 6000 psi by multiplying them by $(6000/f'c)^{1/2}$.

All specimens exhibited a splitting failure; consequently all comparisons were based on the ultimate bond strength. The inverted half-beam specimens showed the epoxy-coated rebar had a 15 percent reduction in bond strength relative to the uncoated rebar specimens after averaging results from all of the tests. The splice type specimens showed that the epoxy-coated rebar had a bond strength reduction ranging from 6 to 29 percent with a mean reduction of 13 percent.

It was concluded that for No. 6 and larger bars, coating thicknesses in the range of 5 to 12 mils did not affect the bond strength. However, results from No. 5 bars indicated that bond strength decreased as coating thickness increased. The reduction in bond strength varied with the different deformation patterns. It was stated that "deformation patterns with larger rib bearing areas were affected less by the epoxy coating."

Increased concrete cover did not produce a significant difference in bond reduction caused by the epoxy coating. However, the trend was that the reduction decreased as the concrete cover increased.

Devries et al. [11] (January 1991) investigated the effect of concrete strength, casting position and anti-bleed agents on the bond strength of uncoated and epoxy-coated rebar. Concrete strengths ranged from 8000 to 15000 psi. All of the mixes contained micro silica ranging in content from 7 to 12 percent. Micro silica was not an intended variable in the study; presumably it was varied to obtain higher concrete strength. The test bars were cast in both the top (at least 12 inches of concrete below the test bar) and bottom position. The presence of an anti-bleed agent (Kelco Gum) was also studied.

Thirty-six splice type specimens similar to those of Treece and Jirsa(1989) were tested. Two bar sizes, No. 6 and No. 9 bars, were tested with no replications of the specimens. The cover was 1.125 inches for all specimens.

The ratio of uncoated to coated rebar bond strengths ranged from 1.30 to 1.38 for the No. 6 bottom cast test bars and 1.10 to 1.40 for the No. 9 bottom cast test bars. It was stated that the ACI modification factor of 1.5 was conservative for all concrete strengths tested and that no limit should be put on the square root of f'c. They stated measured bond strengths, normalized with the OJB equation, showed a decreasing trend in normalized bond strength as f'c increased. No recommendation was made to adjust the modification according to varying f'c.

The top cast bars were found to give conservative

results relative to the ACI equation using a modification factor of 1.3. Top cast bars with the presence of an anti-bleeding agent showed a 5 percent increase in bond strength compared to those of other top cast bars without an anti-bleeding agent.

Hadje-Ghaffari et al. [12] (July 1991) conducted a study which was a continuation of the study done by Choi et al. summarized above. In the continuation study, the added effect of concrete slump, consolidation, transverse reinforcement, and concrete strength were investigated. Slumps varied from 2 to 8 inches and concrete consolidation was varied by either vibrating the concrete or not vibrating the concrete. The concrete compressive strengths were nominally 5000, 6000 and 13000 psi. Only 12 of the 645 specimens evaluated had concrete strengths of 13000 psi.

Higher slumps and vibration improved the bond strength of both epoxy-coated and uncoated bars. The epoxy-coated bars with transverse reinforcement showed bond strengths near those of the uncoated bars without transverse reinforcement. The reduction of bond strength due to epoxy coating decreased about 6 percent with transverse reinforcement present. A somewhat surprising result was that more than doubling the concrete strength had little or no effect on the bond strength. Specimens with 13000 psi concrete compressive strength "showed little or no increase in bond strength"

compared to those with a concrete compressive strength of 6000 psi.

It was suggested that the modification factor for epoxy-coated bars smaller than No. 7 should be 1.25. For larger bars, a modification factor of 1.35 was suggested. A caution was given to applying these modification factors to bar sizes that have not been tested. It was suggested the deformation patterns with the best bond performance be standardized for epoxy-coated bars.

The study concurred with the ACI top-bar modification factor of 1.3 for uncoated rebar. Epoxy-coated top bars should have a combined modification factor of 1.5.

1.2.2.2 Previous Research on Bond and Micro Silica

Relatively little research has been done on the effect of micro silica on the bond behavior of reinforcement in concrete in the United States. The Europeans have done more extensive research on the effects of micro silica. This section summarizes the work published by the Norwegian Institute of Technology, University of Trondheim. The testing was performed at the University of California, Berkeley while O. E. Gjorv was a Visiting Professor.

Gjorv et al. [3] investigated the effect of micro silica on the bond strength of reinforcement in concrete. Variables included micro silica content and concrete strength. The

micro silica content was varied at 0, 8, and 16 percent by weight of cement. Concrete strengths investigated included 3,6,9, and 12 ksi.

The bond strength was determined using pullout type specimens according to ASTM C234. These specimens were similar to the ones used by Clifton et al. above (Figure 1.4). Again it is stated that this type of specimen is unrealistic because concrete surrounding the test bar is in compression. However it does provide a means of relative comparison.

No. 6 deformed and plain test bars with nominal yield strengths of 60 ksi were used. The report did not state the reinforcement deformation pattern nor manufacturer. Four specimens were cast with each concrete mix. Two deformed and two plain bars; one of each was poured in the upper and lower position as defined by ASTM C234.

The bond strength was determined using a slip criteria as specified by ASTM C234. The governing slip criteria for all of the tests was the load occurring at a loaded-end slip of 0.01 inches. This is not the ultimate bond strength. The ultimate bond strength was governed by splitting of the concrete around the bar. The load at the ultimate failure was also reported.

The report stated the addition of micro silica had an "improving effect on the pull-out strength, especially in the high compressive strength range of concrete." This

contradicts the results of Hadje-Ghaffari et al. [12] which saw little or no increase in bond strength when increasing the concrete strength from 6000 to 13000 psi. The 13000 psi mix used in the Hadje-Ghaffari study contained 9 percent micro silica.

The results of the pullout tests were fitted with the following equation:

$$f_{Pull\text{-}out} = K_1 f'c^{K_2} \qquad (1\text{-}4)$$

where $f_{Pull\text{-}out}$ = pull-out strength based on slip criteria, psi
K_1, K_2 = constants
$f'c$ = concrete strength, psi

The values of K_1 and K_2 were not reported. From the fitted data it was concluded that both concrete strength and micro silica had an effect on the pull-out strength.

The concrete around the bar being in compression evokes the question of how realistic are the test specimens. However their results did indicate that micro silica and concrete strength does improve the bond behavior of steel reinforcement in concrete contradicting the results of Hadje-Ghaffari et al. Note: The results found in the current University of Minnesota study also contradict the results of Hadje-Ghaffari et al.

1.3 Objective and Scope

The objective of the current study conducted at the University of Minnesota was to investigate the effect of concrete strength on the bond strength of epoxy-coated and uncoated rebar. Concretes of the same strength were cast with and without micro silica to investigate the effect micro silica on bond behavior. Additionally, the effect of epoxy coating on the rebar strain distribution along the development length was investigated.

The hypothesis by Treece and Jirsa [8] was that reduced adhesion and friction were the primary cause of the decrease in bond strength due to epoxy coating. In this study, load-slip behavior and the rebar strain distribution along the development length were measured experimentally to investigate the differences in load distribution and transfer between the uncoated and epoxy-coated rebar. This information will be used to test and expand on the Treece and Jirsa hypothesis.

A total of 96 inverted half-beam specimens were tested. The concrete strengths ranged from 6000 to 14000 psi with and without micro silica. No. 6 and No. 11 bars were used to determine the effects of concrete strength and micro silica. No. 8 bars were used for the rebar strain distribution tests.

This study adds to the current knowledge to provide a better understanding of why epoxy coating reduces bond

strength. It also provides bond strength data on both epoxy-coated and uncoated rebar specimens in higher strength concrete.

Chapter 2 summarizes the experimental program. Chapter 3 presents the test results and a discussion of how the specimens failed during loading. Chapter 4 describes the evaluation of the results and comparisons with previous research and current design codes. The major conclusions are listed in Chapter 5. Typical results from individual strain gages are given in the Appendix.

Chapter 2: Experimental Program

This chapter describes the experimental program used to determine the bond behavior of epoxy-coated and uncoated reinforcement in both normal and micro silica concrete.

Bond behavior was evaluated on the basis of measured ultimate bond strength and bar slip relative to the concrete. Slip was measured at both the loaded end (loaded-end slip) and the unloaded end of the bar (free-end slip). Inverted half-beam specimens were used for all of the tests. Four specimens were instrumented with internal strain gages to measure the strain distribution along the development length.

The objective was to produce identical uncoated and epoxy-coated rebar specimens with three replications. A total of 96 specimens were tested which were separated into eight different groups. Table 2.1 summarizes all of the groups and their variables.

Each specimen was identified with a specimen label. The specimen labels were as follows:

Specimen Label: $##S%%C&&

$ = G for specimens with strain gages
(blank) for specimens without strain gages
= 06 for No. 6 bars
08 for No. 8 bars
11 for No. 11 bars
S = B for uncoated bars
E for epoxy-coated bars
%% = development length, nearest inch
C = A,B,C (replications, normal concrete)
D,E,F (replications, micro silica concrete)
&& = approximate concrete compressive strength, ksi

2.1 Test Variables

The primary variables included rebar surface condition (epoxy-coated, uncoated), bar size (No. 6, 8, 11), nominal concrete strength (6 to 14 ksi), and concrete type (with and without micro silica). The strain distribution along the development length was also studied.

2.1.1 Bar Surface

The bar surfaces included normal mill scale and fusion bonded epoxy coating. The normal mill scale bars are referred to as uncoated bars throughout the report.

2.1.2 Bar Size

Three bar sizes were tested which included No. 6, No.8, and No. 11 rebar. The No. 6 and No. 11 bars were tested to investigate the effect of the primary test variables. The No. 8 bars were instrumented with internal strain gages to determine the rebar strain distribution along the development length. Strain distribution tests were conducted with 2 uncoated and 2 epoxy-coated No. 8 rebar with normal concrete at 6000 psi.

2.1.3 Concrete Strength and Type

For the No. 6 and No. 11 rebar specimens (Groups 1 to 7) concrete strengths varied from 6000 to 14000 psi. Normal concrete without micro silica was tested at nominal strengths of 6000 and 10000 psi. Concrete with micro silica was tested at nominal strengths of 6000, 10000, 12000 and 14000 psi.

Group specimens were cast with the same concrete for the uncoated and companion epoxy-coated specimens. The effect of micro silica was intended to be compared with tests on normal concrete of the same strength. An inherent variability in material properties exists for concrete. The actual strengths will be discussed in Section 2.2.2.

2.2 Materials

2.2.1 Test Bars

All of the test bars were Grade 60, ASTM A 615 deformed reinforcement as manufactured by North Star Steel Company. The deformation pattern consisted of diagonal ribs joined by two longitudinal ribs along opposite sides (Figure 2.1). The diagonal ribs were inclined at 70 degrees to the longitudinal axis of the bar. The deformation pattern has the N designation.

The epoxy-coated test bars were produced by Simcote Inc.

The 3M Scotchkote epoxy coating was fusion bonded in accordance with ASTM A 775. The coating thickness was not an intended variable in the study. The coating thicknesses were measured with an Elcometer 211, a thumb wheel magnetic pull-off gage. Coating thicknesses were measured over approximately 1 foot of test bar near the development length. Coating thickness measurements were taken in between the deformations, along the longitudinal rib, and on top of the deformations. The larger bars exhibited more variability in coating thickness per bar which was linked to the location of the measurement. For most bars the coating thickness was 1 to 5 mils thicker on one side than the other. Figure 2.2 shows typical coating thickness distributions for the No. 6 and No. 11 bars. The distributions tended to be lump into two ranges representing each side of the bar (Figure 2.2).

The coating thickness of each bar was determined by averaging the coating thickness measurements of each bar. The variability among different bars was not significant. The average coating thicknesses for the No. 6 bars ranged from 5 to 8 mils with one bar having a 10 mil average coating thickness. The No. 11 bars had average coating thicknesses ranging from 10 to 15 mils with one bar having a 7 mil average coating thickness. Average coating thickness for each bar tested is presented in Chapter 4.

Two bars per bar size were measured to determine the related rib area as defined in Chapter 1. The bars were

measured using a 0.001 inch dial gage caliper. The average related rib area was 0.084, 0.080, and 0.087 square inches for the No. 6, No. 8, and No. 11 bars respectively. The average rib heights were 0.086, 0.091, and 0.137 inches for the No. 6, No. 8, and No. 11 bars. The rib heights and bar diameters showed little variability. The rib spacing was determined by measuring the distance between 10 to 12 ribs and dividing by the number of rib spacings.

All bars of the same size were taken from the same heat of steel. For each bar size, two uncoated tension specimens were tested for yield stress, ultimate strength, and percent elongation in 8 inches. Table 2.2 lists the average of the mechanical properties for the two specimens tested. The results were consistent.

2.2.2 Concrete

All of the concrete used was commercially available at the time of testing. The concrete was delivered in a concrete ready-mix truck. The intent was to use concrete mixes that were currently specified for the field.

The 6000 psi normal and micro silica mixes (Groups 1,3) were ordered with 6 percent air entrainment. All other mixes were ordered without air entrainment. Nominal strengths of 6000 and 10000 psi (Groups 1,2) were used for the mixes without micro silica. Nominal strengths for the micro

silica mixes were 6000, 10000, 12000, and 14000 psi (Groups 3-7). The 6000 normal mix (Groups 1,8) is currently specified for structural bridge decks in the State of Minnesota. The 6000 psi micro silica mix is used for standard parking ramp decks. The 10000 to 14000 psi micro silica mixes are used in columns and core walls of multistory buildings.

Concrete cylinders were tested at various ages before testing the bond specimens. Table 2.3 lists actual concrete strength and age at testing for each mix. The age at testing represents the age when the bond specimens were tested. As shown in Table 2.3 concrete strengths for Groups 3 and 5 were significantly different than their specified strength. The actual concrete strength of the Group 3 No. 11 bar specimens cast in nominal 6000 psi micro silica concrete was found to be 8400 psi at 11 days, well above the 28 day design strength. Testing of the Group 3 No. 6 bar specimens cast in the same concrete was interrupted due to instrumentation malfunction. One of the Group 3 No. 6 bar specimens was tested at a concrete strength of 8400 psi (11 days) while the other two were tested with a concrete strength of 9290 psi (142 days). Group 5 concrete (12000 micro silica) attained only 9160 psi in 35 days. This was attributed to lack of moist curing (see Section 2.5.3). The other 12000 and 14000 psi concrete was moist-cured until tested as discussed in Section 2.5.3. Mix proportions are listed in Table 2.4.

2.3 General Test Specimens

The test specimens may be described as inverted half-beam specimens shown schematically in Figure 2.3. The specimens were intended to provide a bond test within a flexural strain field. Before describing the actual test specimens the next section briefly describes the development and lead length selections. A brief background on inverted half-beam specimens was presented in Chapter 1.

2.3.1 Selection of Development Length and Lead Length

Initially, a series of pilot specimens were cast to estimate development lengths to be used for the actual test bars. The pilot study was inconclusive; all of the pilot test bars yielded and showed no signs of cracking due to an excessive lead length (8 in.).

Development lengths used in previous research could have been used. However, the failure loads seen in the previous research could not be guaranteed without duplicating the specimens and variables used. The "blind" pilot study approach was abandoned.

Because research on bond strength is used to gage the required development lengths for design codes, and because the relationship between bond stress and development length is not linear, it is desirable to test specimens that develop

bar stresses close to the desired design code bar stresses. The approach used in this study was to select development lengths that would produce bond failures at stresses near the nominal yield stress without exceeding it. To estimate these development lengths, use was made of the relationship derived by Orangun, Jirsa, and Breen [9] (OJB equation).

The work described by Treece and Jirsa [8] in Chapter 1 correlated very well with the OJB equation [9] also introduced in Chapter 1. The OJB equation was developed primarily with results from splice type bond tests and then checked with the results of development length tests. An evaluation of the OJB equation on inverted half-beam specimens, similar to the ones used in the current study, was required. The inverted half-beam bond strength results of Choi et al. [10] were used in the evaluation.

Table 2.5 shows the average bond stress normalized by the OJB equation for all bar sizes and lead lengths used from the results of Choi et al. [10]. At first glance the results show considerable variation. However in the OJB report [9] it was stated that the OJB equation varies with the bar spacing or side cover.

The effect of bar spacing or side cover was related to the following parameters:

$$C_s/C_bd_b < 3 \qquad U_{test}/U_{OJB} = 1.06$$

$$3 < C_s/C_bd_b < 6 \qquad U_{test}/U_{OJB} = 1.21$$

$$C_s/C_bd_b > 6 \qquad U_{test}/U_{OJB} = 1.64$$

where:

U_{test} = bond stress from test results, psi
U_{OJB} = bond stress from OJB equation, psi
C_s = side concrete cover or half of the clear spacing of bar, in.
C_b = bottom concrete cover, in.
d_b = nominal bar diameter, in.

The OJB report states large values of C_s/C_bd_b as the effect of wide spacing or large side cover.

Table 2.5 gives the values for C_s/C_bd_b for the results from Choi et al. [10]. When considering the effect of wide spacing (C_s/C_bd_b), the variation in the U_{test}/U_{OJB} ratio is explained. During the evaluation, it was noticed that test specimens having lead lengths ranging from 0 to 1 inch gave results closest to those predicted by the OJB equation when considering the value of C_s/C_bd_b. From this observation the lead length for the inverted half-beam specimens used in the University of Minnesota study was selected as 0.5 inch for all test specimens.

This evaluation suggested that the OJB equation was also applicable to inverted half-beam specimens, similar to the

ones used in the University of Minnesota study.

Consequently, the selection of development lengths were guided using the OJB equation, some simple assumptions, and the preliminary test results.

The assumptions used are as follows:

1. Assuming all variables constant except concrete strength and development length the shape of the curve predicted by OJB equation was assumed correct.
2. The variation of the experimental bond stress was directly proportional to the bond stress predicted by the OJB equation (U_{test}/U_{OJB} = constant).

The values of C_s/C_bd_b for the specimens used in this study were 5.0, 2.2, and 1.5 for the No. 6, No. 8, and No. 11 test bar specimens, respectively. Based on data in the OJB report (Figure 14, [9]), values of 1.25, 1.06, 0.94 were taken as the anticipated U_{test}/U_{OJB} ratio.

Letting $U_{test}/U_{OJB} = \alpha$ and assuming uniform bond stress for U_{test} the OJB equation can be rearranged for L_d. The following equation was obtained:

$$L_d = \frac{\frac{f_s d_b}{4\alpha\sqrt{f'c}} - 50 d_b}{1.2 + 3\left(\frac{c}{d_b}\right)} \qquad (2\text{-}1)$$

For the first group a value of 0.75fy was assumed for fs to ensure the test bar did not yield. For Group 1 ($f_s = 0.75f_y$), Equation 2-1, using α values stated above, gave 6 and 11.5 inch development length for the No. 6 and No. 11 tests bar specimens, respectively. After testing Group 1 and 3 test bar specimens the actual values of α were obtained. Group 1 uncoated bar specimens had average α values of 1.10 and 0.82 for the No. 6 and No. 11 bars respectively. Group 3 uncoated bar specimens had average α values of 1.18 and 0.80 for the No. 6 and No. 11 bars respectively. As more test results became available, α could be refined from the actual values of U_{test}/U_{OJB}.

The bar stress, f_s, was taken as 85 to 95 percent of the nominal yield stress when using Equation 2-1 to select development lengths for the remainder of the test groups.

For the next groups (Groups 2,4) α was assumed to be the larger values, 1.18 and 0.82 for the No. 6 and No. 11 test bar specimens respectively. As more results became

available, α was monitored and adjusted as required.

For the No. 8 bars, two pilot specimens were poured and tested to quantify the actual α (U_{test}/U_{OJB}). The pilot specimens had the development length obtained from Equation 2-1 using α (1.06) obtained from the OJB report. The actual α for the No. 8 pilot specimens was near 1.06.

2.3.2 Test Specimens

The gross cross section of all the specimens was 12 inches wide and 18 inches deep. The specimen length was varied with the bar size to reduce shear stresses and produce a more realistic flexural strain field. The No. 6, No. 8 and No. 11 rebar specimens were 36, 42 and 47 inches respectively. Drawings of the cross section for each rebar size are shown in Figures 2.4 to 2.6 with a typical elevation view shown in Figure 2.7.

Auxiliary reinforcement was added to prevent the specimens from failing in flexure and shear. The addition of this reinforcement was not intended to affect the bond behavior. The auxiliary flexural reinforcement was placed in the same location for all specimens to prevent flexural failure in the unbonded region of the test bar. Two bars were placed with each of them centered 2.25 inches from each side and 2.25 inches from the top of the cross section (Figures 2.4-2.6). No. 4, No. 5 and No. 6 uncoated rebar

were used as auxiliary flexural reinforcement for all of the No. 6, No. 8, and No. 11 test bar specimens, respectively. The No. 11 test bar specimens contained No. 3 stirrups at 7.5 in. spacing for concrete strengths from 10000 to 14000 psi to prevent shear failure. The No. 8 test bar specimens also required No. 3 stirrups at 7.5 in. spacing. The stirrup configurations are shown in Figures 2.5 and 2.6 for the No. 8 and No. 11 test bar specimens, respectively. The stirrup spacing was 7.5 inches starting 2 inches from the loaded end of the specimen. The stirrups were designed as open-ended so that they would not confine the concrete around the test bar. The stirrups were only intended to carry the shear stresses. Epoxy-coated stirrups were used with the epoxy-coated test bars and normal stirrups were used with the uncoated test bars.

The cover was taken as the distance from the edge of the concrete to the center of the bar minus one half of the nominal bar diameter, not the measured distance from the edge of the bar deformation to the concrete surface. The concrete cover was originally planned as 2 bar diameters ($2d_b$) for all of the bars. The No. 8 and No. 11 bar covers were changed to control the development length while obtaining the desired bar stress at failure. The cover for the No. 8 bars was increased to limit the development length which allowed an even spacing for the strain gages (see Section 2.4.3). The cover for the No. 11 bars was decreased to make the

development length as long as possible. Nominal concrete cover for the No. 6 test bar specimens was 1.5 inches ($2d_b$). The No. 8 and No. 11 test bar specimens had a nominal cover of 2.5 inches (2.5 and 1.8 d_b, respectively). The actual cover was measured before each specimen was tested.

Development lengths were determined as described in Section 2.3.1. Table 2.1 lists all of the development lengths used in each test group. The development length was controlled by shielding portions of the rebar with PVC pipes (Figure 2.7).

The PVC pipe was centered around the bar using rigid rubber spacers between the bar and the inside of the PVC pipe. The PVC pipe was carefully sealed with general purpose silicon sealant using 6cc syringes. This prevented concrete from seeping in between the test bar and the PVC pipe.

The lead length, the distance from the loaded end concrete face to the beginning of the development length was selected on the basis of the OJB equation [9] and test results from Choi et al. [10] as described in Section 2.3.1. The results of the equation correlated well with a lead length of 0.5 inches when considering the width effect of the specimens. Hence, a lead length of 0.5 inches was selected for all of the test specimens.

The test bar extended the length of the specimen with a minimum of 22 inches extending out the loaded end. All of the test bars were 6 feet long. The bar extended out the

back of the specimen 2 to 3 inches to allow for direct measurement of the free-end slip. Two 3/4 inch PVC lifting ports were located as shown in Figure 2.7. A bar was placed in both lifting ports to aid in lifting the specimens into the test frame.

2.4 Strain Gage Specimens

Four No. 8 test bar specimens were instrumented with internal strain gages. The gages were spaced along the development length to measure the strain distribution in the bar.

The bar was machined in half, gages were installed and the bar was then glued and welded back together so that the concrete rebar interface was not disturbed. This method was first used by Mains [18] in 1948 and provides the determination of undisturbed strain distributions for reinforcement embedded in concrete. The author is not aware of any research of this nature conducted with epoxy-coated rebar.

2.4.1 Fabrication of Rebar

One 6 ft. No. 8 test bar was fabricated from two individual 6 ft. pieces of No. 8 rebar. Each No. 8 bar was machined in half along its length as shown schematically in

Figure 2.8(a). The machining of two whole bars to make one bar allowed for no reduction in the cross section which would be incurred if a single bar was split. Once the bars were halved, a 0.1 in. deep by 0.190 in. wide groove was machined along the center of each half bar as shown in Figure 2.8(b). Figure 2.9 shows the bars being milled in half.

2.4.2 Strain Gages

Strain gages labeled FLA-3-3L-11 manufactured by Tokyo Sokki Kenkyujo Company were used. The gages were ordered with two lead wires attached to eliminate any soldering in the small groove. The wires were seven 0.12 mm(dia), strands. The small size allowed for wires from five gages to fit in the machined groove. The gage length was 3 mm. The gage resistance was 119.8$\pm$0.5 ohms with a gage factor of 2.13.

2.4.3 Strain Gage Positions

The cross section of the rebar was not uniform due to the deformations. This produces a non-uniform strain field along the bar when the bar is under uniform tension. However, for uniform tension, in theory the strain at one point along the bar should be same as another point as long as the two points are in the same position relative to a

deformation. Along the development length, the gages were installed in the same position relative to a deformation. The gages were centered between the top of the deformations as shown in Figure 2.10.

The development length was selected as an even multiple of the deformation spacing. The development length selected was 14 11/32 inches or 27 deformation spacings which allowed for failure at about 95 percent of the nominal yield stress (60 ksi). The development length was predicted as discussed in Section 2.3.1.

The rebar consisted of a top half and a bottom half. The orientation of the bar was such that the top half was next to the concrete cover and the bottom half away from the cover (Figure 2.11).

Each bar contained 16 gages. The top half contained 10 gages evenly spaced along the development length. The bottom half contained 6 gages spaced closer at the loaded end of the development length. Figure 2.12 shows the strain gage layout and gage numbering system. The wires for gages 1 to 5 and 11 to 13 extended out the groove in the loaded direction. The remaining gage wires extended out the groove in the unloaded direction.

Gage 1 located at the front edge of the development length was expected to see all of the external load. Gage 10 located at the free end of the development length was expected to see none of the external load. The gages in the

interior were expected to see part of the external load with the remainder of the load going into the concrete through the transfer of bond.

2.4.4 Strain Gage Installation

The gage positions were laid out to the nearest 1/64 of an inch. However, the size of the groove did not permit the gages to be glued into position with the same accuracy. All of the gages were within 1/32 of an inch from the layout lines. The gages were protected with Micro-Measurements M-Coat A, a polyurethane based coating. The resistance to ground and the gage resistance were measured and recorded after installation.

2.4.5 Gluing and Welding the Half Bars

Once the gages were installed the wires were arranged and taped into the groove using clear book binding tape. The tape had a dual function, as it also provided a 5 mil gap between each bar half as shown in Figure 2.13. This provided a uniform gap of 3-5 mils as specified by the glue supplier.

A 3M flexible epoxy adhesive, 2216 Gray, was used to glue the bars together. The gluing surfaces were cleaned with a solvent and the glue was applied. The bars were then placed in a clamp and cured for about 24 hours (Figure 2.14).

The next day, with the bar still in the clamp, the bar was tack welded. Immediately after welding the welded area was sponged with water to reduce the heat and risk of damaging any strain gage wires. The bars were not welded in the loaded portion of the bar. The weld locations are shown in Figure 2.15.

After welding, the bar was removed from the clamp and wiped clean with acetone. The resistance to ground and the resistance of each gage was recorded. All of the gages exhibited excellent response. At this stage, the surface of the glued bar appeared identical to the surface of a normal bar.

2.5 Placement of Concrete

2.5.1 Formwork

Concrete forms were constructed out of dimensional lumber and 1/2 in. BX underlayment plywood (Figure 2.16). The plywood was sealed by applying 3 to 5 coats of polyurethane. The forms were bolted together to enable disassembly and reassembly.

The forms were treated with Noxcrete form release after the test bars were installed. The bonded area of the test bar was protected during this process to ensure that no release agent spilled on the bar. Holes for the auxiliary flexure reinforcement were sealed with silicon sealant. The

forms were also sealed at the joints to prevent possible leakage of concrete.

2.5.2 Casting

The specimens were cast upside down with the bar in the bottom position. This procedure provided more consistent concrete cover and eliminated top bar effects from the bond investigation. The concrete was poured in two lifts using a crane and bucket. The concrete was shoveled into the forms for the specimens with strain gages. The first lift was approximately 9 inches. All specimens in a group (cast together) received the first lift before any received the second lift. After the first lift was poured the concrete was sampled for the casting of concrete test cylinders. Each lift was vibrated using a concrete vibrator. All specimens were vibrated in the same way. In plan, each 6 by 6 in. square was vibrated by one down and up motion per lift.

2.5.3 Concrete Curing and Stripping of Forms

After the concrete was placed it was cured by covering the forms with 4 mil plastic sheeting. The floor under the forms was soaked with water to help supply a humid environment. For specimens fabricated with nominal compressive strengths in the range of 10000 to 14000 psi, wet

burlap was placed over the exposed concrete before covering them with the 4 mil plastic sheeting. The specimens in the forms remained in this condition until the forms were stripped.

The forms were stripped at 48 hours for all of the concrete pours. After stripping the forms, the specimens were flipped over. Specimens with nominal concrete strengths from 6000 to 10000 psi were then cured in the lab environment until they were tested. Group 5, the 12000 psi mix was also exposed to the lab environment after two days. The Group 5 mix only attained 9160 psi at 35 days probably due to lack of moisture while curing. As a result of the Group 5 mix performance, the specimens with 12000 and 14000 psi concrete (Groups 6,7) were cured under plastic and sprayed down with water every day until they were tested. The moist curing of the 12000 and 14000 psi concrete was to ensure attainment of the specified 28 day strengths.

The concrete test cylinders were cured along side the test specimens for all of the concrete mixes.

2.6 Test Setup

The test frame used for the bond tests is shown in Figures 2.17 and 2.18. The resultant forces on the specimen are shown schematically in Figure 2.3. The bar force was applied with two 77 kip MTS actuators spaced by a yoke beam

that carried the tension grips. Referring to Figure 2.3, Reaction 1 was restrained by a concrete block with a pin support resting on it. Reaction 2 was restrained by tying a beam across the specimen via four tension rods tied to the structural floor. A reaction fixture was mounted to the tied down beam that allowed rotation in both the longitudinal and transverse planes. Reaction 3 was carried into the testing frame by a rocker fitted with a steel plate and a 1/2 inch neoprene pad.

The distance between the test bar and the centriod of Reaction 3 was 12.4 inches. This distance was held constant for all of the specimens.

The actuators simultaneously displaced the rebar in tension at a rate of 0.20 inches per minute. During loading, the total load, loaded-end slip, free-end slip, and strain gages were sampled at approximately one second intervals.

2.6.1 Instrumentation

2.6.1.1 Free-End slip

The free-end slip was measured using a $\pm$0.1 in. Linear Variable Differential Transformer (LVDT) calibrated with a 0.0001 in. dial gage. The free-end slip instrumentation is shown in Figure 2.19. The core rod was connected directly to the test bar using an aluminum angle secured by a stainless steel hose clamp.

2.6.1.2 Loaded-End slip

The loaded-end slip was measured using four ±0.1 in. LVDT's which were calibrated with a 0.0001 in. dial gage. The four LVDT's were mounted on two aluminum frames as shown in Figure 2.20 (plan view). The frame was positioned and secured with hardened set screws. Two connecting rods were attached to hold the frames 4.875 in. (gage length) apart while the set screws were tightened. The connecting rods were then removed. As shown in Figure 2.20, the head length is defined as the distance from the loaded end concrete surface to the loaded-end slip instrumentation. The head length was measured to the nearest 32nd of an inch and was approximately 2 inches for all of the tests. The loaded-end slip (LES) was determined as follows (Figure 2.20).

$$LES = \frac{C1+C2}{2} - \frac{(B1+B2)\,(L_h+L_L)}{2L_G} \qquad (2\text{-}2)$$

where:
- LES = loaded-end slip, in.
- C1 = displacement of LVDT C1, in.
- C2 = displacement of LVDT C2, in.
- B1 = displacement of LVDT B1, in.
- B2 = displacement of LVDT B2, in.
- L_L = lead length, 0.5 in.
- L_g = gage length, 4.875 in.
- L_h = measured head length ≈ 2 in.

The two LVDT's on each side of the bar were used to average out any local effects due to bending in the horizontal plane. Sources of the bending were attributed to unequal gripping, unsymmetric bar section, initial bend in the bar, and specimen misalignment.

2.6.1.3 Strain Gage Instrumentation

The strain gages were used in a quarter bridge configuration with a constant bridge voltage of 2 volts. The signal was amplified 500 times using a MTS 450 Quad Conditioner.

The strain gage and circuit was calibrated using a Micro Measurements resistance box. Resistances were changed in .01 ohm increments and the output voltage from the MTS 450 Quad Conditioner was recorded giving a calibration curve. This calibration was performed on each strain gage circuit used in the testing.

2.6.1.4 Actuator Control and Data Acquisition

During testing the hydraulic actuators and data acquisition were computer controlled; a program written with MTS software toolkits was used. The actuators were run in displacement control. The LVDT's, load cells, and strain gages were recorded by the computer approximately every

second from a MTS 468 data acquisition system.

2.7 Test Procedure

The specimen was aligned along the axis of the grip and then tightened against the main reaction beam, Reaction 3 (Figure 2.3). The alignment was aided by adjusting the position of the reaction apparatuses and the rocker against the main reaction beam. The back end of the specimen was held in place with a pallet jack until load was applied.

The initial load was applied quickly, at a rate of 1.0 in. per minute, to seat the grips. The loading was stopped between 2 and 4 kips to check the instrumentation. After releasing the pallet jack, the specimen was loaded at a rate of 0.2 in. per minute until the specimen failed. As the specimens were loaded the actuator load cells, LVDT's and strain gages were sampled.

Groups 1 and 3 specimens were loaded incrementally to facilitate marking cracks as they progressed. At higher loads some specimens failed under sustained load while marking cracks. To achieve a more consistent loading it was decided that the remaining specimens would be loaded continuously to failure.

Chapter 3: Experimental Results

This chapter presents the results of the experimental program described in Chapter 2. An evaluation of the results and the effect of test variables will be presented in Chapter 4.

3.1 Bar Loads, Initial Cracking Loads and Measured Parameters

The initial cracking load and maximum load of all specimens are presented in Table 3.1 along with other measured data. The ultimate bond strength was derived from the maximum load that occurred during the test. The maximum load was captured by the memory module on the MTS test control equipment which was accurate to the nearest 10 pounds. After maximum load, the bar load dropped approximately 90 percent. A few specimens showed a slight softening after maximum load and then lost about 90 percent of the load. All specimens failed in bond exhibiting a splitting type failure.

In all cases the initial crack occurred in the concrete cover at the loaded end concrete face. The initial cracking load was obtained by physically watching for the initial crack on the surface of the concrete. When a crack was first observed the load was recorded to the nearest kip. Additional discussion of failure and cracking is presented in

Sections 3.4 and 3.5.

Table 3.1 also lists measured concrete cover, coating thickness and actual concrete strength. The cover was measured from the edge of the deformation to the concrete surface. Measurement of the coating thickness and concrete strengths were discussed in Chapter 2, Section 2.2.1.

3.2 Load-Slip Curves

The load slip curves for all of the test specimens are shown in Figures 3.1 to 3.14. Each figure shows the loaded-end slip and free-end slip curve for one group and bar size. Due to instrument failure Groups 1 and 3, No. 11 bars had no slip data.

3.2.1 Load versus Free-End Slip

The free-end slip curves are presented by plotting bar load in kips versus free-end slip in inches. The free-end slip is only plotted until the LVDT readings went outside of their specified range. The last load point before most of the load was lost was within 0.5 percent of the ultimate bond load. The next data point was represented by a load around 90 percent less than the ultimate load with all LVDT's out of their 0.1 inch range. These values were not included in the plots.

The free-end slip curves for the uncoated No. 11 bars had a long plateau before failure which is not typical of splitting type failures. Typical free-end slip behavior for splitting type failures would look similar to the free-end slip curves of the No. 6 bars and the No. 11 epoxy-coated bars. After inspection of the free-end slip data for the uncoated 11 bars it appears a large jump in the slip occurred due to flexural cracking at the end of the development length. The flexural cracking caused the concrete, on which the instrument was referenced off, to rotate (Figure 3.15). Using the Group 7, No. 11 bars as an example, Figure 3.16 shows the free-end slip curve immediately before and after the flexural crack occurred by plotting the next points captured by the acquisition system separately. It can be seen the flexural cracking also caused a drop in load which is discussed in Section 3.4.

Immediately upon loading, the uncoated and epoxy-coated bars began to slip at the free end. The curves were generally smooth and continuous until failure. In general, the epoxy-coated bars slipped more than the uncoated bars for any given load. A more detailed discussion of the slip behavior will be presented in Chapter 4.

3.2.2 Load versus Loaded-End Slip

The loaded-end slip curves are presented by plotting the bar load in kips versus the loaded-end slip in inches. The graphs are plotted to the same load step as the free-end slip curves.

The loaded-end slip curves were more varied than the free-end slip curves and in general had a decreasing slope as load was increased. Some of the variability was caused by possible slip or misalignment of the loaded-end slip instruments. Variability of this nature is most evident in the No. 6 test bar specimens (Figures 3.1 and 3.6). The larger deformation spacing of the No. 11 test bars allowed for a more secure and precise installation of the loaded-end slip instrumentation and thus the variability was reduced for the No. 11 bars.

3.3 No. 8 Bars, Strain Gage Results

The results from the strain gages are summarized with graphs in Figures 3.17 to 3.24 showing the top half and bottom half of the bar separately. The graphs in the figures represent the strain distribution along the development length with increasing bar stress. The X-axis represents the distance from the loaded end of the development length. Typical load versus strain plots for individual gages are

shown graphically in the appendix at the end of the report.

3.3.1 Strain Gage Performance

Overall the results of the strain gages were good. Some of the gages gave unreliable results or were completely dead. These gages were omitted from the results. All but one strain gage for the two epoxy-coated bar specimens gave good results. Strain gage 4 on epoxy bar specimen A was omitted from the data. The uncoated bars had more problems with the strain gages. The uncoated bar specimen B strain gages gave good results except strain gage 14. The bottom half of the uncoated bar specimen B also gave very good results. The strain gages on the top half of the uncoated bar specimen C are questionable except strain gage 1. The caution came from the strain gages having very low resistance to ground readings after pouring the concrete. The resistance to ground for most of the strain gages 2 to 10 ranged from 0.8 to 25 mega ohms. The Strain Gage Technology [17] book gives an absolute minimum resistance to ground of 10 mega ohms with the ideal above 10000 mega ohms. All of the strain gages on the bottom half of the uncoated bar specimen C had resistances to ground equal to or greater than 20000 mega ohms. Only the results of the bottom half of the uncoated bar specimen C will be used in the evaluation.

Strain gage 1 was on the loaded edge of the development

length so the uniaxial tension stiffness (modulus of elasticity) could be obtained. Using Hooke's law and the results of Strain Gage 1 and the load cells, the calculated stiffness ranged from 28000 to 30000 ksi for the four specimens. The accepted value for A615 deformed rebar is 29000 ksi. In some cases, at failure the strain reading for strain gage 1 and 11 decreased. (Figures 3.17-19, 3.22, 2.24). This behavior could not be explained. Strain gage 10 was on the edge of the free end and remained close to zero as expected.

3.4 Specimen Failure

All of the specimens failed in bond by splitting of the concrete around the test bar. There was some variation in the amount and type of cracking that occurred. The following paragraphs describe the crack propagation and failure observed during the tests.

3.4.1 Failure of the No. 11 Test Bar Specimens

The uncoated and epoxy-coated No. 11 test bar specimens with the 11.5 inch development lengths cracked differently than the specimens containing longer development lengths. During loading of the No. 11 test bar specimens with the 11.5 inch development lengths, the initial crack appeared on the

loaded end of the specimens extending from the test bar through the concrete cover to the top of the specimen. As load was increased the bond crack extended along the bar. This was labeled as a bond crack due to the radial tension in the concrete. The specimen failed when the bond crack reached the end of the development length. Two of the uncoated bar specimens exhibited flexural cracking at about 7 inches from the loaded end of the specimens which did not affect the results.

Initially, the No. 11 test bar specimens with the 22.5 and 24 in. development lengths and stirrups behaved similarly to the No. 11 test bar specimens with 11.5 inch development lengths. Figure 3.25 shows how the cracks propagated with increasing load for the No. 11 uncoated test bar specimens. Referring to Figure 3.25(a), the initial bond crack was observed on the loaded end of the specimen. As the specimen was loaded this bond crack extended along the bar and most specimens exhibited flexural cracking usually occurring at a stirrup position (Figure 3.25(b)). In some cases the interaction of the bond crack with the flexural cracking caused the bond crack to meander along the centerline of the bar (Figure 3.27). After this stage the uncoated bar specimens behaved differently than the epoxy-coated rebar specimens.

Referring to Figure 3.25(c), the uncoated bar specimens exhibited a flexural crack occurring at the end of the

development length when the bond crack had propagated along approximately 75 percent of the development length. This flexural crack caused a slight drop in load. With the load increasing, the bond crack continued to propagate along the bar. When the bond crack extended to the end of the development length the specimen failed (Figure 3.25(d)). At failure, cracks often flared out into the unbonded region (Figure 3.25(e)). The cracks on the loaded end face also were not visible until failure for the uncoated bar specimens.

Only a few epoxy bar specimens behaved similarly to the uncoated bar specimens. The generalized crack propagation for the epoxy-coated test bar specimens is shown in Figure 3.26. The epoxy-coated bar specimens differed from the uncoated bar specimens in that the flexural cracking at the end of the development length occurred simultaneously with the bond crack reaching the end of the development length. This can be seen by comparing Figures 3.25(c,d) and 3.26.(c,d). At failure the flexural crack at the end of the development length interacted with the local shear stresses causing the flexural crack to flare into the unbonded region as shown in Figure 3.26(e).

3.4.2 Failure of the No. 6 Test Bar Specimens

In general, the No. 6 test bar specimens exhibited similar behavior to the No. 11 test bar specimens. There were some slight differences that will be noted.

Both the uncoated and epoxy-coated No. 6 test bar specimens with 6 in. development lengths failed suddenly after initial bond cracks occurred or simultaneously occurred at failure. Both the epoxy-coated and uncoated No. 6 test bar specimens with 8.5 in. development lengths exhibited flexural cracks at the end of the development length prior to failure. This was similar to the behavior observed for the No. 11 uncoated test bar specimens as stated in Section 3.4.1 with the exception that there was no indication of a drop in load. For the No. 6 test bar specimens, flexural cracking at the end of the development length prior to failure was independent of the bar surface condition.

3.4.3 Failure of the No. 8 Test Bar Specimens

The No. 8 test bar specimens with 14.34 in. development length failed similarly to the No. 11 test bar specimens with 22.5 and 24 in. development lengths. Most of the uncoated bar specimens exhibited flexural cracking causing a drop in load prior to failure.

The fabrication of the strain gaged No. 8 rebar did not

appear to affect the specimen behavior. The behavior of the strain gage specimens was the same as that of the specimens with the original rebar.

3.5 Post Failure Observations

After testing each group of specimens, specimens were broken open to inspect the rebar and the concrete surface in contact with the rebar. A minimum of four specimens per group were examined. This included one epoxy-coated rebar specimen and one uncoated bar specimen of each bar size.

3.5.1 Concrete Surface in Contact with Bonded Rebar

For the uncoated rebar specimens the concrete surface in contact with the rebar was relatively smooth with a dull finish. There was no indication that this condition varied for any of the concrete strengths. The concrete surface in contact with the epoxy-coated rebar was smooth with a very glassy finish. This condition was also consistent for all concrete strengths. Figure 3.28 shows pictures of the concrete surface that was in contact with the rebar.

3.5.2 Bonded Rebar Surface

In general, the rebar surface for all uncoated rebar specimens showed signs that the concrete had good adhesion with the steel. Small particles of concrete still adhered to the rebar upon removal. In areas where the concrete had failed, concrete particles were lodged against the pull side of the deformations. This will be discussed further in Section 3.5.3.

In general, the rebar surface for all epoxy-coated rebar specimens showed no sign of concrete adhering to the epoxy. The epoxy coating was abraded only in the last 25 percent of the development length. This was attributed to the concrete at the front of the development length being displaced away from the rebar due to wedge action.

For both uncoated and epoxy-coated rebar in micro silica concrete, there was no visual evidence of an increase in adhesion as compared to the rebar in normal concrete.

3.5.3 Failure of Concrete at Rebar Deformations

The failure of the concrete at the rebar deformations varied with the concrete strength and development length. The No. 6 and No. 11 rebar specimens at 6360 and 9290 psi (Groups 1,3) showed no signs of concrete crushing, shearing, or any distress to the epoxy coating. This was most likely

due to the low failure stress that was limited by the shorter development lengths and lower concrete strength.

The No. 6 and No. 11 rebar specimens at 9160 to 10470 psi (Groups 2,4,5) showed signs of concrete failure at the rebar deformation. This failure may be described as concrete powder adhering to the rebar deformations and concrete missing from the concrete key as shown in Figure 3.29(b). This was labeled as concrete crushing in front of the rebar deformation. An important fact is that this failure only occurred at the end of the development length. Only the last 9 to 10 deformations showed evidence of concrete crushing.

The No. 6 rebar specimens at 12030 and 13375 psi (Groups 6,7) behaved similar to those cast with the nominal 6000 psi mixes (Groups 1,3). There were no signs of concrete failure or abrasion of the epoxy coating.

The No. 11 rebar specimens at 12030 and 13375 psi (Groups 6,7) showed signs of concrete failure at the rebar deformations. As shown in Figure 3.29(a), the failure may be described as a partial shearing of the concrete keys. It appeared that only slight crushing occurred with a sliver of concrete being removed. Again this shearing of the concrete keys only occurred at the last 9 to 10 deformations. The rebar deformations showed signs of severe distress with deposits of concrete powder. This type of failure is most likely related to the larger stiffness and compressive strength of micro silica concrete. The lower strength micro

silica mixes at 9280 and 9140 psi (Groups 4,5) exhibited crushing of the concrete in front of the deformation without exhibiting a shearing of the concrete key.

Chapter 4: Evaluation of Experimental Results

This chapter presents an evaluation of the results presented in Chapter 3. The general behavior of epoxy-coated reinforcement is evaluated to understand why epoxy coating lowers bond resistance. Upon establishing this understanding, the effects of test variables, comparisons with previous research, and comparisons with design codes will be evaluated.

The effects of test variables include: bar surface (epoxy coating, uncoated), concrete strength, bar size, and concrete type. The effect of epoxy coating on the rebar strain distribution will also be evaluated.

Comparison with most of the previous research described in Chapter 1 will be discussed. Comparisons to the ACI and AASHTO design codes along with the design equation proposed by ACI Committee 408 will also be made.

4.1 Evaluation of General Behavior

The obvious interpretation of the results of Chapter 3 is that epoxy coating reduces the bond resistance of deformed reinforcement. This is not new knowledge, but before the effects of tests variables can be understood, an attempt at understanding the general behavior is imperative. If the difference in behavior of epoxy-coated and uncoated specimens

is understood improvements regarding the coating might be suggested.

4.1.1 Why Do Epoxy Coatings Reduce Bond Strength?

The above question has no direct quantitative answer. The current investigation supports and expands the failure hypothesis of Treece and Jirsa [8] which states that the reduction in bond strength caused by epoxy coating is due to decreased friction for splitting type bond failures.

Another possible reason for the decrease in bond strength due to epoxy coatings is that the coating decreases the related rib area which then decreases the bond strength and stiffness.

4.1.1.1 Reduced Friction with Epoxy Coating

Treece and Jirsa [8] described a failure hypothesis that is supported by quantitative results from the current investigation. Their hypothesis will be expanded and revised with support from the results of this investigation. Treece and Jirsa state that "the primary reason for the reduction in bond strength appears to be the loss of adhesion between the concrete and epoxy-coated bars..." which destroys "most or all of the friction capacity." Uncoated bars have good adhesion to concrete. Treece and Jirsa stated reduced

friction of epoxy-coated bars increases the radial pressure component which sets up radial tension in the concrete cover. Their key point then becomes the bond strength is controlled by the magnitude of the radial pressure that the concrete cover can resist.

The results of this study show that companion epoxy-coated and uncoated test bar specimens exhibit initial splitting of the concrete cover at different loads. The epoxy-coated specimens exhibit initial cracking of the concrete cover at loads that are 91 percent of the uncoated specimens initial cracking loads (Table 4.1). The bar load corresponding to the splitting of the concrete cover is directly related to radial pressure exerted by the bar on the surrounding concrete. The lower splitting loads for the epoxy-coated bars supports the hypothesis of Treece and Jirsa [8]. A further extension of the hypothesis is what happens after splitting of the concrete cover.

The behavior after cracking can be investigated by evaluating the slip curves before and after initial cracking of the concrete cover. To expand the hypothesis of Treece and Jirsa [8] the slip curves for the Group 7, No. 11 bars will be used. Figure 4.1 shows the slip curves with the range of initial cracking loads for both the epoxy-coated and uncoated bar specimens. As observed in Figure 4.1, after initial cracking the epoxy-coated bars showed an increased rate in free-end slip while the rate of increase in free-end

slip for the uncoated bars remained constant.

The same behavior is seen on the loaded-end slip curve. After initial cracking, the slope of the curve decreases more for the epoxy-coated bar than for the uncoated bars. The effect of epoxy coating on slip is discussed in more detail in Section 4.2.2.

Treece and Jirsa attributed better friction of uncoated bars to better adhesion. As discussed in Chapter 1, overall adhesion between the concrete and steel is lost at low bar stresses, but the adhesion which improves bond performance is that of the concrete particles which remain attached to the bar surface. Reported by this study and other studies, after failure of the bond specimen localized concrete particles were observed to still adhere to the uncoated bar. The interlock of these particles with the adjacent concrete develops friction. The friction developed at the rib face is most significant in resisting wedge action (or slip). On areas of the bar without local adhesion, friction was developed due to the roughness of the rebar surface produced when hot rolled. Blast clean bars have shown bond strengths in between those of epoxy-coated and uncoated bars (Johnston and Zia, 1975 [7]). The roughness of the blast clean bars is most likely between that of epoxy-coated and uncoated bars. The lack of localized concrete particles adhering to the epoxy and the smoothness of the coating decreased the ability to develop significant friction forces especially after

initial bond cracks had occurred.

4.1.1.2 Reduced Related Rib Area with Epoxy Coating

Related rib area, α_{sb}, was introduced and defined in Chapter 1. The application of epoxy coating to a deformed bar reduces the "effective" related rib area. The related rib area is proportional to, F_R, the area of a transverse rib above the bar core. This area is dependent on the height of the transverse rib. The definition of F_R is intended to mean the area available for bearing against the concrete. Referring to Figure 4.2, the epoxy coating reduces the effective bearing area on the concrete. The coating at the top of the deformation cannot provide much bearing resistance and thus cannot be included in the "effective" related rib area. The end result is that related rib area is decreased. The effective height is reduced by twice the coating thickness (Figure 4.2).

Work done by Martin and Noakowski (1981) showed that bond strength and stiffness decrease with decreasing related rib area. It should be noted that their test specimens failed by pullout and had short bond lengths.

A solution to the reduced related rib area with epoxy-coated bars would be to increase the height of the deformation to offset the coating thickness so that the epoxy-coated and uncoated rebar had the same "effective"

related rib area.

The reduced friction between the epoxy coating and concrete and the reduced effective bearing area cannot resist the wedging action of the bar. The friction developed by the uncoated bar and larger effective related rib area are enough to resist wedge action and allow significant bearing between the deformation and concrete after initial bond cracks have occurred. In addition to increasing the deformation height of epoxy-coated bars, grit might be added to the epoxy to increase the friction between the concrete and the rebar surface (as is done for epoxy-coated prestressing cables).

4.2 Effect of Test Variables

4.2.1 Effect of Epoxy Coating

The epoxy coating affected the ultimate bond strength, slip, and strain distribution along the development length. The epoxy coating decreased the ultimate bond strength and increased the bar slip for all of the test groups. The effect on strain distribution is discussed in Section 4.2.1.3.

4.2.1.1 Effect of Epoxy Coating on Ultimate Bond Strength

As discussed in Chapter 1 the ultimate bond strength was defined as the maximum average bond stress developed by a

specimen. The ultimate bond strength was calculated using the maximum bar load during the test divided by the development length and nominal bar perimeter (see Table 3.1).

The ultimate bond strength of the epoxy-coated bar specimens will be compared to the ultimate bond strength of the uncoated bar specimens. For comparison, the ultimate bond strengths of the three replications were averaged to obtain a representative ultimate bond strength for both the uncoated and epoxy-coated bars. Unless otherwise stated in this section the ultimate bond strength refers to the average of the three replications.

To compare the ultimate bond strengths, the ultimate bond strength of the uncoated bar specimens was divided by the ultimate bond strength of the companion epoxy-coated bar specimens thus yielding a ratio. The ratio will be referred to as the ultimate bond strength ratio. Only epoxy-coated bar specimens with the same development length as the uncoated bar specimens were compared with an ultimate bond strength ratio. Because the development lengths were the same the ultimate bond strength ratio could have been be calculated by using the average maximum loads.

If the ultimate bond strength ratio equals one, then the epoxy-coated bar specimens had the same ultimate bond strength as the uncoated bar specimens. If the ultimate bond strength ratio was greater than one, say 1.5, then the uncoated bar specimens had an ultimate bond strength 1.5

times larger than the epoxy-coated bar specimens. In other words, the uncoated bar specimen developed 1.5 times the force of the epoxy-coated bar before bond failure.

For all test groups, the ultimate bond strength ratio was greater than one, in other words the epoxy-coated bar specimens had a lower ultimate bond strength than the uncoated bar specimens for all cases. Table 4.2 lists the ultimate bond strengths and the ultimate bond strength ratios for all of the test groups. Figure 4.3 is a scatter plot of the ultimate bond strengths for all of the specimens. Figure 4.3 gives some indication of the amount of variability within the test groups. All specimens in an individual group had the same concrete compressive strength.

The lower bound for ultimate bond strength of the epoxy-coated bars is represented by the highest bond ratio. The highest bond ratio for all of the tests was 1.33, thus for this case the uncoated bars had a bond strength 1.33 times higher than the epoxy-coated bars. This occurred for test Group 2, 10000 psi normal concrete with No. 11 bars.

The ultimate bond strength ratios ranged from 1.01 to 1.08 and 1.20 to 1.33 for the No. 6 and No. 11 bars, respectively. The average of the ultimate bond strength ratios for all No. 6 bars was 1.04 and the average for all No. 11 bars was 1.26. The bond ratios varied with concrete strength and will be discussed in Section 4.2.1.

Johnson and Zia(1982) obtained bond ratios of 1.17 for

both No. 6 and No. 11 bars. However, their specimens were limited in number and contained transverse reinforcement which produced a combined splitting and pullout failure.

Treece and Jirsa(1989) obtained ratios ranging from 1.15 to 1.82 with an overall average of 1.5 and stated there was no variation for coating thickness, bar size, and concrete strength. The diamond shape deformation patterned was used which tends to amplify the effect of epoxy coating thus giving larger ultimate bond strength ratios (poorer performance of epoxy-coated bars).

Hadje-Ghaffari et al. [12] obtained bond ratios ranging from 1.01 to 1.25 and 1.01 to 1.37 for No. 6 and No. 11 bars, respectively. The overall average was 1.12 for all No. 6 bars and 1.20 for all No. 11 bars. The N shape deformation pattern, the same as used in this study, gave bond ratios of 1.08 for the No. 6 bars and 1.35 for the No. 11 bars. These results are similar to those obtained in the current study despite large differences in development lengths and concrete strengths.

4.2.1.2 Effect of Epoxy Coating on Bar Slip

The load-slip relationship gives some insight into how the rebar and concrete interact at the rebar concrete interface. The slip is a function of three main components: adhesion, friction, and the wedge action in front of the

rebar deformation. These components are associated with the rebar concrete contact surface. However, it is virtually impossible separate these components experimentally. The effect of epoxy coating on the loaded end and free-end slip is evaluated and discussed in the next two sections.

4.2.1.2.1 Effect of Epoxy Coating on Free-End Slip

The initial slope of the free-end slip curves will be evaluated. The initial slope indicates a relative comparison of which bars are slipping more than others for the same change in load. The initial slope of the free-end slip curve was obtained by simple linear regression analysis of the first 20 data points. This corresponded with loads of approximately 8, 14, and 20 kips for the No. 6, No. 8, and No. 11 bars, respectively. Any irregular points due to spurious voltage jumps etc. were discarded before conducting the regression analysis.

The representative value of the initial slope was taken as the average of three replications for each set of epoxy-coated and uncoated bars. Tables 4.3 and 4.4 lists all of the initial slopes obtained from the free-end slip curves, the average initial slope of the three replications, and the ratio of the uncoated to epoxy-coated free-end slip curve initial slopes.

The initial slope of the free-end slip curves exhibited

a great deal of variability. In general the epoxy-coated specimens had initial slopes less than those of the uncoated bar specimens thus producing more slip for the same change in load. The initial slopes obtained for the uncoated bar specimens ranged from one to two times the initial slope of the epoxy-coated bar specimens. However, for Groups 4 and 6 No. 11 bars the epoxy-coated bar specimens had average initial slopes about 5 percent greater than the uncoated bars (Table 4.4). The average was skewed by one of the three initial slopes being significantly larger than the other two replications (greater than 20000 kip/inch). Discarding the larger value of initial slope gave average initial slopes for the epoxy-coated bar specimens less than those of the uncoated bar specimens for Groups 4 and 6, No. 11 bars.

The reduction in initial slope supports the hypothesis that the reduced related rib area due to the coating thickness is reducing bond stiffness. Better adhesion exhibited by the uncoated bars would also tend to give larger bond stiffness. Another possible reason for the initial decrease in bond stiffness is the epoxy coating could have compressed between the deformation and the concrete.

4.2.1.2.2 Effect of Epoxy Coating on Loaded-End slip

The loaded-end slip represents the bar slip plus the elongation of the bonded rebar. The epoxy-coated specimens had larger loaded-end slip than the uncoated bar specimens. As stated before, there was a lot of variability in the loaded-end slip data. The data from Group 7, No. 11 bars will be used as representative slip curves to evaluate the effect of the epoxy coating.

To evaluate the effect of the epoxy coating on loaded-end slip a secant stiffness was used. Referring to Figure 4.4, there are two distinct secant slopes on the loaded-end slip curves. The transition point (0.004 in. slip) was chosen to approximate when initial bond cracks had occurred. In region 1 (Figure 4.4) little or no deterioration of the concrete had occurred. However the loaded-end slip stiffness of the epoxy-coated bars was less than that of the uncoated bar specimens. The transition from region 1 to region 2 was represented by a decrease in the secant stiffness. This reduction was due to cracking of the concrete cover. As the load was increased the epoxy-coated bars slipped significantly more than the uncoated bars. As stated above the epoxy-coated bars cannot develop enough friction to resist the wedge action of the bar. After cracking of the concrete cover (bond crack) friction at the rib face becomes more significant in resisting wedge action. Just before

failure, the loaded-end slip curves tended to flatten.

The other loaded-end slip data is more variable but generally follows the stated behavior. The transition from region 1 to 2 for the No. 6 bars is less drastic with a continuous decrease in slope instead of a soft kink as shown with the No. 11 bar specimens. This can be seen by examining the slip curves presented in Section 3.2.

4.2.1.3 Effect of Epoxy Coating on the Strain Distribution Along the Development Length

The rebar strain distribution along the development length is an indicator of how the load is distributed and transferred from the rebar to the concrete. This section describes the differences observed between the strain distributions of the No. 8 epoxy-coated and uncoated rebar.

The effects of the epoxy coating can be described for low, medium, and high stress levels. At low level stress (10 ksi) the epoxy-coated rebar showed strain in the rebar throughout the entire development length (see Figure 4.5). The uncoated bars showed noticeable amounts of strain only in the first 8 to 10 inches. As expected strain gage 1 at the loaded end showed nearly the same strain for both the coated and uncoated bar specimens (same level of stress). Strain gage 10 on the edge of the free end gave strains near zero for both coated and uncoated bar specimens. All of the strain gages between gages 1 and 10 (inside the development

length) for the epoxy-coated bar specimens produced larger strains than those on the uncoated bar specimens at low stress levels (Figure 4.5).

The strain distribution results at low level stress imply the uncoated bars transferred load to the concrete over a shorter length than the epoxy-coated bars. The epoxy-coated bars developed noticeable load over the entire development length (14.3 inches) while the uncoated bars developed the same load within 8 to 10 inches.

For the uncoated bar specimens, strain was not observed throughout the entire development length until the bar was loaded to 20-30 ksi stress (medium stress levels). As the stress level was increased the uncoated bar specimens developed an initial bond crack at 30 ksi and the epoxy-coated bar specimens developed the crack at 28 ksi on average. This also coincided with the loads at which the strain distribution between the coated and uncoated bar specimens were almost the same (Figure 4.6).

As higher stress levels were reached (above 30 ksi) the bond crack propagated further along the development length. This occurred as the wedge action of the deformation pushed the concrete away and thus decreased the transfer of load to the concrete. The deterioration of the bond produced large increases in strain especially near the loaded end where the greatest extent of concrete deterioration had occurred.

At 45 ksi the uncoated bars exhibited the same or larger

strains than the epoxy-coated bars (Figure 4.7). The increased rate of slip for the epoxy-coated bars was possibly relieving the load and not allowing enough bond resistance to increase the load at a significant rate. This would be similar to a mobilized friction situation. The uncoated bars were able to resist slip (wedge action) which allowed strain in the deteriorated regions to increase and more efficient transfer of load to the concrete in the area where the concrete was not deteriorated.

Despite similar failure loads for the epoxy-coated and uncoated bars, the strain distributions were different at failure. The uncoated No. 8 strain gage bars exhibited an ultimate bond strength 2 percent higher than the epoxy-coated No. 8 strain gage bars. This differed from the No. 8 bars without strain gages which showed a 10 percent increase with uncoated bars as compared to epoxy-coated bars. The reason for the difference was not obvious. Possibly the excessive handling of the uncoated gaged bars during fabrication allowed for the natural roughness of the bar to be reduced.

At failure, the uncoated bars showed an almost uniform strain in the first 3 to 4 inches of the development length (Figure 4.8). This was most likely due to a loss of bond transfer in that area and the ability of the remaining development length to restrain load without significant slip.

At failure, the epoxy-coated bars showed a trend to produce uniform strain in only the first 1.5 inches of the

development length. However the strains in the epoxy-coated bar dropped off more rapidly than those of the uncoated bar (Figure 4.8). The rapid reduction was probably due to the excessive slip in the area of the development length that was still transferring load. As the bar slips at a faster rate, the resistance to load is relieved due to the lack of friction between the epoxy and the concrete and also the reduced effective bearing area.

It seems the epoxy coating has the most effect on the strain distribution at low bar stress and near failure. The differences at low stress do not seem to affect the ultimate strength behavior. Excessive slip due to decreased friction and bearing area explains why epoxy coatings decrease ultimate bond strength. It cannot be adhesion alone since the global adhesion has been broken at lower stress levels. If the slip could be reduced (increased friction and related rib area) then the ultimate bond strength of epoxy-coated reinforcement would most likely increase.

4.2.2 Effect of Concrete Strength

The concrete strength had a significant effect on the bond strength of both epoxy-coated and uncoated rebar and consequently the ultimate bond strength ratio that was discussed in Section 4.1.

4.2.2.1 Effect of Concrete Strength on the Ultimate Bond Strength Ratio (Uncoated/Epoxy-coated)

The results of this study showed that the bond strength reduction due to epoxy coating varied with concrete strength. Figures 4.9 and 4.10 show the relationship between the ultimate bond strength bond ratio and concrete strength for the No. 6 and No. 11 bars, respectively. The ultimate bond strength ratio, uncoated/epoxy-coated, as defined in Section 4.1.1 generally decreased with increasing concrete strength for the No. 6 bars. The slight decreasing trend for the No. 6 bars was judged as insignificant. The No. 11 bars showed a more significant trend of increased ultimate bond strength ratios with increasing concrete strength as shown by the best fit line through the data (Figure 4.10).

The development lengths were not the same for all of the tests and produced different bar stresses at failure. The ultimate bond strength ratio is considered to be unaffected by the development length and bar stress at failure. This is supported by past tests that were done by Hadje-Ghaffari et al. (1991) [12] who obtained similar bond ratios as the current study when their development lengths and bar stresses were significantly different than those of the current study. However more research is needed to investigate the effect of bar stress and development lengths on the ultimate bond strength ratio for epoxy-coated and uncoated reinforcement.

The ultimate bond strength ratios were also affected by

the concrete type and will be discussed more in Section 4.2.4.2.

4.2.2.2 Effect of Concrete Strength on the Ultimate Bond Strength

One of the objectives of this study was to investigate the effect of high strength concrete on the bond strength of uncoated and epoxy-coated bars. The No. 6 and No. 11 bars were evaluated with development lengths that were nearly the same.

The No. 6 bars in Groups 1,6, and 7 had development lengths within a quarter of an inch; a direct effect of concrete strength can be determined. As the concrete strength was increased the bond strength increased (Figure 4.11). The rate of increase in bond strength was nearly the same for the uncoated and epoxy-coated bar specimens thus not much change in the ultimate bond strength ratio with increasing concrete strength (Figure 4.9). Figure 4.11 shows that around 8500 to 10000 psi the rate of increase in bond strength is drastically decreased. The author acknowledges the fact that the data is sparse in the transition area. However there still exists a decreased rate in bond strength as the concrete strength increased above 8000 to 9000 psi.

Tests by Hadje-Ghaffari et al. [12] compared 6000 psi concrete to 13000 psi concrete for bottom cast uncoated No. 6 bars and found there was no increase in bond strength. The

results of the current investigation and work by Gjorv et al. [3] and DeVries et al. [11] clearly show that bond strength increased with increased concrete strength for No. 6 bars. However, the rate of increase in bond strength decreased as the concrete strength increased.

There are a few possible reasons for the decreased rate of bond strength at higher concrete strengths. Higher strength concretes are much stiffer. The binder strength is approaching strengths comparable to that of the coarse aggregate strength. Under the same increase in load, the bond crack opens and propagates at a faster rate than in less stiff concrete. This was observed in the current study. It was noticed at concrete strengths from 10000 to 14000 psi, failures were more explosive. It was also noted, especially for the 12000 and 14000 psi concretes, that once the initial bond crack appeared, the crack propagation was much faster than in the 6000 psi concrete. This behavior is common for stiffer materials.

The No. 11 bars in Groups 2,4,5,6, and 7 had comparable development lengths at 24, 24, 24, 24, and 22.5 inches respectively with nominal concrete strengths at 9000 to 14000 psi. Groups 1 and 3 had development lengths at 11.5 inches for concrete strengths below 9000 psi. Figure 4.12 shows the rate of increase for the lower strength concrete tends to be higher than the rate of increase for the higher strength concrete. There was no increase in bond strength observed

above 12000 psi for the uncoated bar specimens (Figure 4.12). The bond strength of the epoxy-coated bar specimens increased at a slower rate than the uncoated specimens and decreased at concrete strengths above 12000 psi. The relative drop in bond strength of the epoxy-coated bar specimens explains the increase in ultimate bond strength ratios with concrete strength (Figure 4.10).

Another possible reason for the decreased rate in bond strength with increased concrete strength, was the failure mode of the concrete in front of the deformations. The No. 11 bars at 12000 and 14000 psi had evidence of small slivers of concrete sheared off due to the deformations bearing on the concrete keys as discussed in Section 3.5.3. When the concrete crushes in front of the deformation it is confined by the surrounding concrete and can still provide some additional mechanical bearing with the deformation. When the sliver of concrete is sheared off only wedging of the sliver and friction between the sliver and surrounding concrete can provide additional increase in strength. Also the effective wedge angle is decreased thus decreasing the bond resistance.

4.2.3 Effect of Bar Size

The bar size has been discussed indirectly throughout Chapter 4. However this section will summarize the effects of bar size.

The most significant effect was on the reduction of bond strength due to the epoxy coating. As stated in Section 4.2.1, the average ultimate bond strength ratio for No. 11 bars was 21 percent greater than that of the No. 6 bars. In other words epoxy coating has a more detrimental effect on the bond performance of larger epoxy-coated bars relative to uncoated bars. The limited data for the No. 8 bars without strain gages showed that the ultimate bond strength ratio for the No. 8 bars fell between the ultimate bond strength ratios of the No. 6 and No. 11 bars. The reason for the differences due to bar size is not apparent; a possible explanation is the transverse strain relative to bar size.

The effect of transverse strain is dependent on bar size and would tend to be detrimental to the bond performance. For the same bar stress transverse strains will increase with the diameter of the bar. Though small, the effect of transverse strain is cumulative with the effect of epoxy coating. Theoretical transverse strains at the nominal yield point reduce the nominal radius of the bar by 0.8, 1.0, and 1.5 mil for the No. 6, No. 8, and No. 11 bars respectively. These reductions in radius are equivalent to 6 to 30 percent of the allowable coating thicknesses for epoxy-coated bars (5-12 mil).

Micro silica seemed to increase the bond strength of the No. 11 bars more than that of the No. 6 bars. This is discussed further in Section 4.2.4.

4.2.4 Effect of Micro Silica Concrete Relative to Normal Concrete

Originally Group 1 would be compared to Group 3 and Group 2 would be compared to Group 4. The two sets of groups represent nominal compressive strengths of 6000 and 10000 psi concrete with and without micro silica. The effect of micro silica can only be compared directly for Groups 2 and 4 (10000 psi concrete) because the Group 3 (6000 psi micro silica concrete) gained strengths well above 6000 psi in only 4 days while the Group 1 normal concrete remained near its design strength of 6000 psi. The Group 2 specimens had normal concrete and the Group 4 specimens had micro silica concrete (10 percent). From the results of the 10000 psi concrete tests with and without micro silica it is evident that the micro silica had effects on both the ultimate bond strength and bar slip.

4.2.4.1 Effect of Micro Silica Concrete on Ultimate Bond Strength

The concrete strengths for Groups 2 and 4 were 9704 and 9284 psi, respectively. Before comparison of the two groups, the ultimate bond strength of the three replications was normalized by the square root of the corresponding actual concrete strength.

The No. 6 uncoated bars showed a 2.5 percent increase in

ultimate bond strength when using the micro silica concrete. The epoxy-coated No. 6 bars showed no difference in bond strength when comparing micro silica concrete to normal concrete. These results are much different than those obtained by Gjorv et al. [3]. Gjorv did not test epoxy-coated bars but found in some cases for uncoated No. 6 bars an increase of 30 percent in bond strength with micro silica. The difference could be linked to the specimen type. Gjorv used the smaller pull-out type specimens defined in Chapter 1.

The No. 11 bars showed a significant increase in bond strength with micro silica concrete. When comparing Groups 2 and 4, the No. 11 uncoated bars showed an 8 percent increase in ultimate bond strength and the epoxy-coated bars showed a 16 percent increase when using micro silica. These numbers are possibly inflated by the fact the Group 2 (10000 psi, normal concrete) had bond strengths 5 percent below what were expected using the prediction method from Chapter 2. The value of α (defined in Section 2.3.1) of 0.74 for Group 2 No. 11 bars was lower than that from Groups 1 and 3 No. 11 bars (α=0.80). It appears that the micro silica may help the larger bars more than the smaller ones. The limited data suggests more research is needed to determine the effect micro silica has on the bond behavior of deformed reinforcement.

4.2.4.2 Effect of Micro Silica on the Ultimate Bond Strength Ratio

The slight decrease in ultimate bond strength ratios for the No. 6 bars as discussed in Section 4.2.1.1 and 4.2.3 could have come from the addition of micro silica but it is not likely. Group 6, 12000 psi concrete had only 5 percent micro silica and did not show any reduction in ultimate bond strength ratio compared with the 10000 and 14000 psi concrete with 10 percent micro silica. The No. 11 bars showed a significant decrease in the ultimate bond strength ratio (uncoated/epoxy-coated) when comparing micro silica concrete to normal concrete. Figure 4.13 shows the best fit lines through the normal concrete and micro silica concrete data for the ultimate bond strength ratios versus concrete strength. The author recognizes that the normal concrete data is only represented by two data points and thus lacks statistical validity. However the lines were nearly parallel and the normal concrete line represented a 9 percent increase in the ultimate bond strength ratio when compared to the micro silica line.

Overall, micro silica does effect bond but with the limited data on micro silica content, the most efficient micro silica content or type cannot be stated quantitatively. However at least 5 percent micro silica tends to help increase the ultimate bond strengths of epoxy-coated No. 11 bars.

4.2.4.3 Effect of Micro Silica on Bar Slip

If the micro silica somehow adheres to the bar or provides more friction, a difference in slip behavior should be observed. When comparing the No. 6 bar load versus free-end slip curves, the micro silica concrete shows little difference than the normal concrete (Figure 4.14). This makes sense when considering that the ultimate bond strengths were nearly the same for the No. 6 bars in normal concrete and micro silica concrete. The No. 11 rebar slip curves for Groups 2 and 4 (nominal 10000 psi with and without micro silica) show that the uncoated bars and the epoxy-coated bars in micro silica have initial slopes noticeably greater than the epoxy-coated and uncoated bars in normal concrete (Figure 4.15). This helps to explain the increase in bond strength for the No. 11 bars with micro silica concrete.

The No. 11 bars have a much larger surface area than the No. 6 bars which could allow for increased adhesion if the micro silica concrete has enhanced adhesion properties to the epoxy.

4.3 Comparisons with ACI and AASHTO Design Codes

In this section the bond strengths observed for the higher strength concretes are examined with respect to current design equations. The current design equations were developed with results from bond tests on concrete strengths well below 10000 psi.

4.3.1 Comparison with ACI and AASHTO Bond Stress

4.3.1.1 Comparison with ACI 318-89 and AASHTO

Before making any comparisons a review of the current bond stress equation is presented. The ACI 318-89 and the AASHTO design equations (ACI/AASHTO) for basic development length are the same. The current equation for the development length of No. 11 bars and smaller was derived from the bond stress equation from the ACI 318-63 code.

$$U_u = 9.5\frac{\sqrt{f'_c}}{d_b} \qquad (4\text{-}1)$$

The design code assumes an average uniform bond stress over the development length. The equation for the average uniform bond stress is:

$$U_u = \frac{f_s A_b}{\pi d_b l_d} \qquad (4\text{-}2)$$

By setting equation 4-1 equal to equation 4-2 ($f_s = 1.25 f_y$) an expression for ld, the ACI/AASHTO design expression for the basic development length can be obtained.

Equation 4-1 above with the 1.25 safety factor applied to fs was used to compare the ACI/AASHTO codes relative to the experimental results. Figures 4.16 and 4.17 show the experimental ultimate bond stress normalized by the ACI/AASHTO expression (equation 4-1 divided by 1.25) for No. 6 and No. 11 bars respectively.

The No. 6 bars were found to give conservative results for both the uncoated and epoxy-coated bars for all concrete strengths. The normalized bond stress was nearly unaffected by concrete strength.

Equation 4-1 was also conservative for the uncoated and epoxy-coated No. 11 bars for all concrete strengths. Also obvious in Figure 4.17, the ACI/AASHTO expression are much more conservative for Groups 1 and 3. The ACI/AASHTO expression is intended to predict the bond stress when the

bar yields. Groups 1 and 3 failed at about 50 percent of the nominal yield stress due to the 11.5 inch development length. The other groups with development lengths of 22.5 to 24 in. failed at loads that were 85 to 96 percent of the nominal yield. Bond specimens designed to fail significantly lower than the yield stress would show much more conservativeness than specimens failing near the yield stress. Specimens that fail in bond significantly below the yield stress have relatively shorter development lengths. Because bond stress is inversely proportional to development length, specimens with short development lengths will exhibit bond stresses much larger than those predicted by the design code equation which are independent of development length.

4.3.1.2 Comparison to ACI Committee 408 Recommended Bond Equation

The ACI 408 bond equation was derived from the OJB equation presented in Chapters 1 and 2. Instead of applying a safety factor to the bar stress (fs = 1.25fy) as did ACI 318/AASHTO, the bar stress is assumed as the nominal yield stress and a strength reduction factor (0.8) is applied for the ACI 408 equation.

Rearranging the OJB equation and assuming fs as 60,000 psi (fs = fy) an approximate expression for the development length is obtained:

$$l_{db}=\frac{5500A_b}{\phi K\sqrt{f'c}} \qquad (4\text{-}3)$$

where l_{db} = basic development length, in.
A_b = nominal bar area, in^2
ϕ = 0.8, strength reduction factor
K = cover parameter define by ACI 408
f'c = nominal concrete strength, psi

By setting equation 4-3 equal to equation 4-2 with fs = 60000 psi, an expression for the ACI 408 bond stress is obtained:

$$U=2.78K\frac{\sqrt{f'c}}{d_b} \qquad (4\text{-}4)$$

Figures 4.18 and 4.19 show the experimental results normalized by Equation 4-4. The No. 6 bar specimens gave conservative results with normalized bond stresses about 2. Similar to the ACI 318/AASHTO comparison the normalized bond stress was unaffected by concrete strength. However for the No. 6 bars the ACI 408 expression was slightly more conservative than the ACI 318/AASHTO expression.

The normalized bond stresses for the No. 11 bars (Figure

4.19) gave nearly identical results as the ACI 318/AASHTO comparison. The ACI 408 was slightly less conservative than the ACI 318/AASHTO which made the ACI 408 equation unconservative for epoxy-coated No. 11 bars in Groups 2 and 4-7 (no modification factor). Groups 1 and 3 which failed significantly lower than the nominal yield stress were much more conservative which was similar to the ACI 318/AASHTO comparison.

4.3.1.3 Design Modification Factors

According to ACI/AASHTO the specimens in this study required a modification factor of 1 for the uncoated bars and 1.5 for the epoxy-coated bars. The epoxy-coated specimens that gave unconservative results without the epoxy coating modification factor gave conservative results when the factor was applied. Unconservative results without the modification factor only occurred when comparing the epoxy-coated No. 11 test bar results to the ACI 408 expression.

The following chapter presents the conclusions and design recommendations.

Chapter 5: Conclusions

5.1 General

It was found in the investigation reinforcement coating, concrete strength, bar size and concrete type affect the bond behavior of deformed reinforcement in concrete.

The following sections state the conclusions based on the evaluation of experimental results and comparisons with design codes. The last two sections give recommendations for design and future research.

5.2 Conclusions from Experimental Results

1. Epoxy coatings reduce bond strength because the friction developed between the coating and concrete cannot resist the wedge action of the bar after initial splitting has occurred. Also, the epoxy coating reduces the effective bearing area of the deformation.
2. Epoxy-coated test bar specimens exhibit initial bond cracks at lower loads than uncoated test bar specimens. Reduced friction at the rib face with epoxy-coated bars increases the radial tension stresses in the concrete around the bar causing the bond cracks to form at lower bar load.

3. Epoxy-coated bars have different strain distributions than uncoated bars at low bar stress and near bond failure. At low bar stress the epoxy-coated bars developed the same load as uncoated bars but over a much longer length. Near failure the epoxy-coated bars showed less strain in the bar than the uncoated bars. The epoxy-coated bars were unable to resist slip which caused the strain in the epoxy-coated bar to be relieved.

4. Epoxy coating reduces the ultimate bond strength as compared to uncoated bars for the concrete strengths tested (6 to 14 ksi). This is especially true for No. 11 bars in higher strength concrete.

5. The reduction in bond strength due to epoxy coating increased with bar size. On average, the ultimate bond strength ratios (uncoated/epoxy-coated) for all No. 6, No. 8, and No. 11 bars were 1.04, 1.10, and 1.26, respectively.

6. For No. 6 bars, the ultimate bond strength ratio (uncoated/epoxy-coated) was unaffected by concrete strength. For No. 11 bars, the ultimate bond strength ratio increased as concrete strength increased.

7. The ultimate bond strength of epoxy-coated and uncoated No. 6 bars increased with concrete strength (6-14 ksi). The rate at which the bond strength increased with concrete strength was nearly the same for uncoated and epoxy-coated No. 6 bars. The bond strength of epoxy-coated and uncoated No. 11 bars increased with concrete strength up to 12 ksi. Above 12 ksi concrete strength, the uncoated No. 11 bars exhibited no significant change in bond strength while the epoxy-coated bars exhibit a decrease in bond strength. The rate of increase in bond strength with concrete strength was lower for epoxy-coated No. 11 bars as compared to uncoated No. 11 bars.
8. Epoxy-coated bars slip more than uncoated bars. For epoxy-coated bars, the load-slip behavior is affected mostly from the splitting of the concrete around the bar. Load-slip behavior for uncoated bars seemed unaffected by initial bond cracks.
9. The addition of micro silica improved bond strength. The improvement in bond strength for the No. 6 bars was insignificant while the No. 11 bars exhibited an 8 and 16 percent increase in bond strength for uncoated and epoxy-coated bars, respectively.

10. For No. 11 bars, the addition of micro silica reduced the negative effect of the epoxy coating. The ultimate bond strength ratio (uncoated/epoxy-coated) was decreased by 9 percent with the addition of micro silica. It appears that No. 6 bars were unaffected by the addition of micro silica.

5.3 Conclusions from Comparisons with ACI and AASHTO.

1. For No. 6 bars, the ACI 318/AASHTO and ACI 408 were conservative in predicting the bond strength of both uncoated and epoxy-coated bars for the concrete strengths tested (6-14 ksi).
2. For No. 11 bars, the ACI 318/AASHTO was conservative for uncoated and epoxy-coated bars for the concrete strengths tested (6-14 ksi), even without modification factors for epoxy coating.
3. The ACI 408 was conservative for No. 11 uncoated bars for the concrete strengths tested (6-14ksi). The ACI 408 was unconservative for some of epoxy-coated No. 11 bars (Groups 2, 4-7), however, when the current modification factor for epoxy coating was applied to the ACI 408 expression, it gave conservative results for the concrete strengths tested (6-14 ksi).

4. ACI 318/AASHTO was slightly less conservative than ACI 408 for No. 6 bars. For No. 11 bars, the ACI 408 was slightly less conservative than ACI 318/AASHTO.

5.4 Design Recommendations

5.4.1 Epoxy-Coated Modification Factor

Only the ACI 318 and the AASHTO design recommendations for bottom cast bars can be addressed by this investigation. In this investigation only specimens with concrete cover less than $3d_b$ were tested and thus only recommendations are made for that case. For bar sizes No. 3 to No. 11, the current ACI 318/AASHTO modification factor for epoxy-coated bars is 1.5 for concrete cover less than 3 bar diameters ($3d_b$) or a clear spacing between bars less than 6 bar diameters.

This investigation found lower bound modification factors for epoxy-coated bars of 1.08, 1.10, and 1.33 for No. 6, No. 8, and No. 11 bars, respectively. From the results of this study the modification factor for epoxy-coated bars could be reduced to at least 1.33 for No. 9, No. 10, and No. 11 bars; No. 6, No. 7, and No. 8 bars could have a modification factor of 1.10. The data on the No. 8 bars were limited and to simplify the design code a modification factor of 1.33 could be used for bar sizes No. 6 thru No. 11. No recommendations could be made on other bar sizes outside the

sizes tested in this investigation. A caution is stated that the modification factors recommended above can only be used with bars having the N deformation pattern.

The 1.5 modification factor in the current codes was derived from tests (Treece and Jirsa [8]) done on bars having a diamond shaped deformation pattern. Hadje-Ghaffari et al. [12] investigated other less efficient deformation patterns which did not include the diamond shape deformation pattern. Hadje-Ghaffari et al. (1991) [12] proposed a development length modification factor of 1.25 for No. 6 bars and smaller and a factor of 1.35 for No. 7 bars and larger. But contradictory to Hadje-Ghaffari et al. the diamond deformation pattern is still being used in the production of epoxy-coated bars in some parts of the United States. Currently over 50 percent (23 of 44) of the rebar manufactures produce diamond shape deformation patterns. Thus it is possible that the diamond shape deformation pattern may continue to be used for epoxy coating. Also the diamond shape deformation is considered by some epoxy coating companies to be the easiest to coat. Despite possible differing political opinions the production of epoxy-coated bars should be limited to the most efficient deformation patterns. Economically, this may not be feasible but more efficient deformation patterns should not be taxed by designed codes.

The modification factors in the current ACI 318/AASHTO

codes should remain unchanged as long as the diamond deformation pattern is used and it is still common place not to specify the type of deformation pattern in contract specifications. The modification factors proposed by Hadje-Ghaffari et al. (1991) and endorsed by this study could be used for the N, C, and S deformation patterns if specified in contract specifications.

5.4.2 Limited Concrete Strengths for Design

Based on results of this investigation the concrete strength in design code equations should be limited to 12000 psi for No. 7 bars and larger and 14000 psi for No. 6 bars until more bond research is done with higher strength concretes.

5.5 Recommendations for Future Research

There are still unanswered questions regarding the behavior of epoxy-coated bars and the use of epoxy-coated and uncoated bars in high strength concrete. The following list of recommendations should be considered in future research on the bond behavior of reinforcement in concrete.

1. What is the effect of development length and bar stress at failure on the ultimate bond stress ratio for uncoated and epoxy-coated bars?
2. The effect of related rib area on bond should be investigated by evaluation of current data and new research.
3. Will increased rib height to compensate for the reduction in effective rib bearing area increase the bond strength of epoxy-coated bars?
4. More information is needed on the bond strength of bars in high strength concrete. Tests should be done with bar sizes No. 3 thru No. 5, No. 7 thru No. 10, and larger than No. 11 bars.
5. More information is needed on the effect of micro silica on bond strength. Is there an optimum content or type?

6. Can grit be applied to epoxy-coated bars to increase friction between the coating and the concrete? This would also help to validate the failure hypothesis for epoxy-coated rebar.
7. What is the bond strength of bars at bar stress levels in the strain hardening region?
8. If the development length of epoxy-coated bars is multiplied by the design modification factors or their bond ratios does the bond strength increase by the same factor (probably not as much).
9. Analytical models with multiple deformations should be created to predict the strain distributions of uncoated and epoxy-coated bars. The analytical model then could be used to study the effects of friction and other parameters influencing bond.
10. Are there other coatings or methods that would perform better than fusion bonded epoxy coatings?

REFERENCES

1. ACI Committee 318. (1989). "Building Code Requirements for Reinforced Concrete (ACI 318-83) and Commentary-ACI-318R-89," American Concrete Institute, Detroit, MI..

2. *Standard Specifications for Highway Bridges*, 14th Edition, American Association of State Highway and Transportation Officials, Washington D.C., 1989.

3. Gjorv, Odd E., Monteiro, Paulo J. M., Mehta, P. Kumar, "Effect of Condensed Silica Fume on the Steel-Concrete Bond," BML Report 86.201, Division of Building Materials the Norwegian Institute of Technology, University of Trondheim, Trondheim, Norway, May, 1986.

4. Clifton, James R., Beeghly, Hugh F., and Mathey, Robert G. (1975). "Nonmetallic Coatings for Concrete Reinforcing Bars," Building Science Series, No. 65, National Bureau of Standards, Washington, DC, 1975.

5. ACI Committee 408, Subcommittee on Repeated Loadings, "State-of-the-Art Report, Bond Under Cyclic Loading", Draft, January, 1990.

6. Lutz, Leroy A., Gergley, Peter, "The Mechanics of Bond and Slip of Deformed Bars in Concrete," ACI Journal, Proceedings Vol. 64, No. 11, November 1967, pp 711-721.

7. Johnston, David W. and Zia, Paul., "Bond Characteristics of Epoxy-coated Reinforcing Bars," Report No. FHWA-NC-82-002, Federal Highway Administration, Washington, DC, 1982.

8. Treece, R. A. and Jirsa, J. O., "Bond Strength of Epoxy-Coated Reinforcing Bars," ACI Materials Journal, Vol. 86, No. 2, March-April, 1989.

9. Orangun, C. O., Jirsa, J. O., and Breen, J. E., "A Reevaluation of Test Data on Development Length and Splices, " Journal of the American Concrete Institute,Proceedings Vol. 74, No. 3, March,

10. Choi, Oan C., Hadje-Ghaffari, H., Darwin, David, and McCabe, Steven L., "Bond Epoxy-Coated Reinforcement to Concrete: Bar Parameters," SL Report 90-1,University of Kansas Center for Research, Lawrence, Kansas, January 1990.

11. DeVries, Richard A., Moehle, Jack P., Hester, Weston, "Lap Splice Strength of Plain and Epoxy-Coated Reinforcements: An Experimental Study Considering Concrete Strength, Casting Position, and Anti-Bleeding Additives," Report No. UCB/SEMM-91/02, Department of Civil Engineering, University of California, Berkeley, California, January 1991.

12. Hadje-Ghaffari, Hossain, Darwin, David, and McCabe, Steven L., "Effects of Epoxy-Coating on the Bond of Reinforcing Steel to Concrete," SM Report No. 28, The University of Kansas Center for Research, Inc, Lawrence Kansas, July 1991.

13. ASTM. (1989). "Standard Specification for Deformed and Plain Billet-Steel Bars for Concrete Reinforcement," (ASTM A 615-87a) 1989 Annual Book of ASTM Standards, Vol. 1.04, American Society for Testing and Materials, Philadelphia, PA.

14. ASTM. (1989). "Standard Specification for Epoxy-Coated Reinforcing Steel Bars," (ASTM A 775/A 775M-88a) 1989 Annual Book of ASTM Standards, Vol. 104, American Society for Testing and Materials, Philadelphia, PA,

15. CEB - Comite Euro-International Du Beton, "Bond Action and Bond Behavior of Reinforcement - State of the Art Report," Bulletin No.151, Paris, France, December, 1981.

16. ACI Committee 408, "Suggested Development, Splice, and Standard Hook Provisions for Deformed Bars in Tension," Report No. ACI 408.1r-79, American Concrete Institute, Detroit, Michigan, CONCRETE INTERNATIONAL, July 1979, pp. 47-61.

17. A.J. Window and G.S. Holister, Strain Gauge Technology, London, Applied Science Publishers, 1983.

18. Mains R.M., "Measurement of the Distribution of Tensile and Bond Stresses along Reinforcing Bars," ACI Journal, Proceedings V. 48, No. 9, Nov. 1951, pp. 225-252.

19. Rehm, G.: Úber die Grundlägen des Verbundes zwischen Stahl und Beton. (The fundamentals of bond between steel reinforcement and concrete.) Deutscher Ausschuss fűr Stahlbeton. Heft 138, 1961, p. 59.

20. Soretz, S., Hölzenbein, H.: Einfluss der Rippenabmessungen von Betonbewehrungsstäben auf den Verbund und die Biegefähigkeit. Betonstahl in Entwicklung. Tor-Isteg Steel Corporation. Luxenburg, Heft 69, 1980, p. 34.

21. Martin H. and Noakowski, P.: Verbundverhalten von Betonstählen, Untersuchungen auf der Grundlage von Ausziehversuchen, Shriftenreihe auf der Deutscher Ausschuss fűr Shahlbeton, Heft 319, p. 239.

Table 2.1

Test Variables and Group Definitions

Group No.	Nominal Concrete Strength (psi)	Percent Micro Silica (%)	Bar Size	Development Length (inch)	Cover (inch)
1	6000	0	#6	6	1.5
			#11	11.5	2.5
2	10000	0	#6	8.5	1.5
			#11	24	2.5
3	6000	7.5	#6	6	1.5
			#11	11.5	2.5
4	10000	10	#6	8.5	1.5
			#11	24	2.5
5	12000	10	#6	7	1.5
			#11	24	2.5
6	12000	10	#6	6.25	1.5
			#11	24	2.5
7	14000	10	#6	5.75	1.5
			#11	22.5	2.5
8	6000	0	#8	14.34	2.5

Table 2.2

Mechanical Properties of Test Bars

Bar Size	Yield Strength (ksi)	Ultimate Strength (ksi)	% Elong. in 8 inches
#6	62.1	97.7	16.9
#8	62.5	101.4	15.9
#11	69.2	108.9	15

Table 2.3

Actual Concrete Strength and Age at Testing

Group No.	Bar Size	Nominal Concrete Strength (psi)	Actual Concrete Strength (psi)	Age at Testing (day)
1	#6	6000	6650	15
1	#11	6000	6360	28
2	#6	10000	9705	13
2	#11	10000	10470	28
3	#6	6000	9290	142
3	#11	6000	8400	11
4	#6,#11	10000	9285	42
5	#6,#11	12000	9160	35
6	#6,#11	12000	12030	21
7	#6,#11	14000	13975	28
8	#8	6000	5630	26

Table 2.4

Concrete Mix Proportions

Group No.	Nominal Concrete Strength (psi)	Percent Micro Silica (%)*	W/C Ratio (lb)	Cement (lb)	Aggregate		Slump (inch)
					Coarse (lb)	Fine (lb)	
1,8	6000	0	0.38	693	1782 R	1162	3
2	10000	0	0.3	800 200 F	1790 L	950	4
3	6000	7.5 S	0.4	610	1700 R	1230	4
4	10000	10 S	0.32	705	1725 R	1250	4
5	12000	10 S	0.3	730	1725 R	1250	4
6	12000	5 D	0.29	950 T	1800 L	1060	3
7	14000	10 D	0.29	975 T	1800 L	1007	3

* Percent micro silica by weight of cement
S Micro silica slurry
D Dry micro silica powder
F Fly ash
T Cement + Fly ash
L Limestone
R River Stone

Note: All mixes except for Groups 1 and 8 contained superplasticizer to obtain desired slump

Table 2.5

Comparison of
OJB Equation to Results from
Choi et al. (1989)

#5 Bars C_s/C_bd_b = 5.36	
Lead Length	Uncoated U_{TEST}/U_{OJB}
0	0.88
0.5	1.18
1	1.18
1.5	1.28
2.375	1.63
3.75	1.95

#6 Bars C_s/C_bd_b = 3.67	
Lead Length	Uncoated U_{TEST}/U_{OJB}
0.5	1.18
2.75	1.52

#8 Bars C_s/C_bd_b = 2	
Lead Length	Uncoated U_{TEST}/U_{OJB}
0.5	1
3.75	1.657

#11 Bars C_s/C_bd_b = 1.1	
Lead Length	Uncoated U_{TEST}/U_{OJB}
1.5	0.93

Table 3.1

Test Results and Measured Parameters

Group No.	Specimen Label	Concrete Strength (psi)	Develop. Length (inch)	Cover (inch)	Coating Thickness (mils)	Maximum Load (kip)	Initial Cracking Load (kip)
Group 1	06B06A06	6650	6	1.59	0	17.16	12
	06B06B06	6650	6	1.56	0	16.80	**
	06B06C06	6650	6	1.50	0	17.27	17
	06E06A06	6650	6	1.59	7	15.90	12
	06E06B06	6650	6	1.69	7	15.92	14
	06E06C06	6650	6	1.59	10	16.84	12
	11B11A06	6360	11.5	2.47	0	42.03	*
	11B11B06	6360	11.5	2.44	0	41.68	28
	11B11C06	6360	11.5	2.47	0	41.86	18
	11E11A06	6360	11.5	2.47	*	33.15	16
	11E11B06	6360	11.5	2.50	*	34.30	22
	11E11C06	6360	11.5	2.50	*	33.97	19
Group 2	06B08A10	9705	8.5	1.69	0	27.26	20
	06B08B10	9705	8.5	1.56	0	26.68	18
	06B08C10	9705	8.5	1.63	0	27.42	15
	06E08A10	9705	8.5	1.50	8	25.05	*
	06E08B10	9705	8.5	1.44	7	25.70	15
	06E08C10	9705	8.5	1.59	7	26.50	14
	11B24A10	10470	24	2.50	0	80.63	31
	11B24B10	10470	24	2.41	0	76.06	25
	11B24C10	10470	24	2.44	0	80.97	28
	11E24A10	10470	24	2.44	6	59.94	25
	11E24B10	10470	24	2.53	9	55.69	23
	11E24C10	10470	24	2.50	8	62.79	23
Group 3	06B06D08	8400	6	*	0	20.96	*
	06B06E08	9290	6	*	0	21.19	*
	06B06F08	9290	6	1.56	0	21.41	*
	06E06D08	9290	6	1.56	6	20.62	*
	06E06E08	9290	6	1.44	6	19.35	*
	06E06F08	9290	6	1.56	7	19.90	*
	11B11D08	8400	11.5	2.22	0	45.12	26
	11B11E08	8400	11.5	2.47	0	48	27
	11B11F08	8400	11.5	2.44	0	48.93	26
	11E11D08	8400	11.5	2.47	*	40.7	29
	11E11E08	8400	11.5	2.47	*	41.09	24
	11E11F08	8400	11.5	2.22	*	36.47	23

See end of table for footnotes

Table 3.1

Test Results and Measured Parameters
(continued)

Group No.	Specimen Label	Concrete Strength (psi)	Develop. Length (inch)	Cover (inch)	Coating Thickness (mils)	Maximum Load (kip)	Initial Cracking Load (kip)
Group 4	06B08D10	9285	8.5	1.59	0	26.92	19
	06B08E10	9285	8.5	1.56	0	27.19	16
	06B08F10	9285	8.5	1.63	0	27.46	16
	06E08D10	9285	8.5	1.44	8	23.79	15
	06E08E10	9285	8.5	1.59	7	25.66	12
	06E08F10	9285	8.5	1.66	7	26.15	14
	11B24D10	9285	24	2.44	0	75.80	33
	11B24E10	9285	24	2.47	0	80.33	27
	11B24F10	9285	24	2.47	0	84.95	28
	11E24D10	9285	24	2.41	11	66.25	*
	11E24E10	9285	24	2.47	10	62.49	*
	11E24F10	9285	24	2.44	14	66.16	29
Group 5	06B07D09	9160	7	1.59	0	24.12	15
	06B07E09	9160	7	1.59	0	25.12	17
	06B07F09	9160	7	1.59	0	25.01	19
	06E07D09	9160	7	1.63	6	23.18	16
	06E07E09	9160	7	1.59	6	23.83	17
	06E07F09	9160	7	1.50	6	24.17	14
	11B24D09	9160	24	2.47	0	84.72	29
	11B24E09	9160	24	2.47	0	82.59	35
	11B24F09	9160	24	2.47	0	88.94	32
	11E24D09	9160	24	2.47	12	71.93	28
	11E24E09	9160	24	2.47	10	67.19	30
	11E24F09	9160	24	2.41	10	70.11	28
Group 6	06B06D12	12030	6.25	1.63	0	23.95	21
	06B06E12	12030	6.25	1.69	0	23.87	20
	06B06F12	12030	6.25	1.47	0	22.70	16
	06E06D12	12030	6.25	1.59	6	22.82	**
	06E06E12	12030	6.25	1.63	5	22.91	19
	06E06F12	12030	6.25	1.63	6	22.96	19
	11B24D12	12030	24	2.47	0	89.85	47
	11B24E12	12030	24	2.50	0	89.22	39
	11B24F12	12030	24	2.47	0	91.57	43
	11E24D12	12030	24	2.38	15	68.51	43
	11E24E12	12030	24	2.47	7	72.62	38
	11E24F12	12030	24	2.44	11	74.28	34

See end of table for footnotes

Table 3.1

Test Results and Measured Parameters
(continued)

Group No.	Specimen Label	Concrete Strength (psi)	Develop. Length (inch)	Cover (inch)	Coating Thickness (mils)	Maximum Load (kip)	Initial Cracking Load (kip)
Group 7	06B06D14	13975	5.75	1.50	0	21.34	18
	06B06E14	13975	5.75	1.69	0	23.19	17
	06B06F14	13975	5.75	1.66	0	21.50	16
	06E06D14	13975	5.75	1.59	5	21.25	17
	06E06E14	13975	5.75	1.59	7	22.03	15
	06E06F14	13975	5.75	1.53	7	21.82	18
	11B22D14	13975	22.5	2.47	0	85.01	36
	11B22E14	13975	22.5	2.47	0	81.38	35
	11B22F14	13975	22.5	2.47	0	86.89	34
	11E22D14	13975	22.5	2.44	11	63.74	38
	11E22E14	13975	22.5	2.44	12	66.13	38
	11E22F14	13975	22.5	2.47	11	62.00	29
Group 8	08B14A06	5630	14.34	2.47	0	43.30	18
	08B14B06	5630	14.34	2.47	0	42.04	18
	08B14C06	5630	14.34	2.53	0	44.08	16
	08E14A06	5630	14.34	2.47	7	38.9	19
	08E14B06	5630	14.34	2.53	9	39.55	15
	08E14C06	5630	14.34	2.53	8	38.98	14
	G8B14A06	5630	14.34	2.50	0	41.72	20
	G8B14B06	5630	14.34	2.50	0	39.71	28
	G8E14A06	5630	14.34	2.53	8	40.47	21
	G8E14B06	5630	14.34	2.47	7	39.01	23

* Data not taken

** Initial crack occured at failure

Specimen Label: $##S%%C&&

$ = G for specimens with strain gages
(blank) for specimens without strain gages

= 06 for No. 6 bars
08 for No. 8 bars
11 for No. 11 bars

S = B for uncoated bars
E for epoxy-coated bars

%% = the development length, nearest inch

C = A,B,C (three replications for normal concrete specimens)
D,E,F (three replications for micro silica concrete specimens)

&& = Concrete compressive strength, ksi

Table 4.1

Initial Cracking Load Ratios

Group No.	Bar Size and Surface	Average Maximum Load (kip)	Average Initial Cracking Load (kip)	Initial Cracking Ratio: Uncoated/Epoxy	Ratio of Initial Cracking Load to Maximum Load
Group 1	#6 Uncoated	17.08	15.27	1.21	0.89
	#6 Epoxy	16.22	12.67		0.78
	#11 Uncoated	41.86	23.00	1.21	0.55
	#11 Epoxy	33.81	19.00		0.56
Group 2	#6 Uncoated	27.12	17.67	1.08	0.65
	#6 Epoxy	25.75	16.33		0.63
	#11 Uncoated	79.22	28.00	1.18	0.35
	#11 Epoxy	59.47	23.67		0.40
Group 3	#6 Uncoated	21.19	**	**	**
	#6 Epoxy	19.96	**		**
	#11 Uncoated	47.35	26.33	1.04	0.56
	#11 Epoxy	39.42	25.33		0.64
Group 4	#6 Uncoated	27.19	17.00	1.24	0.63
	#6 Epoxy	25.20	13.67		0.54
	#11 Uncoated	80.36	29.33	1.01	0.37
	#11 Epoxy	64.97	29.00		0.45
Group 5	#6 Uncoated	24.75	17.00	1.09	0.69
	#6 Epoxy	23.73	15.67		0.66
	#11 Uncoated	85.42	32.00	1.12	0.37
	#11 Epoxy	69.74	28.67		0.41
Group 6	#6 Uncoated	23.51	19.00	0.94	0.81
	#6 Epoxy	22.90	20.27		0.89
	#11 Uncoated	90.21	43.00	1.12	0.48
	#11 Epoxy	71.80	38.33		0.53
Group 7	#6 Uncoated	22.01	17.00	1.02	0.77
	#6 Epoxy	21.70	16.67		0.77
	#11 Uncoated	84.43	35.00	1.00	0.41
	#11 Epoxy	63.96	35.00		0.55
Group 8	#8 Uncoated	43.14	17.33	1.08	0.40
	#8 Epoxy	39.14	16.00		0.41
	#8G Uncoated	40.72	24.00	1.09	0.59
	#8G Epoxy	39.74	22.00		0.55

G = Strain gage specimen

** = Data not taken

Table 4.2

Bond Strength Ratios: Uncoated/Epoxy-Coated

Group No.	Bar Size and Surface	Average Ultimate Strength (kip)	Ultimate Strength Bond Ratio: Uncoated/Epoxy
Group 1	#6 Uncoated	17.08	1.05
	#6 Epoxy	16.22	
	#11 Uncoated	41.86	1.24
	#11 Epoxy	33.81	
Group 2	#6 Uncoated	27.12	1.05
	#6 Epoxy	25.75	
	#11 Uncoated	79.22	1.33
	#11 Epoxy	59.47	
Group 3	#6 Uncoated	21.19	1.06
	#6 Epoxy	19.96	
	#11 Uncoated	47.35	1.20
	#11 Epoxy	39.42	
Group 4	#6 Uncoated	27.19	1.08
	#6 Epoxy	25.20	
	#11 Uncoated	80.36	1.24
	#11 Epoxy	64.97	
Group 5	#6 Uncoated	24.75	1.04
	#6 Epoxy	23.73	
	#11 Uncoated	85.42	1.22
	#11 Epoxy	69.74	
Group 6	#6 Uncoated	23.51	1.03
	#6 Epoxy	22.90	
	#11 Uncoated	90.21	1.26
	#11 Epoxy	71.80	
Group 7	#6 Uncoated	22.01	1.01
	#6 Epoxy	21.70	
	#11 Uncoated	84.43	1.32
	#11 Epoxy	63.96	
Group 8	#8 Uncoated	43.14	1.10
	#8 Epoxy	39.14	
	#8-G Uncoated	40.72	1.02
	#8-G Epoxy	39.74	

G = Strain gage specimen

Table 4.3

Initial Slope of Free-End Slip Curves
No. 6 Bars

Group No.	Specimen Label	Initial Slope (kip/in)	Average Initial Slope (kip/in)	COV (%)	Initial Slope Ratio **
Group 1	06B06A06	20451			
	06B06B06	21942			
	06B06C06	21079	21158	2.9	
	06E06A06	19165			
	06E06B06	19591			
	06E06C06	16710	18488	6.9	1.14
Group 2	06B08A10	39635			
	06B08B10	*			
	06B08C10	45218	42426	6.6	
	06E08A10	34534			
	06E08B10	32353			
	06E08C10	27338	31408	9.6	1.35
Group 3	06B06D08	*			
	06B06E08	*			
	06B06F08	23007	23007		
	06E06D08	22141			
	06E06E08	19467			
	06E06F08	18300	19969	8.1	1.15
Group 4	06B08D10	37298			
	06B08E10	31598			
	06B08F10	37353	35416	7.6	
	06E08D10	33322			
	06E08E10	31080			
	06E08F10	36836	33746	7.0	1.05
Group 5	06B07D09	28375			
	06B07E09	33475			
	06B07F09	26488	29446	10.0	
	06E07D09	26604			
	06E07E09	25056			
	06E07F09	28657	26772	5.5	1.10
Group 6	06B06D12	26164			
	06B06E12	25581			
	06B06F12	29999	27248	7.2	
	06E06D12	12828			
	06E06E12	16475			
	06E06F12	11966	13756	14.2	1.98
Group 7	06B06D14	28008			
	06B06E14	31052			
	06B06F14	28079	29046	4.9	
	06E06D14	19279			
	06E06E14	13829			
	06E06F14	21236	18115	17.3	1.60

* = No data due to instrumentation problems
** = Uncoated/Epoxy
G = Strain Gage Specimen
COV = Coefficient of Variation

Table 4.4

Initial Slope of Free-End Slip Curves
No. 11 Bars

Group No.	Specimen Label	Initial Slope (kip/in)	Average Initial Slope (kip/in)	COV (%)	Initial Slope Ratio **
Group 1	11B11A06	*			
	11B11B06	*			
	11B11C06	*	*	*	
	11E11A06	*			
	11E11B06	*			
	11E11C06	*	*	*	*
Group 2	11B24A10	91580			
	11B24B10	82452			
	11B24C10	100330	91454	8.0	
	11E24A10	60452			
	11E24B10	86268			
	11E24C10	72617	73112	14.4	1.25
Group 3	11B11D08	*			
	11B11E08	*			
	11B11F08	*	*	*	
	11E11D08	*			
	11E11E08	*			
	11E11F08	*	*	*	*
Group 4	11B24D10	94726			
	11B24E10	85864			
	11B24F10	118626	99739	13.9	
	11E24D10	126075			
	11E24E10	102457			
	11E24F10	82781	103771	17.1	0.96
Group 5	11B24D09	87488			
	11B24E09	92057			
	11B24F09	102725	94090	6.8	
	11E24D09	76488			
	11E24E09	81092			
	11E24F09	93258	83613	8.5	1.13
Group 6	11B24D12	84588			
	11B24E12	85765			
	11B24F12	92560	87638	4.0	
	11E24D12	84479			
	11E24E12	81706			
	11E24F12	108156	91447	13.0	0.96
Group 7	11B22D14	99589			
	11B22E14	101394			
	11B22F14	98713	99898	1.1	
	11E22D14	78009			
	11E22E14	83975			
	11E22F14	89679	83888	5.7	1.19

* = No data due to instrumentation problems
** = Uncoated/Epoxy
G = Strain Gage Specimen
COV = Coefficient of Variation

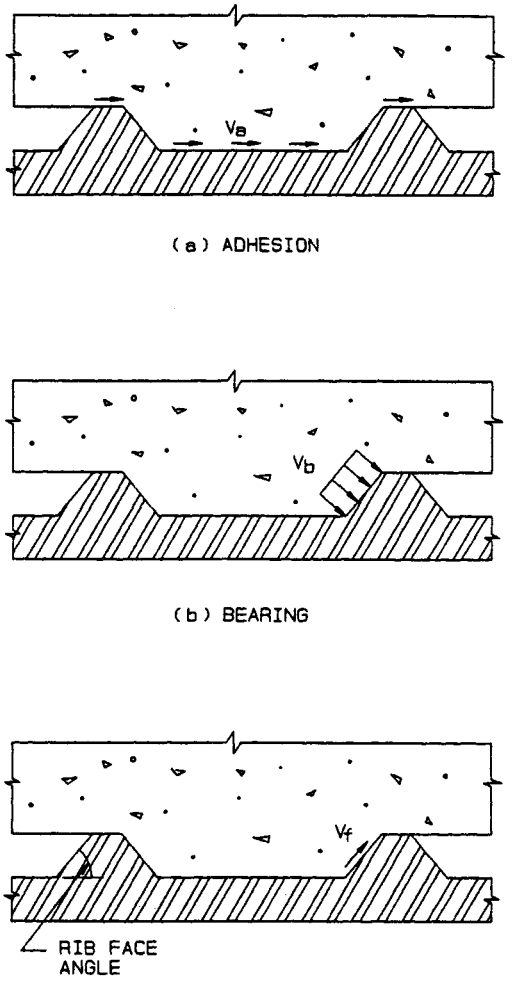

Figure 1.1 Bond Mechanisms for Deformed Reinforcement in Concrete

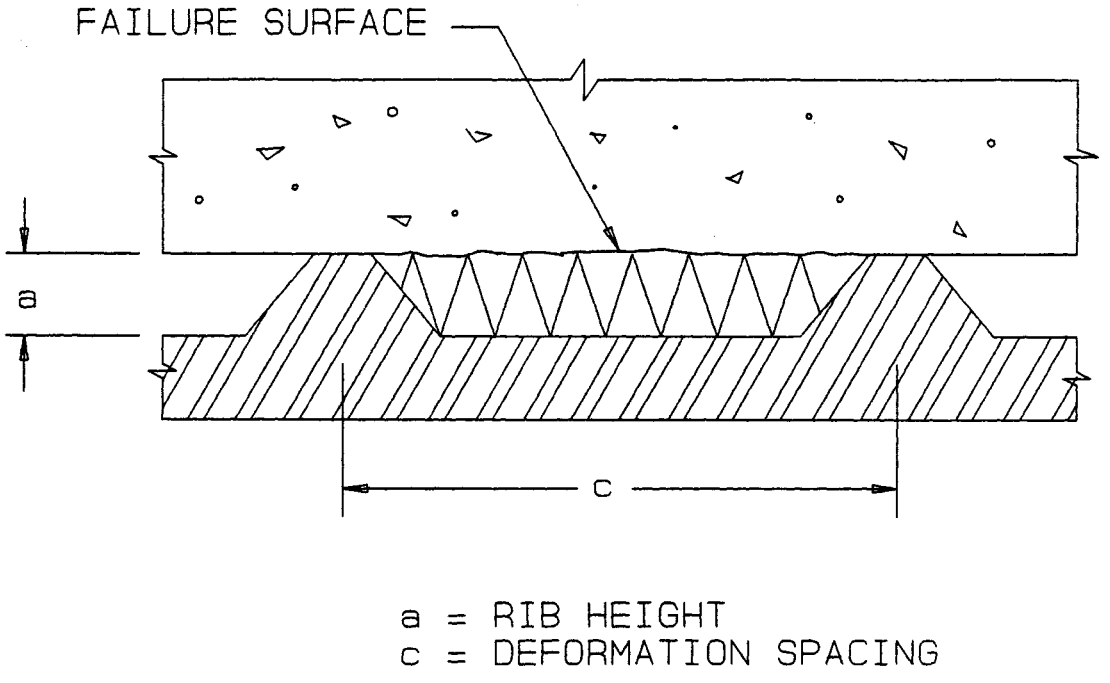

Figure 1.2 Pull Out Type Bond Failure

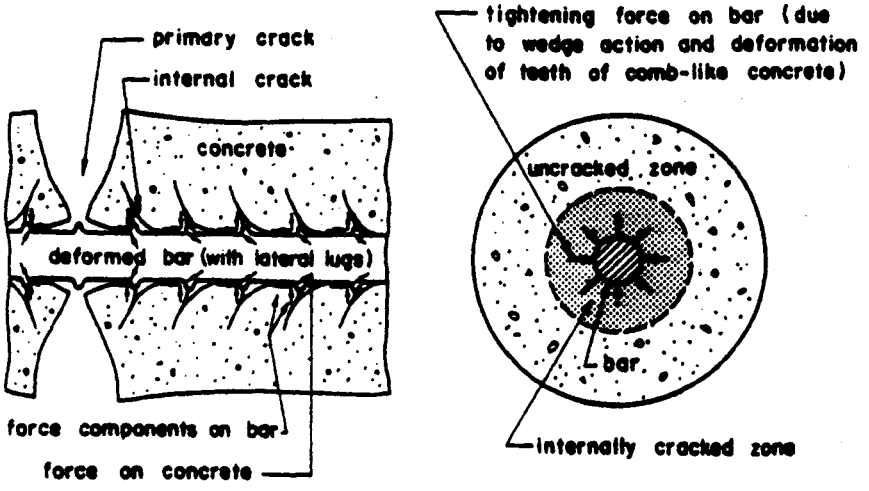

[Eligahausen, 1983].

Figure 1.3 Splitting Type Bond Failure

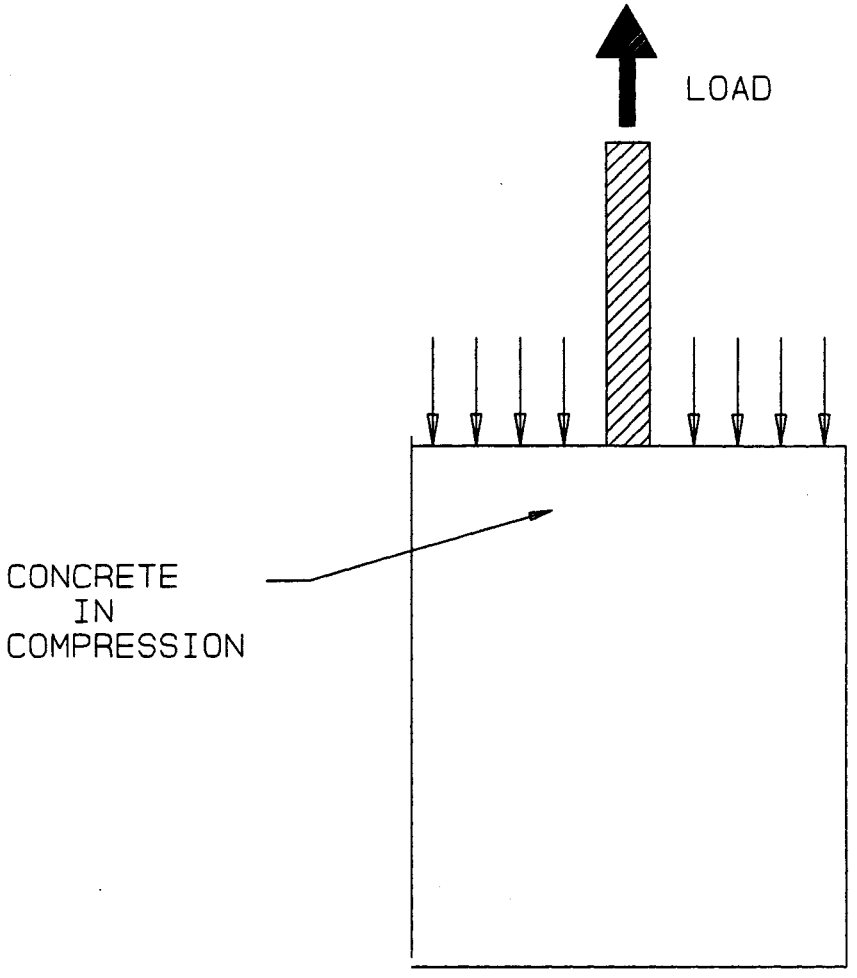

Figure 1.4 Pull Out Type Bond Specimen

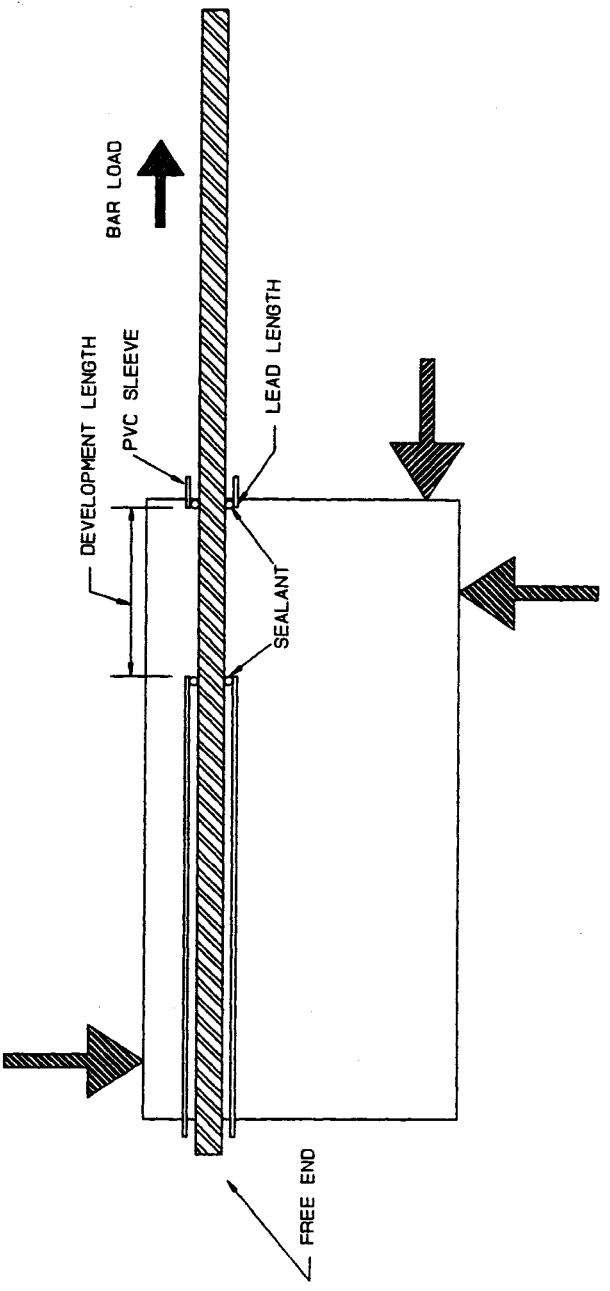

Figure 1.5 Inverted Half-Beam Bond Specimen

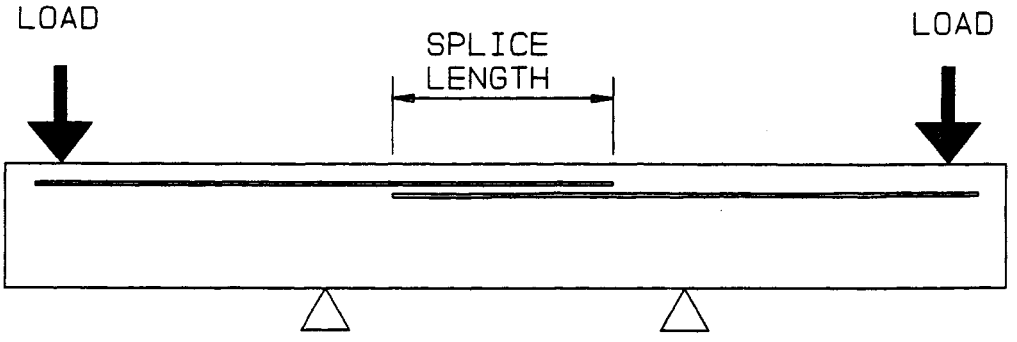

Figure 1.6 Splice Type Bond Specimen

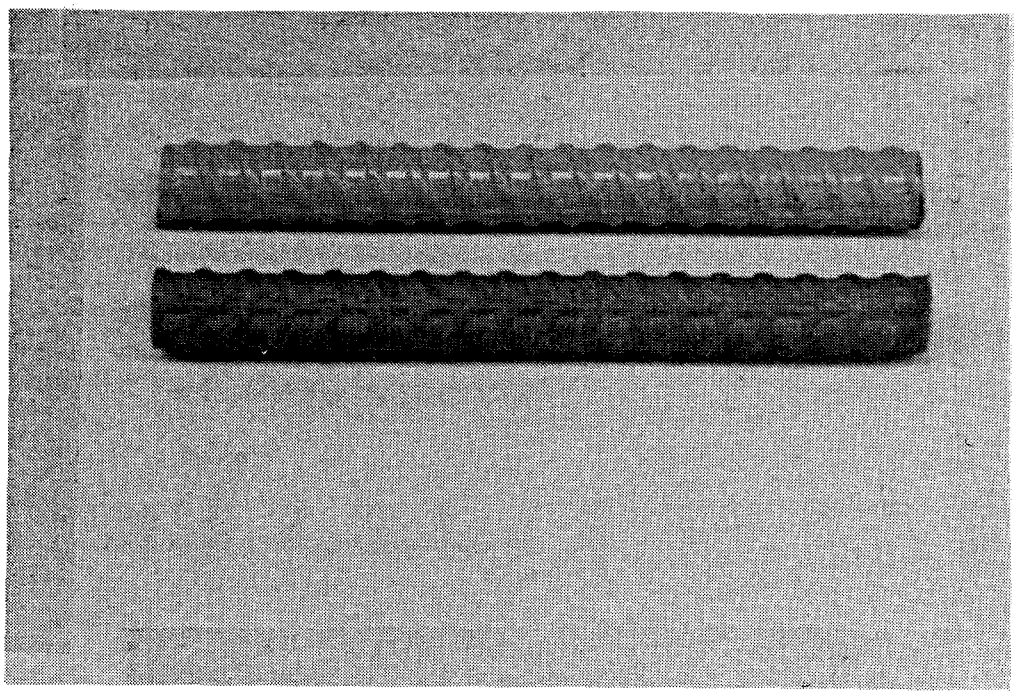

Figure 2.1 Test Bars

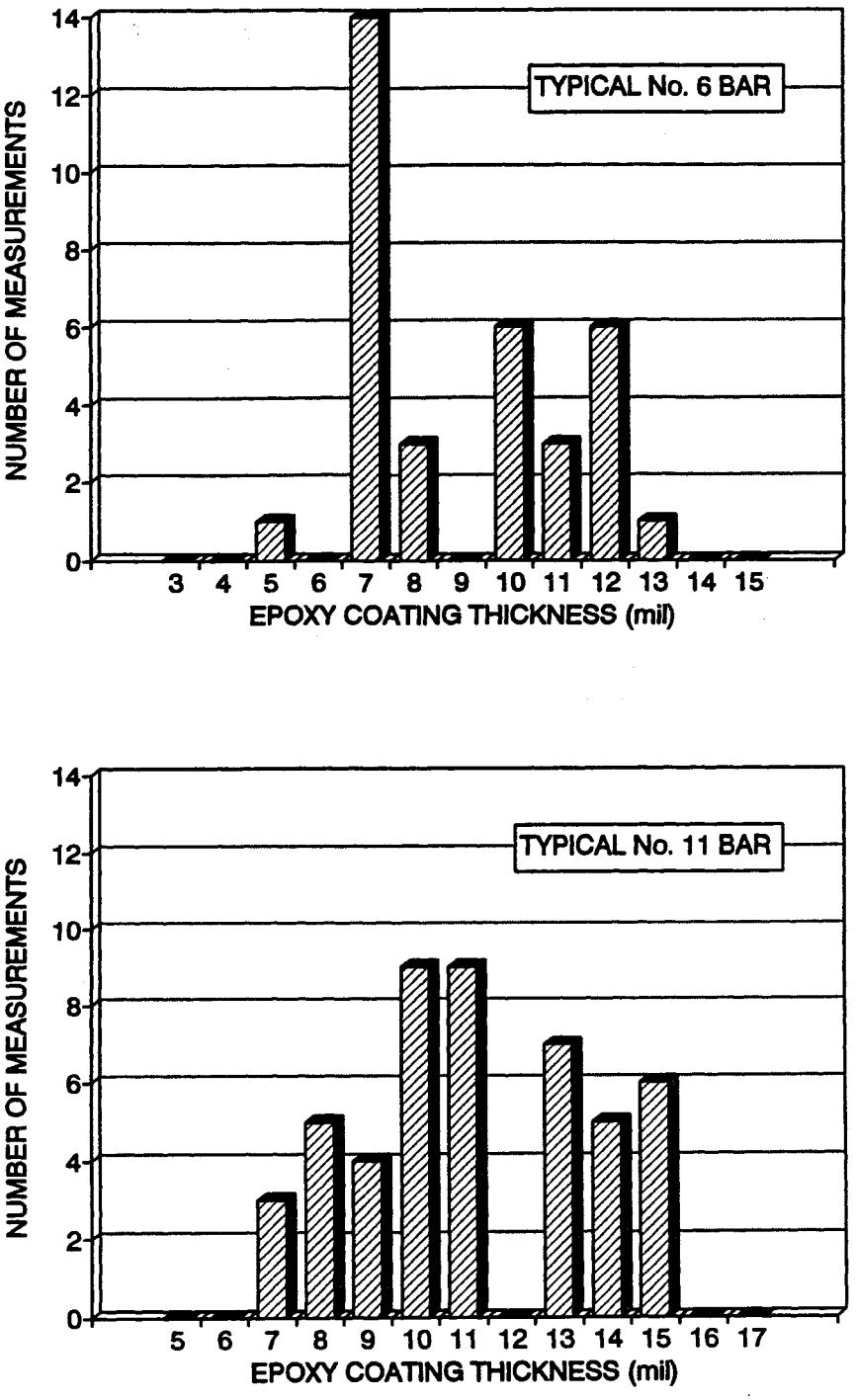

Figure 2.2 Typical Coating Thickness Distribution

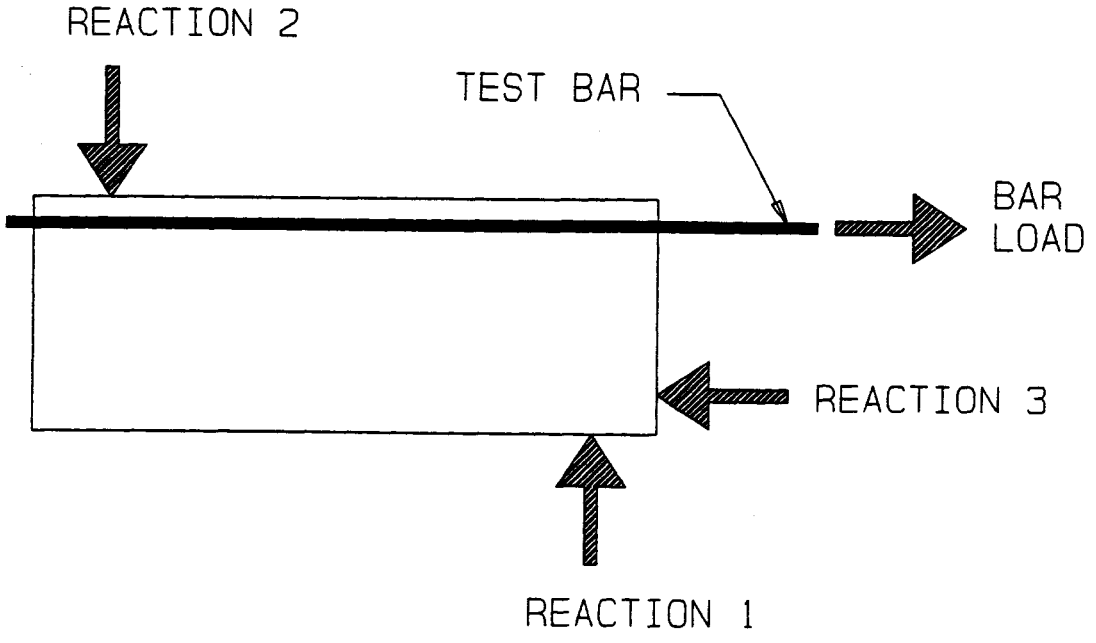

Figure 2.3 Schematic of Inverted Half-Beam Specimen with Resultant Forces

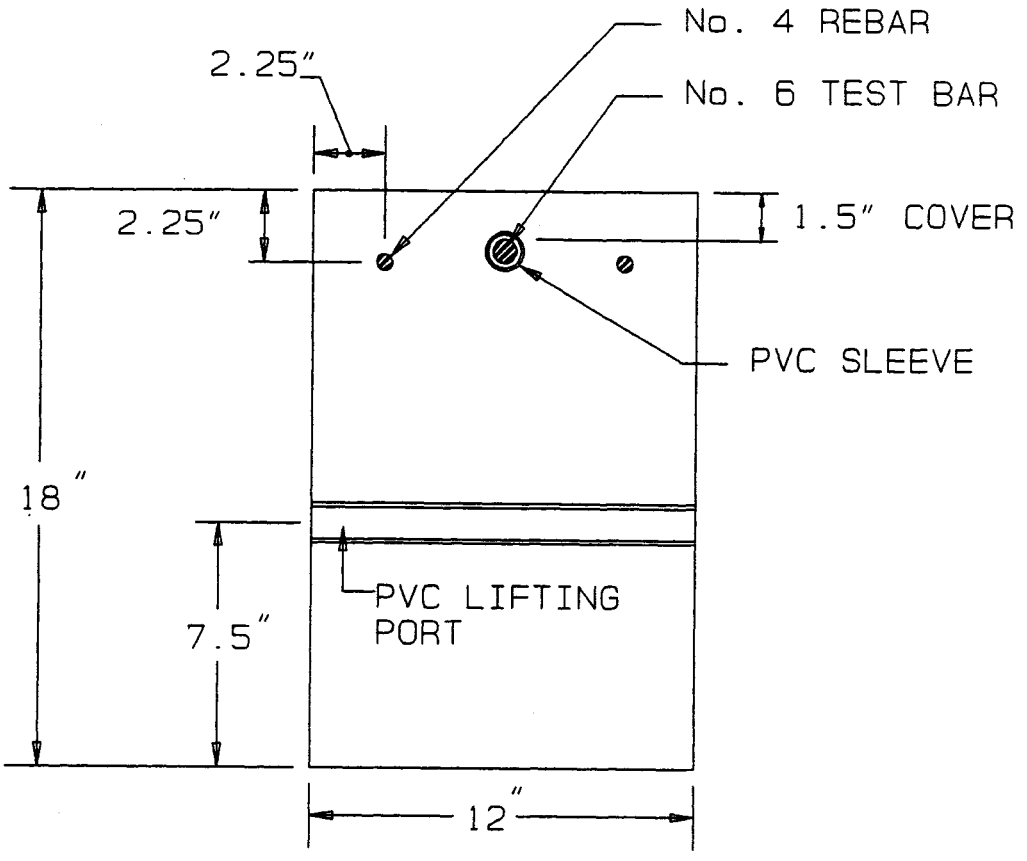

Figure 2.4 Cross Section of No. 6 Test Bar Specimen

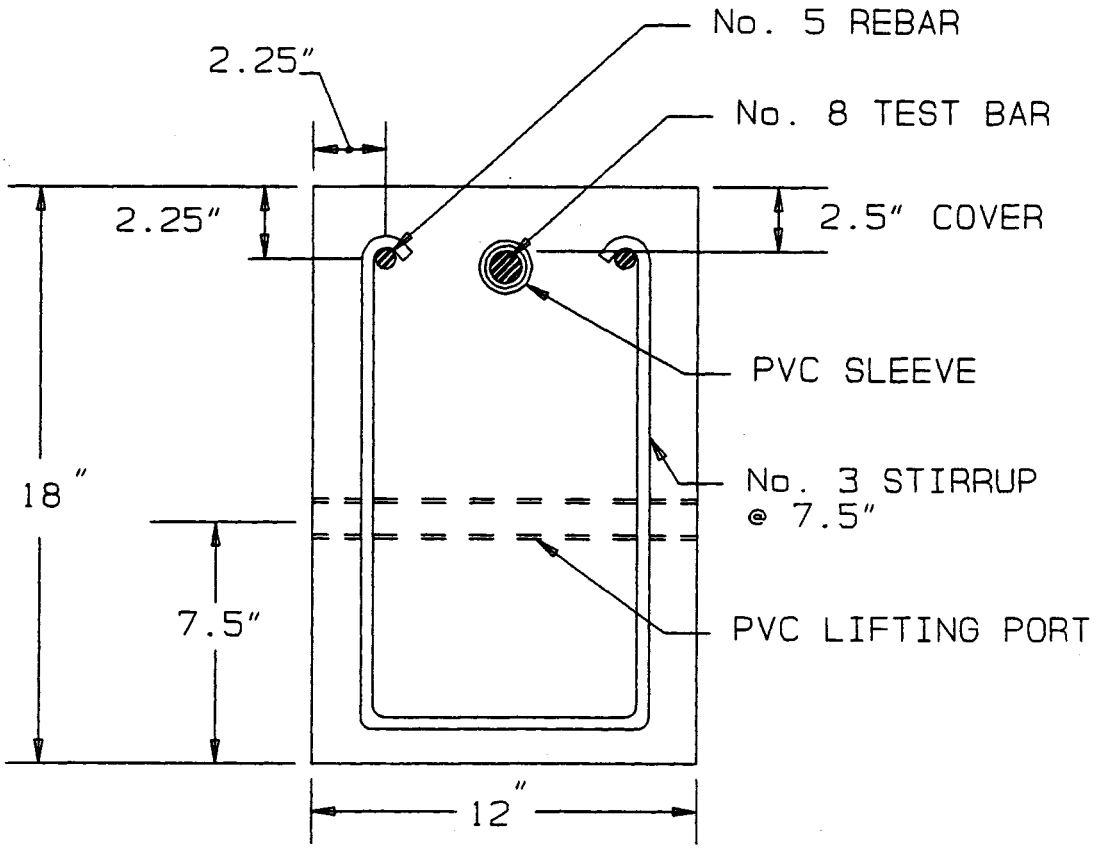

Figure 2.5 Cross Section of No. 8 Test Bar Specimen

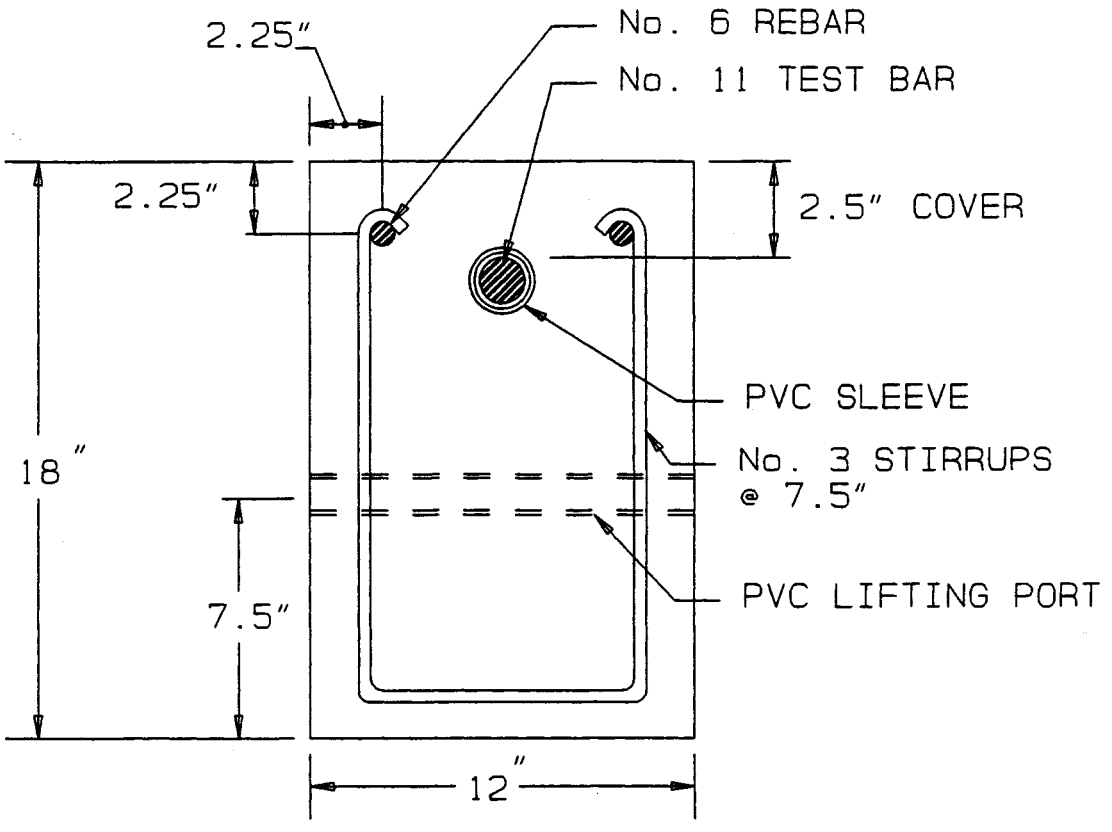

Figure 2.6 Cross Section of No. 11 Test Bar Specimen

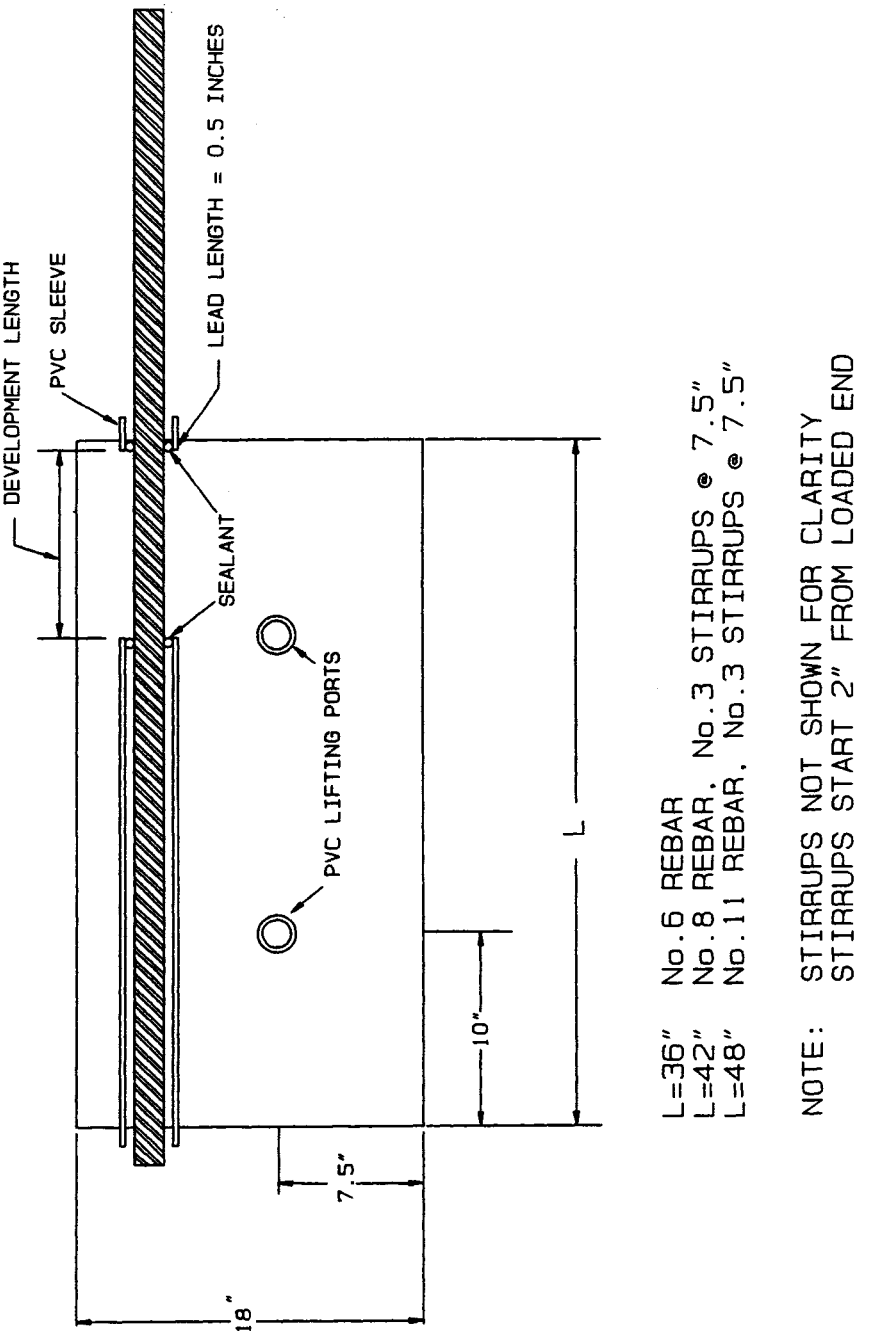

Figure 2.7 Typical Specimen Elevation

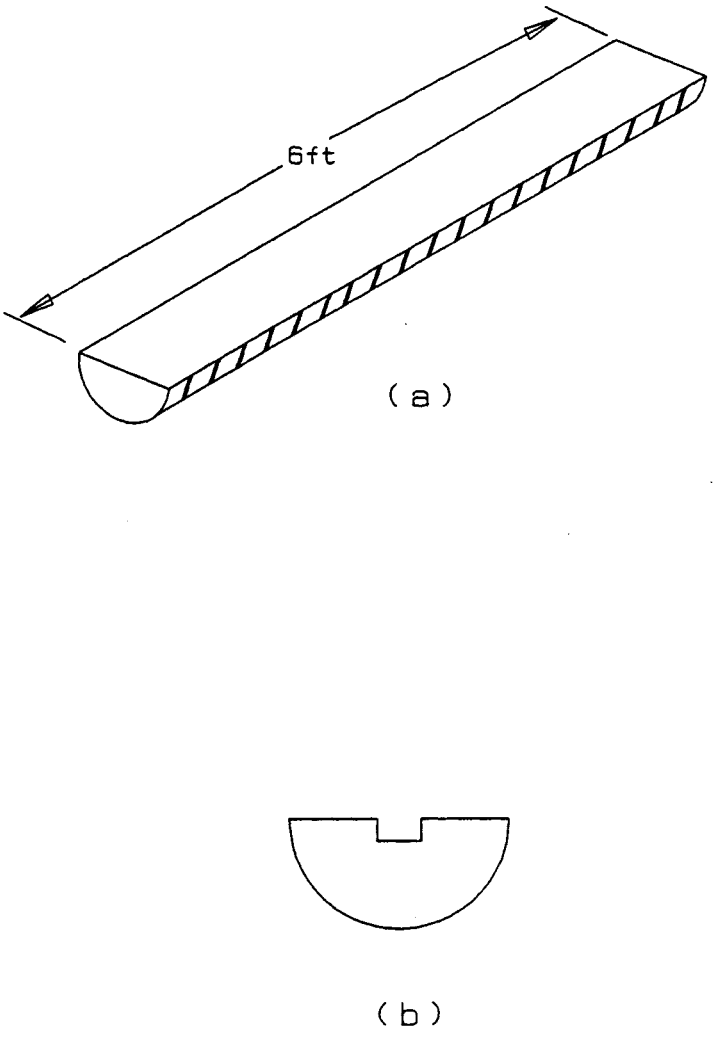

Figure 2.8 Bar Fabrication. (a) No. 8 Bar Milled in Half (b) Cross Section of Grooved No. 8 Half Bar

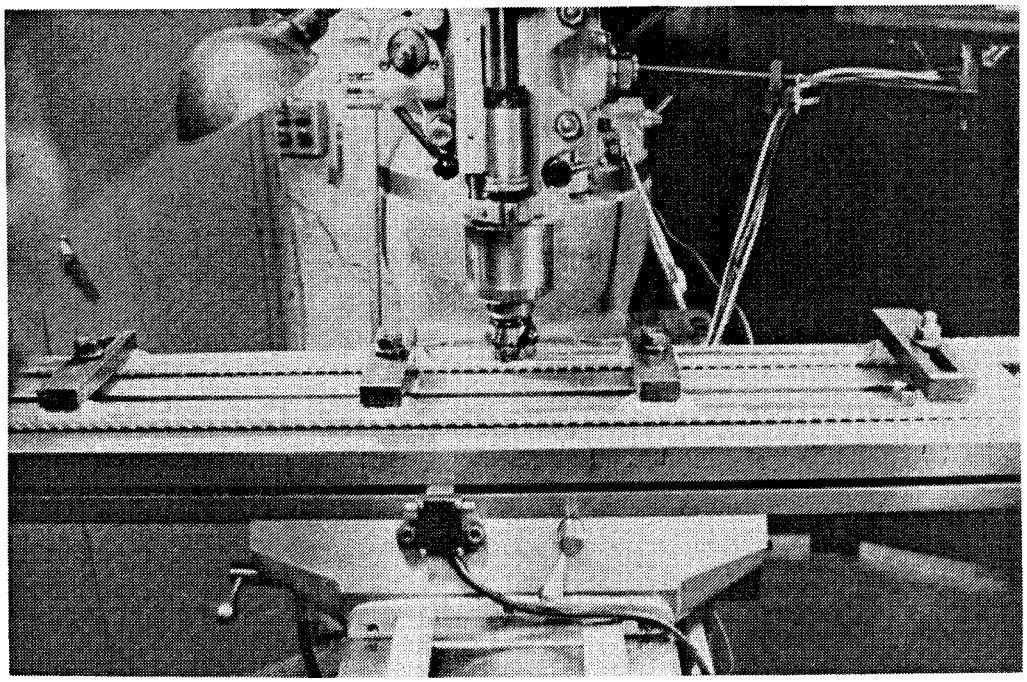

Figure 2.9 No. 8 Bars Being Milled in Half

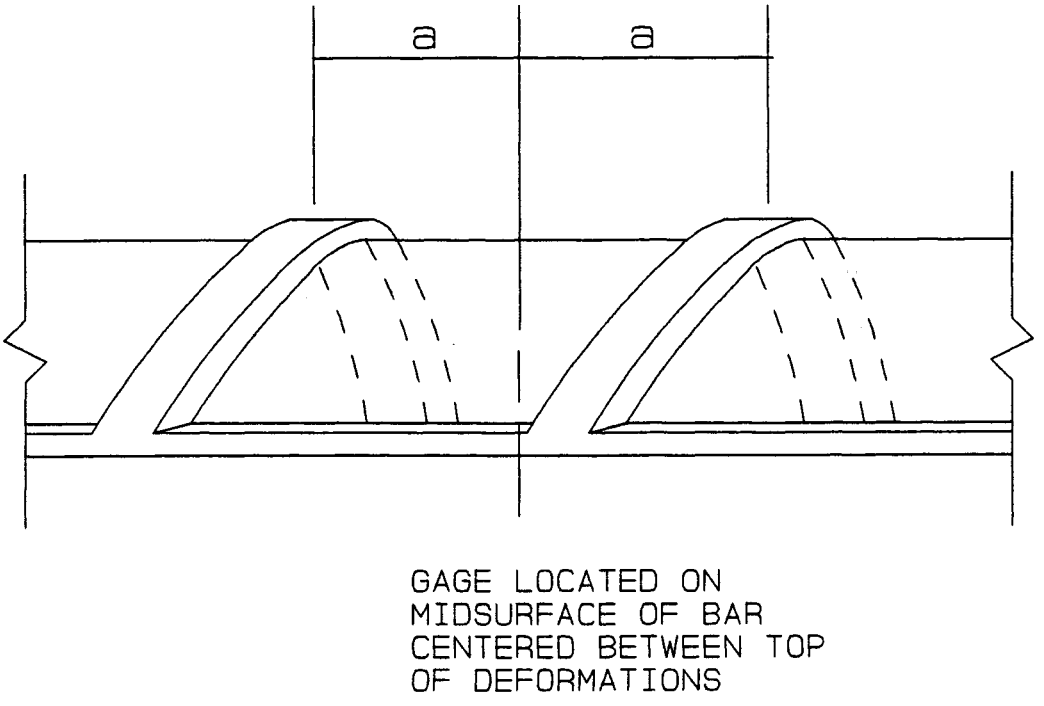

Figure 2.10 Strain Gage Position Relative to the Rebar Deformation

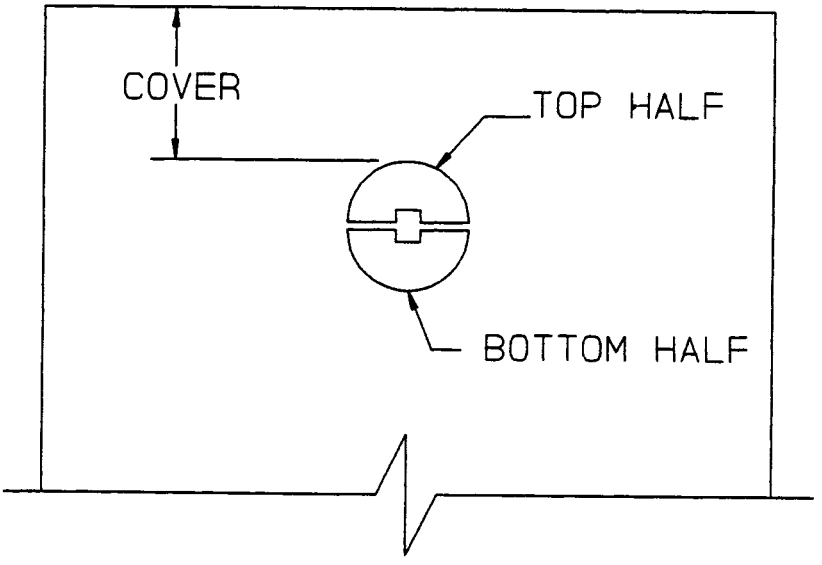

Figure 2.11 Half Bar Orientation for Strain Gage Specimens

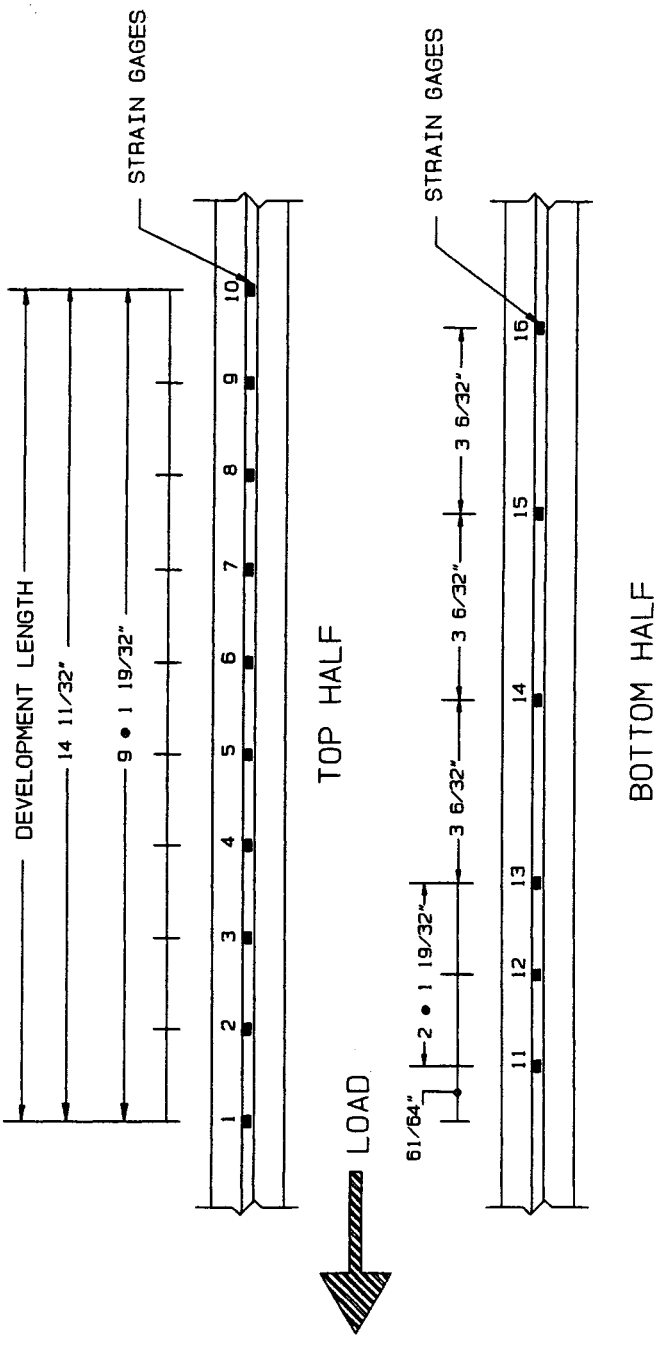

Figure 2.12 Strain Gage Layout and Strain Gage Numbering System

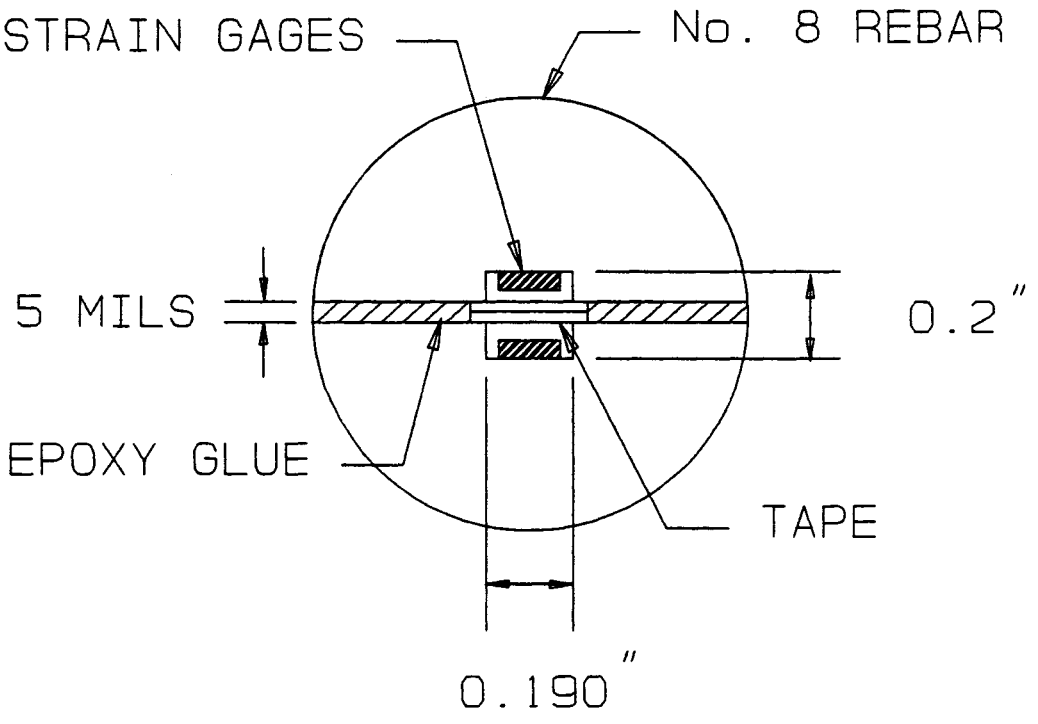

Figure 2.13 Cross Section of Glued Strain Gage Bar

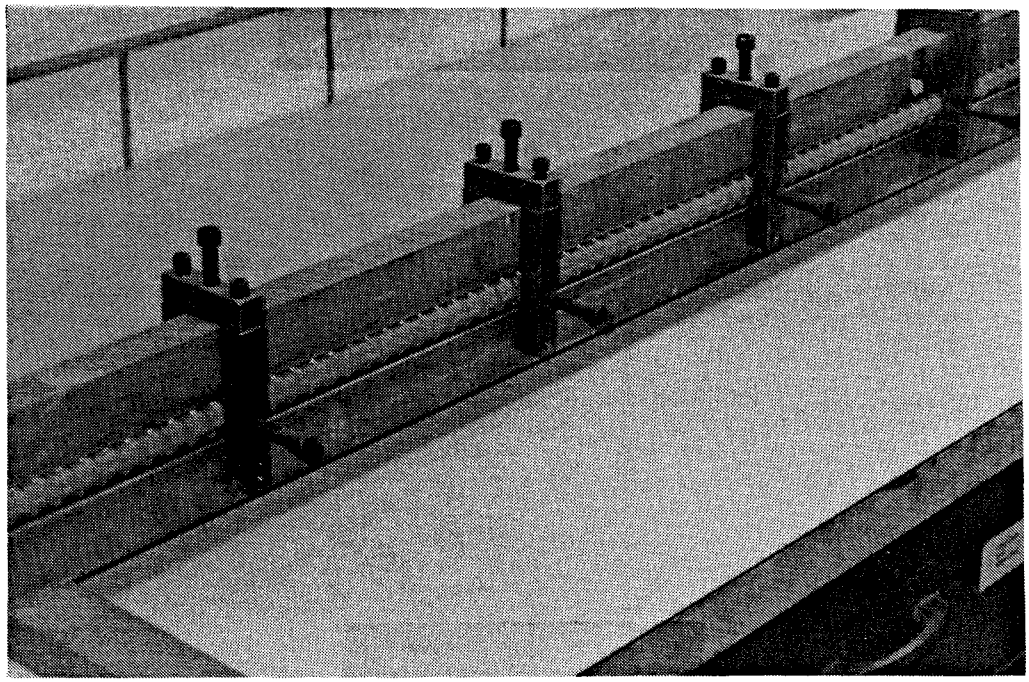

Figure 2.14 Clamping Jig used for Gluing Half Bars

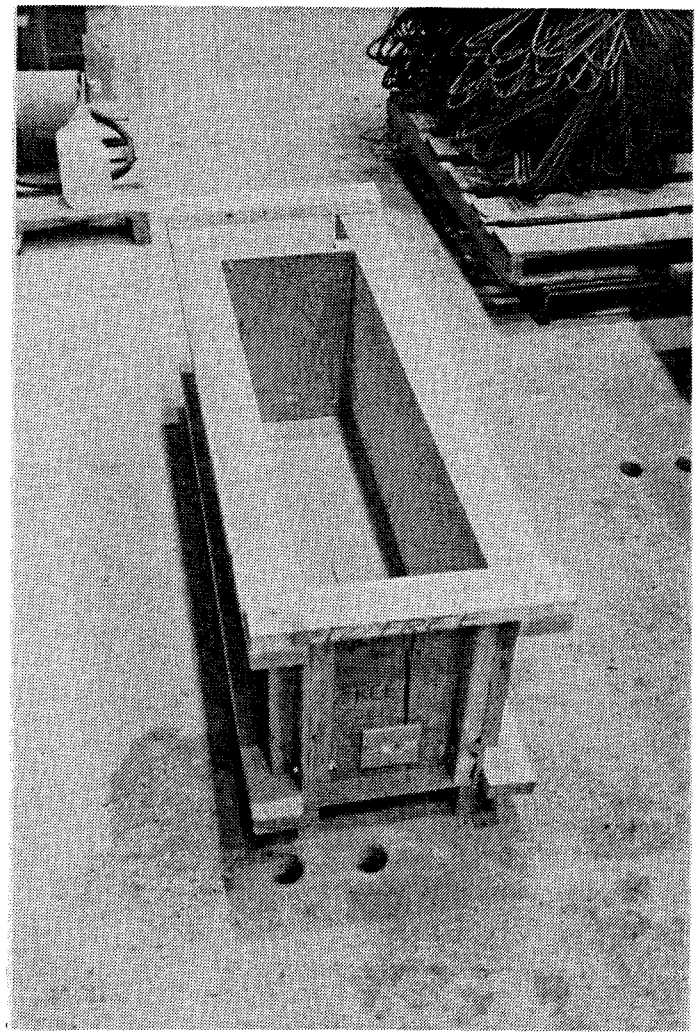

Figure 2.16 Concrete Forms used for Casting Specimens

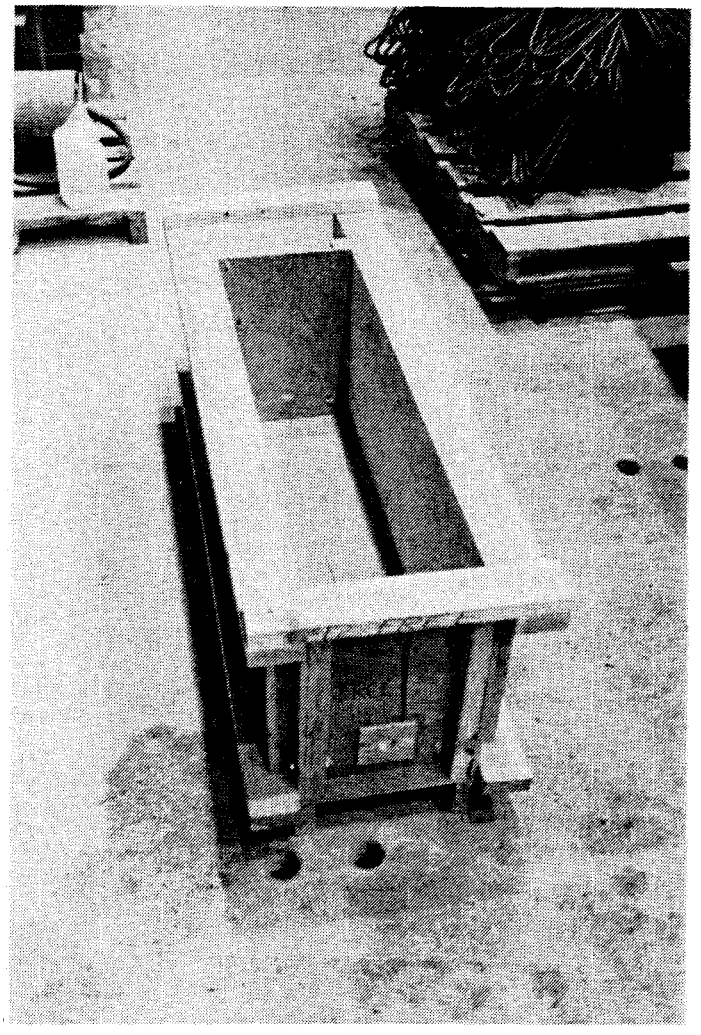

Figure 2.16 Concrete Forms used for Casting Specimens

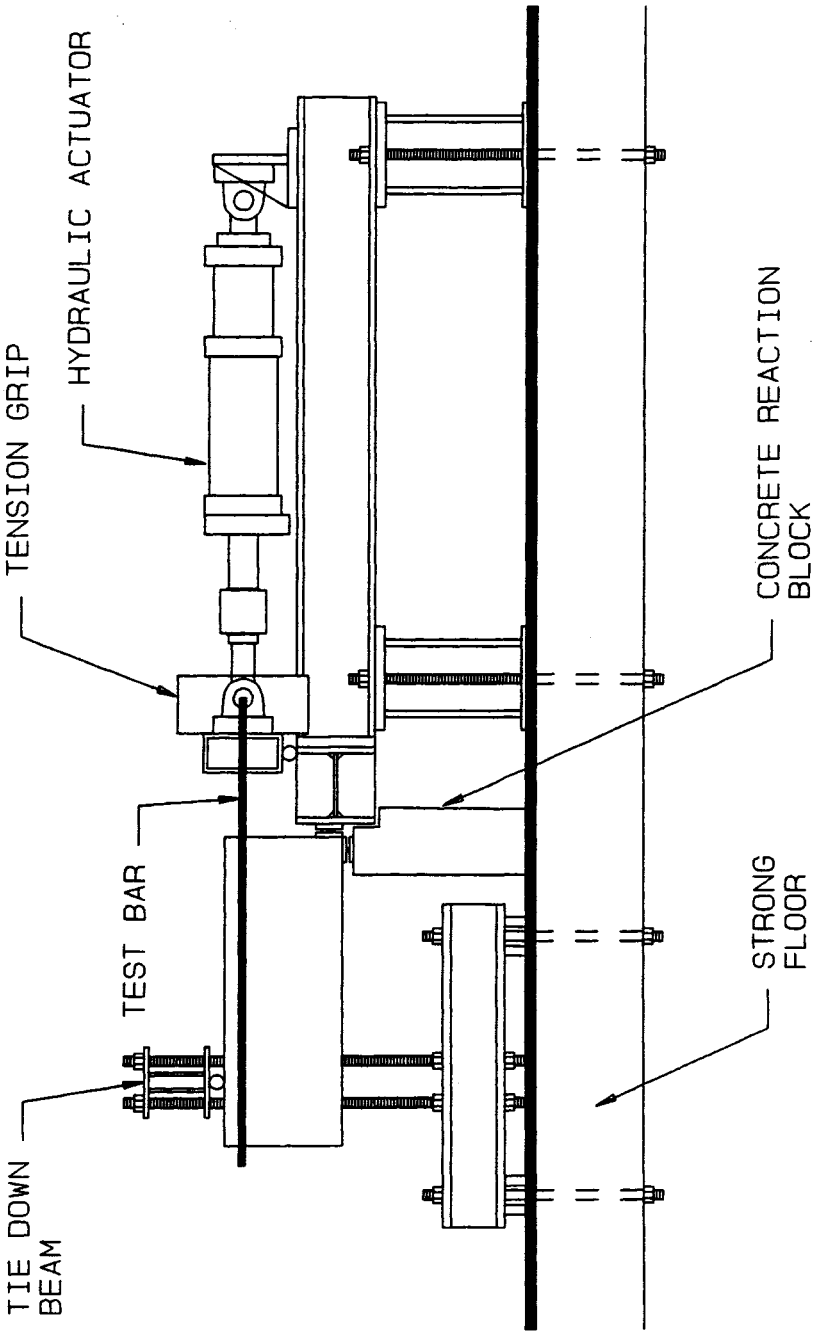

Figure 2.17 Testing Frame, Side View

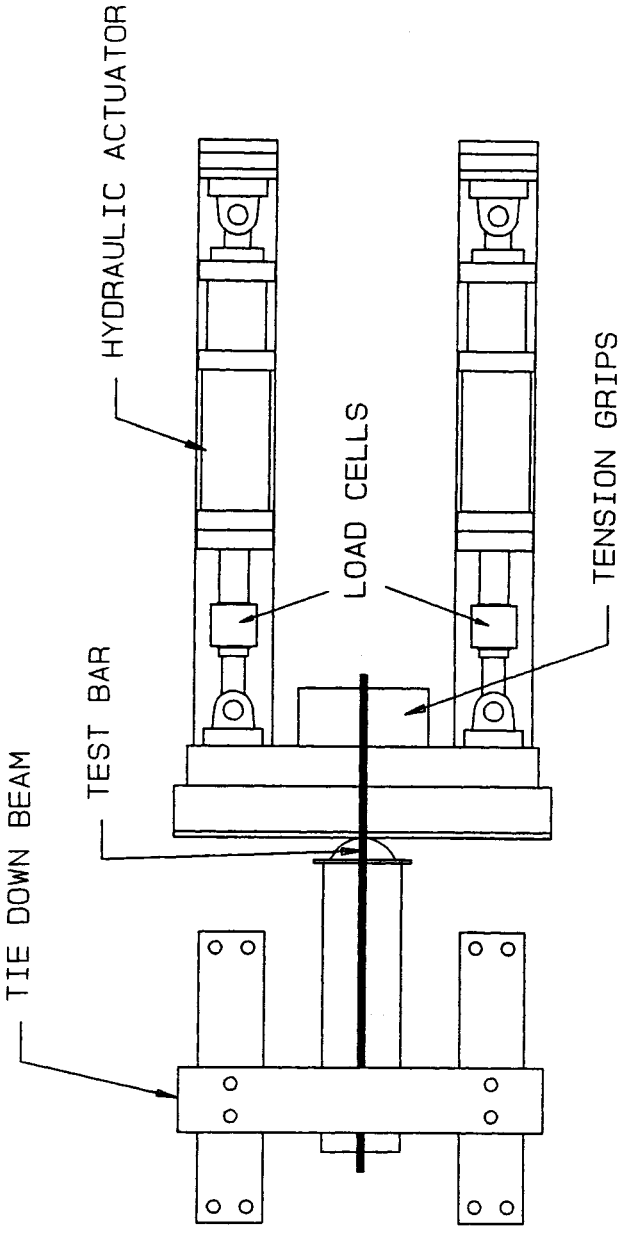

Figure 2.18 Testing Frame, Top View

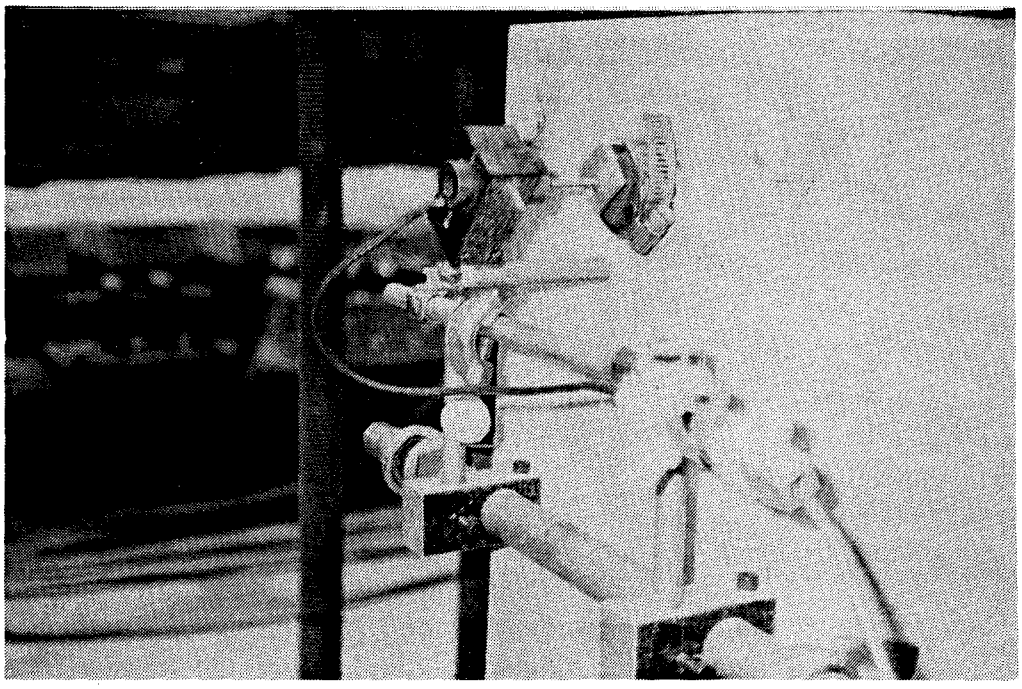

Figure 2.19 Free End Slip Instrumentation

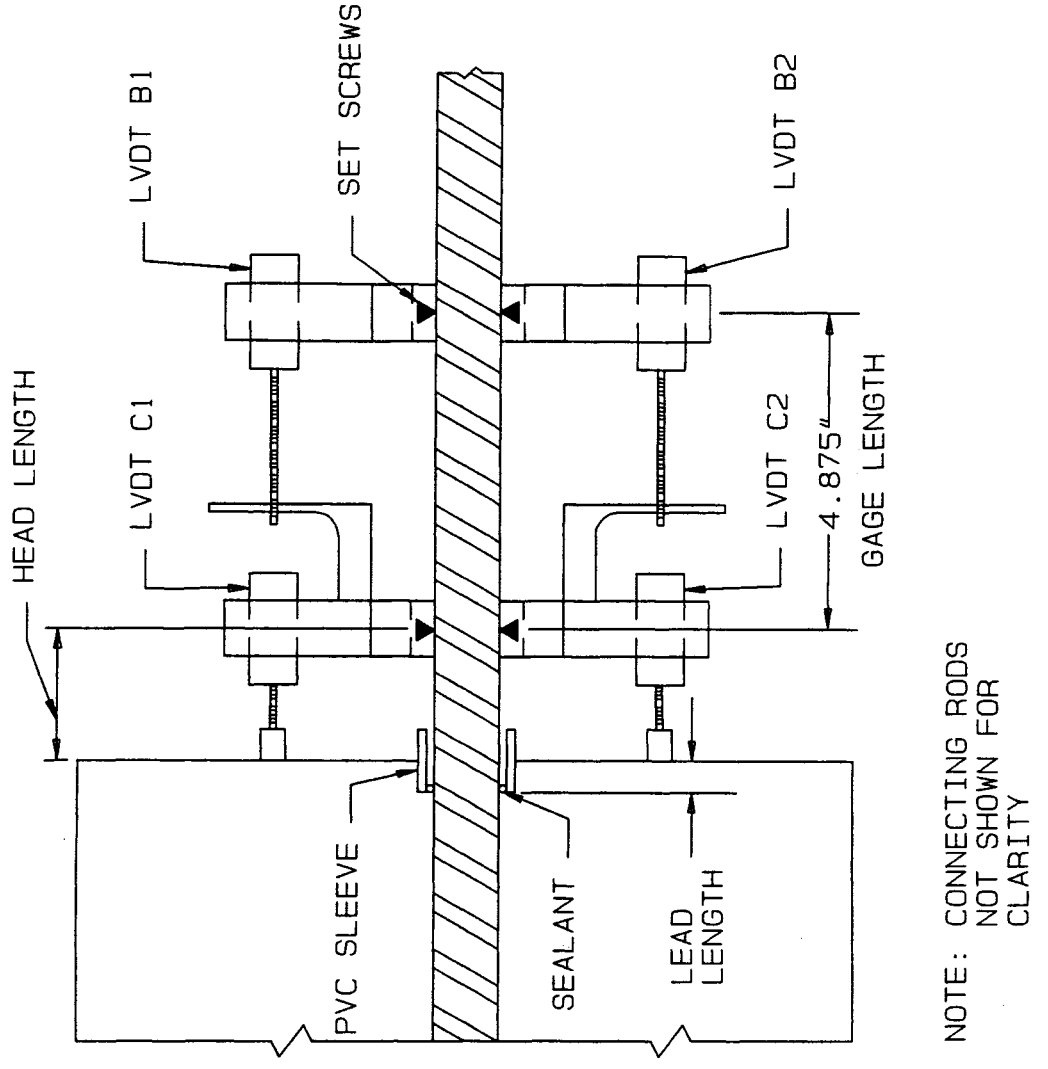

Figure 2.20 Loaded-End Slip Instrumentation

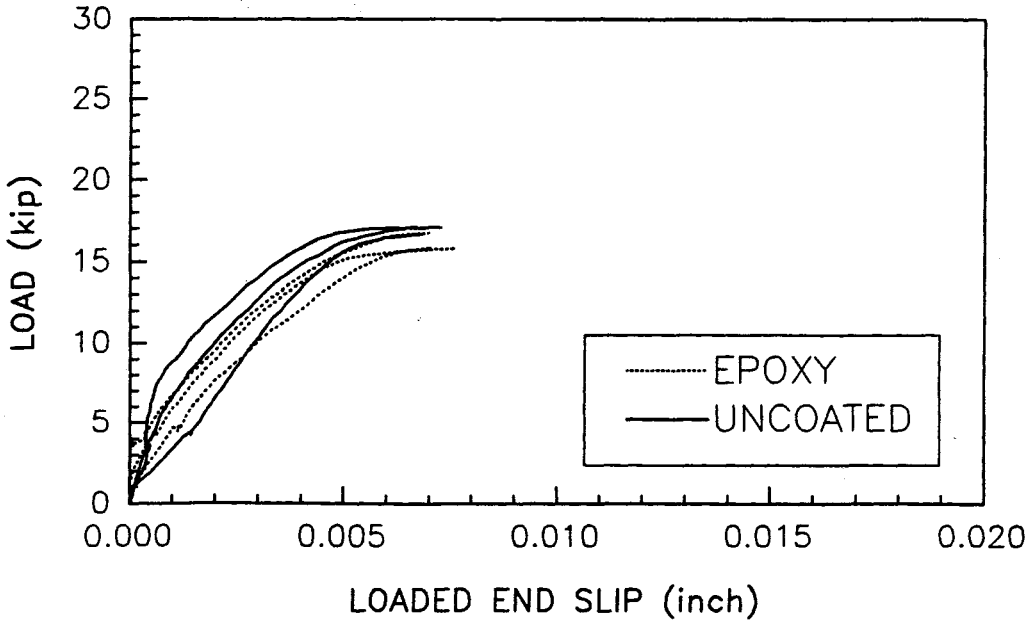

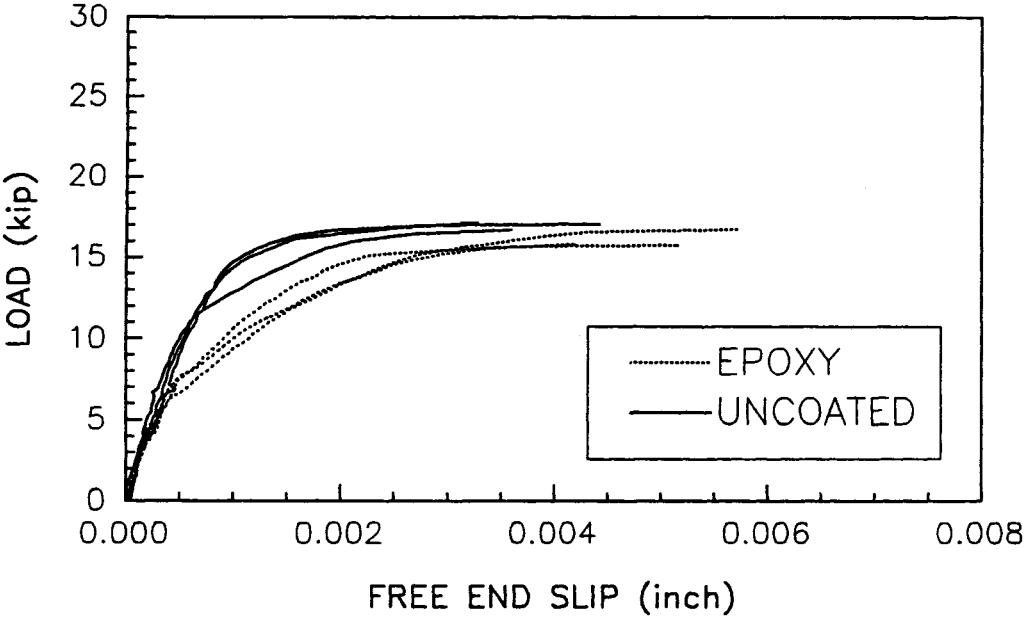

Figure 3.1 Rebar Slip Curves for Group 1, No. 6 Bars.

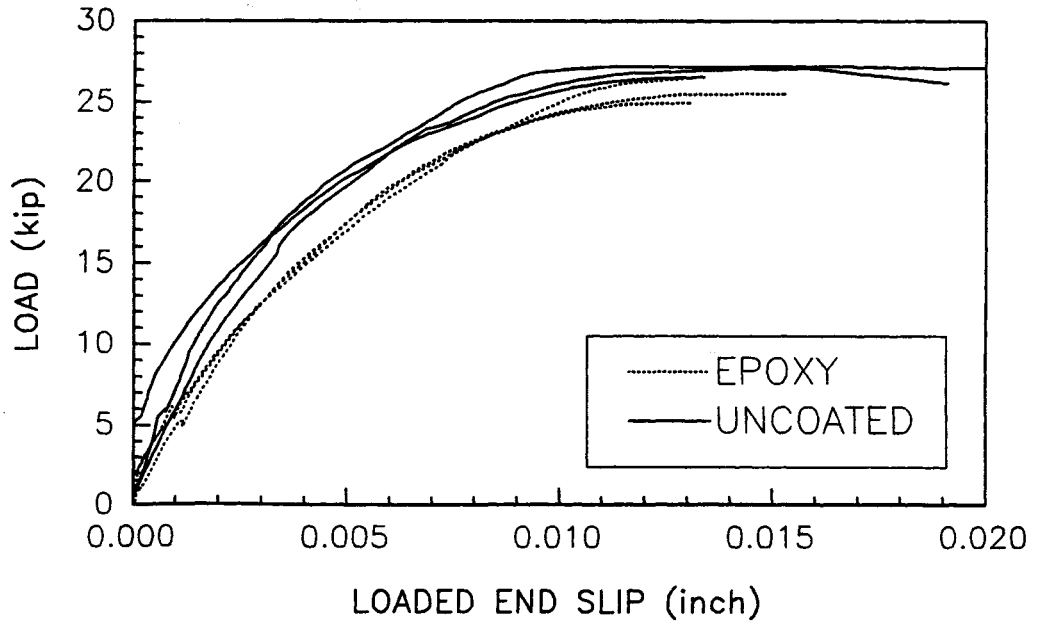

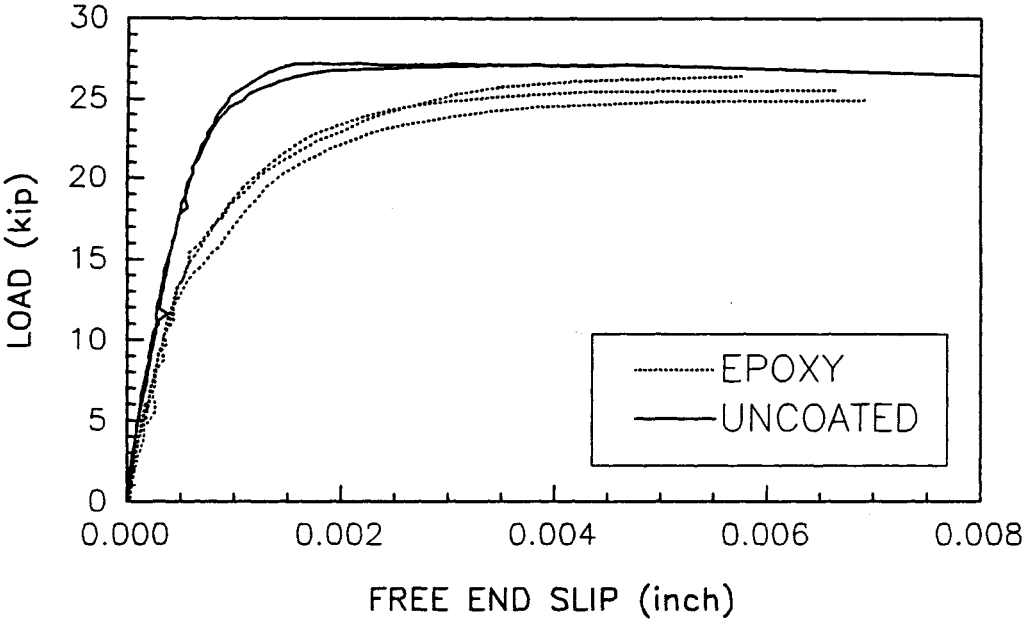

Figure 3.2 Rebar Slip Curves for Group 2, No. 6 Bars.

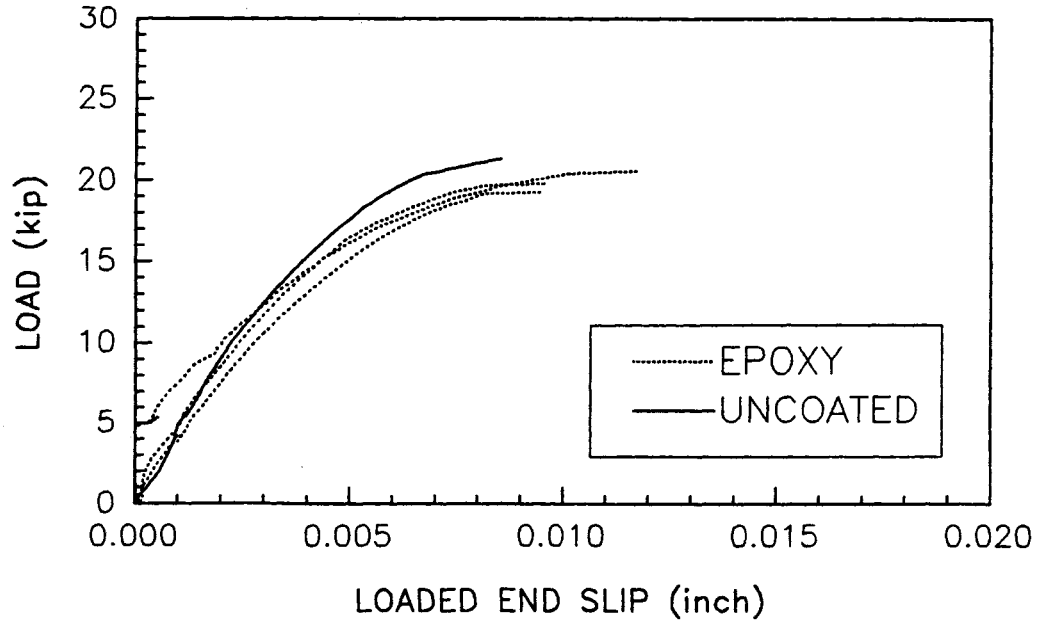

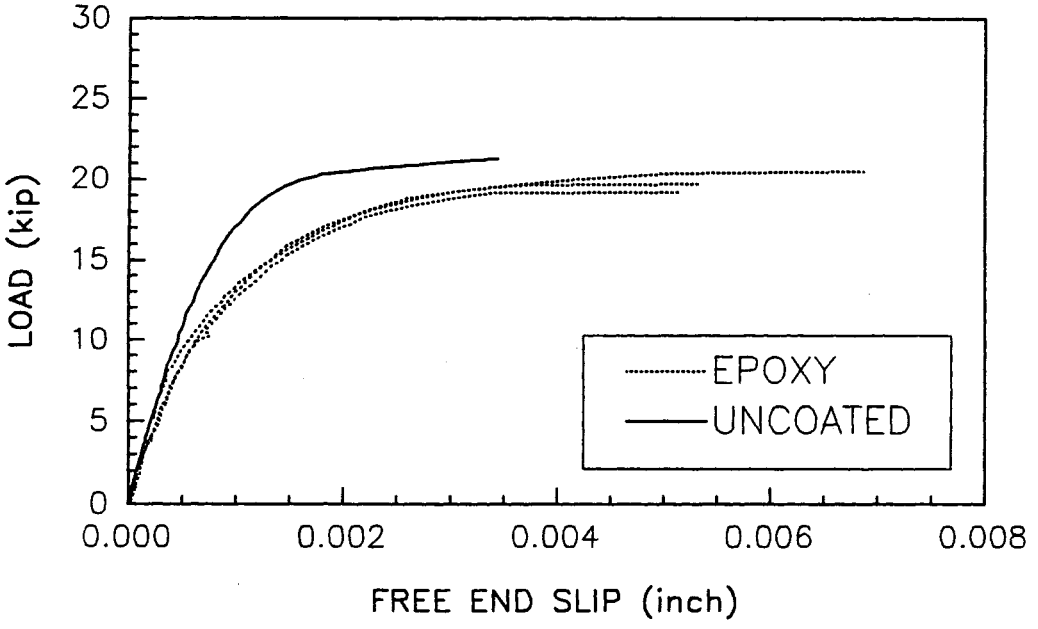

Figure 3.3 Rebar Slip Curves for Group 3, No. 6 Bars.

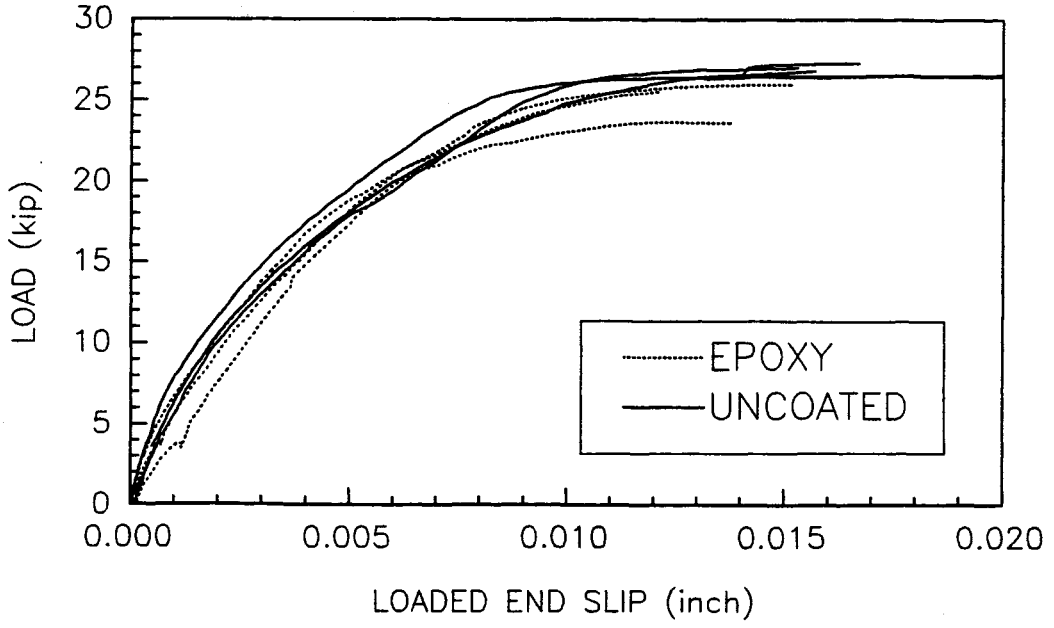

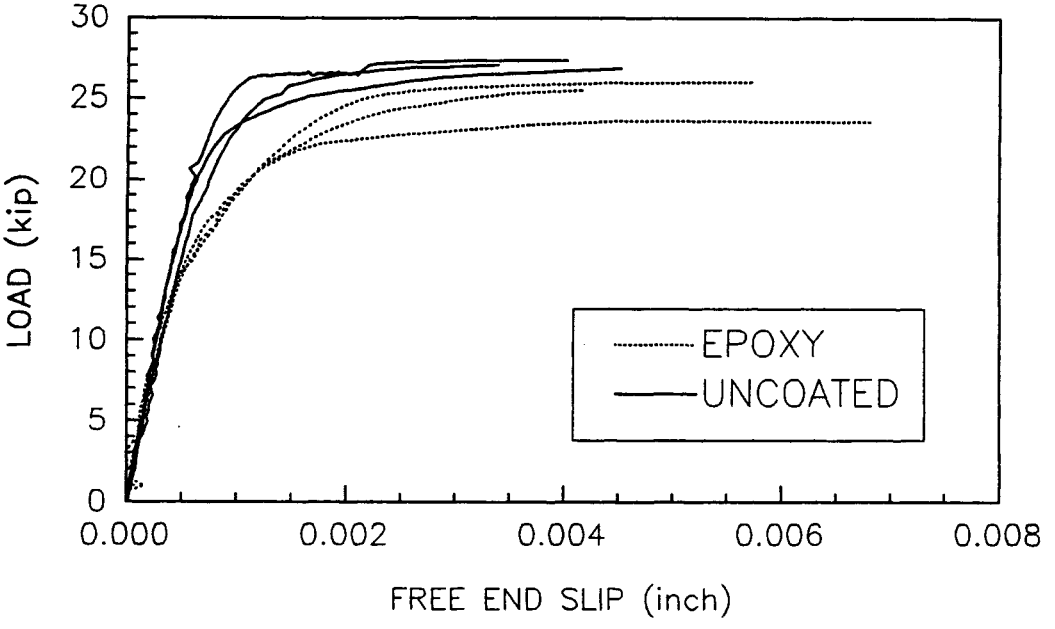

Figure 3.4 Rebar Slip Curves for Group 4, No. 6 Bars.

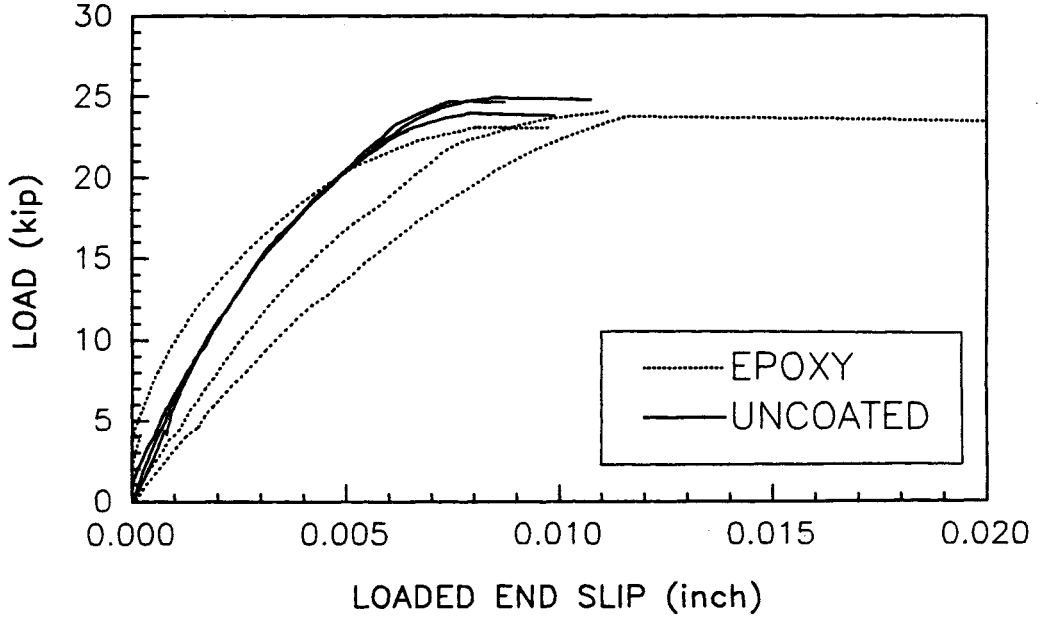

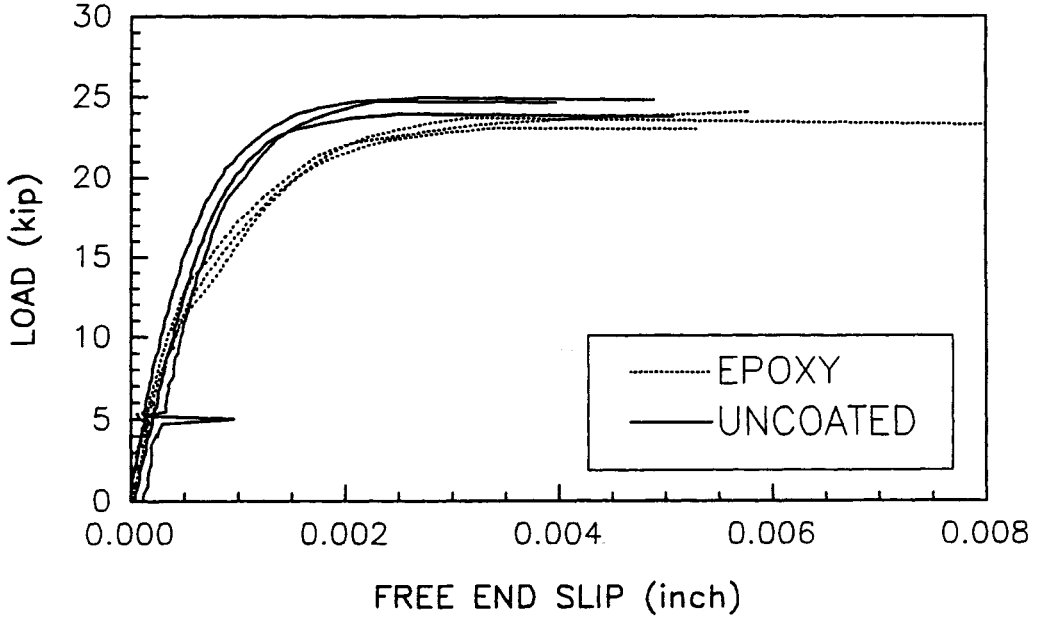

Figure 3.5 Rebar Slip Curves for Group 5, No. 6 Bars.

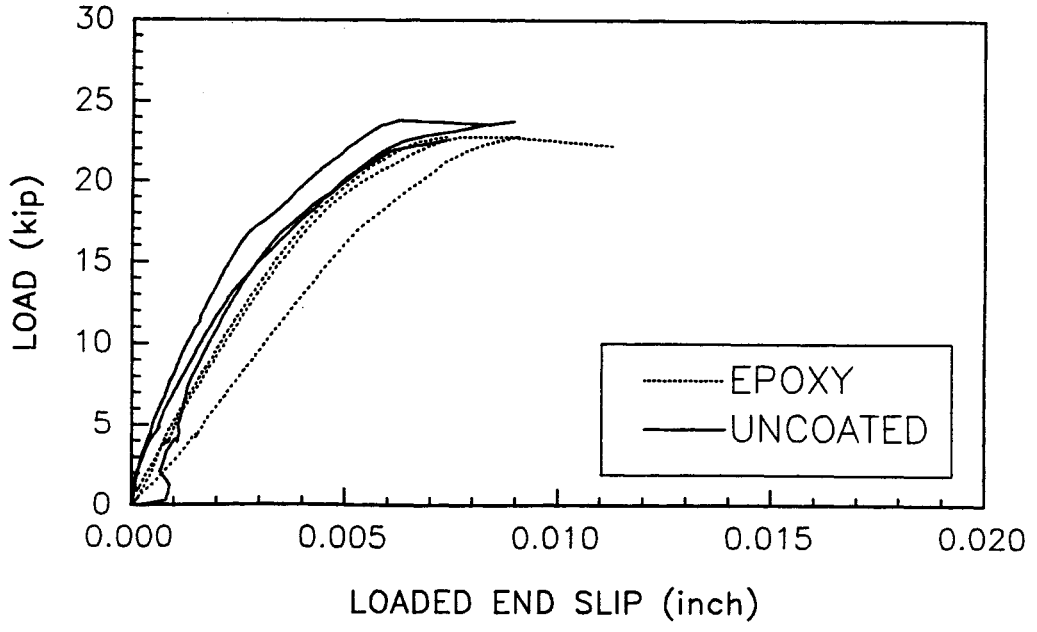

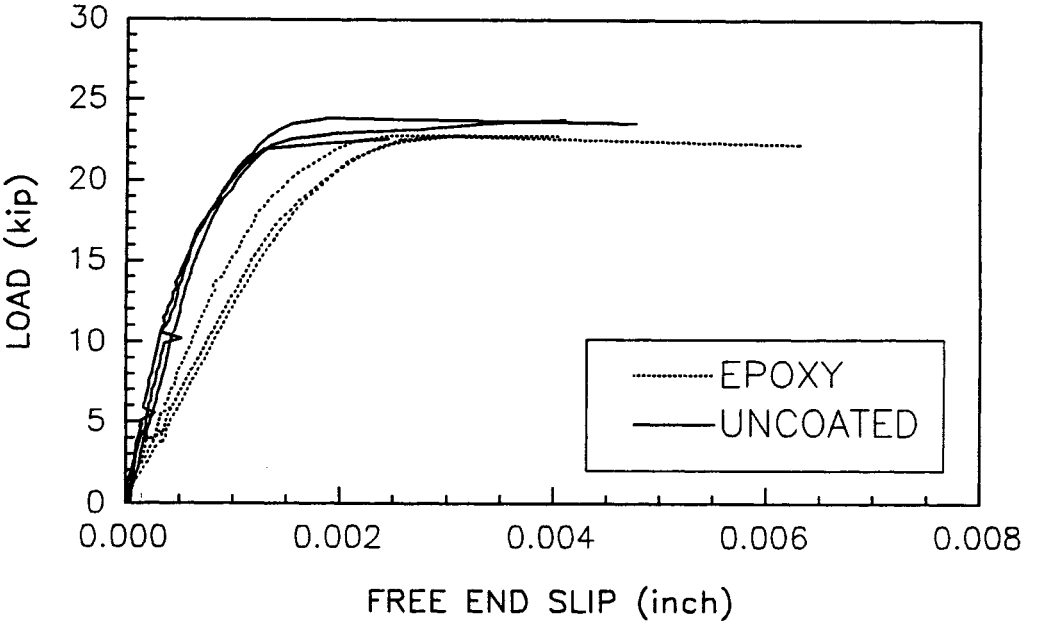

Figure 3.6 Rebar Slip Curves for Group 6, No. 6 Bars.

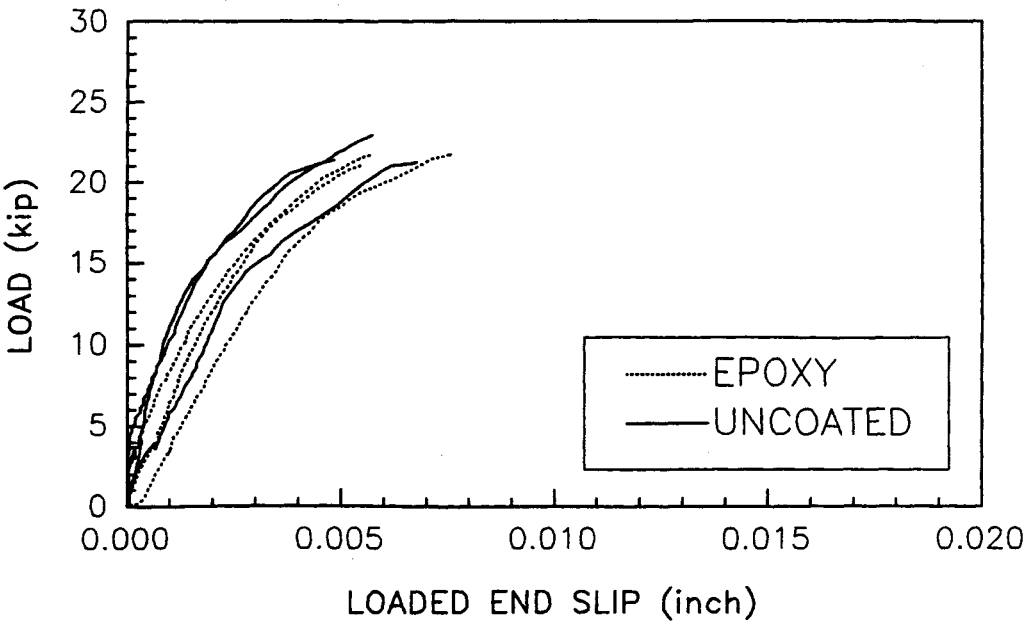

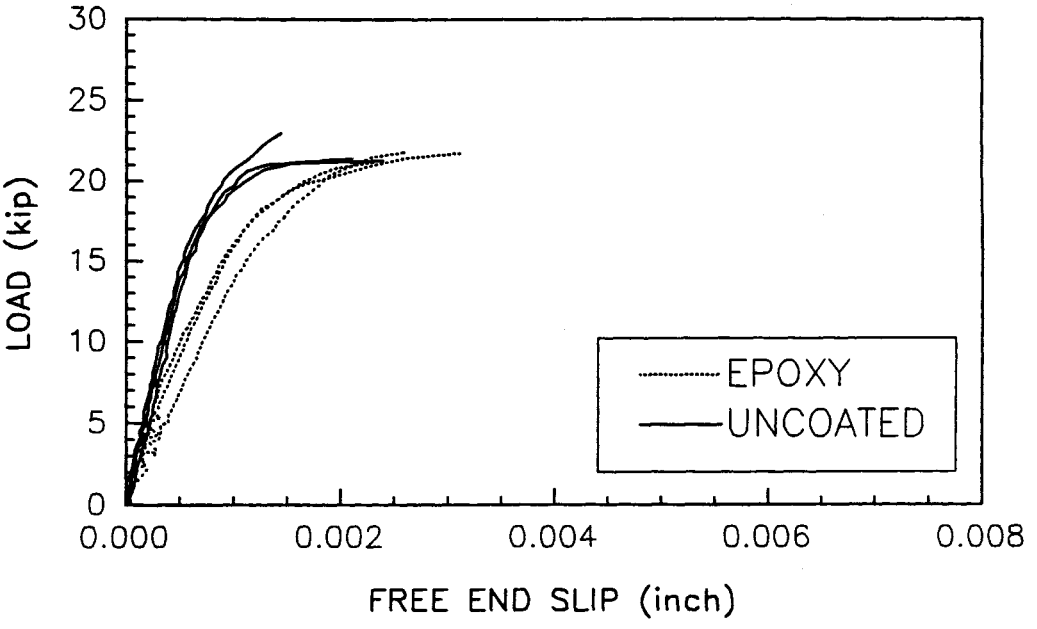

Figure 3.7 Rebar Slip Curves for Group 7, No. 6 Bars.

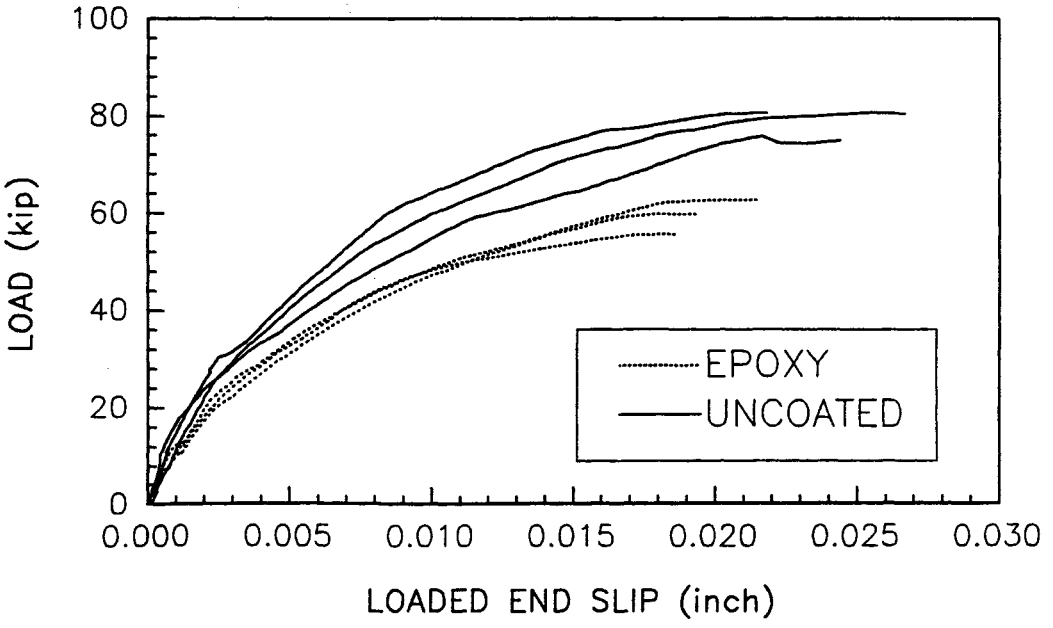

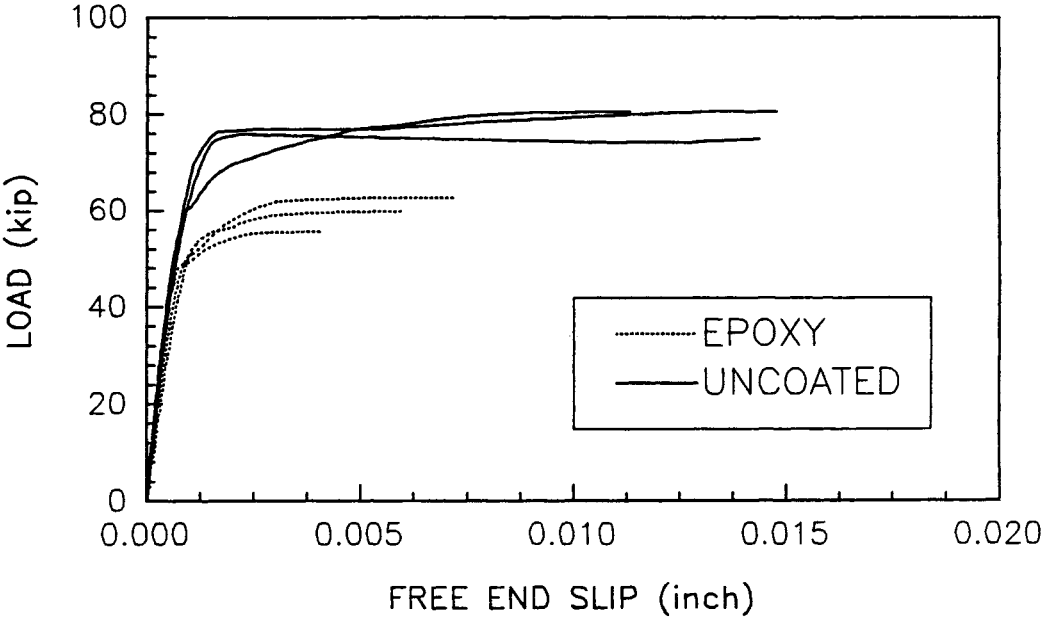

Figure 3.8 Rebar Slip Curves for Group 2, No. 11 Bars.

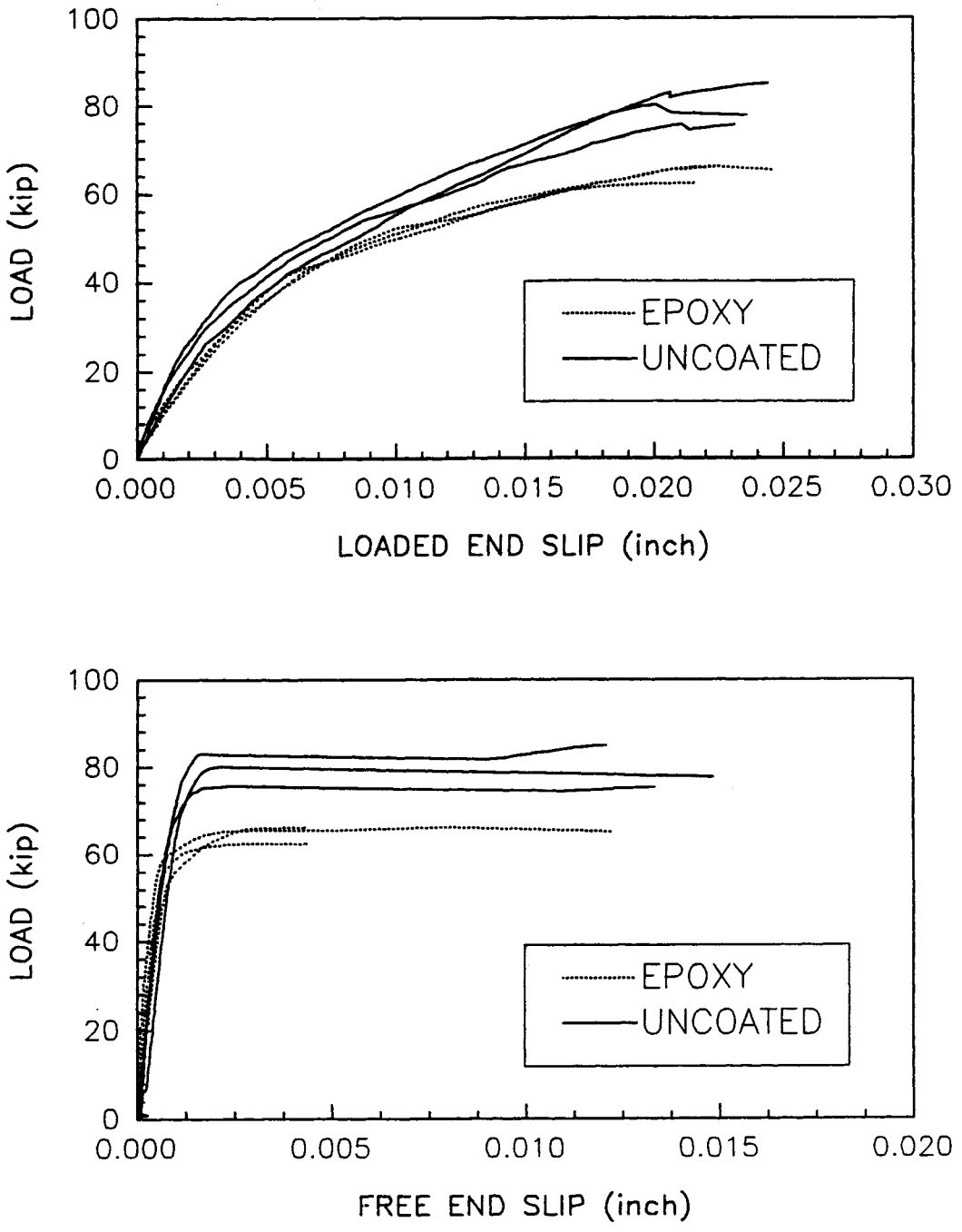

Figure 3.9 Rebar Slip Curves for Group 4, No. 11 Bars.

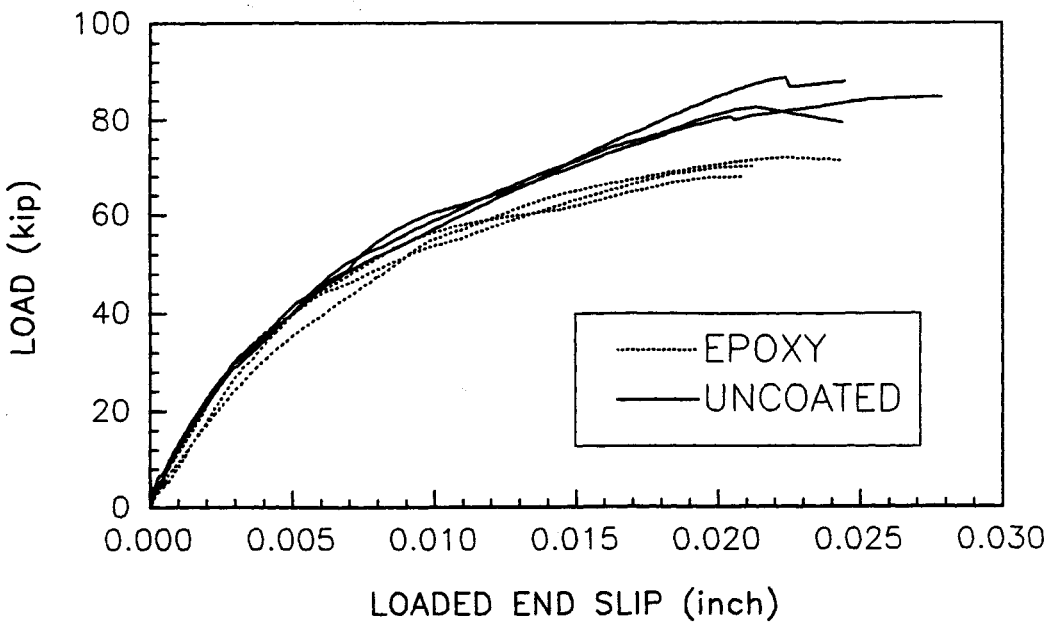

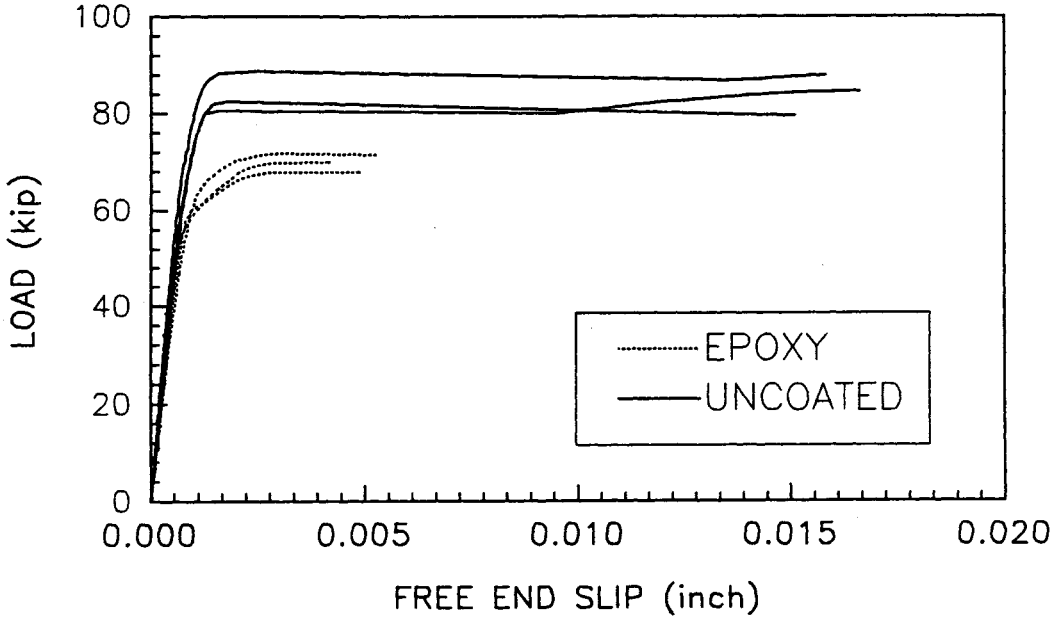

Figure 3.10 Rebar Slip Curves for Group 5, No. 11 Bars.

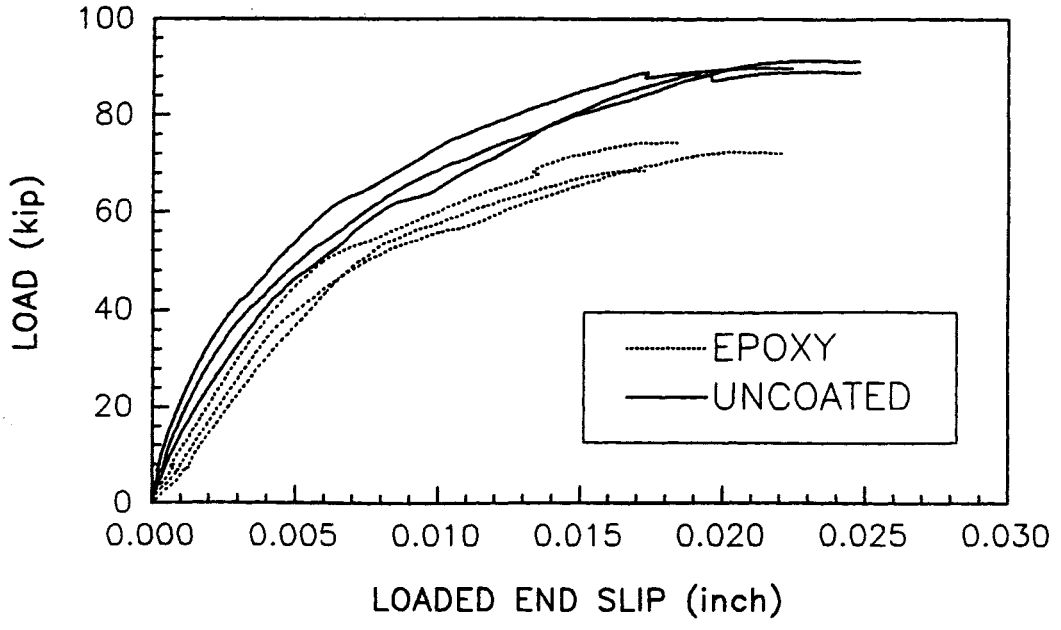

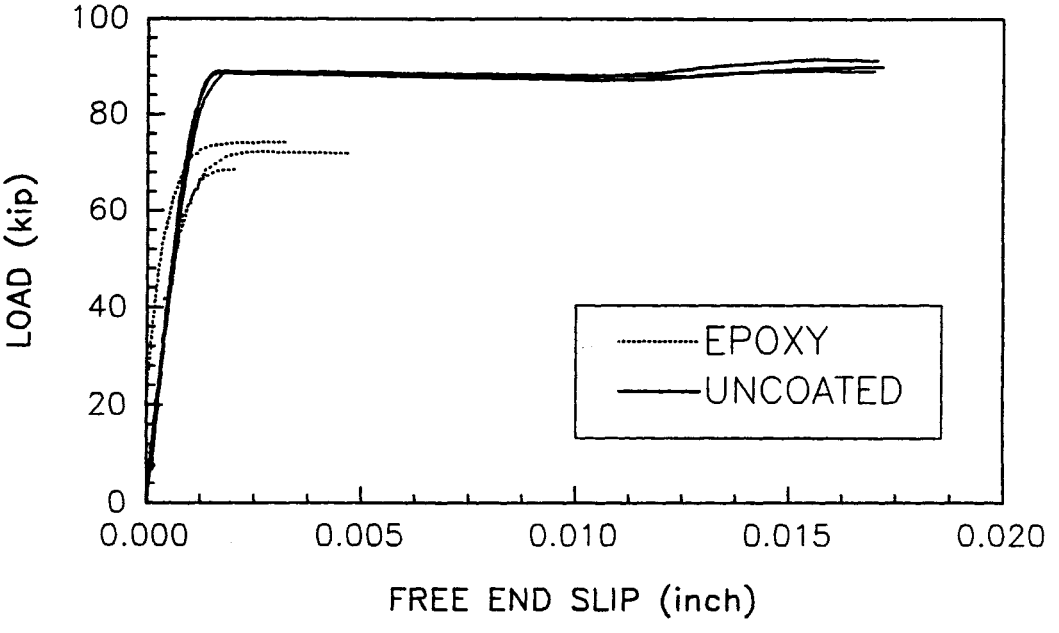

Figure 3.11 Rebar Slip Curves for Group 6, No. 11 Bars.

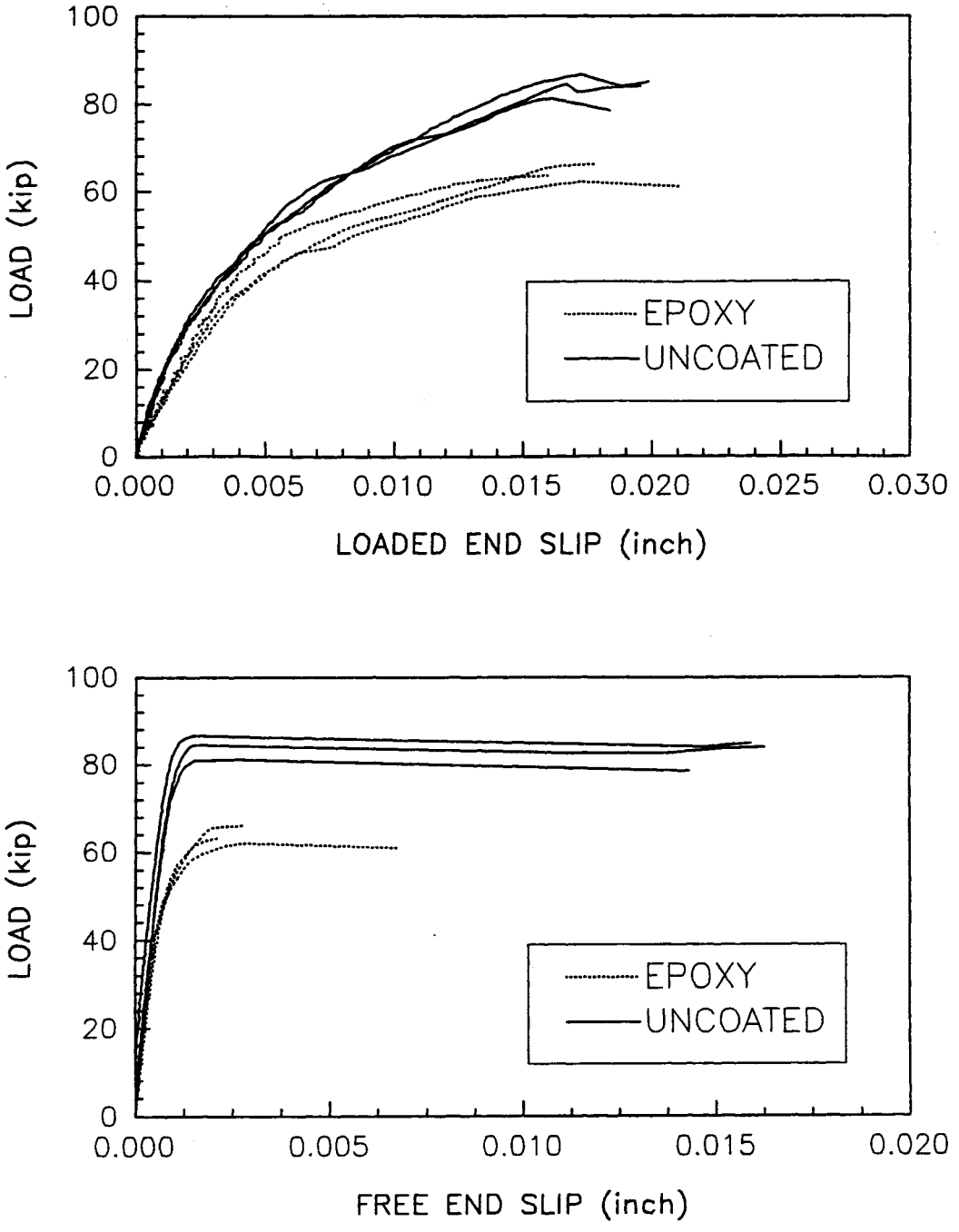

Figure 3.12 Rebar Slip Curves for Group 7, No. 11 Bars.

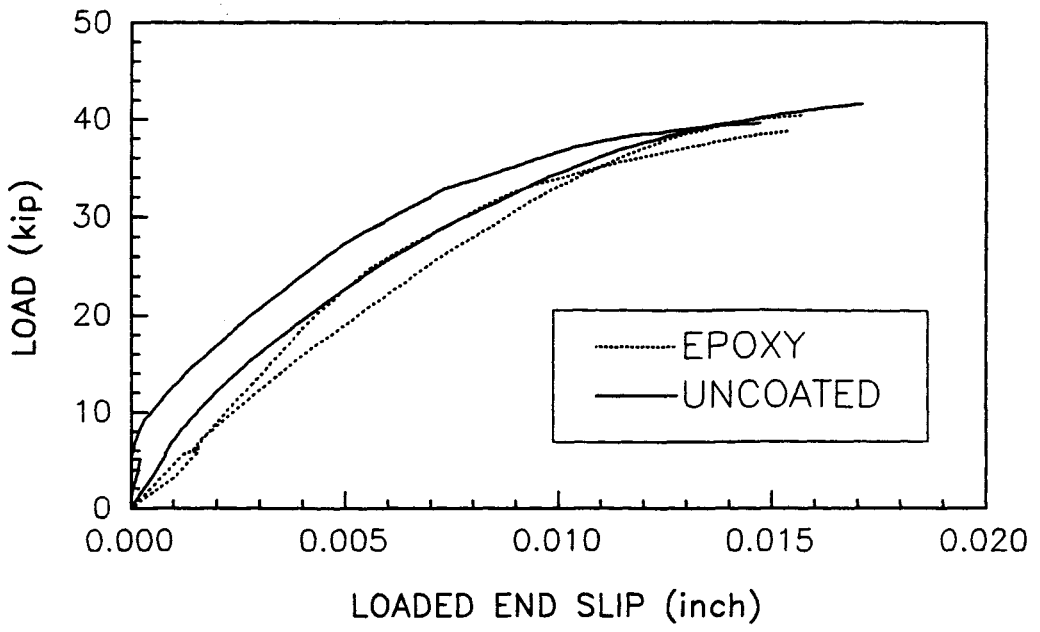

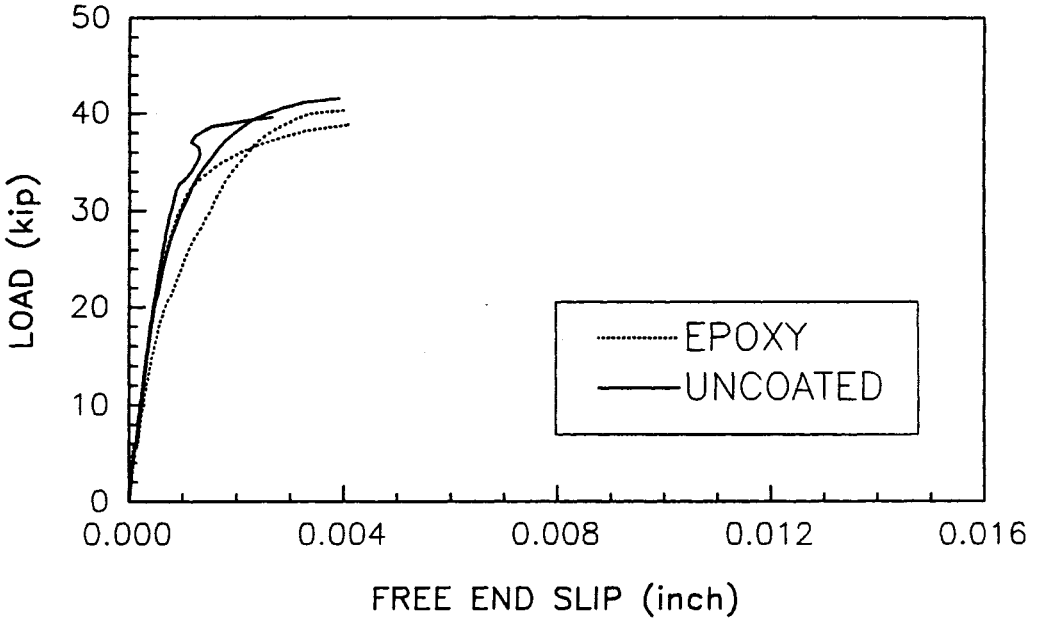

Figure 3.13 Rebar Slip Curves for Group 8, No. 8 Bars with Strain Gages.

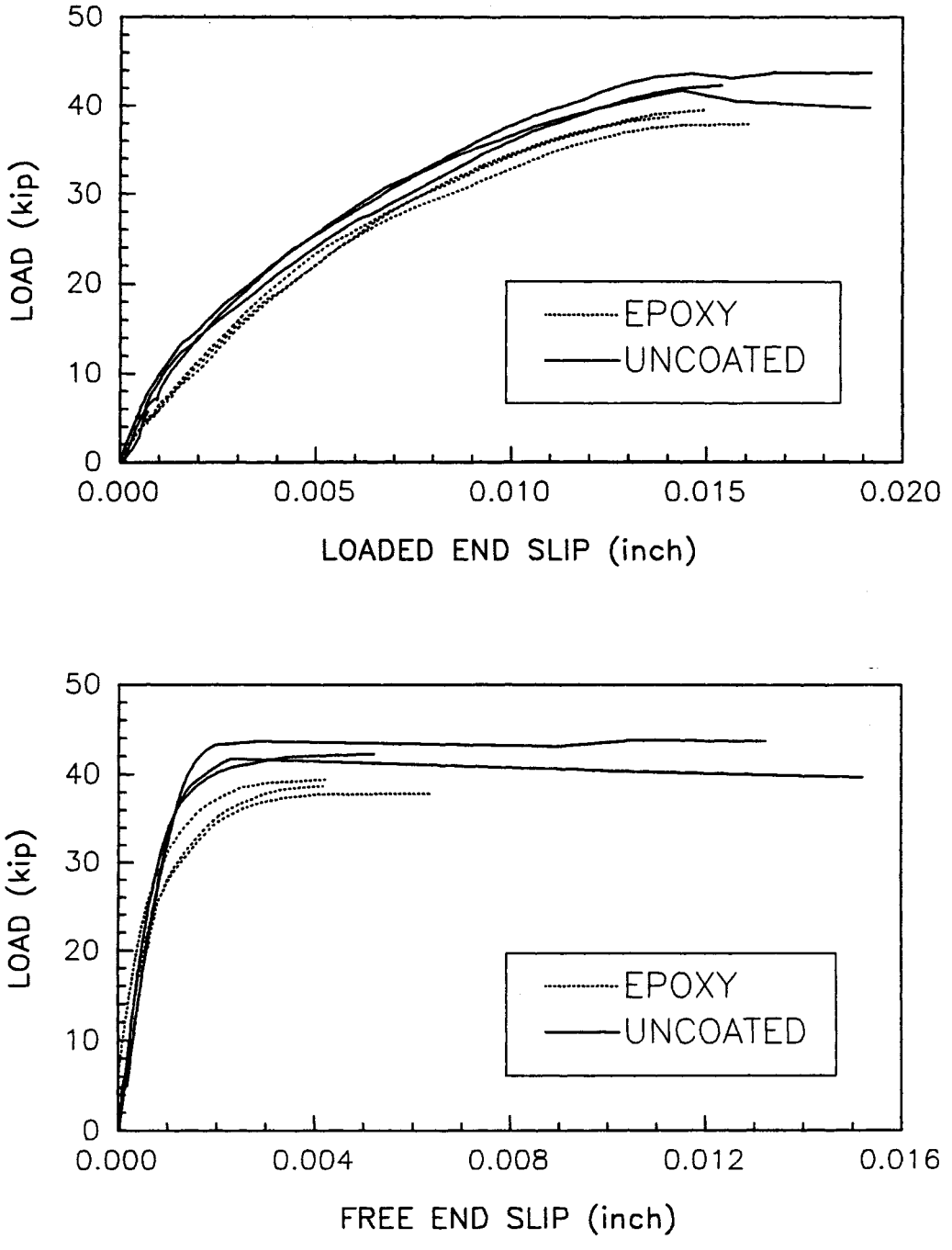

Figure 3.14 Rebar Slip Curves for Group 8, No. 8 Bars without Strain Gages.

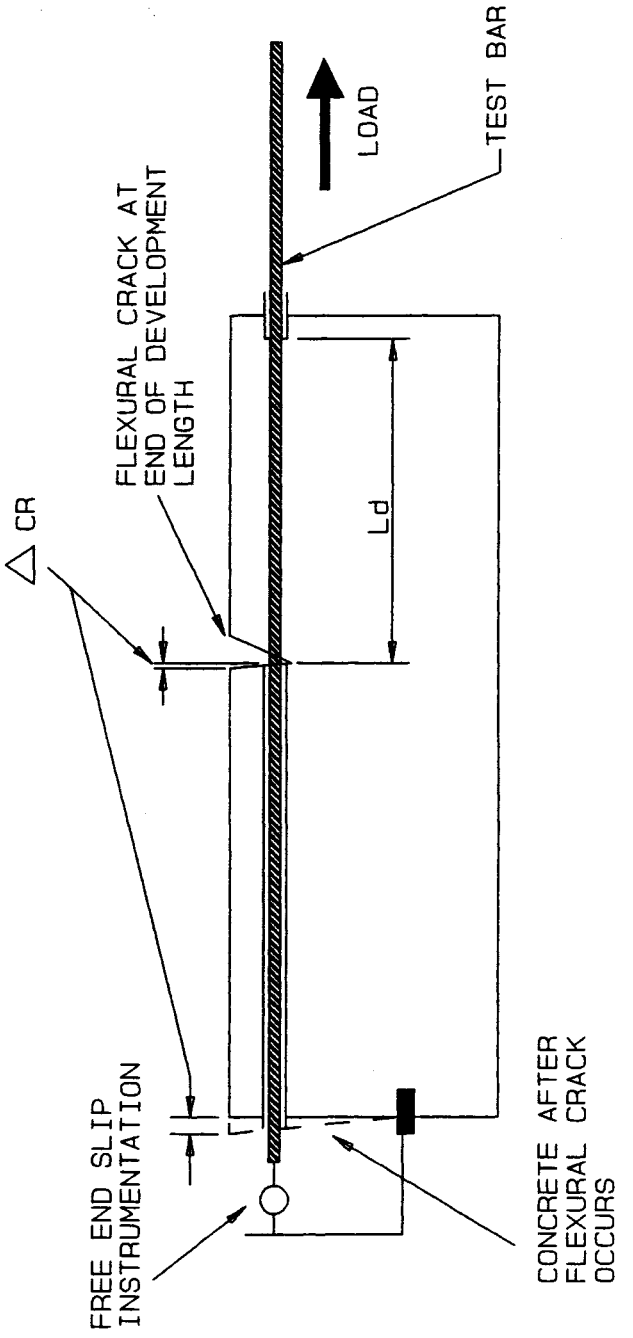

Figure 3.15 Rotation of Specimen Due to Flexural Cracking

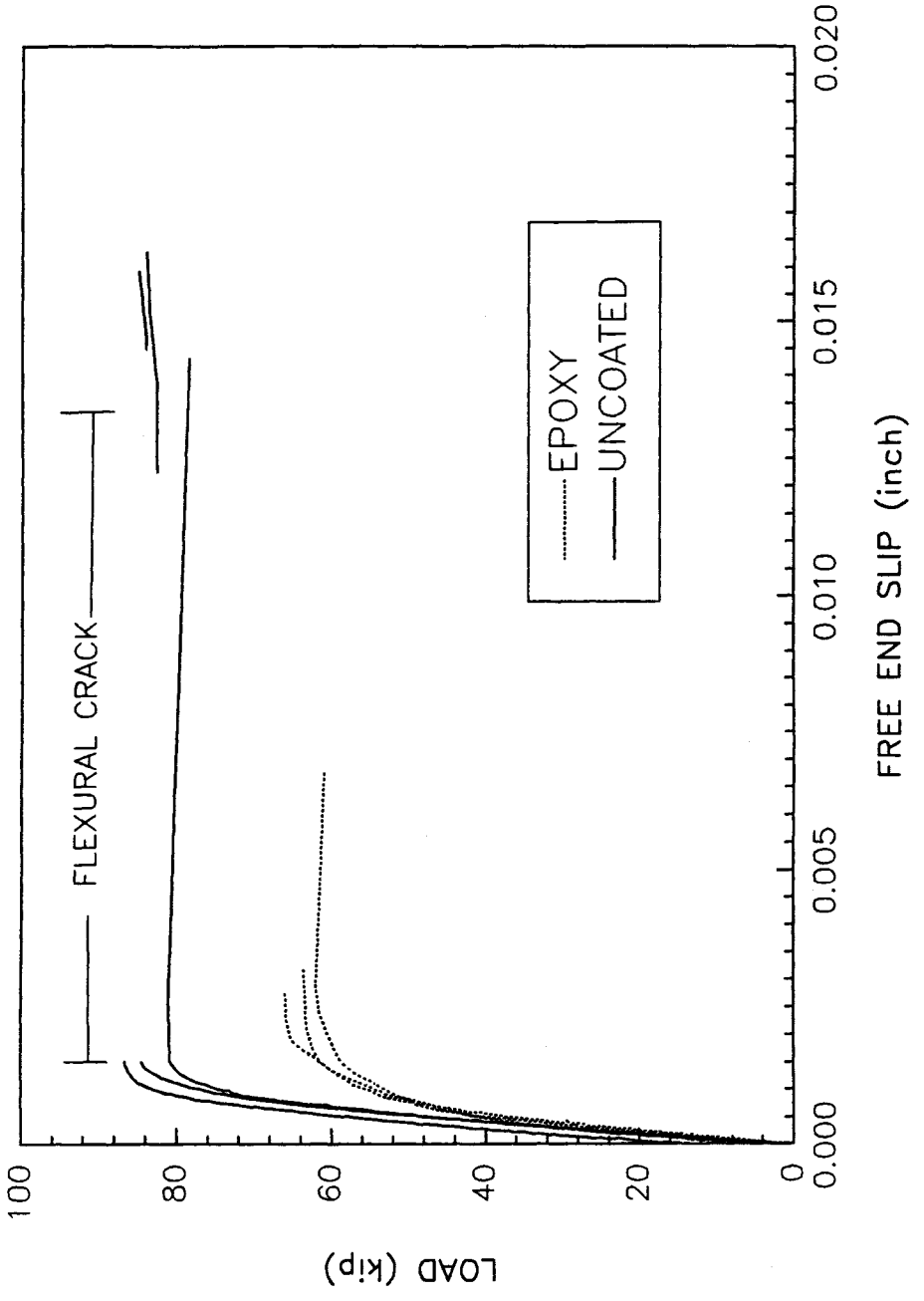

Figure 3.16 Effect of Flexural Cracking on Free-End Slip Group 7, No. 11 Bars

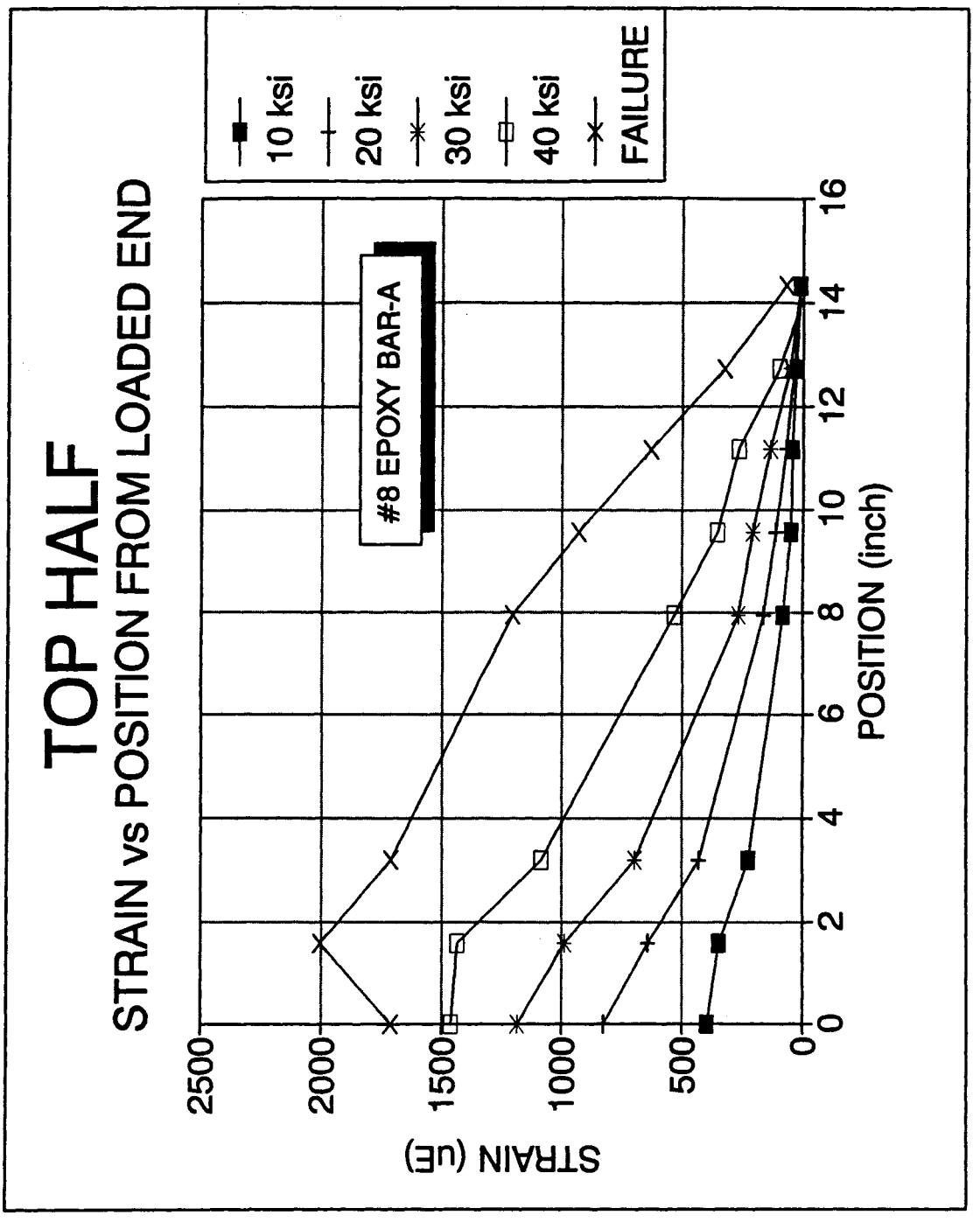

Figure 3.17 Strain Distribution Along the Development Length. Top Half of No. 8 Epoxy-Coated Rebar Specimen, 08E14A06.

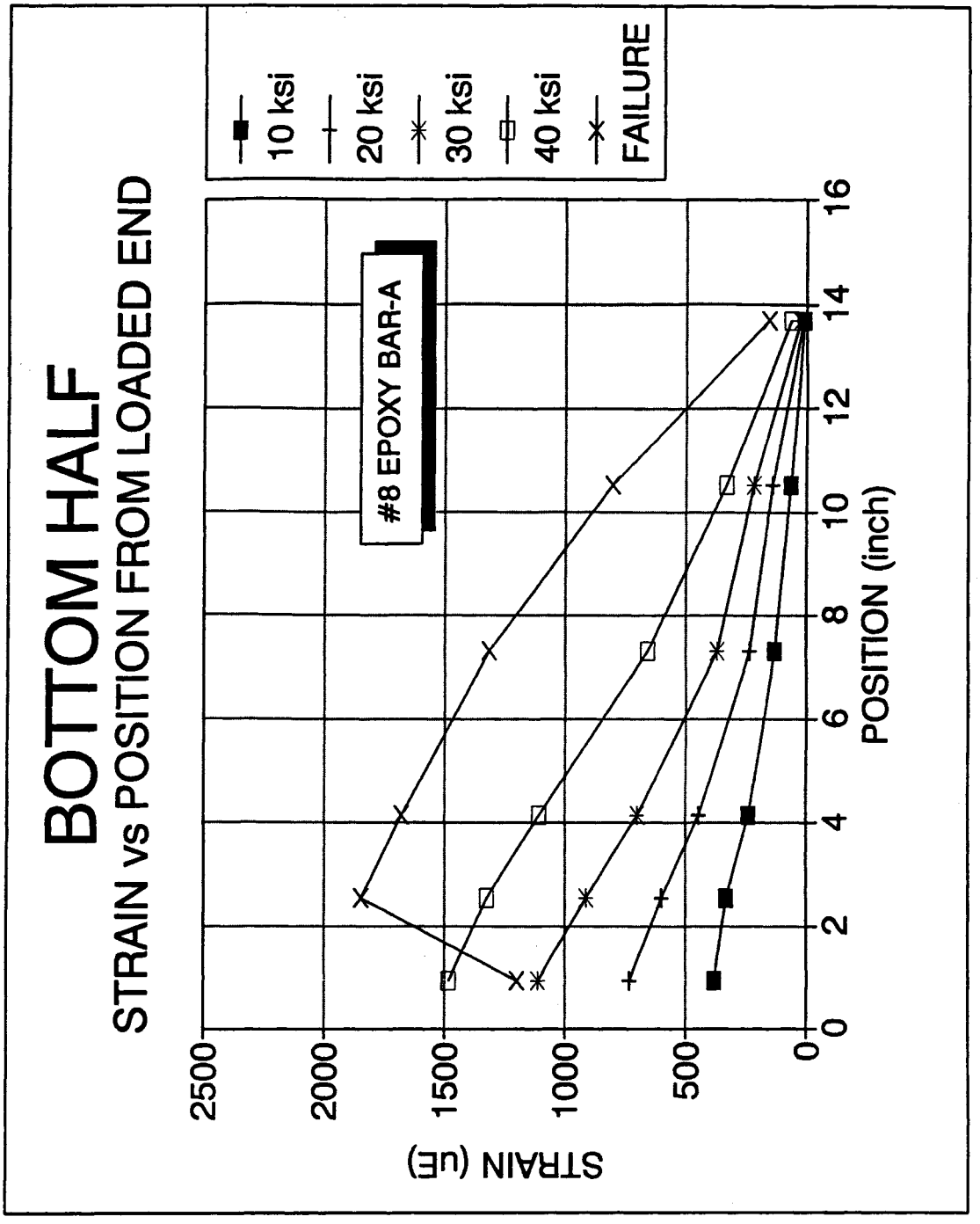

Figure 3.18 Strain Distribution Along the Development Length. Bottom Half of No. 8 Epoxy-Coated Rebar Specimen, 08E14A06.

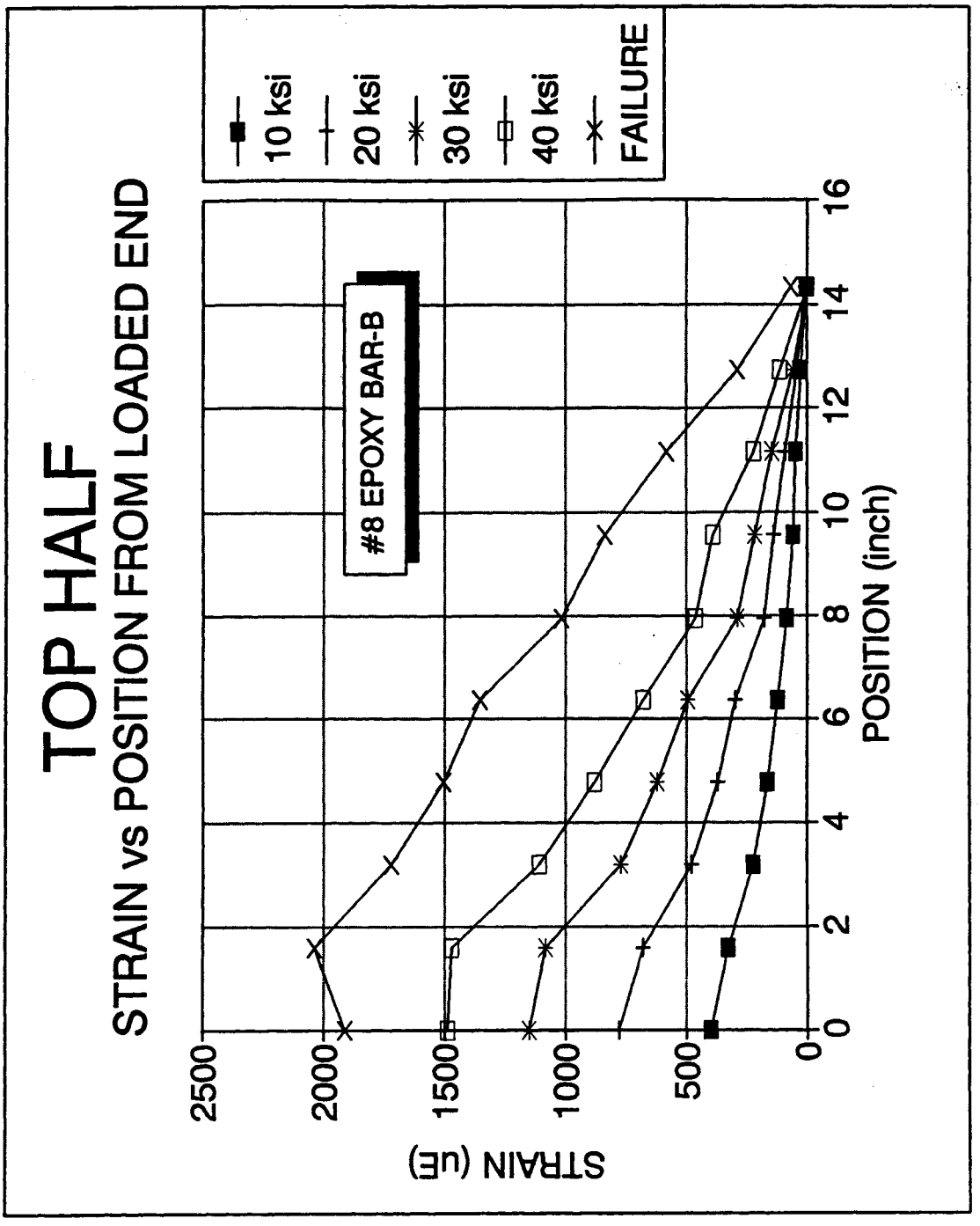

Figure 3.19 Strain Distribution Along the Development Length. Top Half of No. 8 Epoxy-Coated Rebar Specimen, 08E14B06.

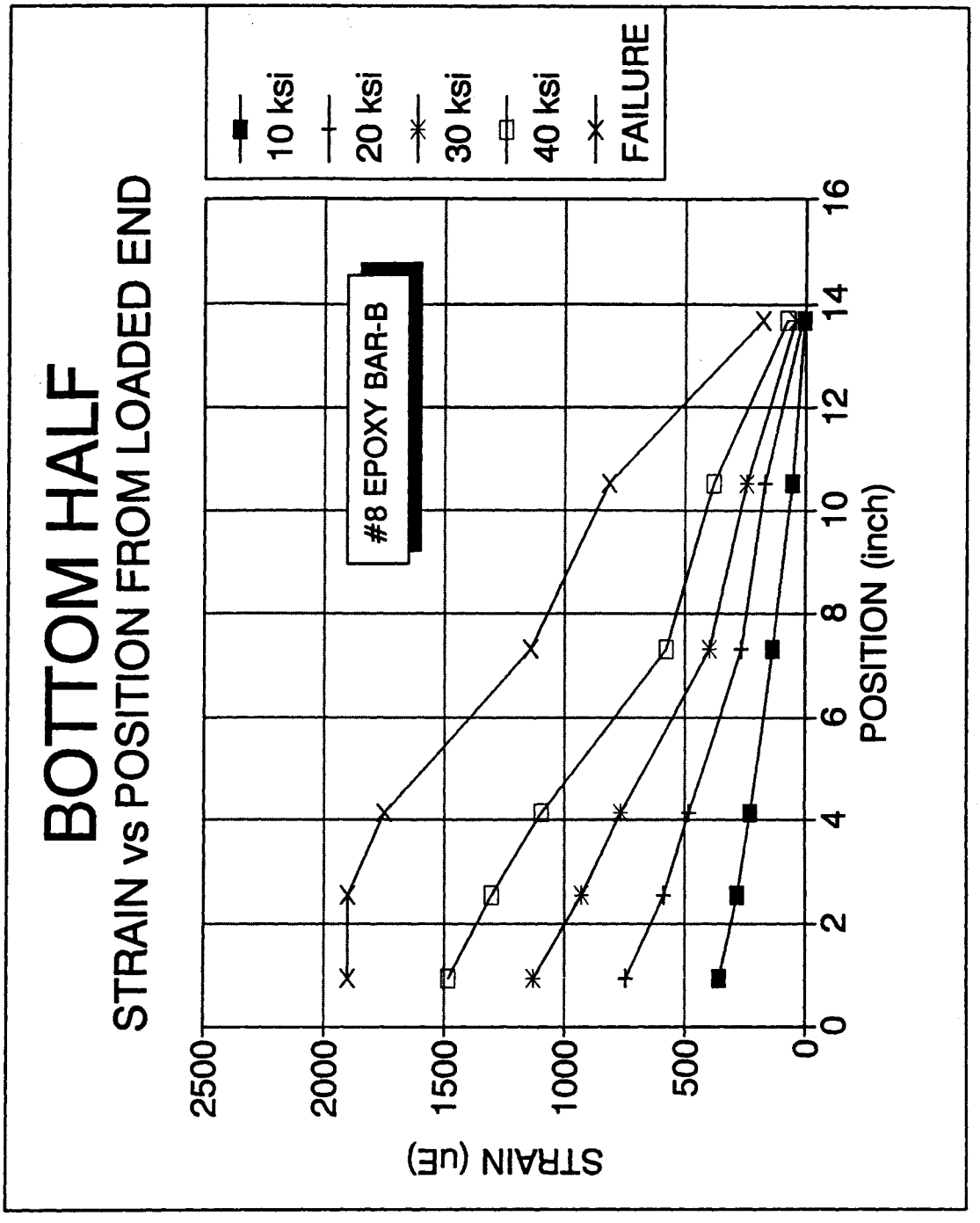

Figure 3.20 Strain Distribution Along the Development Length. Bottom Half of No. 8 Epoxy-Coated Rebar Specimen, 08E14B06.

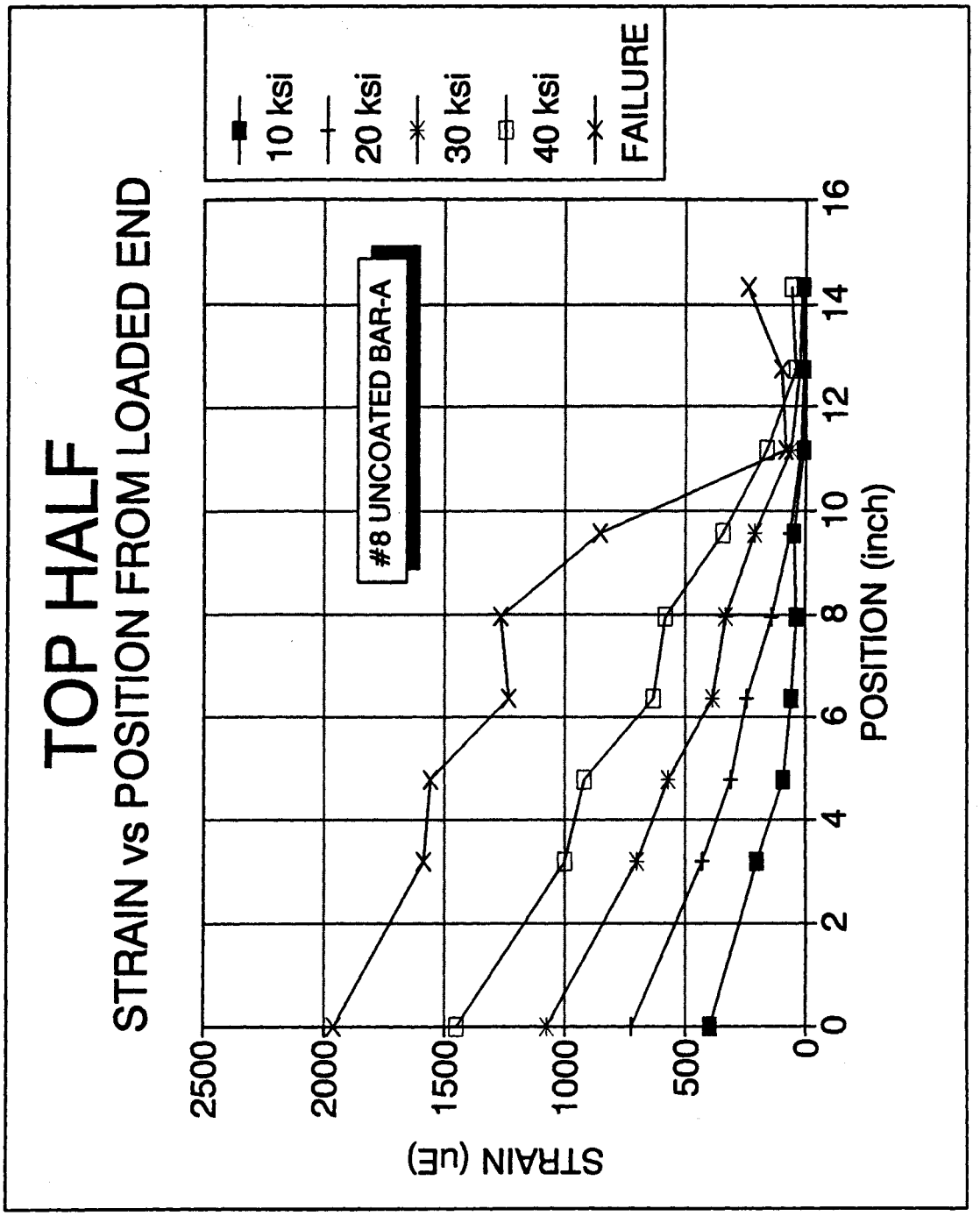

Figure 3.21 Strain Distribution Along the Development Length. Top Half of No. 8 Uncoated Rebar Specimen, 08B14A06.

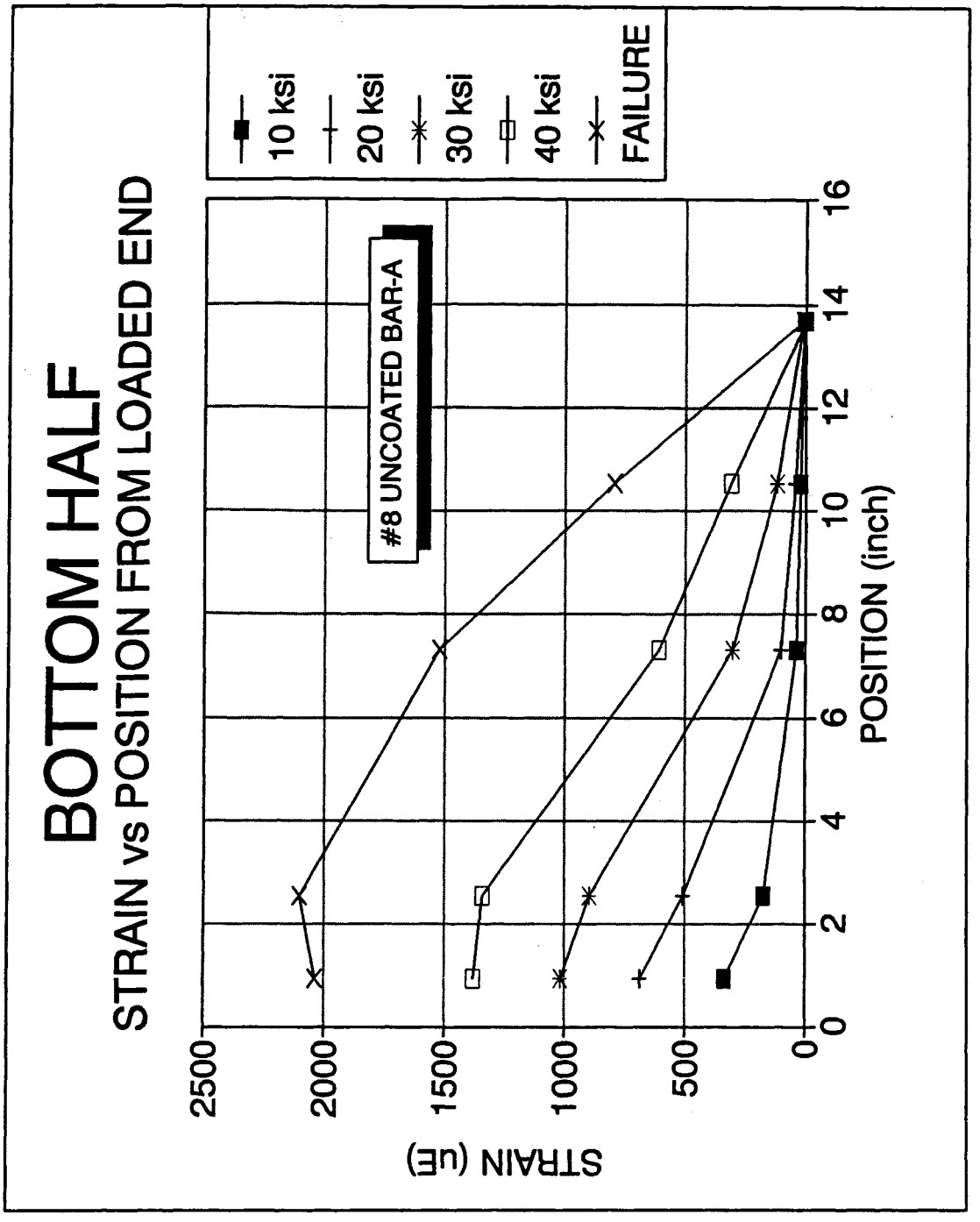

Figure 3.22 Strain Distribution Along the Development Length. Bottom half of No. 8 Uncoated Rebar Specimen, 08B14A06.

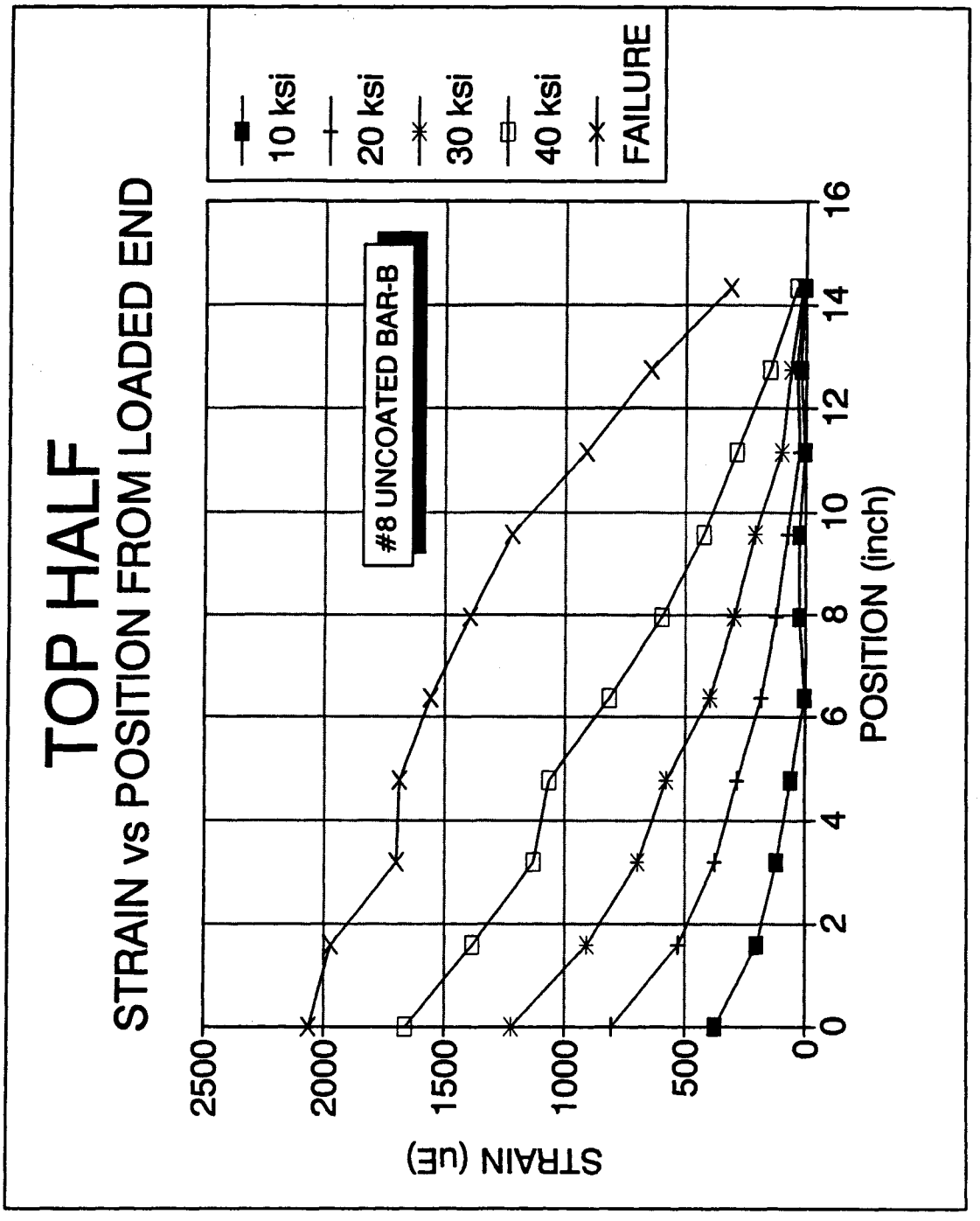

Figure 3.23 Strain Distribution Along the Development Length. Top Half of No. 8 Uncoated Rebar Specimen, 08B14B06.

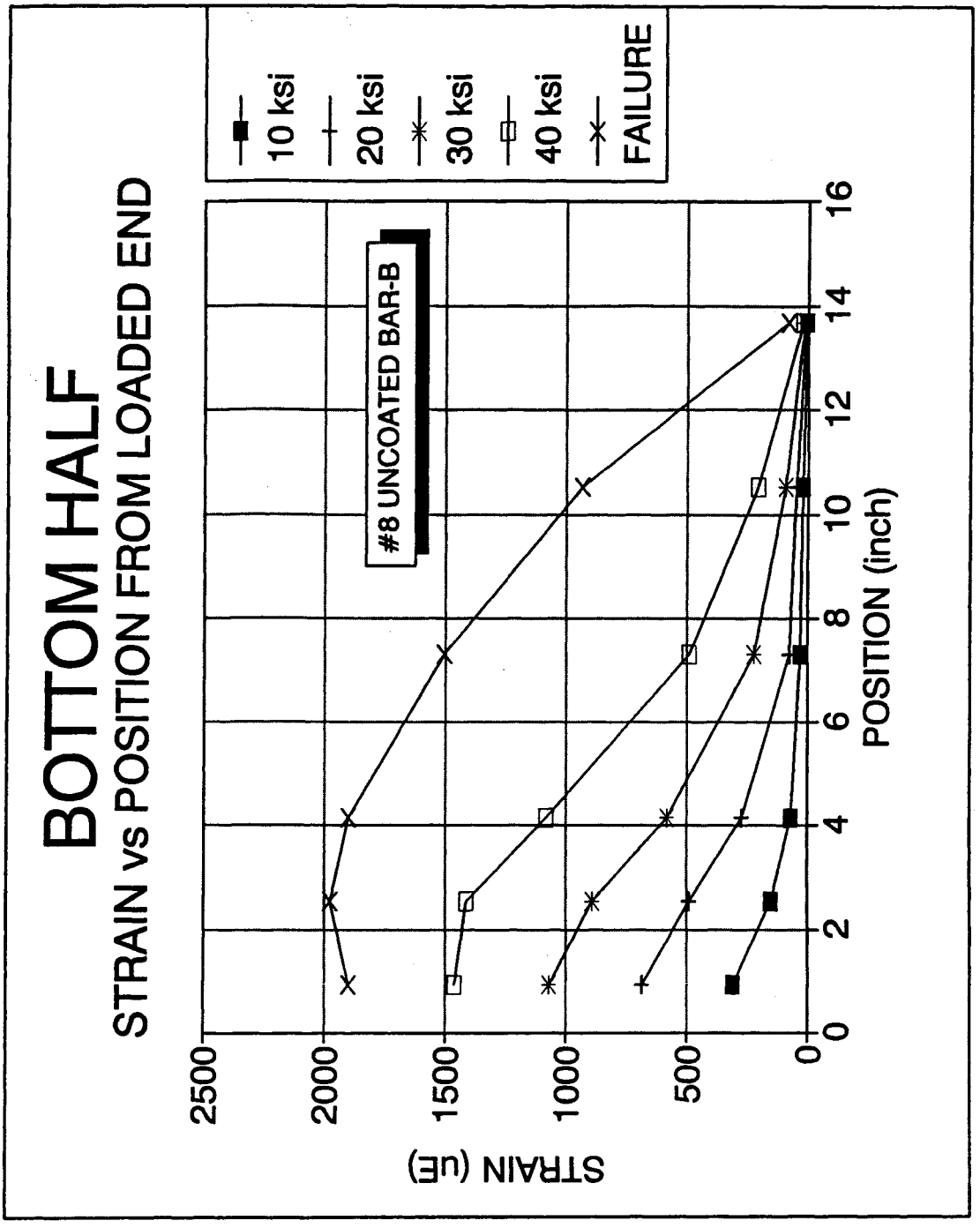

Figure 3.24 Strain Distribution Along the Development Length. Bottom Half of No. 8 Uncoated Rebar Specimen, 08B14B06.

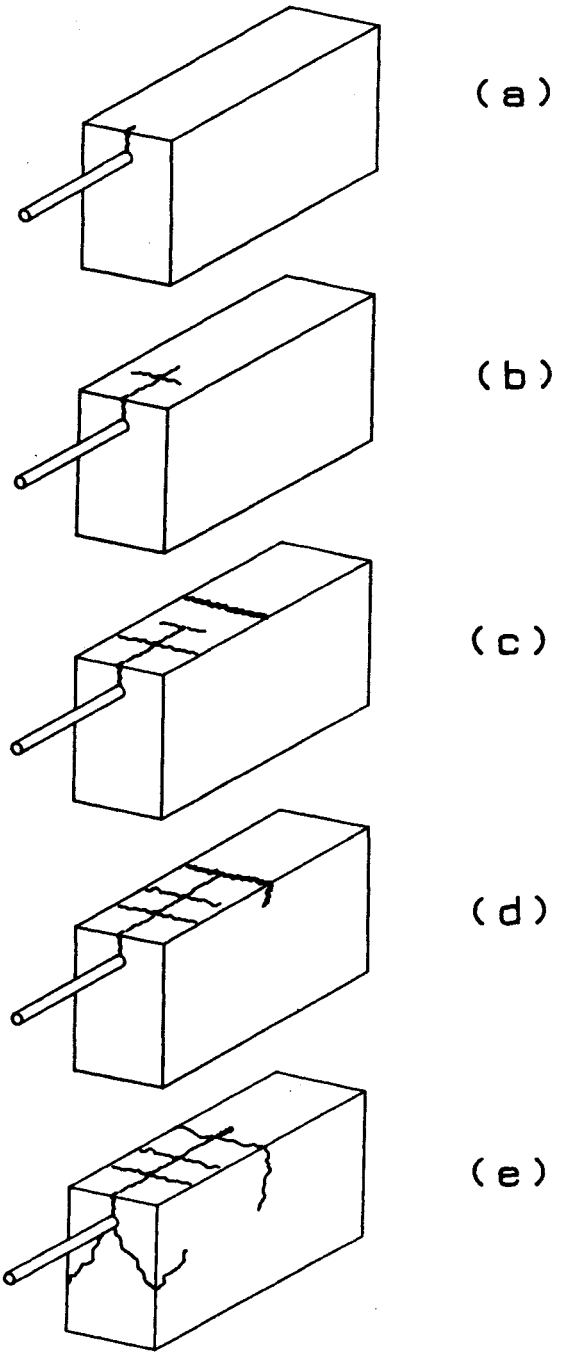

Figure 3.25 Generalized Crack Propagation for No. 11 Uncoated Bars.

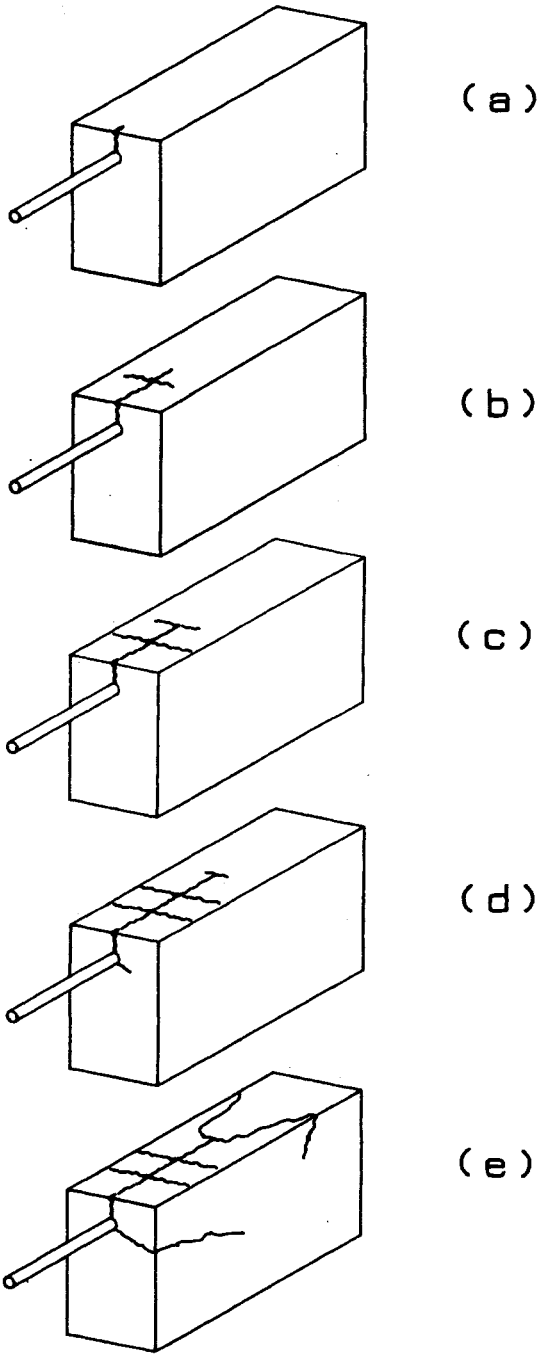

Figure 3.26 Generalized Crack Propagation for No. 11 Epoxy-Coated Bars.

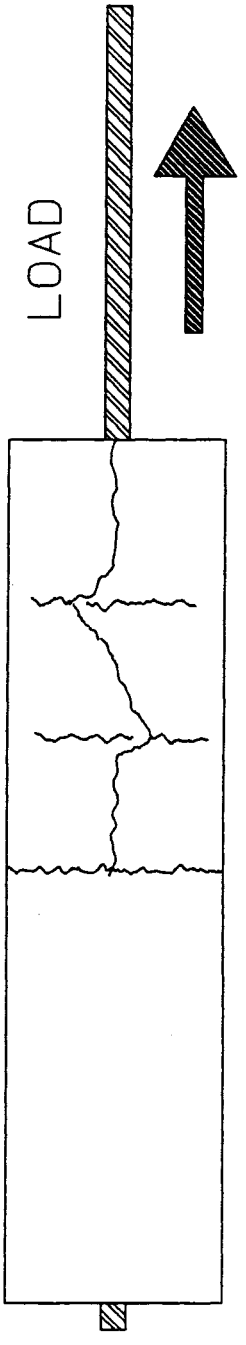

Figure 3.27 Meandering Bond Crack.

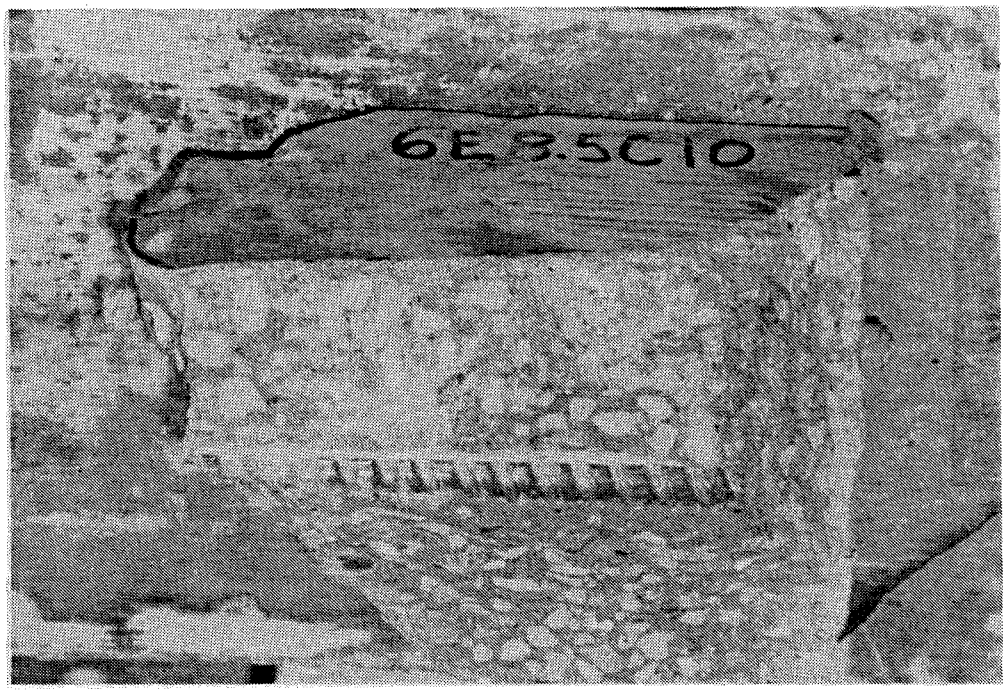

EPOXY-COATED

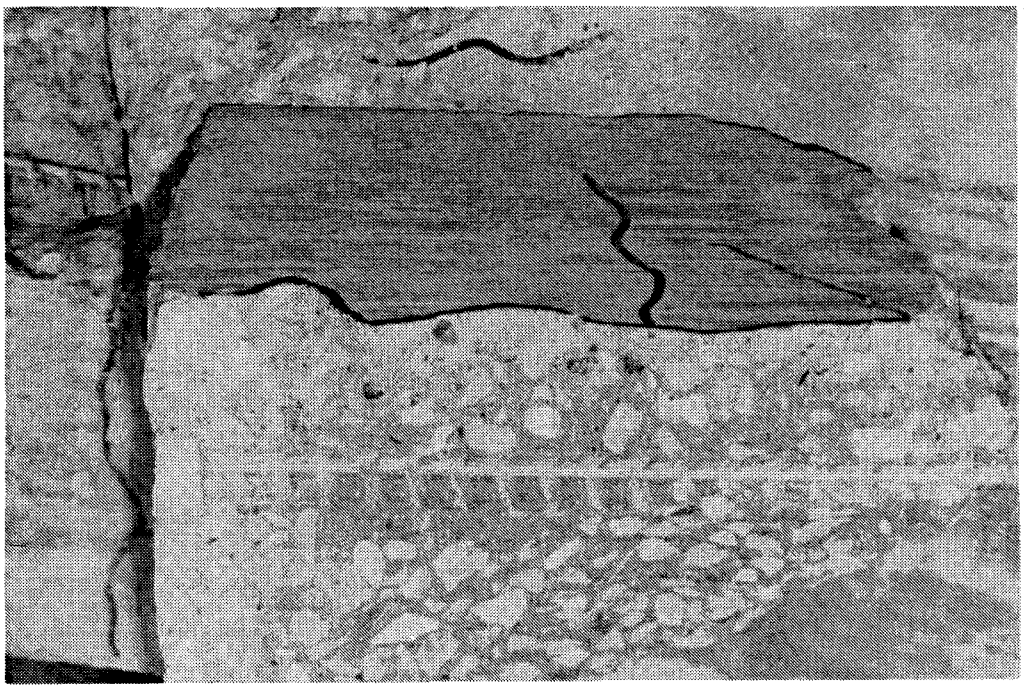

UNCOATED

Figure 3.28 Concrete Surface in Contact with the Bonded Rebar (after testing).

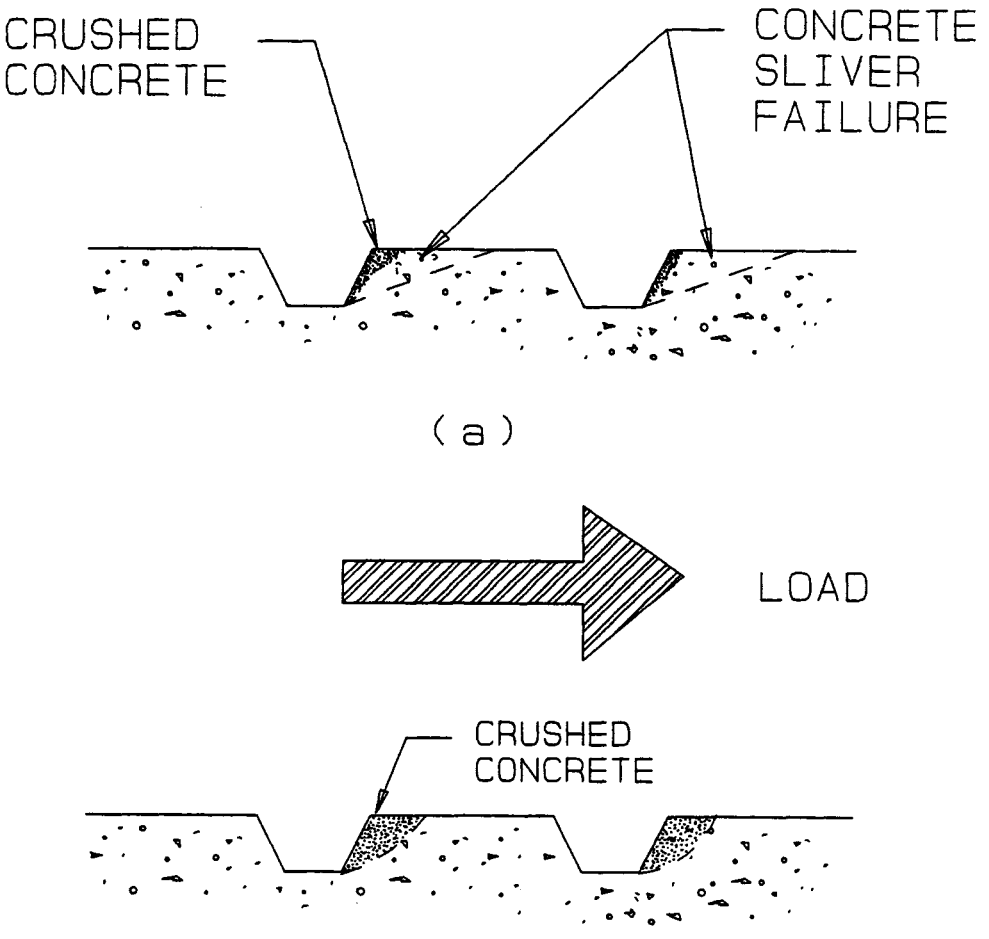

Figure 3.29 Failure of Concrete in Front of Rebar Deformation

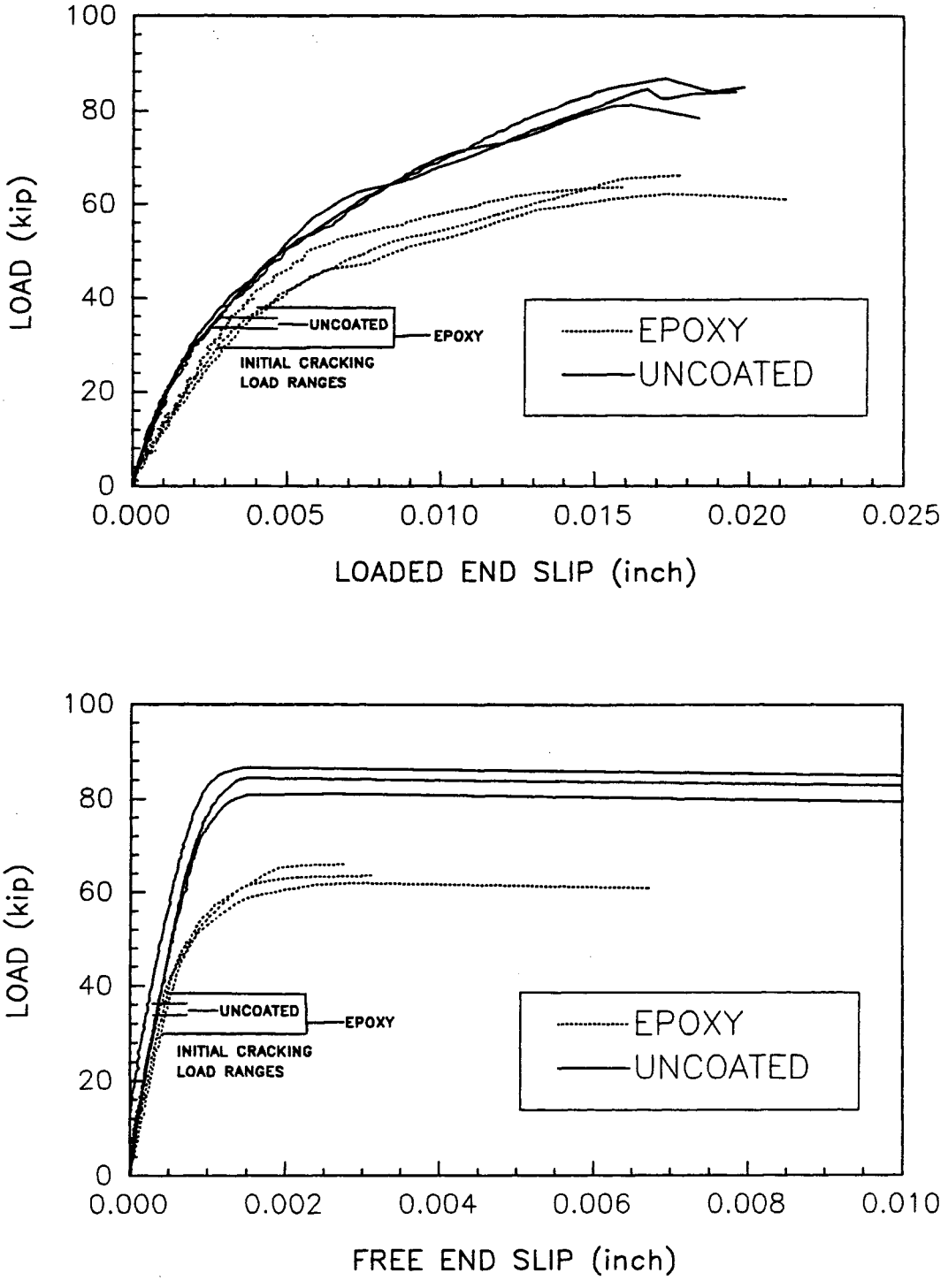

Figure 4.1 Effect of Initial Cracking Load on Slip Group 7, No. 11 Bars

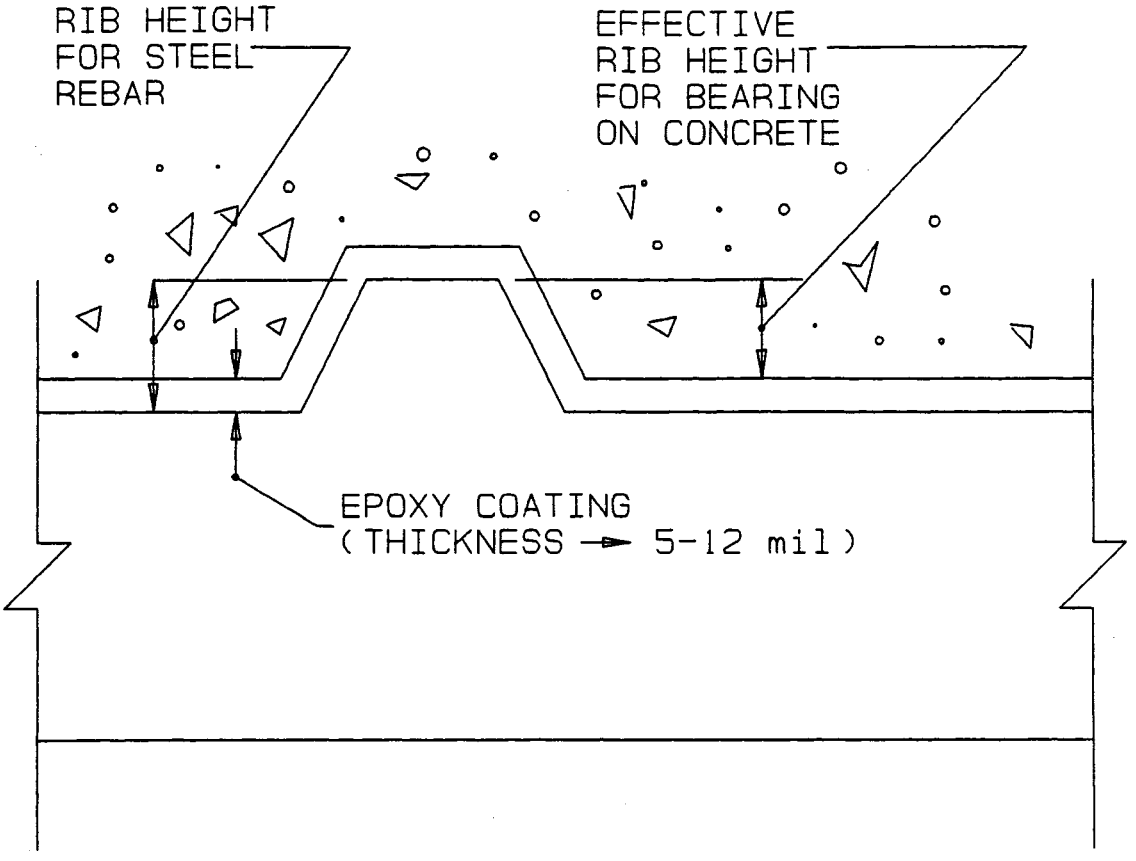

Figure 4.2 Reduced Rib Height with Epoxy Coatings

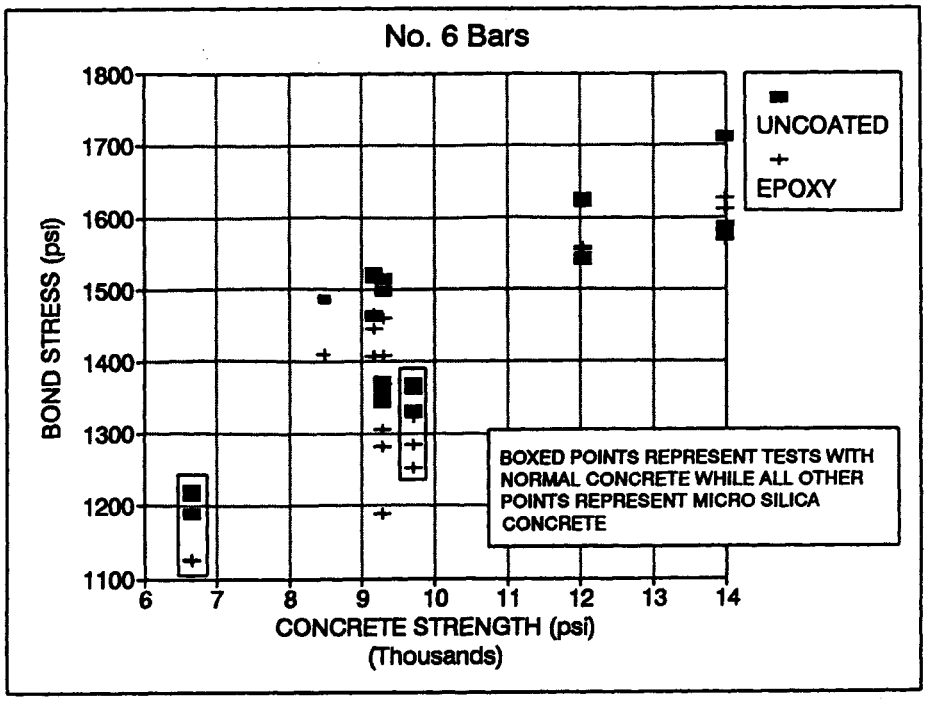

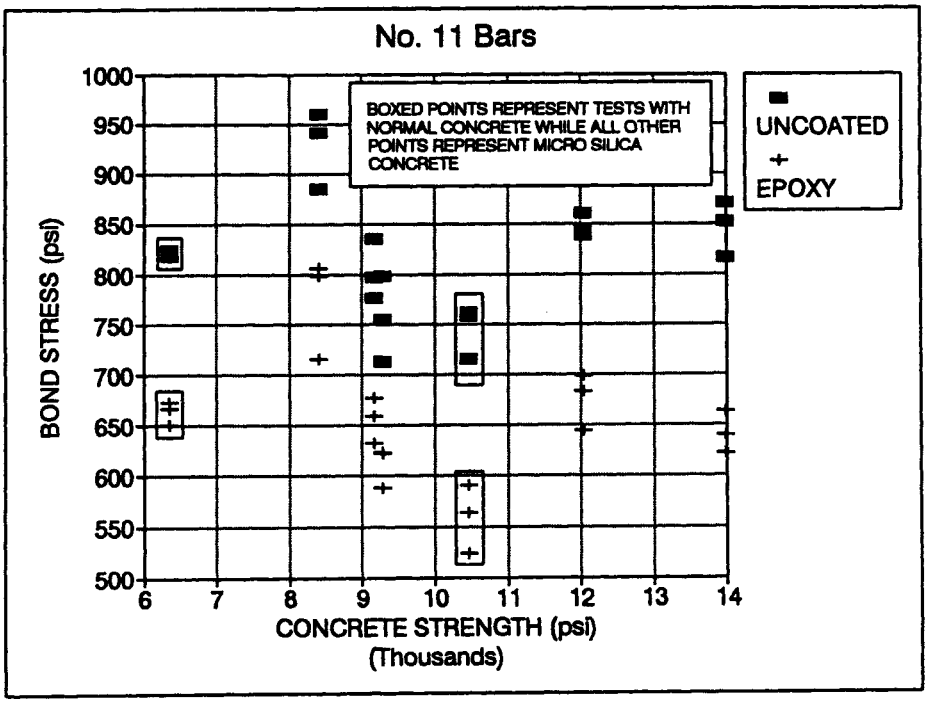

Figure 4.3 Scatter Plot of Ultimate Bond Strengths

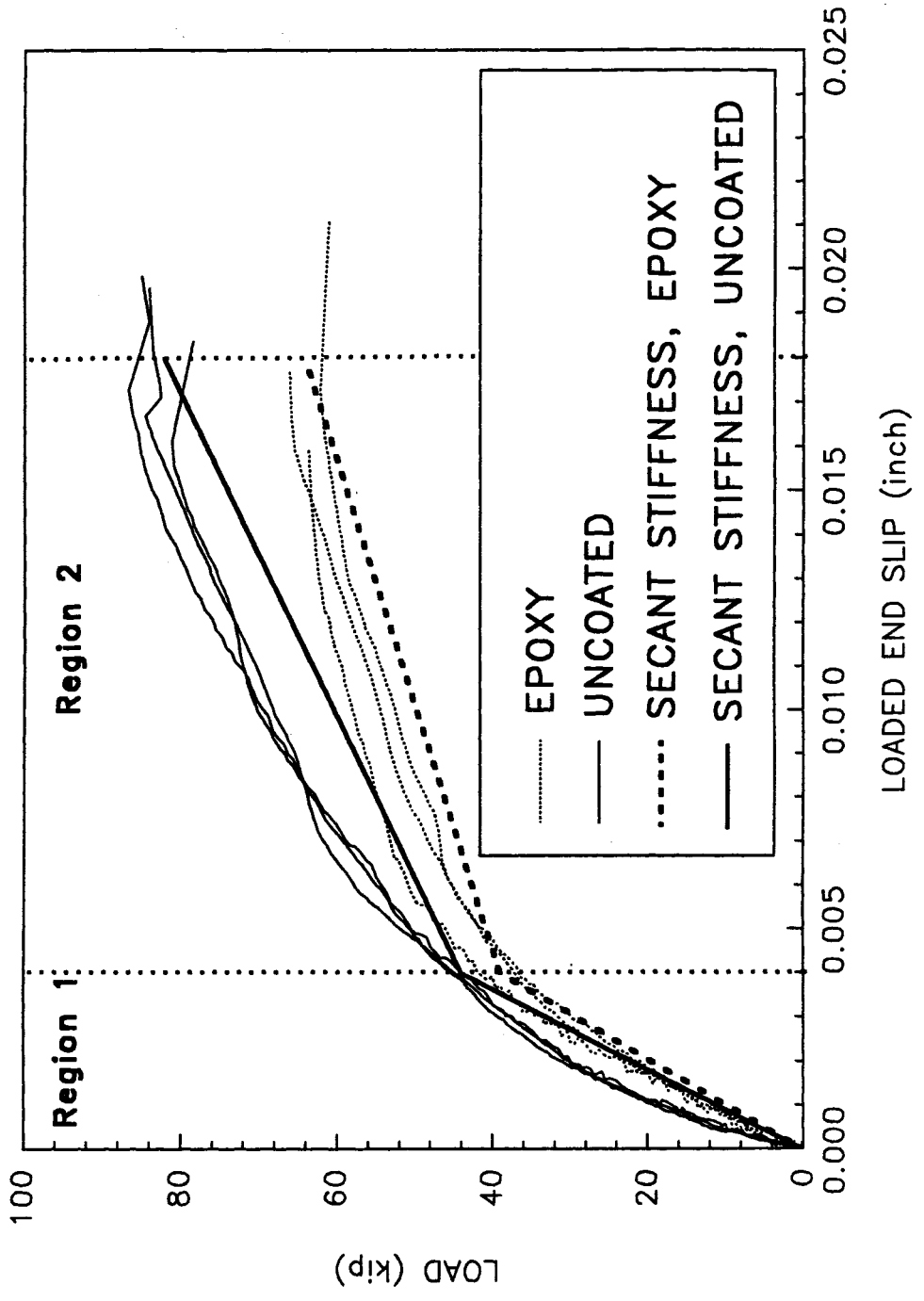

Figure 4.4 Effect of Epoxy Coating on Loaded-End Slip Group 7, No. 11 Bars

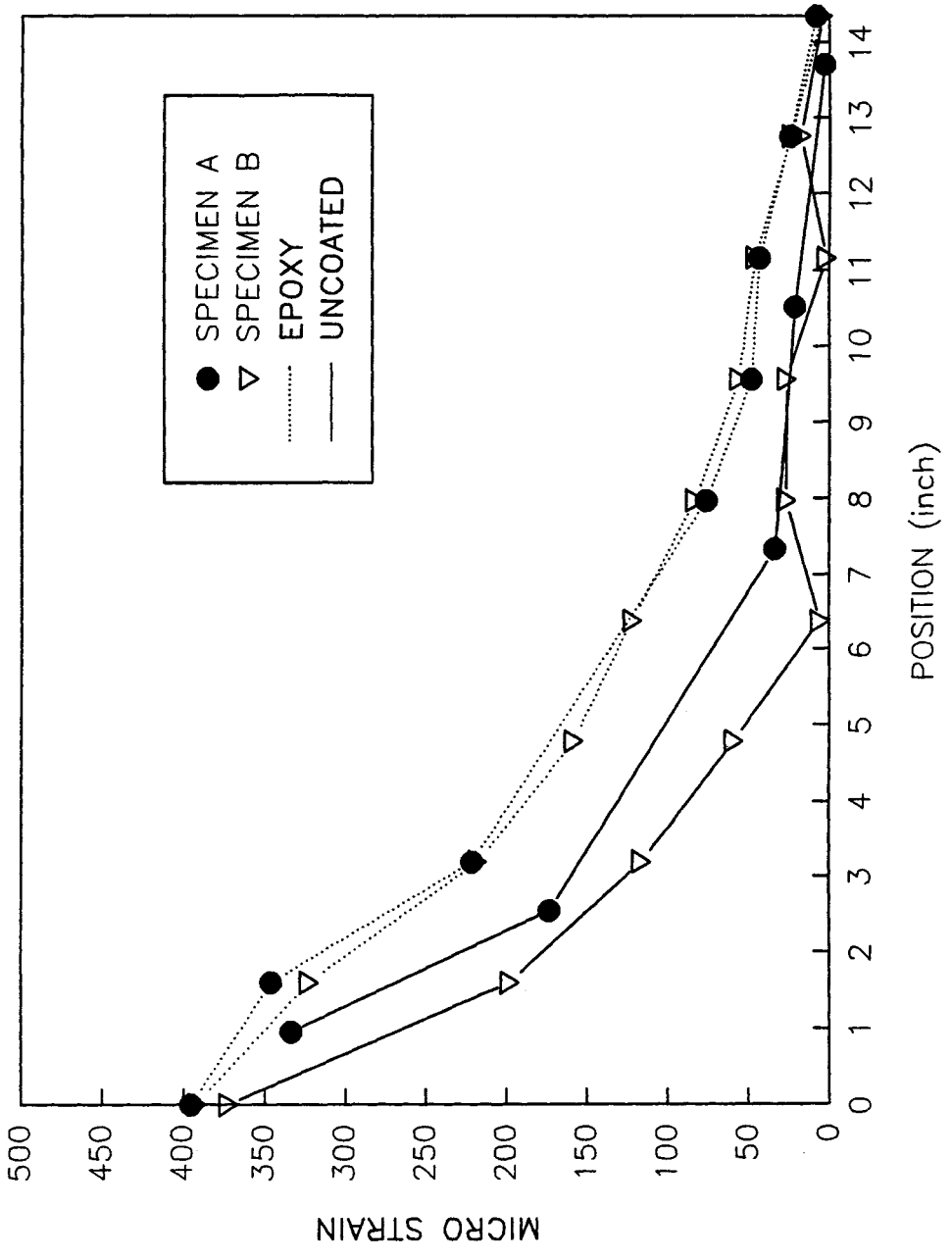

Figure 4.5 Strain Distribution Comparison for Stress Level of 10 ksi.

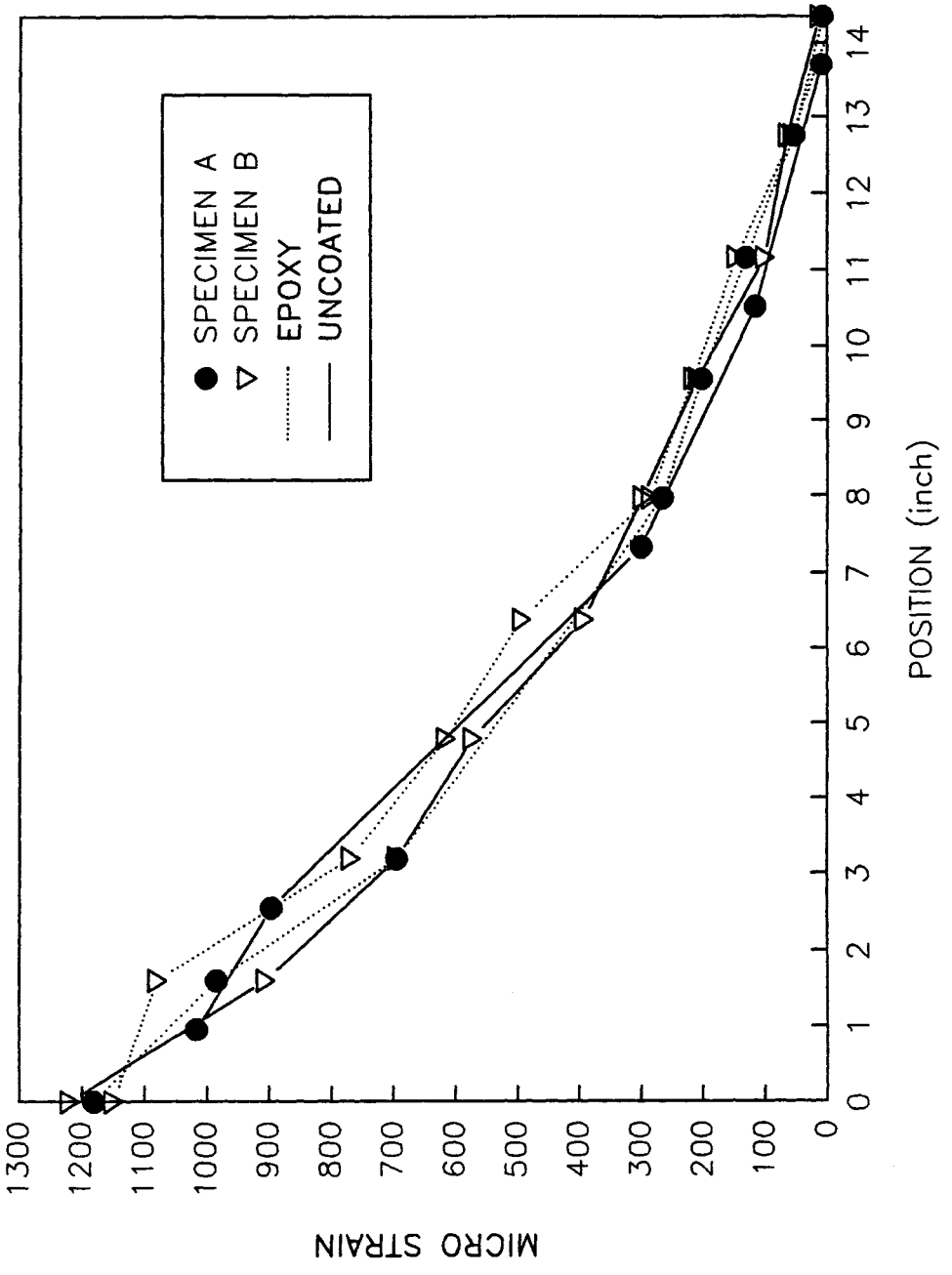

Figure 4.6 Strain Distribution Comparison for Stress Level of 30 ksi.

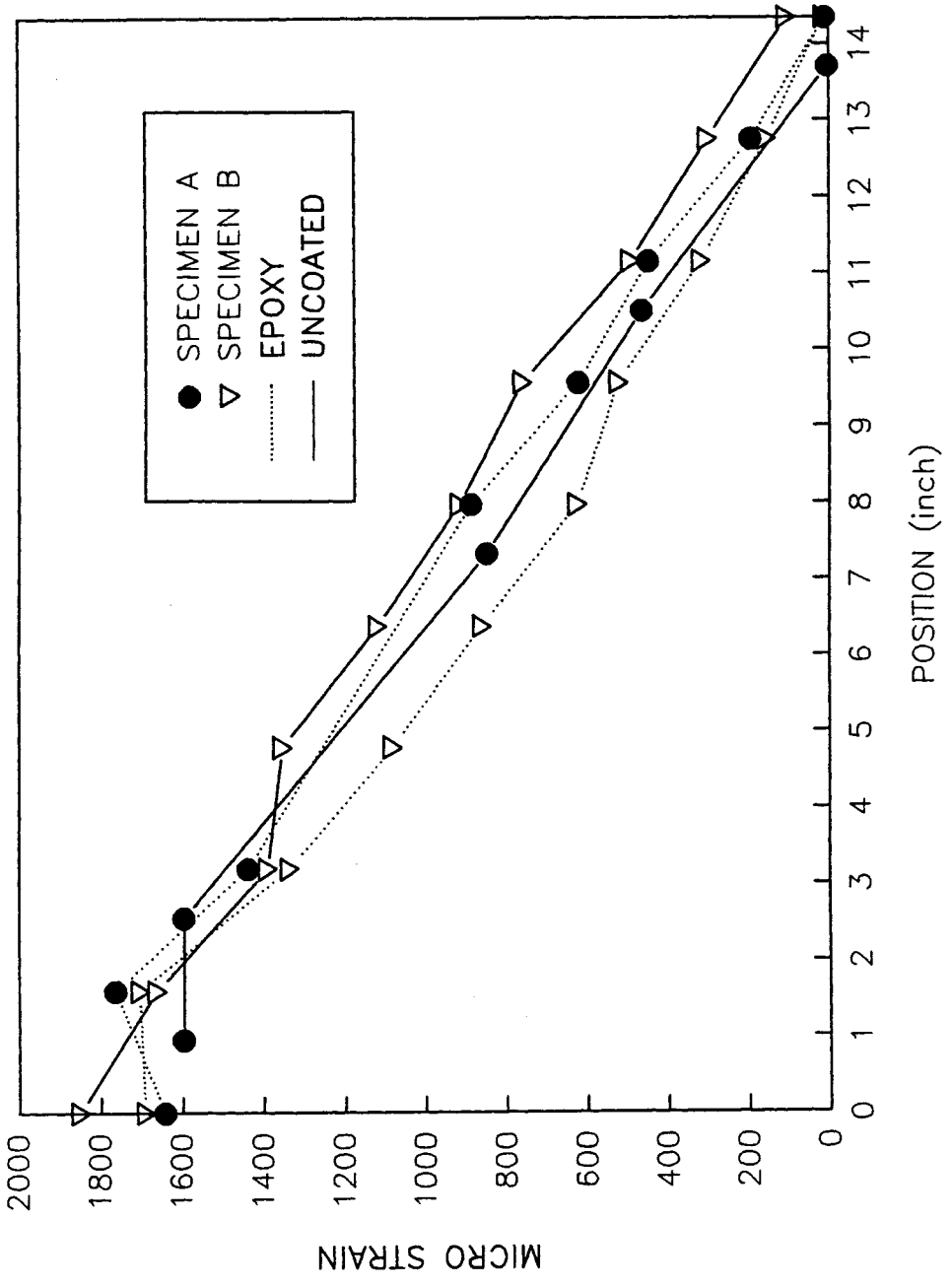

Figure 4.7 Strain Distribution Comparison for Stress Level of 45 ksi.

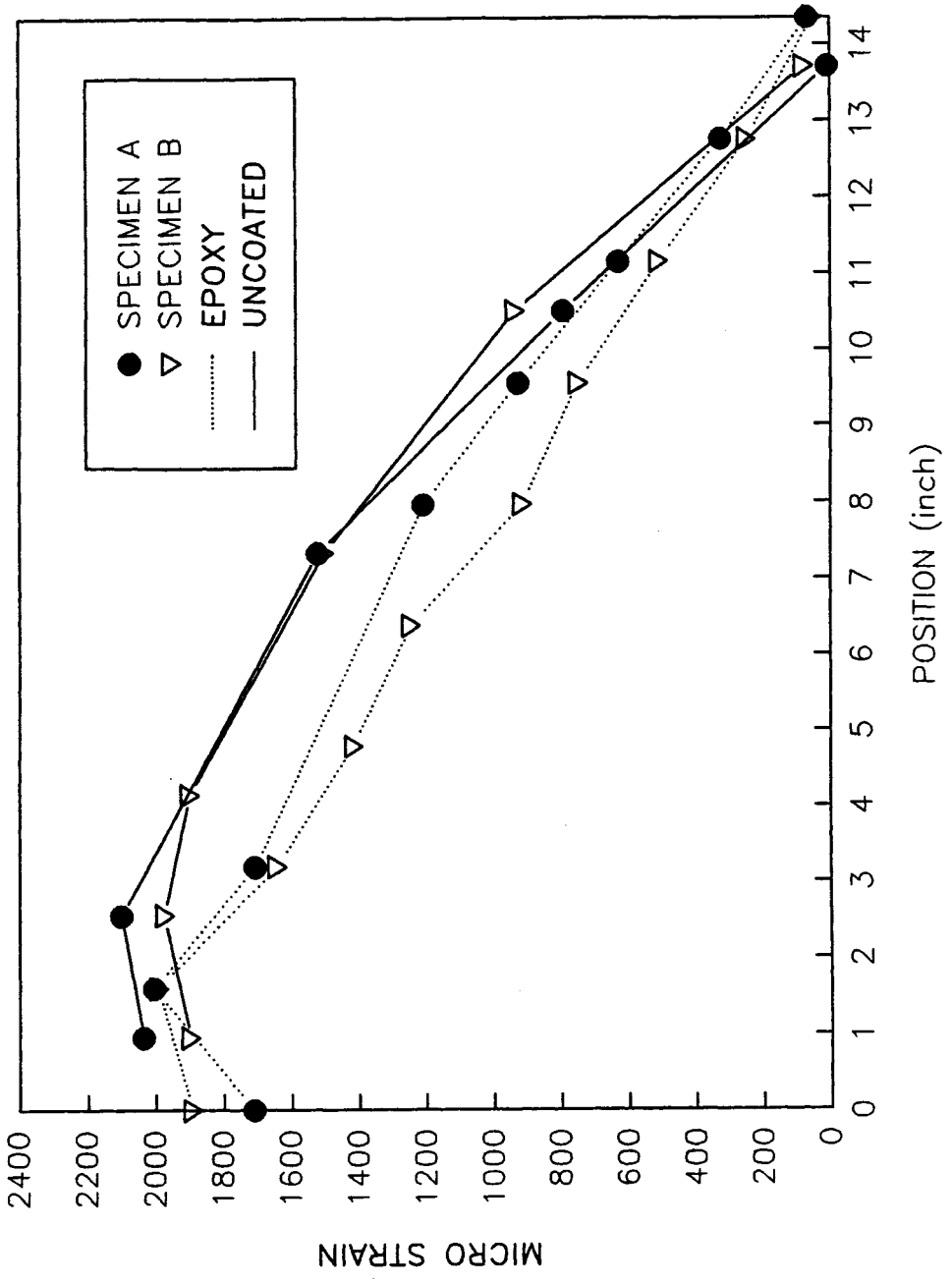

Figure 4.8 Strain Distribution Comparison at Failure

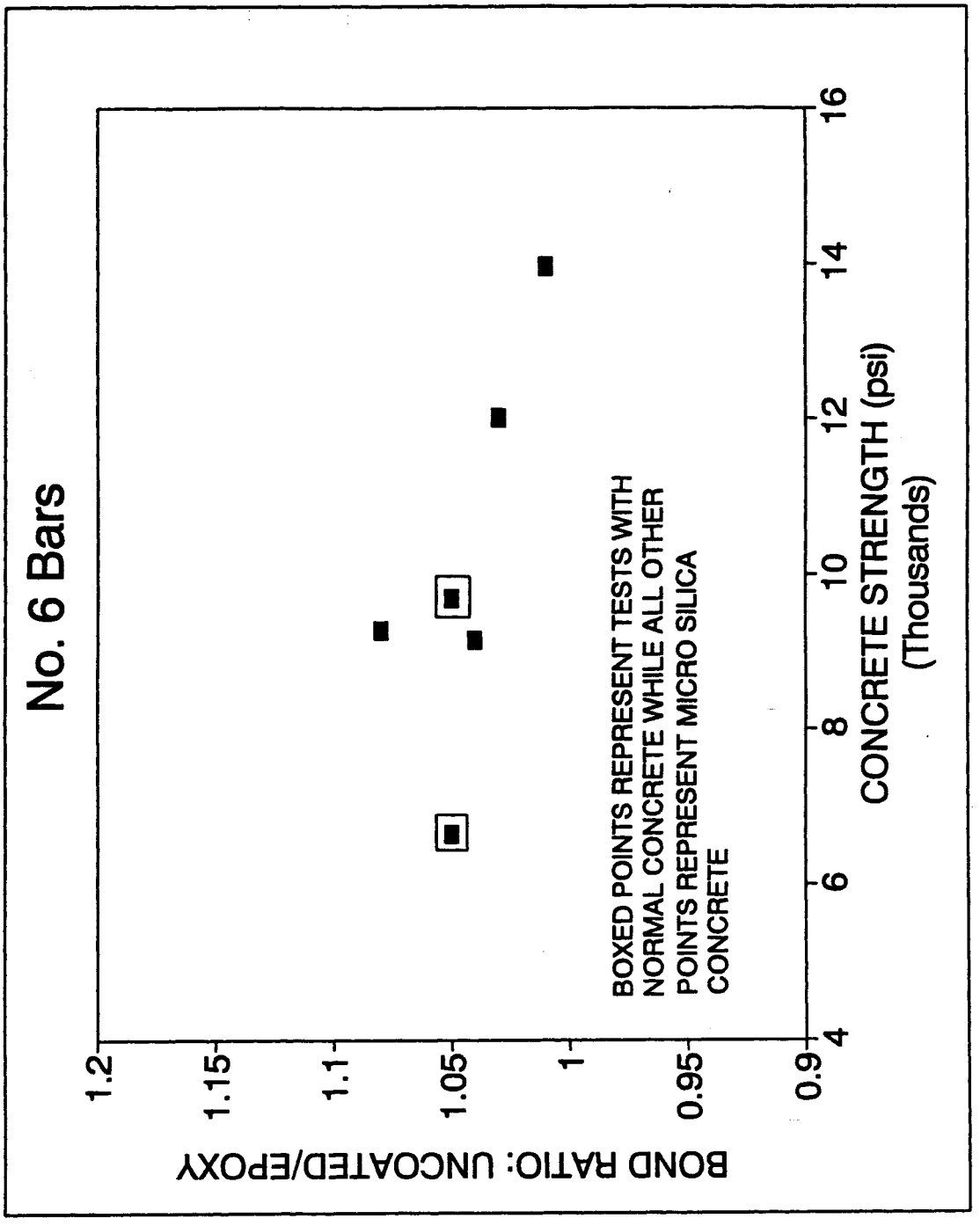

Figure 4.9 No. 6 Bars, Ultimate Bond Strength Ratio versus Concrete Strength

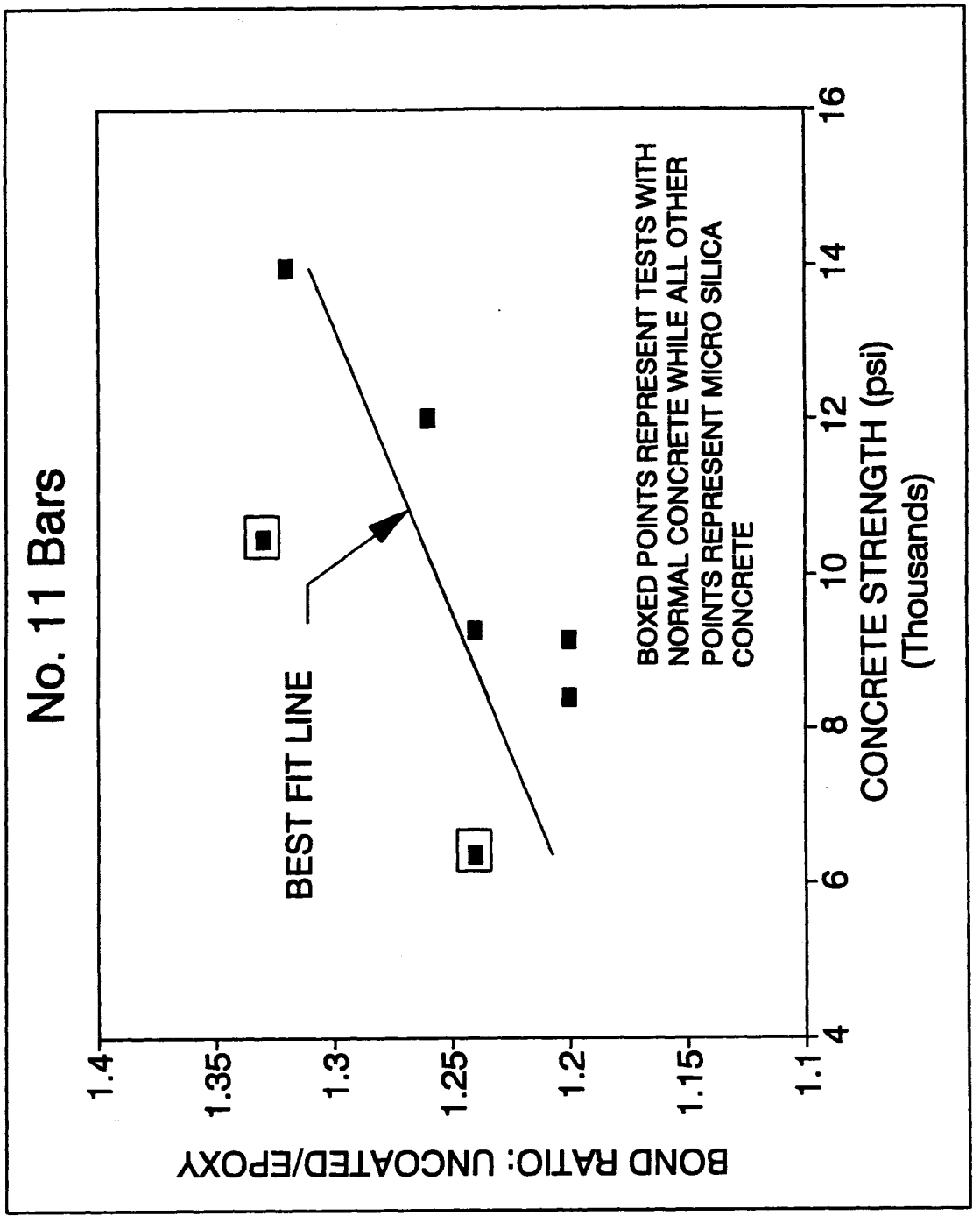

Figure 4.10 No. 11 Bars, Ultimate Bond Strength Ratio versus Concrete Strength

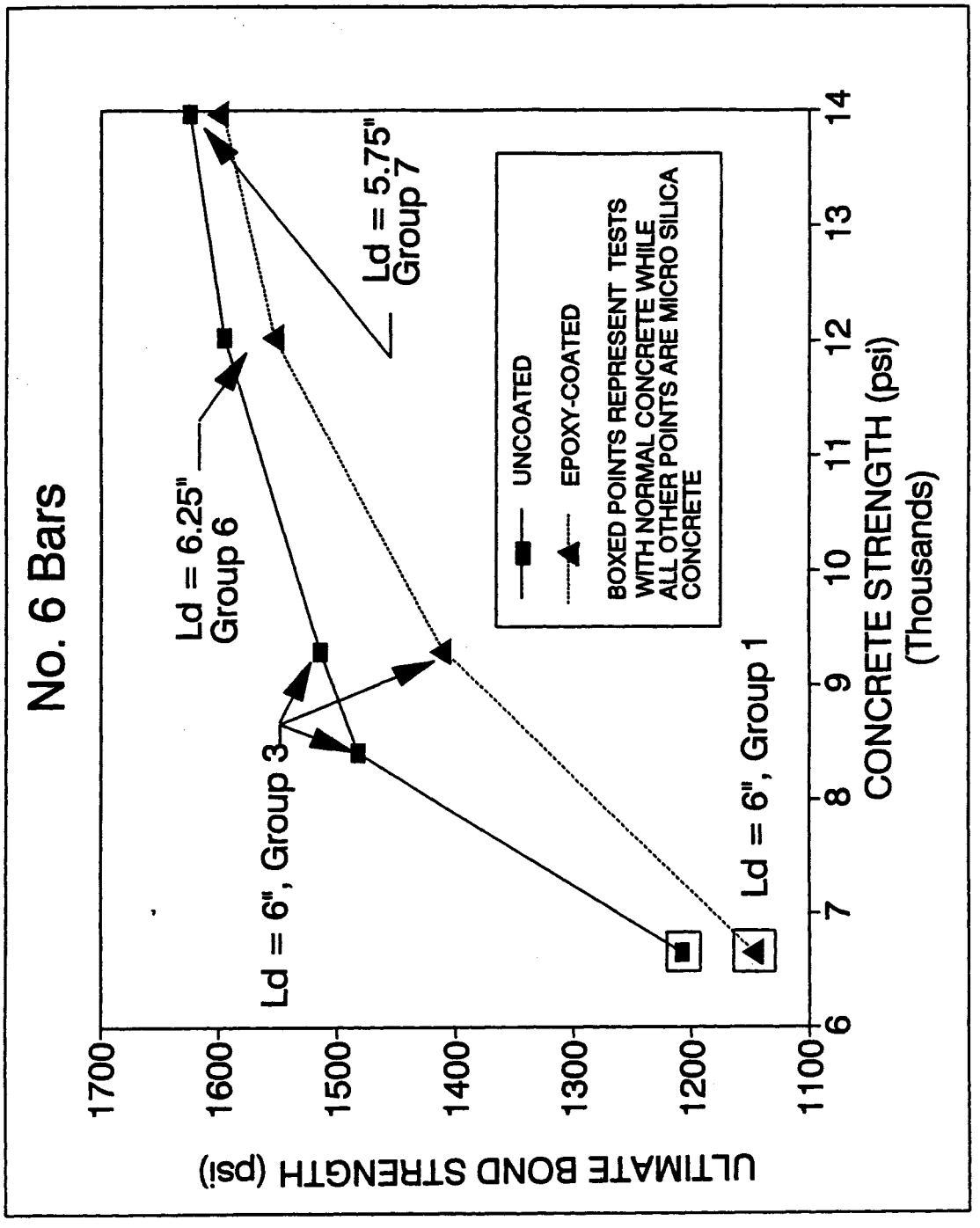

Figure 4.11 No. 6 Bars, Bond Strength versus Concrete Strength

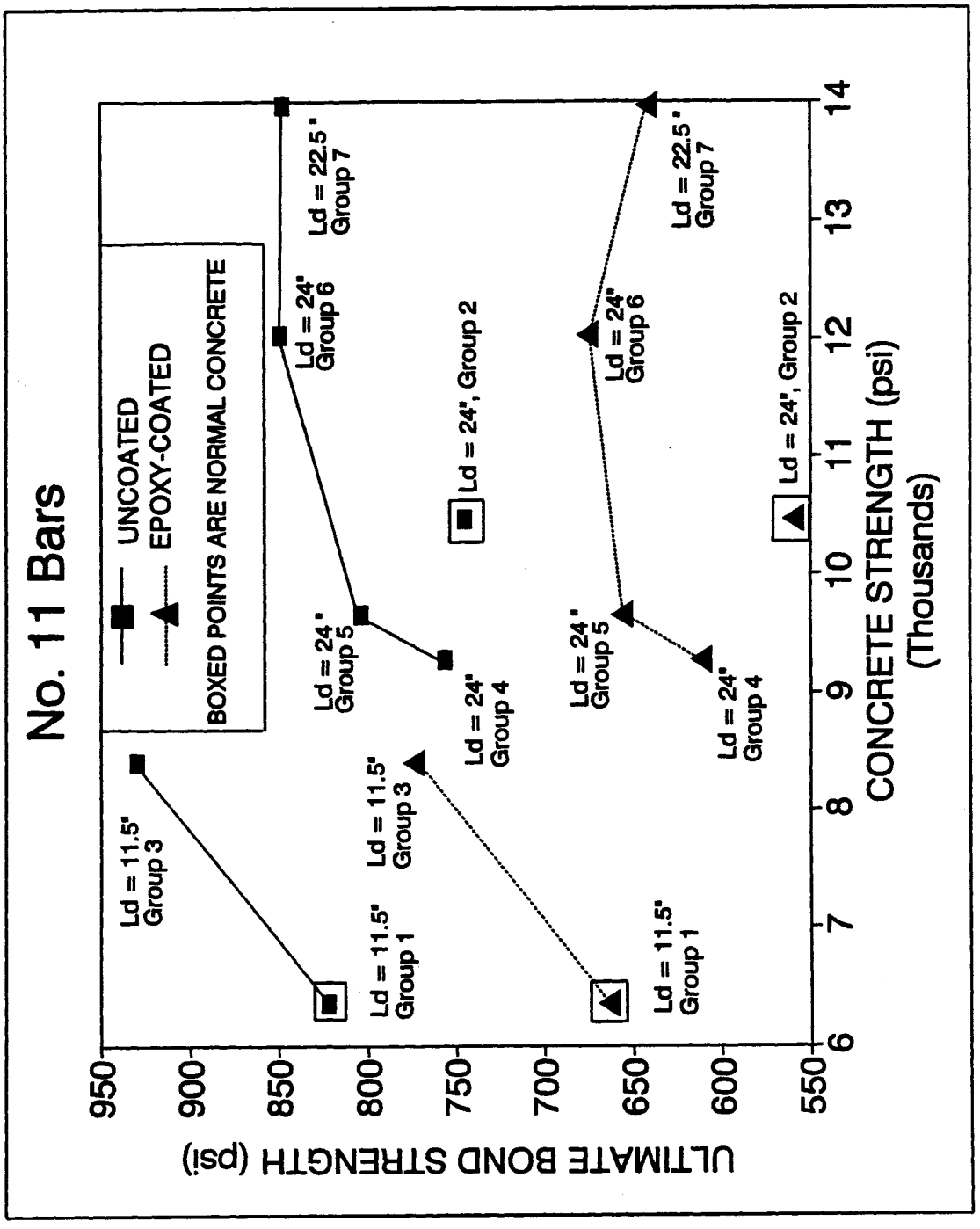

Figure 4.12 No. 11 Bars, Bond Strength versus Concrete Strength

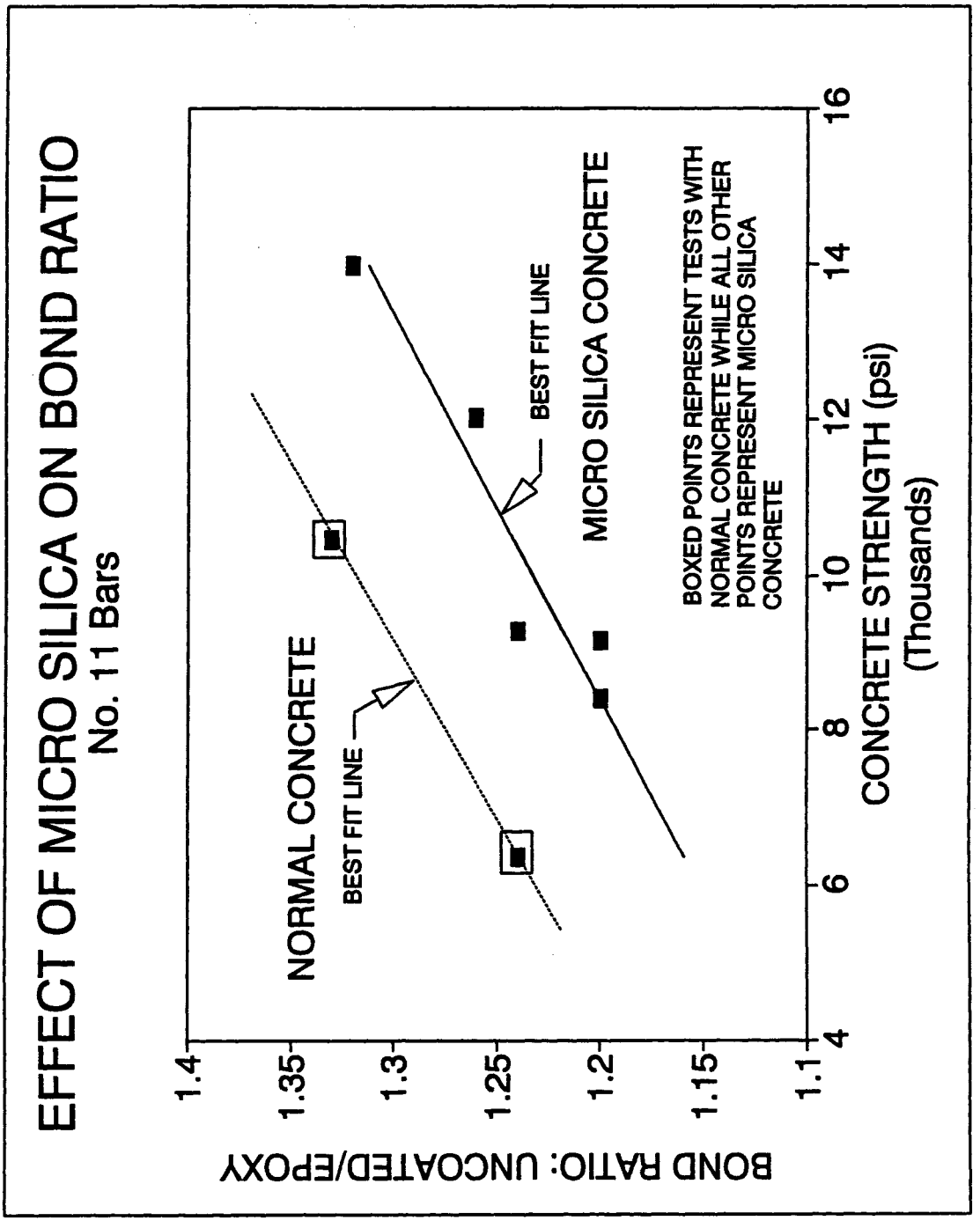

Figures 4.13 Effect of Concrete Type on Bond Strength Ratio for No. 11 Bars

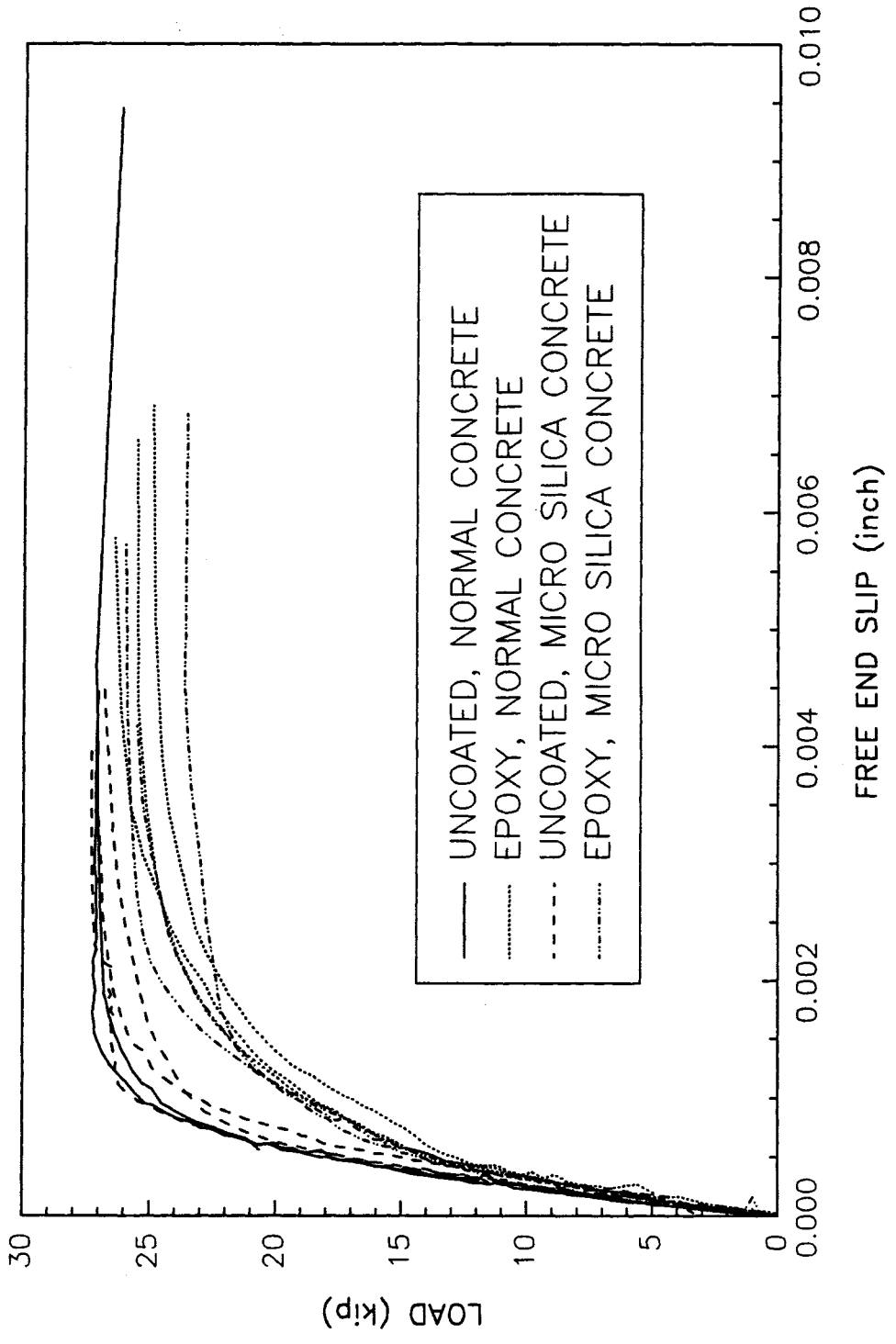

Figure 4.14 Comparison of Free-End Slip for No. 6 Bars in Micro Silica and Normal Concrete

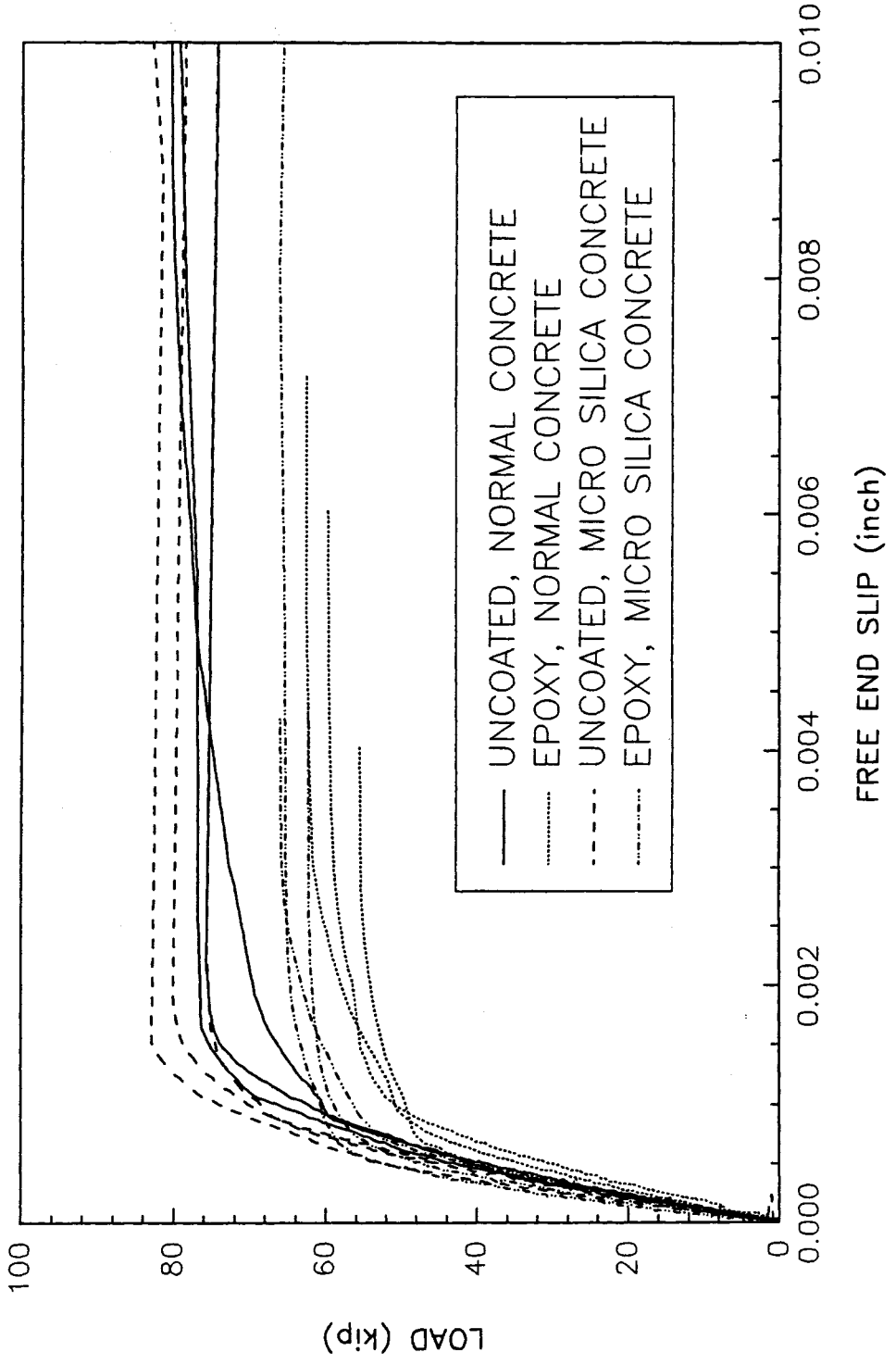

Figure 4.15 Comparison of Free-End Slip for No. 11 bars in Micro Silica and Normal Concrete

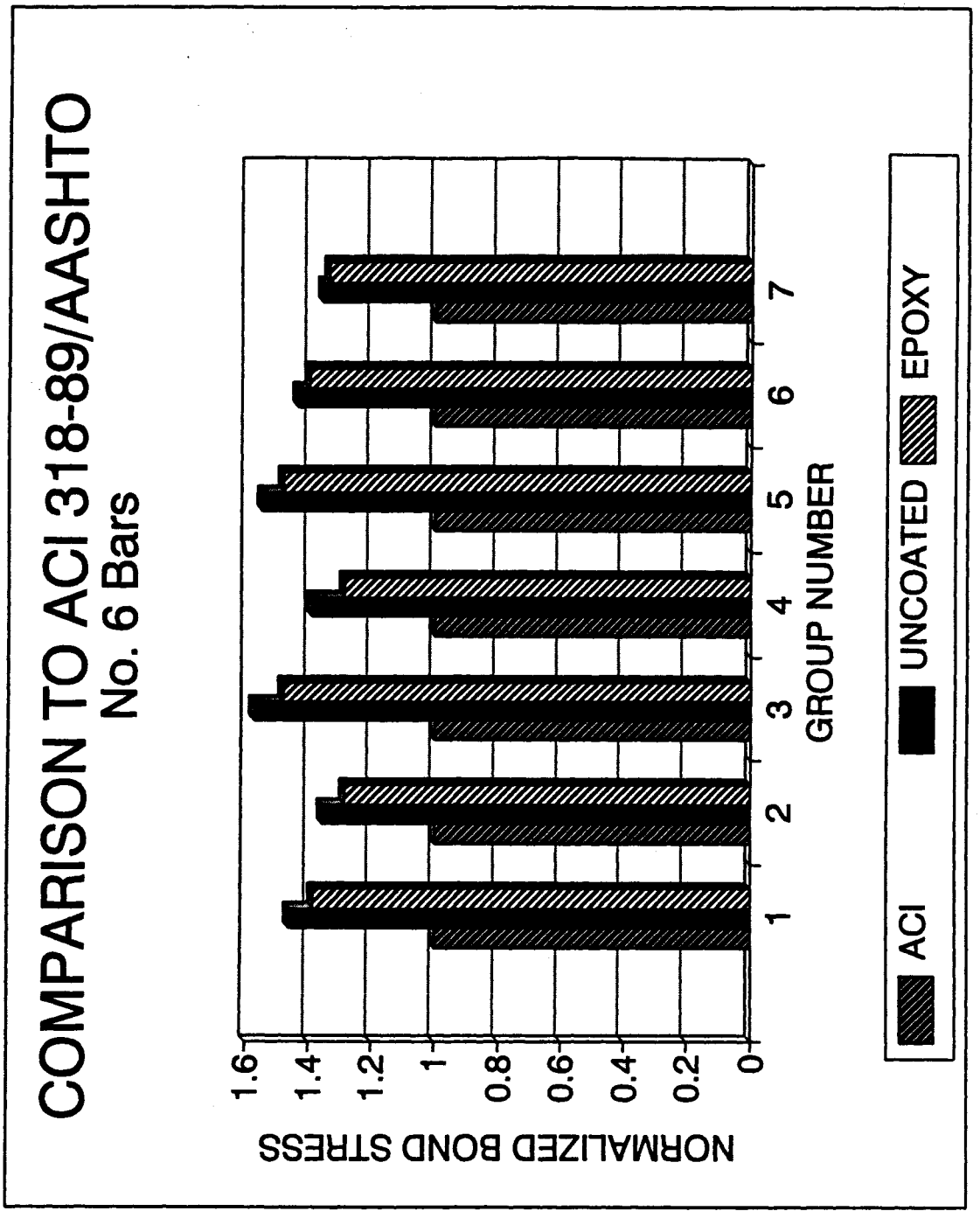

Figure 4.16 No. 6 Bars, Comparison of Test Results to ACI/AASHTO Design Code

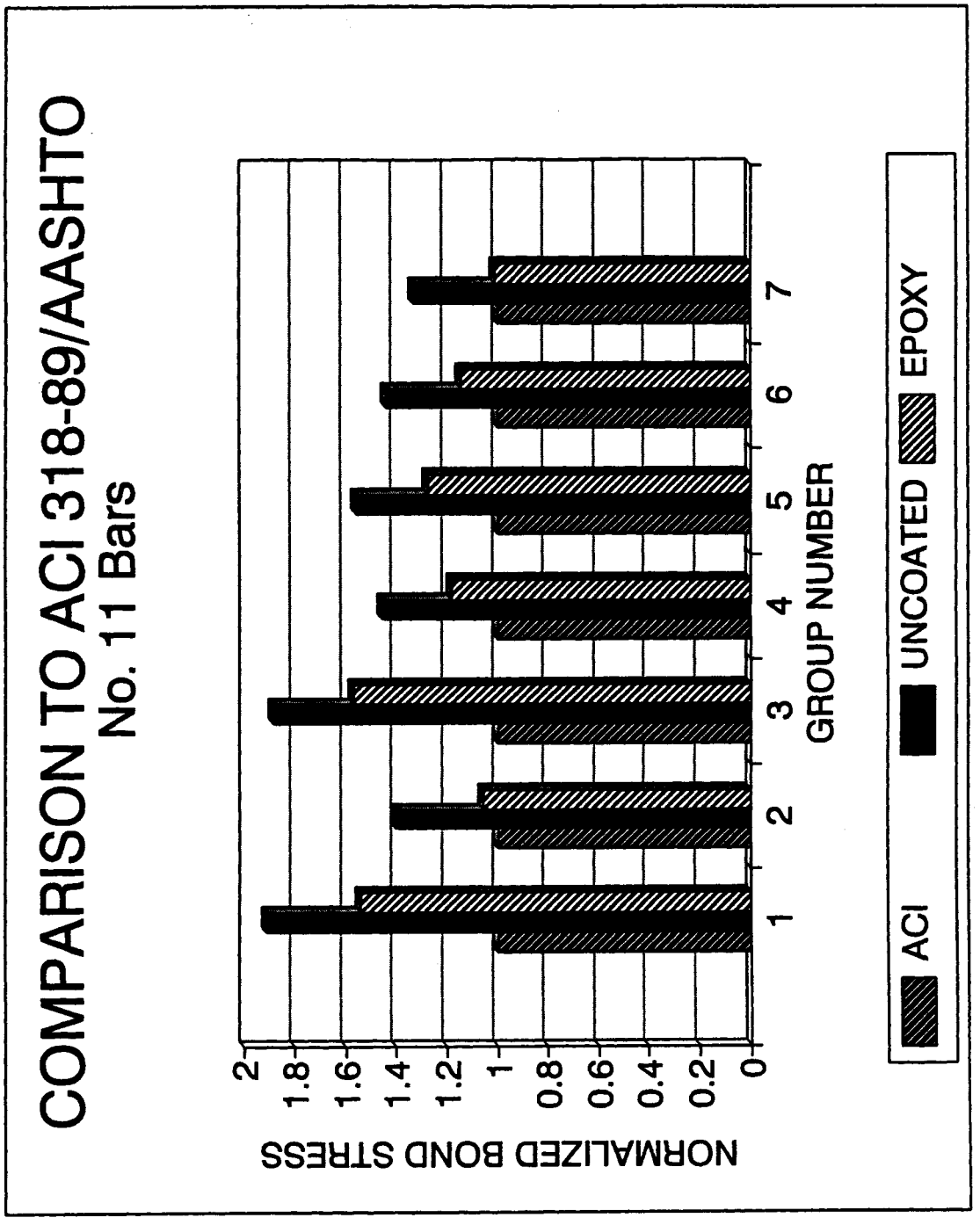

Figure 4.17 No. 11 Bars, Comparison of Test Results to ACI/AASHTO Design Code

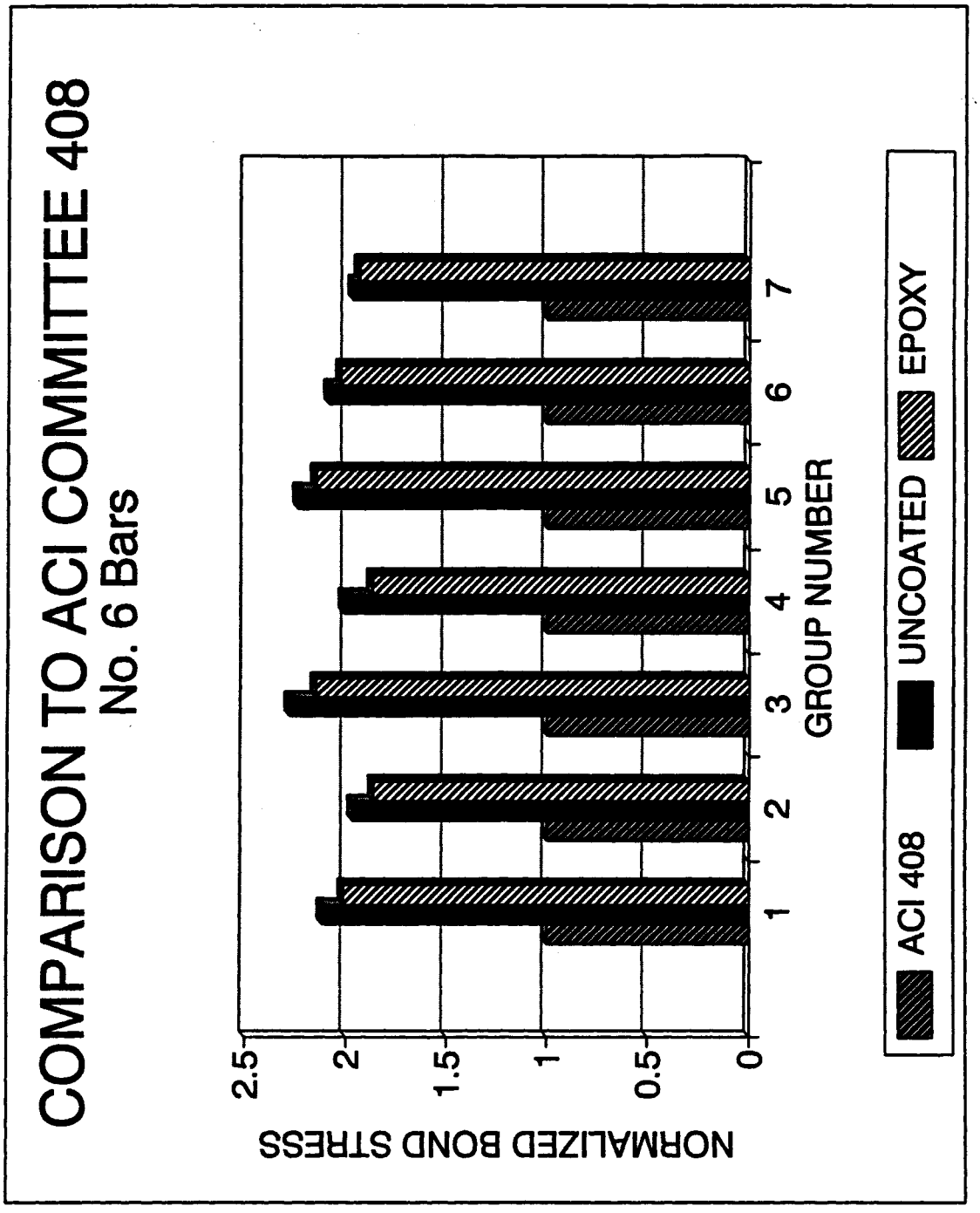

Figure 4.18 No. 6 Bars, Comparison of Test Results to ACI Committee 408

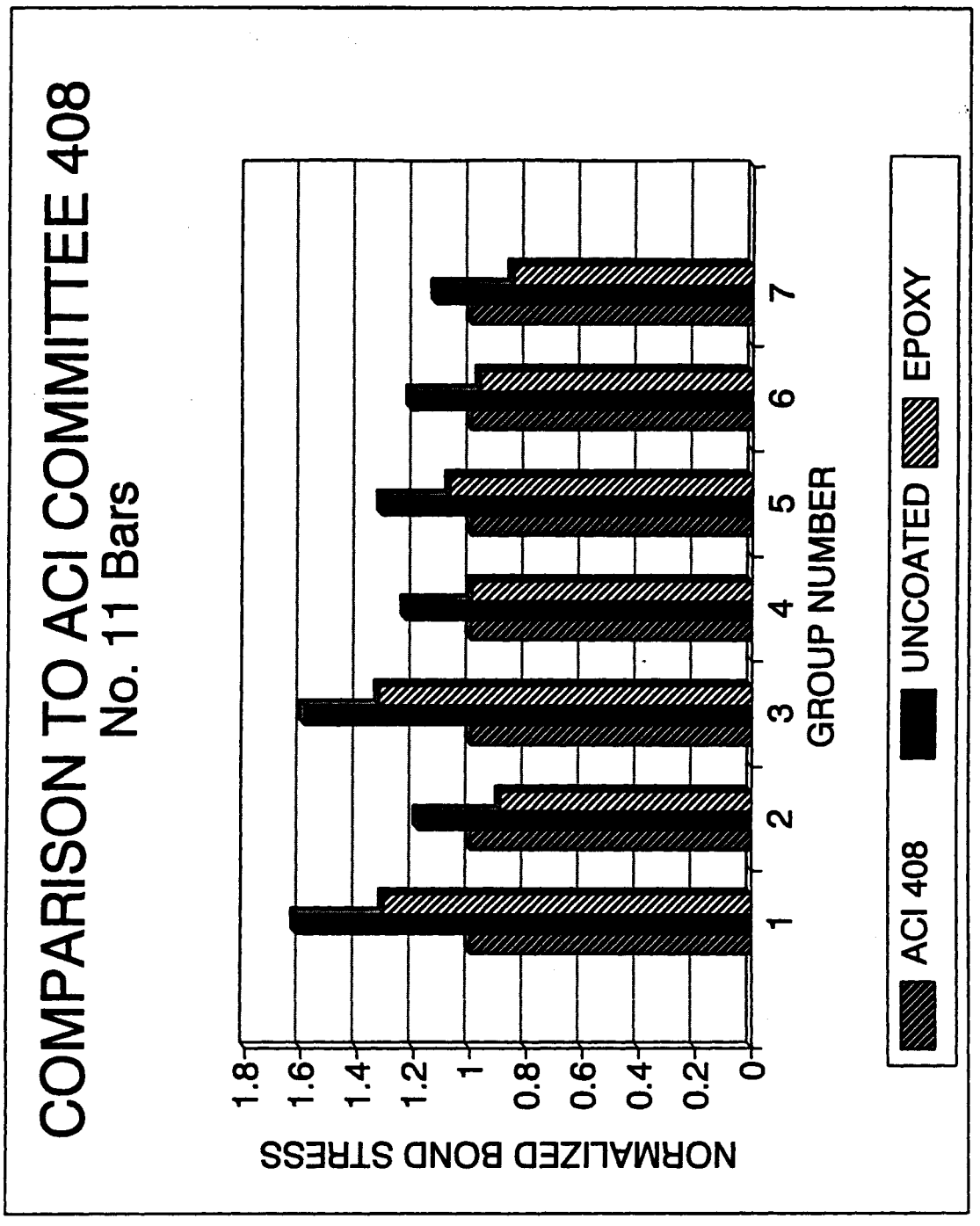

Figure 4.19 No. 11 Bars, Comparison of Test Results to ACI Committee 408

APPENDIX

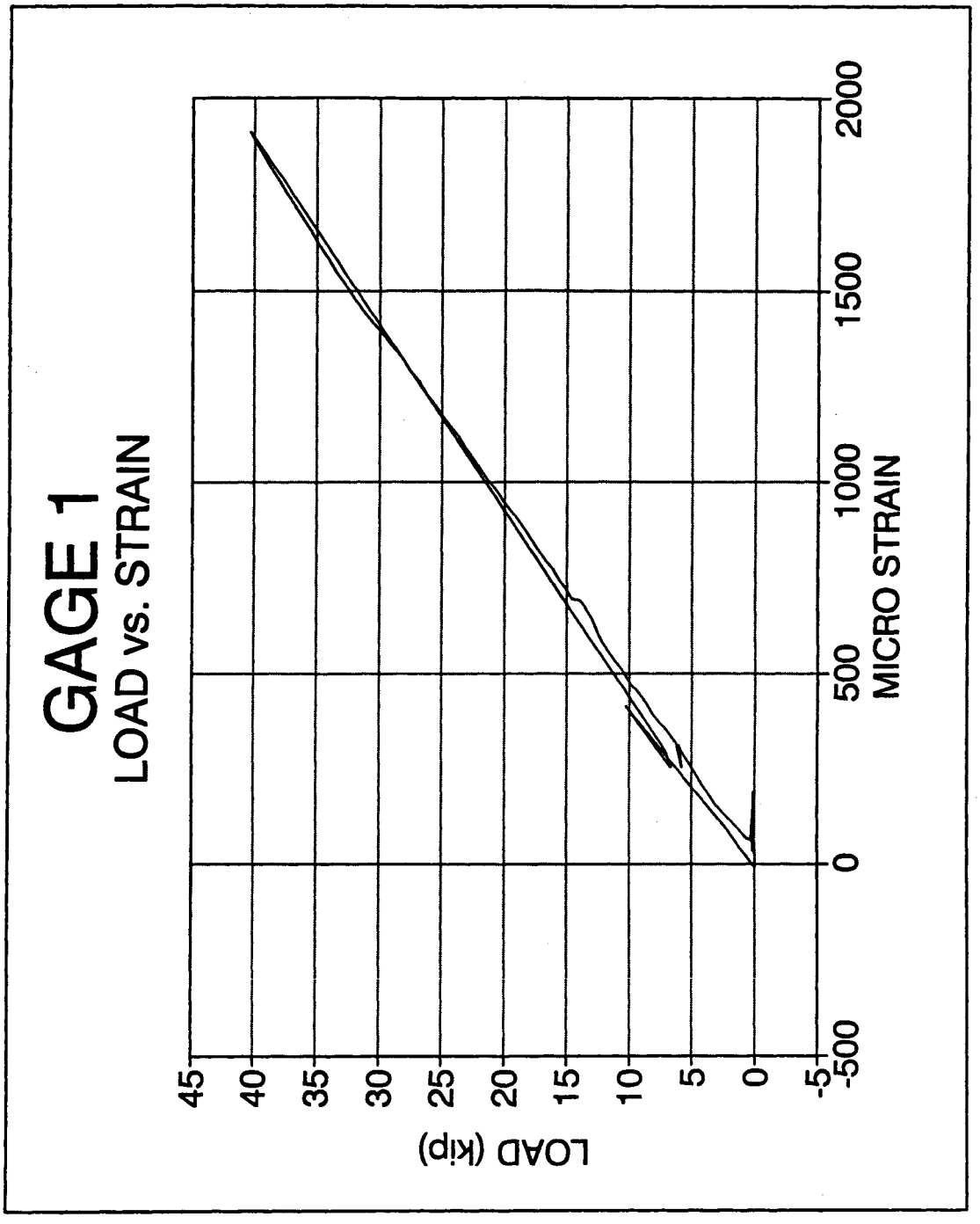

No. 8 Epoxy-Coated Bar Specimen B, Strain Gage 1

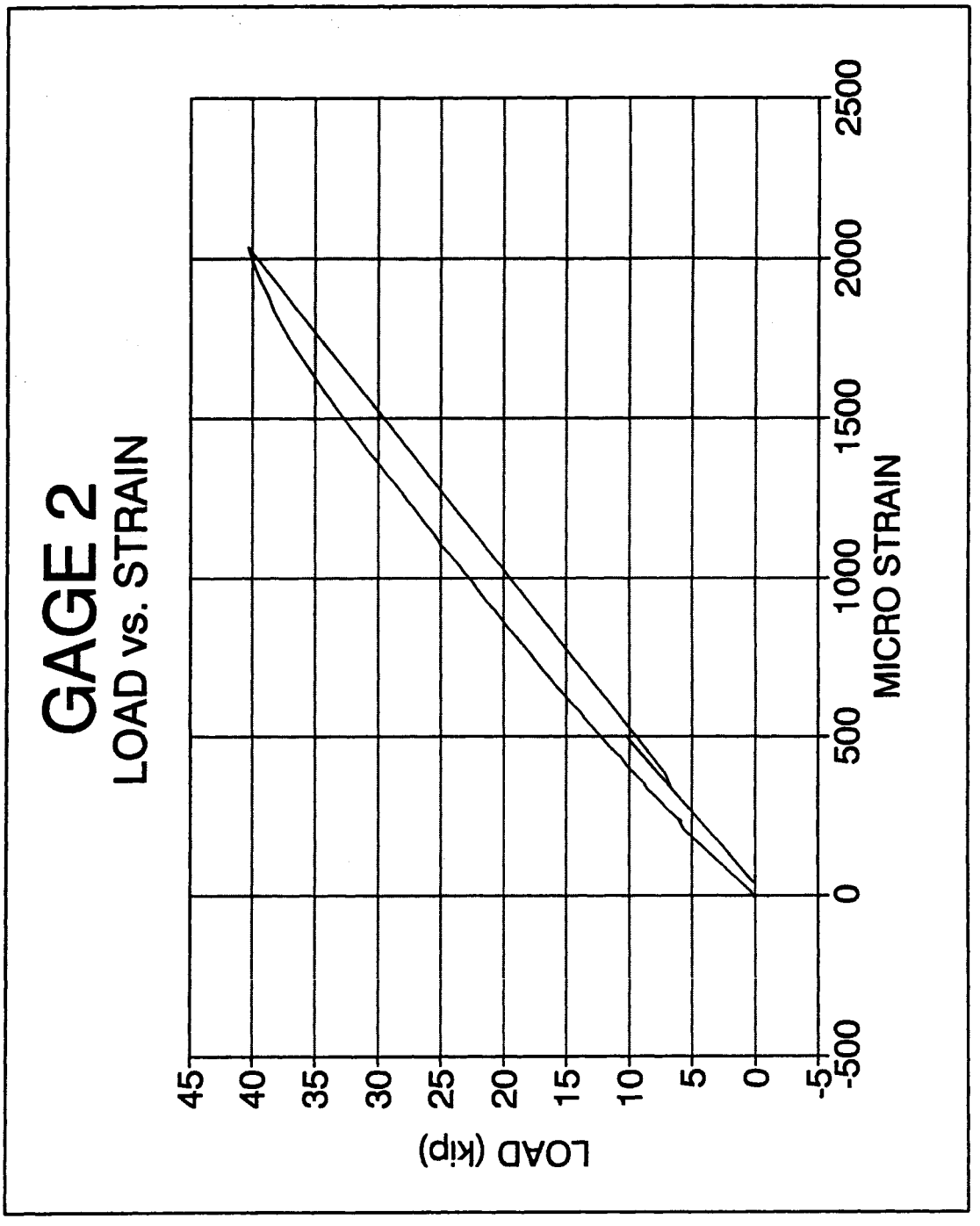

No. 8 Epoxy-Coated Bar Specimen B, Strain Gage 2

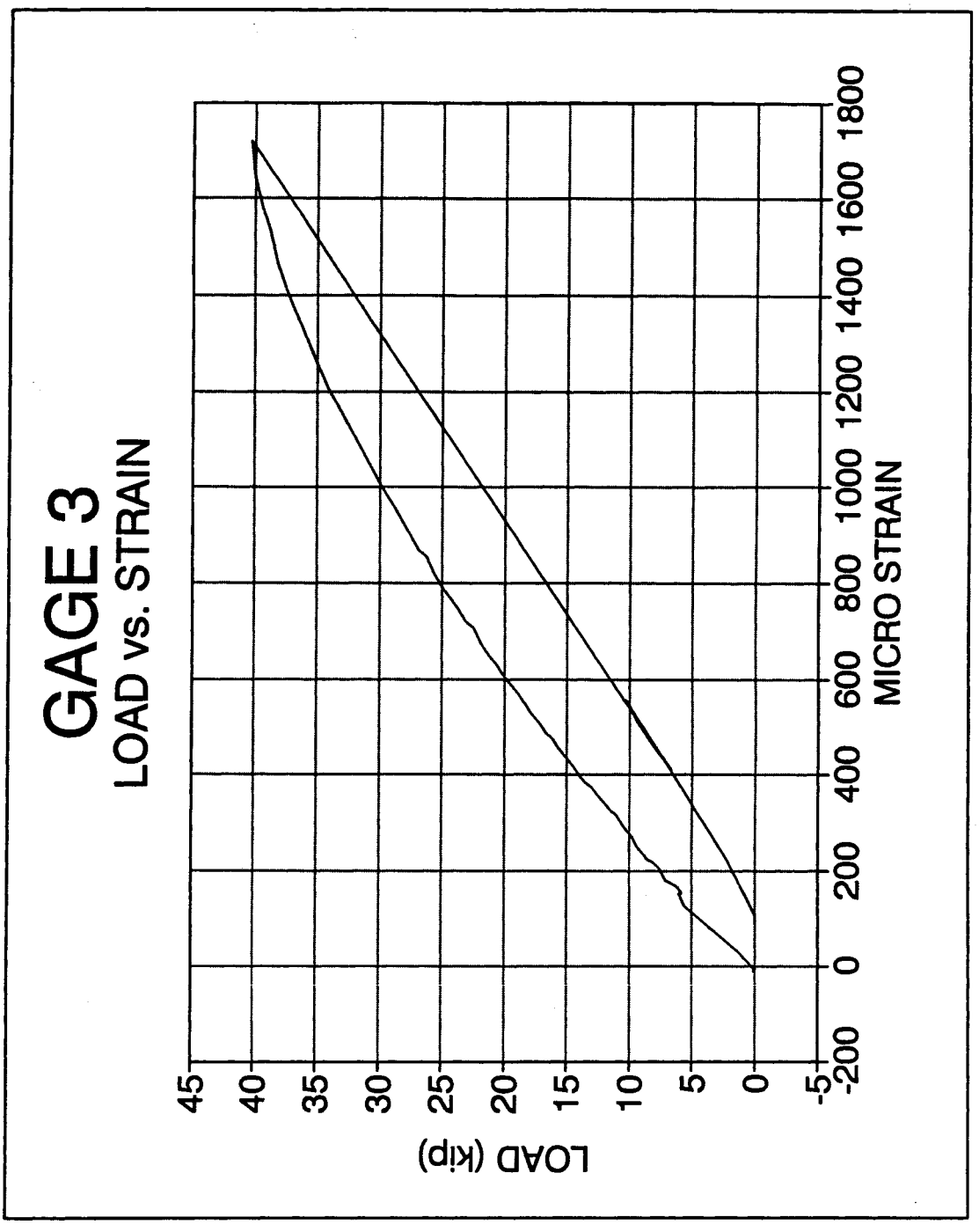

No. 8 Epoxy-Coated Bar Specimen B, Strain Gage 3

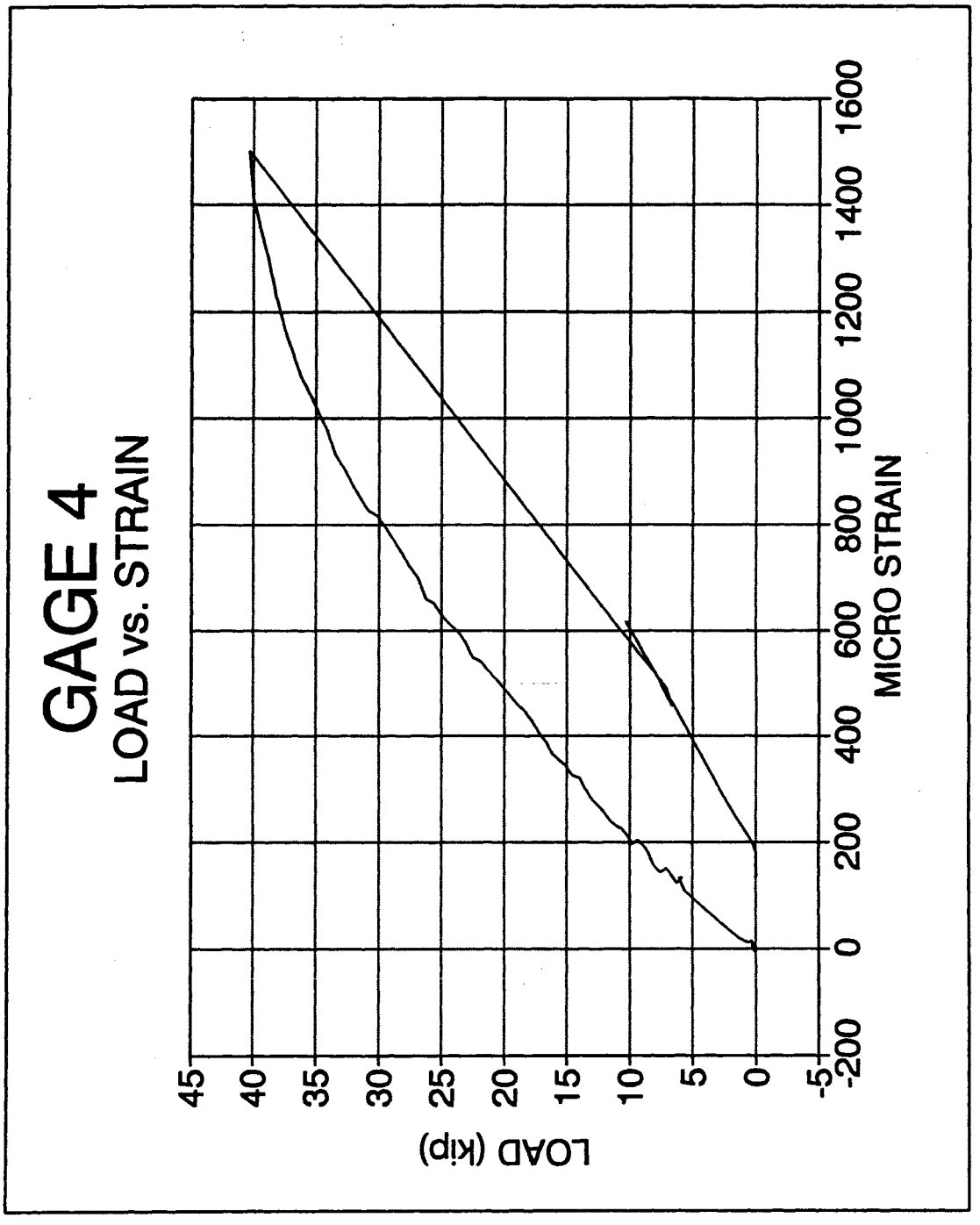

No. 8 Epoxy-Coated Bar Specimen B, Strain Gage 4

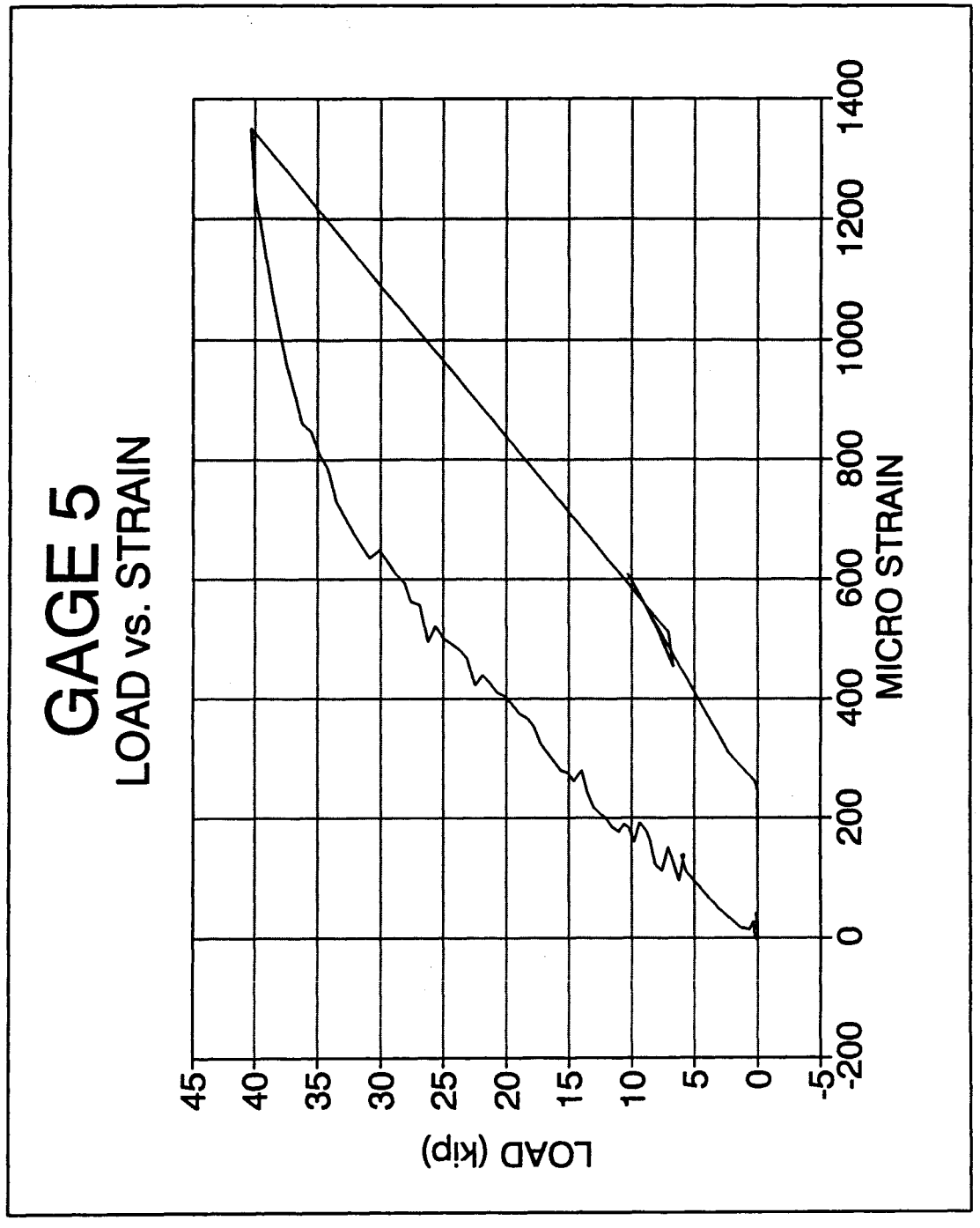

No. 8 Epoxy-Coated Bar Specimen B, Strain Gage 5

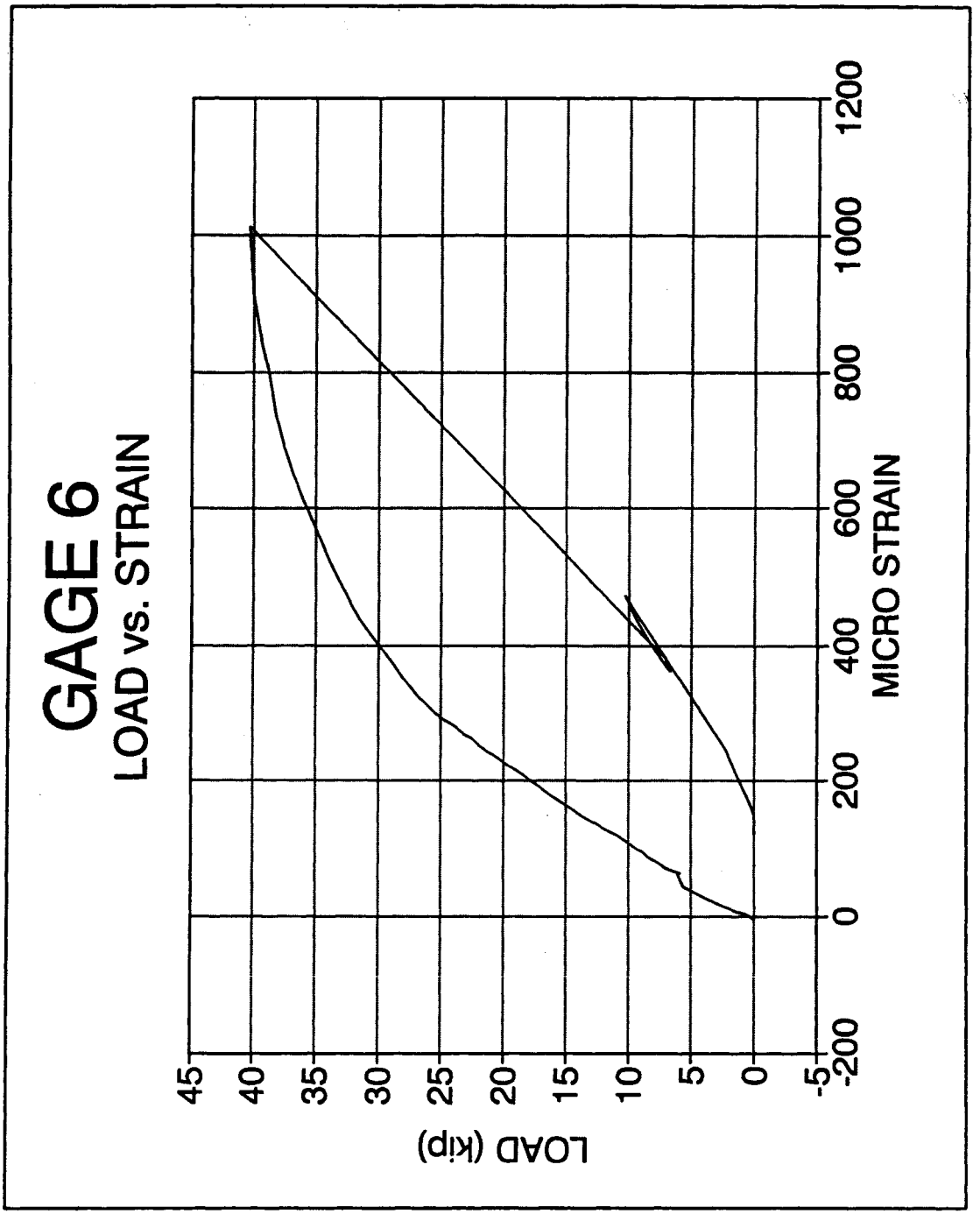

No. 8 Epoxy-Coated Bar Specimen B, Strain Gage 6

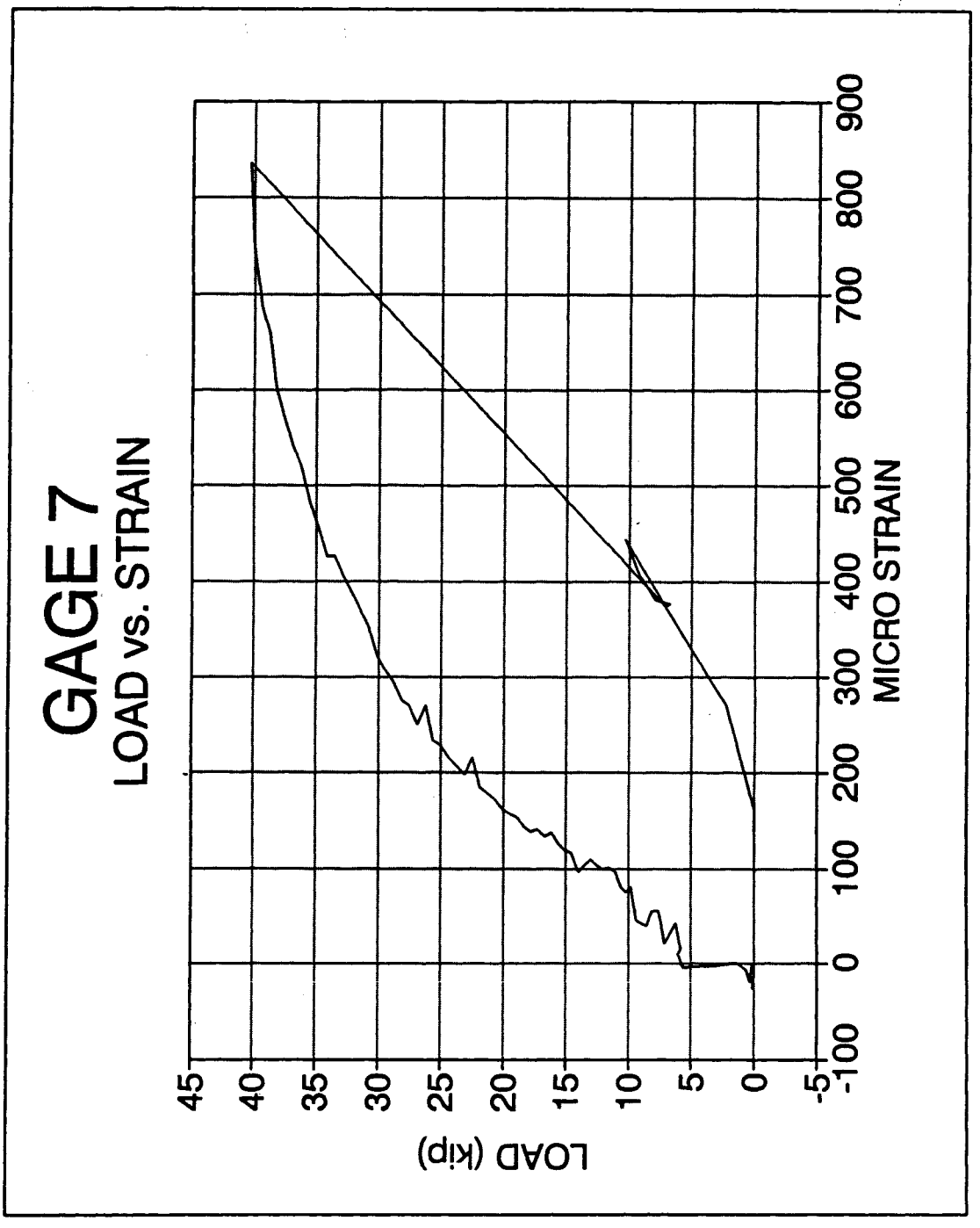

No. 8 Epoxy-Coated Bar Specimen B, Strain Gage 7

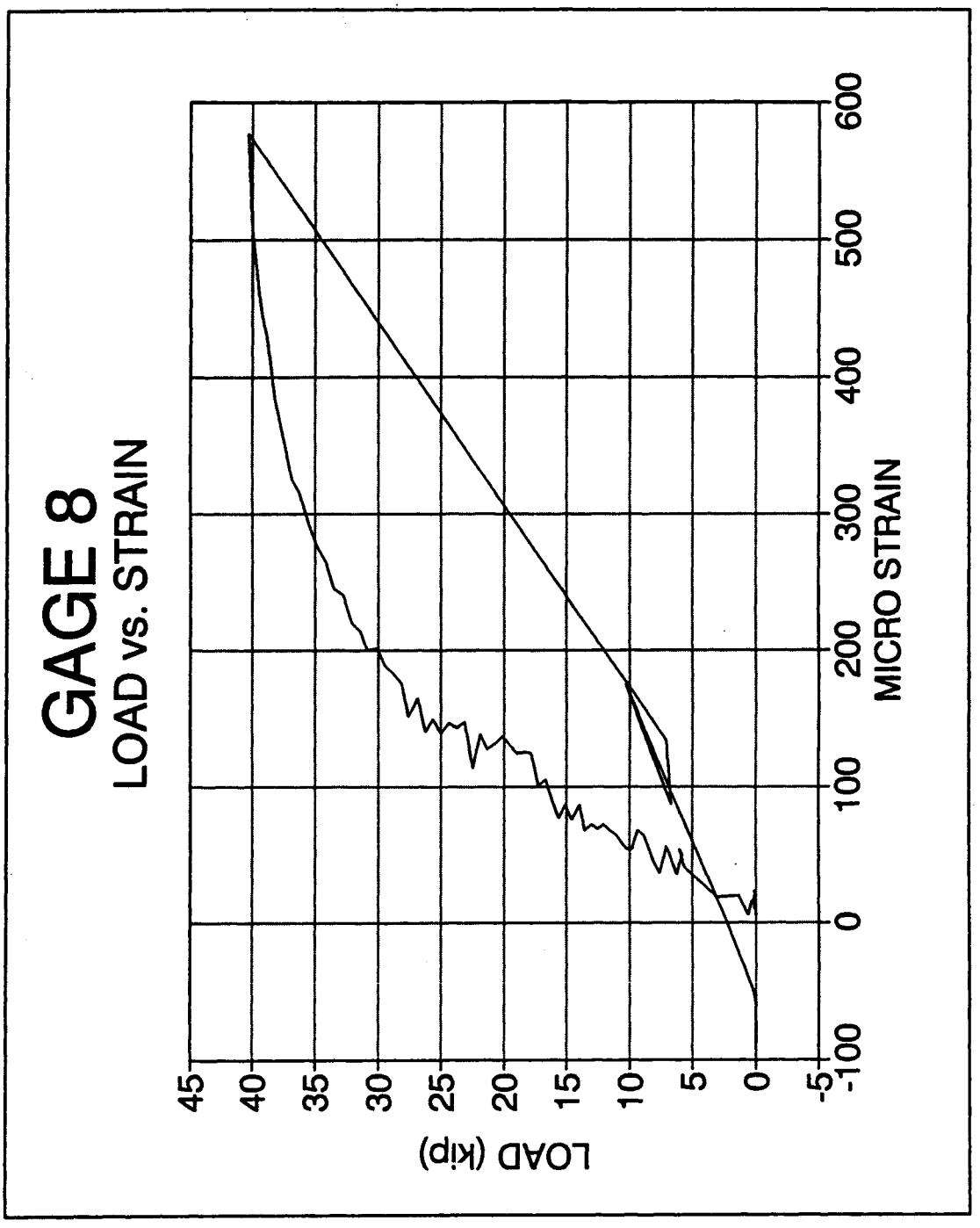

No. 8 Epoxy-Coated Bar Specimen B, Strain Gage 8

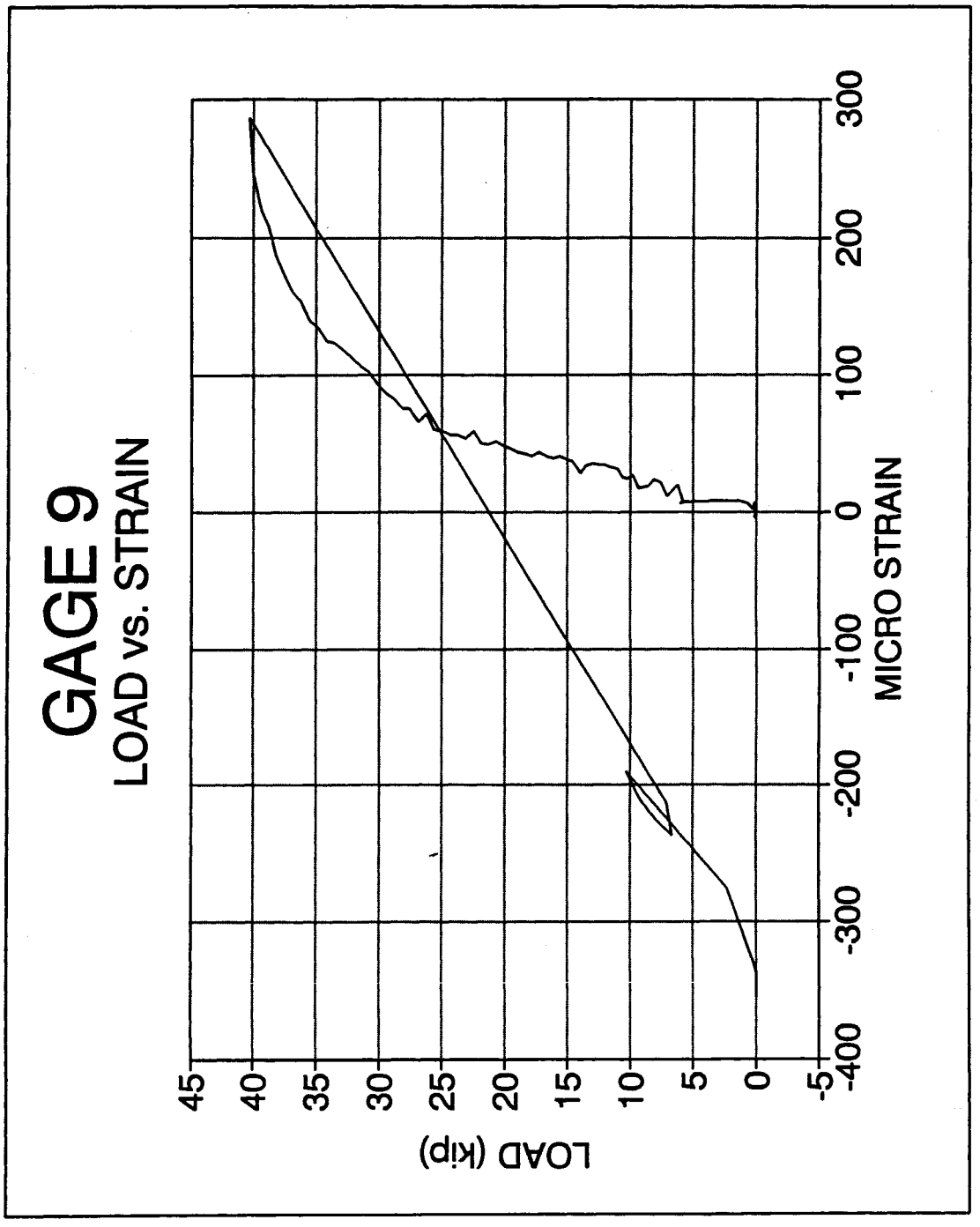

No. 8 Epoxy-Coated Bar Specimen B, Strain Gage 9

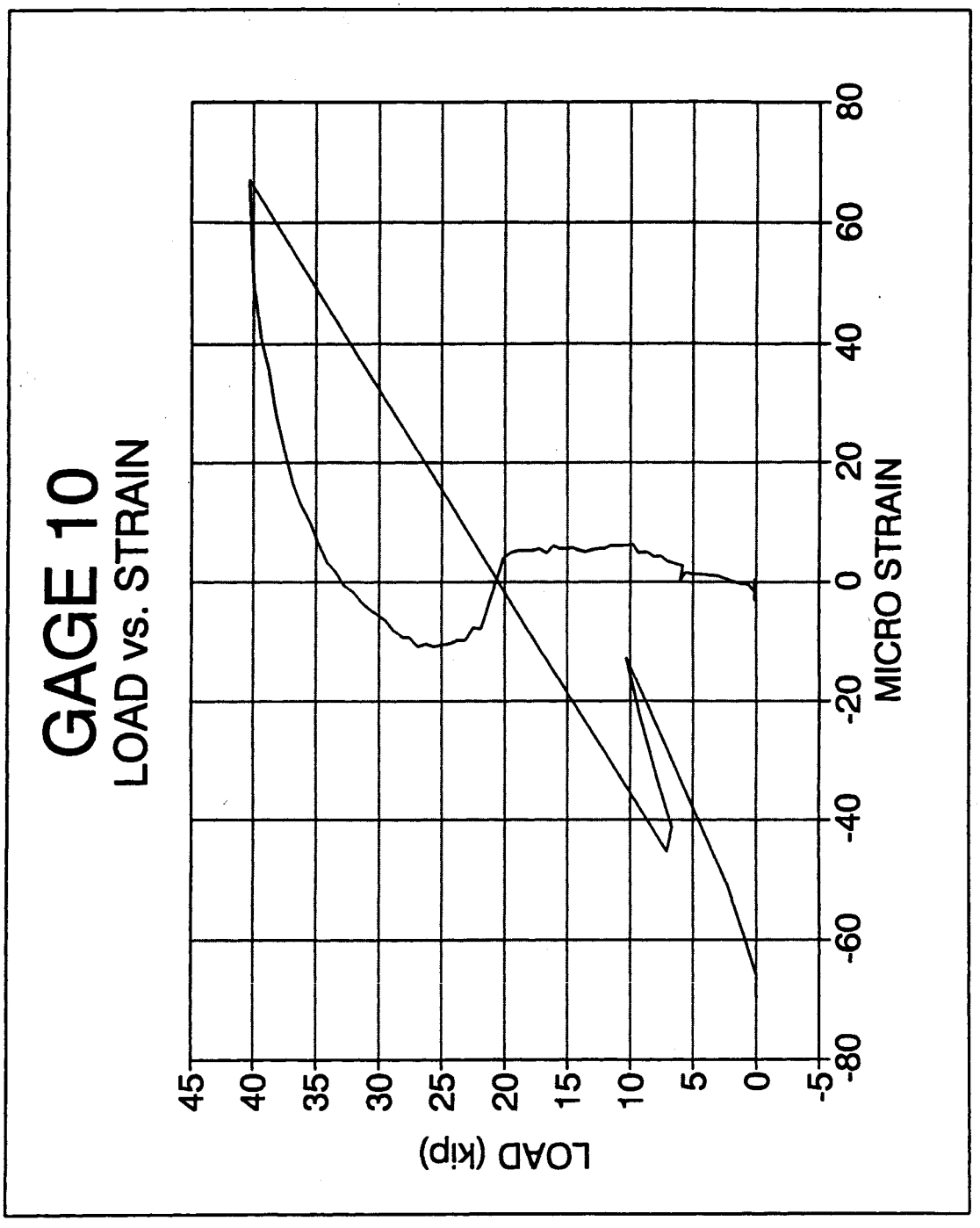

No. 8 Epoxy-Coated Bar Specimen B, Strain Gage 10

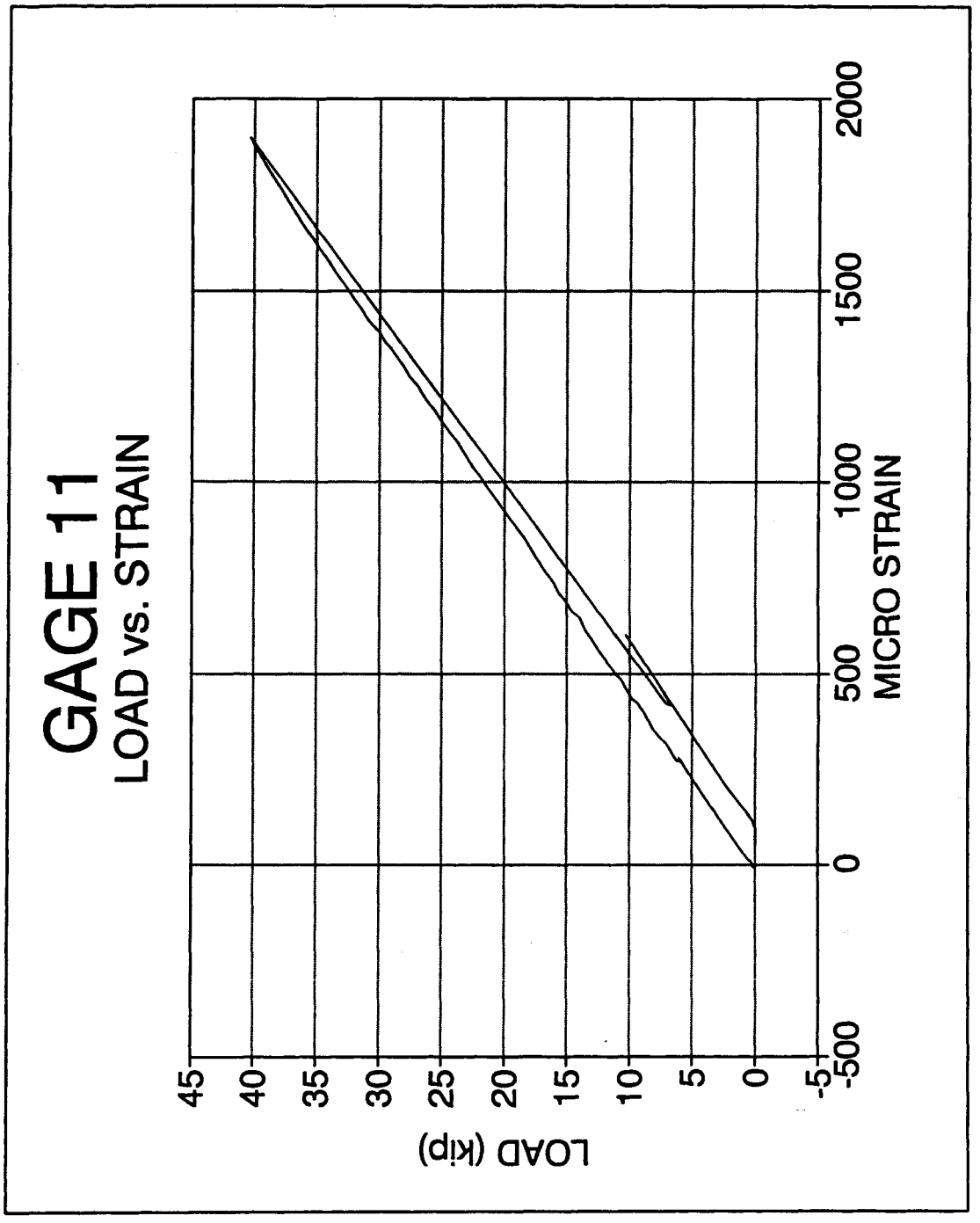

No. 8 Epoxy-Coated Bar Specimen B, Strain Gage 11

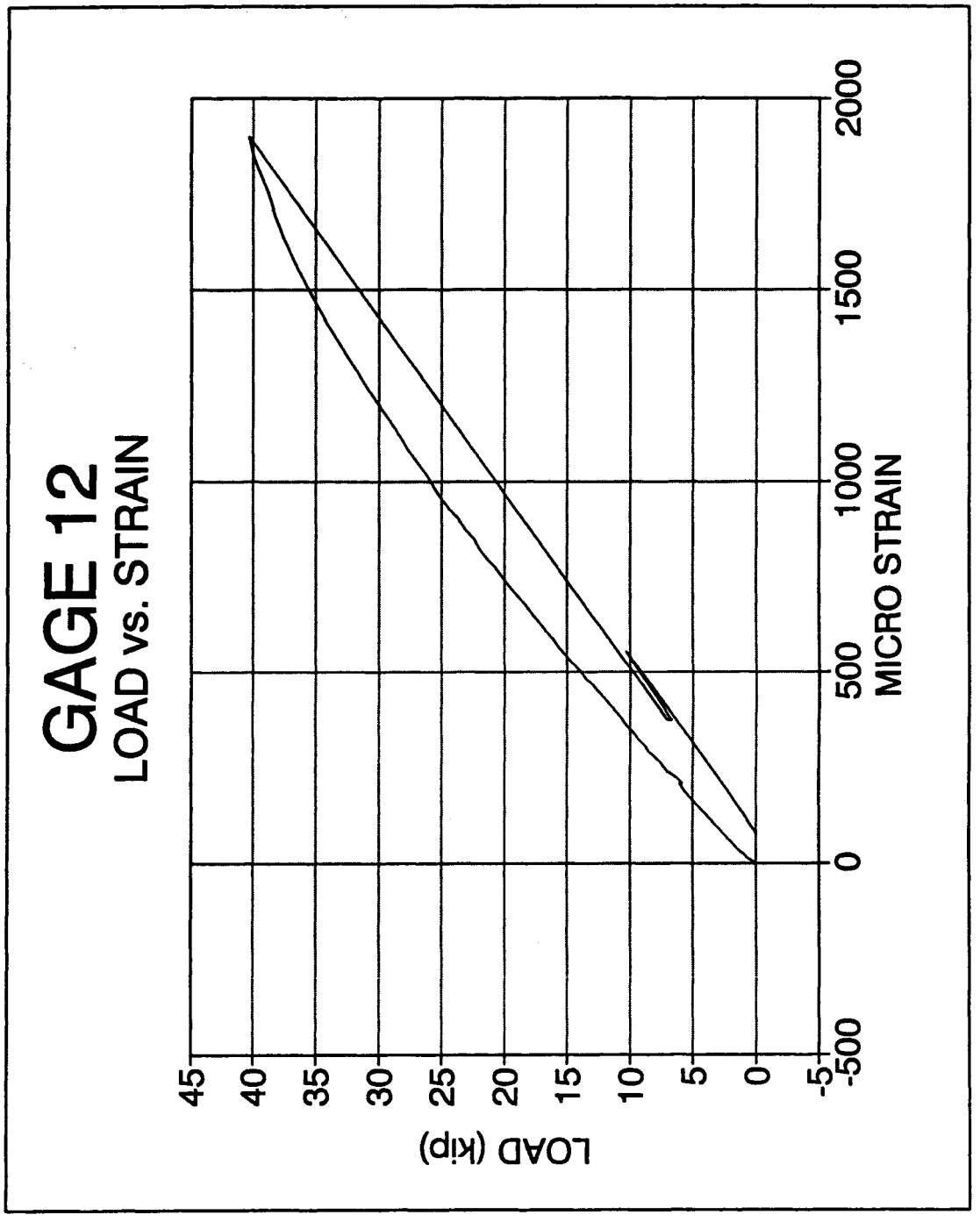

No. 8 Epoxy-Coated Bar Specimen B, Strain Gage 12

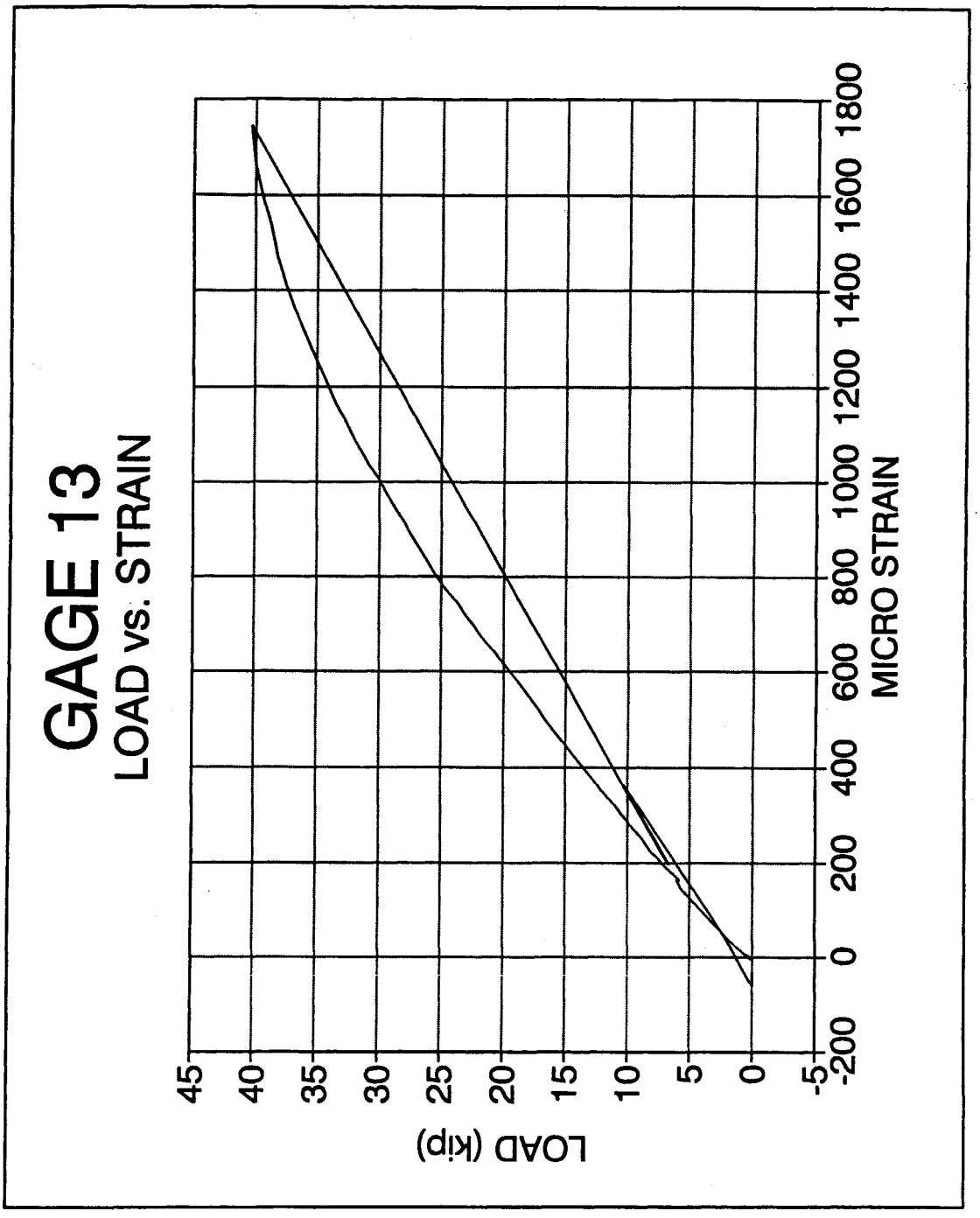

No. 8 Epoxy-Coated Bar Specimen B, Strain Gage 13

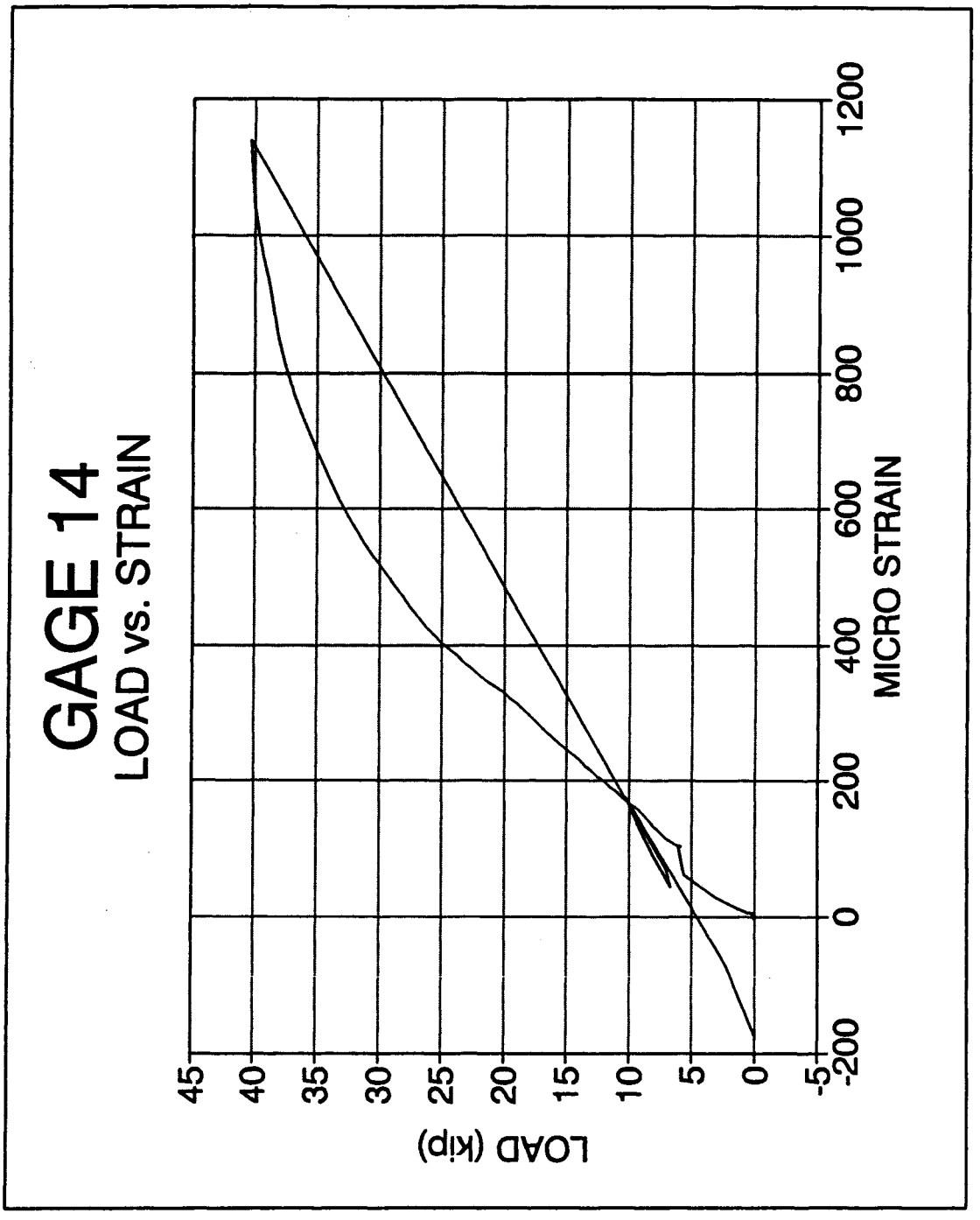

No. 8 Epoxy-Coated Bar Specimen B, Strain Gage 14

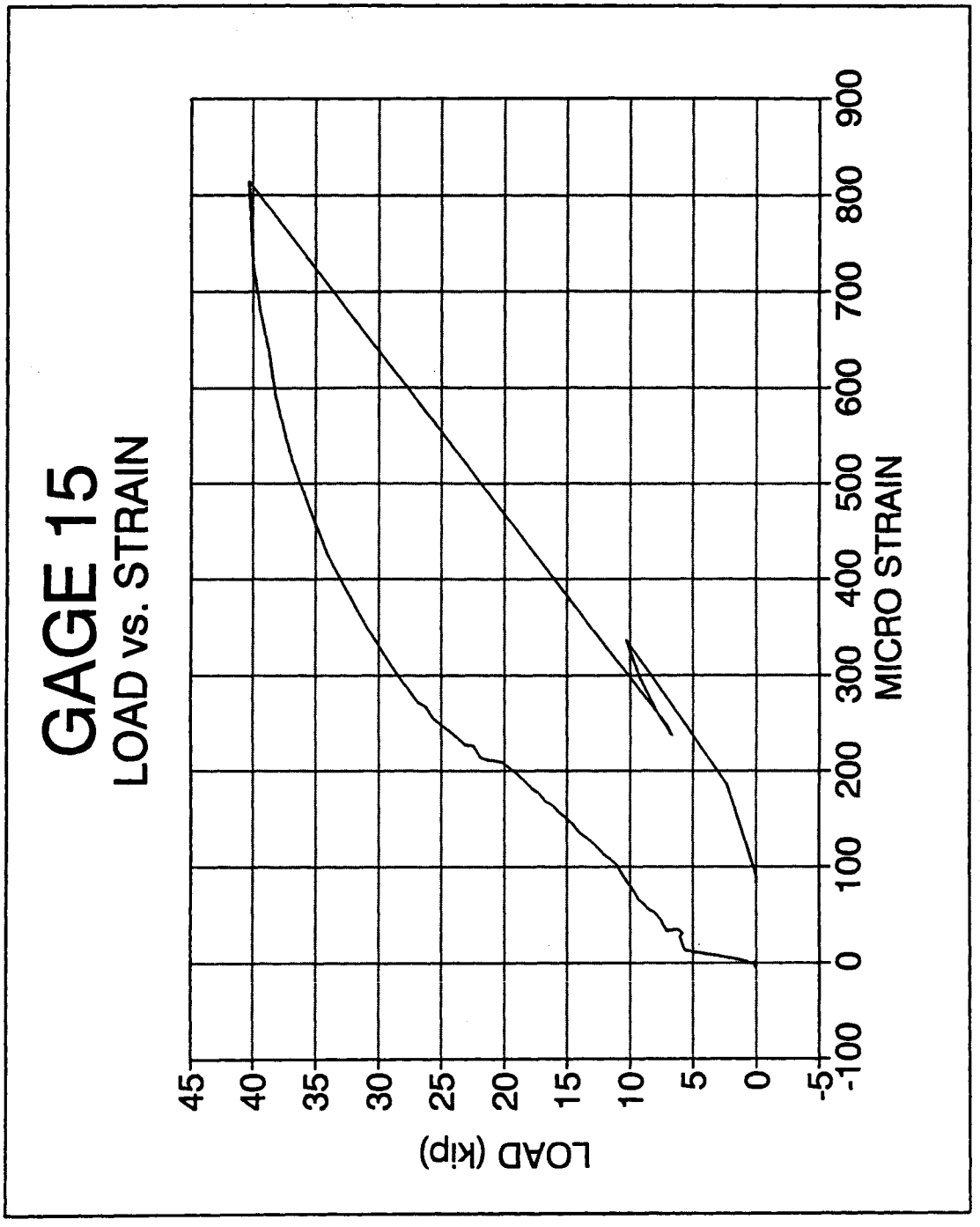

No. 8 Epoxy-Coated Bar Specimen B, Strain Gage 15

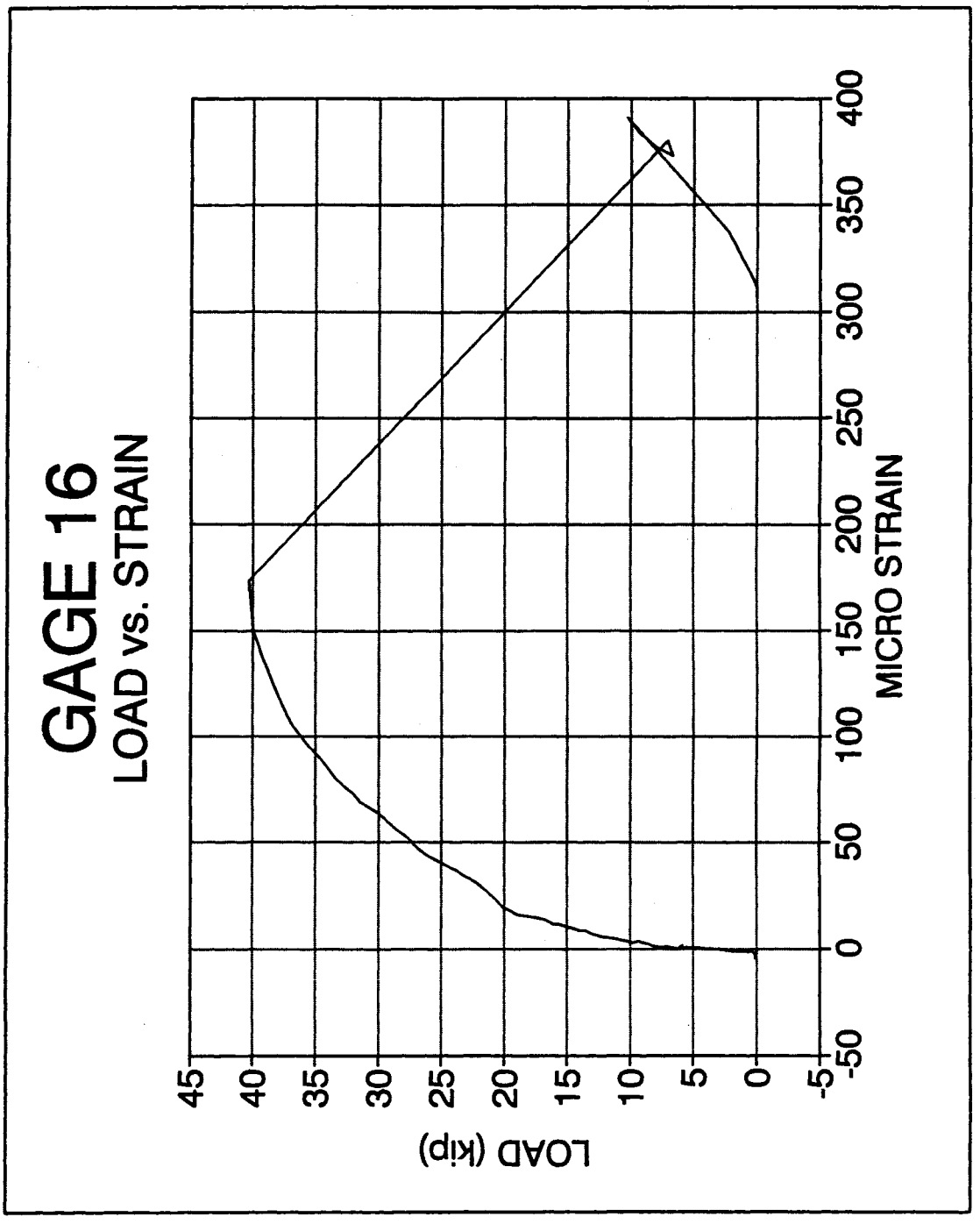

No. 8 Epoxy-Coated Bar Specimen B, Strain Gage 16